NAVAL POSTGRADUATE SCHOOL
Monterey, California

THESIS

**COMPARISON OF CHANNEL EQUALIZATION
FILTERING TECHNIQUES IN UNDERWATER
ACOUSTIC COMMUNICATIONS**

by

Ryan J. Kuchler

June 2002

Thesis Advisor:	Charles W. Therrien
Thesis Co-Advisor:	Kevin B. Smith

Approved for public release; distribution is unlimited.

THIS PAGE INTENTIONALLY LEFT BLANK

REPORT DOCUMENTATION PAGE		*Form Approved OMB No. 0704-0188*

Public reporting burden for this collection of information is estimated to average 1 hour per response, including the time for reviewing instruction, searching existing data sources, gathering and maintaining the data needed, and completing and reviewing the collection of information. Send comments regarding this burden estimate or any other aspect of this collection of information, including suggestions for reducing this burden, to Washington headquarters Services, Directorate for Information Operations and Reports, 1215 Jefferson Davis Highway, Suite 1204, Arlington, VA 22202-4302, and to the Office of Management and Budget, Paperwork Reduction Project (0704-0188) Washington DC 20503.

1. AGENCY USE ONLY *(Leave blank)*	2. REPORT DATE June 2002	3. REPORT TYPE AND DATES COVERED Master's Thesis	
4. TITLE AND SUBTITLE: Comparison of Channel Equalization Filtering Techniques in Underwater Acoustic Communications		5. FUNDING NUMBERS	
6. AUTHOR(S) Kuchler, Ryan			
7. PERFORMING ORGANIZATION NAME(S) AND ADDRESS(ES) Naval Postgraduate School Monterey, CA 93943-5000		8. PERFORMING ORGANIZATION REPORT NUMBER	
9. SPONSORING /MONITORING AGENCY NAME(S) AND ADDRESS(ES) N/A		10. SPONSORING/MONITORING AGENCY REPORT NUMBER	

11. SUPPLEMENTARY NOTES The views expressed in this thesis are those of the author and do not reflect the official policy or position of the Department of Defense or the U.S. Government.

12a. DISTRIBUTION / AVAILABILITY STATEMENT Approved for public release; distribution is unlimited.	12b. DISTRIBUTION CODE

13. ABSTRACT *(maximum 200 words)*

In this thesis, underwater acoustic communications signal processing techniques, which are used to equalize the distortional effects associated with the ocean as a communications channel, are investigated for a shallow water ocean environment. The majority of current signal processing techniques employ a Finite Impulse Response (FIR) filter. Three equalization filters were investigated and presented as alternatives; they were the passive time-reversed filter, the inverse filter, and the Infinite Impulse Response (IIR) filter. The main advantage of the passive time-reversed filter and the inverse filter is simplicity of design. Bit error rates for the time-reversed filter were consistently around 10^{-1} and those for the inverse filter were greater than 10^{-1}. However, inability of the passive time-reversed filter to completely eliminate multipath components and the ill-conditioned nature of the inverse filter made it difficult to achieve Probability of Error results below 10^{-1}. Research into the development of an array receiver using a time-reversed filter should improve calculated bit error rates. Simulations of the IIR filter were conducted with limited success. The main advantage of an IIR filter is that fewer parameters are required in the design of the filter. However, the potential for instability in the filter is a significant limitation. Probability of Error results were found to be on the order of those for current FIR filters at close ranges. Unfortunately, instability issues arose for receivers as range from the source increased. This research on the IIR filter is still in the embryonic stage, whereas research using FIR filters is relatively highly developed. Further research is needed to address the issue of instability in IIR filters in order to make them an effective signal processing technique employable in underwater acoustic communications.

14. SUBJECT TERMS Underwater Acoustic Communications, Infinite Impulse Response Filter, Inverse Filter, Passive time-reversed FIlter			15. NUMBER OF PAGES 169
			16. PRICE CODE
17. SECURITY CLASSIFICATION OF REPORT Unclassified	18. SECURITY CLASSIFICATION OF THIS PAGE Unclassified	19. SECURITY CLASSIFICATION OF ABSTRACT Unclassified	20. LIMITATION OF ABSTRACT UL

THIS PAGE INTENTIONALLY LEFT BLANK

**COMPARISON OF CHANNEL EQUALIZATION FILTERING TECHNIQUES
IN UNDERWATER ACOUSTIC COMMUNICATIONS**

Ryan J. Kuchler
Lieutenant, United States Navy
B.S., United States Naval Academy, 1993

Submitted in partial fulfillment of the
requirements for the degree of

MASTER OF SCIENCE IN ELECTRICAL ENGINEERING

from the

**NAVAL POSTGRADUATE SCHOOL
June 2002**

Author: Ryan J. Kuchler

Approved by: Charles W. Therrien
                 Thesis Advisor

                 Kevin B. Smith
                 Co-Advisor

                 Jeffrey B. Knorr
                 Chairman, Department of Electrical and Computer Engineering

THIS PAGE INTENTIONALLY LEFT BLANK

ABSTRACT

In this thesis, underwater acoustic communications signal processing techniques, which are used to equalize the distortional effects associated with the ocean as a communications channel, are investigated for a shallow water ocean environment. The majority of current signal processing techniques employ a Finite Impulse Response (FIR) filter. Three equalization filters were investigated and presented as alternatives; they were the passive time-reversed filter, the inverse filter, and the Infinite Impulse Response (IIR) filter. The main advantage of the passive time-reversed filter and the inverse filter is simplicity of design. Bit error rates for the time-reversed filter were consistently around 10^{-1} and those for the inverse filter were greater than 10^{-1}. However, inability of the passive time-reversed filter to completely eliminate multipath components and the ill-conditioned nature of the inverse filter made it difficult to achieve Probability of Error results below 10^{-1}. Research into the development of an array receiver using a time-reversed filter should improve calculated bit error rates. Simulations of the IIR filter were conducted with limited success. The main advantage of an IIR filter is that fewer parameters are required in the design of the filter. However, the potential for instability in the filter is a significant limitation. Probability of Error results were found to be on the order of those for current FIR filters at close ranges. Unfortunately, instability issues arose for receivers as range from the source increased. This research on the IIR filter is still in the embryonic stage, whereas research using FIR filters is relatively highly developed. Further research is needed to address the issue of instability in IIR filters in order to make them an effective signal processing technique employable in underwater acoustic communications.

THIS PAGE INTENTIONALLY LEFT BLANK

TABLE OF CONTENTS

LIST OF FIGURES

LIST OF TABLES

THIS PAGE INTENTIONALLY LEFT BLANK

ACKNOWLEDGMENTS

THIS PAGE INTENTIONALLY LEFT BLANK

EXECUTIVE SUMMARY

With the state of communications technology available today, the Department of Defense and the U. S. Navy are focused on improving information collection, synthesis and dissemination throughout the battlespace. The concept of Network Centric Warfare relies on the merging of many information sources on land, in the air, on the sea, and under the sea. In support of integrating submerged assets into the overall concept of Network Centric Warfare, much research is being conducted in the field of underwater acoustic communications.

Since the majority of military naval operations occur in waters in the littoral regions of the world, there are multiple obstacles to the development of an efficient underwater acoustic communications system. The shallow water channel characteristics of littoral regions pose many problems. The most significant adverse affects to underwater acoustic communications in these regions are ambient noise and multipath arrivals, which can cause fading and intersymbol interference (ISI). Many techniques exist which try to mitigate the affects of the shallow water channel either through modulation schemes or equalization through signal filtering. This thesis focused on some additional signal processing methods to mitigate the shallow water channel effects.

Currently, the majority of research on signal processing techniques to improve underwater acoustic communications focuses on the use of adaptive forms of Finite Impulse Response (FIR) filters. Though the research has produced useful results, FIR filters have the disadvantage of complex design and large memory requirements. Alternatives to the FIR filter are presented in this thesis. These alternatives are the passive time-reversed filter, the inverse filter, and the Infinite Impulse Response (IIR) filter; these filters were analyzed to determine their effectiveness in underwater acoustic communications. The advantage of these filters is simplicity of design. However they each have their own disadvantages. Specifically, the passive time-reversed filter can minimize but never eliminate multipath returns, the inverse filter is known to be ill-conditioned, and the IIR filter can potentially have stability issues.

The objective of this thesis was to determine the suitability of the three filters as signal processing techniques for underwater acoustic communications. By simulating selected receiver locations with bit rates ranging from about 10,000 bits per second to 30,000 bits per second, it was possible to evaluate and make comparisons among the effectiveness of each of the filters. The simulations produced mixed results ranging from poor performance to some limited success (bit error rates below 10^{-2}). Overall, the inverse filter performed poorly because of its ill-conditioned behavior. The passive time-reversed filter was limited in its ability to equalize the channel and produce bit error rates below 10^{-1}, however it consistently produced bit error rates around 10^{-1}. The IIR filter was successful in producing bit error rates below 10^{-1}, but still on a limited basis. Stability proved to be a significant issue, along with the complete removal of multipath structures. In the cases where the IIR filter was stable and able to remove all the multipath returns, the IIR filter produced bit error rates below 10^{-2}, and in some instances down to 10^{-4}.

The results of this thesis were based on a single point receiver (single hydrophone) whereas most of the results reported in the literature on time-reversal use an array to provide focusing in space as well as time and significantly improve performance. Therefore the results reported in this thesis are not discouraging. These results suggest that the time-reversed filter and the IIR filter might be viable methods for equalizing the ocean channel and removing multipath structures. Further investigation and development of these approaches may prove fruitful in the development of a useful ocean channel equalization method.

I. INTRODUCTION

A. A BRIEF HISTORY OF U. S. NAVAL UNDERWATER ACOUSTIC COMMUNICATIONS

Since the 1940s, the United States Navy has been using underwater acoustic communications to communicate to and from underwater vehicles. Typical platforms carrying underwater acoustic communications systems are submarines, surface ships, deep submergence recovery vehicles (DSRV's) and a small number of shore facilities. The original communications systems operated in the 8-12 kHz band and were used solely for voice transmissions [Ref. 1].

Throughout the Twentieth Century technological developments allowed improvements in underwater acoustic communications. However, the improvements utilized by the U.S. Navy still centered on voice communications only. Some of these improvements came in the form of lower frequency bands which provided better range performance [Ref. 1]. It was not until the late 1970's that reliable digital communications began to be developed [Ref. 2].

Over the past two decades, rapid technological developments in digital communications have shifted the world to a computer-network-based information and electronics culture. In response, the Department of Defense (DoD) and the Navy have developed two key doctrines that, in part, are designed to incorporate the new information technology. The DoD doctrine is called Network Centric Warfare, while the corresponding Navy doctrine is known as *Forward, From the Sea*. [Ref. 1] DoD's Network Centric Warfare posits that "networks can help the military achieve informational dominance, leading to: speed of command, and ability to organize from the bottom up." [Ref. 1] In *Forward, From the Sea*, the Navy envisions expanding missions for the submarine force "which require effective communication while the submarine is submerged at speed and depth." [Ref. 1]

The implication of these doctrines is that the DoD and the U.S. Navy, in particular, need to develop advanced underwater acoustic communications systems that can transmit to, and receive from, undersea platforms while operating at speed and depth.

The types of data to be transmitted are extensive. They range from command and control, and telemetry data of Unmanned Undersea Vehicles (UUV's) to battlespace information and intelligence in the form of images, video, and text. [Ref. 3]

With large amounts of information required successfully to complete the desired missions, there is much interest in maximizing data rate and bandwidth efficiency. Since the majority of military applications for underwater acoustic communications occurs in the littoral regions, complex conditions adverse to reliable communications exist that limit the ability to design simple systems that achieve the desired military specifications. Therefore, there is much interest in the U.S. Navy to develop advanced signal processing algorithms and methods to counter the adverse effects of the ocean environment.

B. SOME NEGATIVE EFFECTS OF THE OCEAN ENVIRONMENT ON UNDERWATER ACOUSTIC COMMUNICATIONS

The ocean environment presents several obstacles to reliable underwater acoustic communications. Among the most troublesome are ambient noise and multipath. There are two possible effects of multipath; fading and intersymbol interference (ISI). It is these obstacles that make designing an underwater acoustic communications system challenging. [Ref. 4, 5]

Ambient noise poses a problem to underwater acoustic communications by potentially masking a signal. The sources for ambient noise can be categorized into two groups - natural noise and man-made noise. While both noise groups degrade the ability of communications systems to receive an intelligible signal, they each have their own characteristics. Natural noise consists of marine life, surface noise due to sea state, wind, and wave height, as well as noise from terrestrial sources like earthquakes. Natural noise mainly affects the frequency spectrum below 10 Hz and above 300 Hz. Man-made noise is typically derived from shipping noise and oil rigs. In the littoral regions there is also potential for shoreline industrial facilities to create ambient noise. The majority of man-made noise is found between 10 and 300 Hz. [Ref. 6]

There are several methods available for minimizing the effects of ambient noise. All the methods, however, attempt to achieve one goal – to increase the signal-to-noise

ratio (SNR), or the ratio of the received signal power to the received noise power. The simplest method is to transmit the signal with enough power to ensure that the SNR is high at the intended receiver. However, this method reduces covertness and requires significantly increasing power as the noise level increases. Other methods available take advantage of the nature of the ambient noise. For example, omni-directional noise can be reduced by using a directional receiver, or array, and directional noise can be reduced by avoiding pointing the receiver in the direction of the noise. [Ref. 6]

Multipath is a significant problem in underwater acoustic communications in general, but most particularly in littoral regions because of the shallow channel nature of the ocean. Multipath distortion occurs when a single transmitted signal reflects off either the ocean surface or the ocean bottom and takes multiple paths to the intended receiver, arriving as multiple signals. Depending on the strength of the transmitted signal, reflected signals could be received as a series of discrete arrivals over time at a particular range. When the multiple signals from the same transmitted signal arrive at the intended receiver close enough together in time that their phases destructively interfere with each, thus reducing the energy of the original signal, the multipath phenomenon is referred to as fading. When the reflected signals arrive at the intended receiver sufficiently separated in time, there is potential that the signals will overlay different data on each other. When a reflected signal arrives at the intended receiver at the same time as a subsequently transmitted signal, then the multipath phenomenon is called intersymbol interference (ISI). Intersymbol interference is a significant problem for underwater acoustic communications because often the multipath arrivals can span a large amount of time relative to the data rate, thus overlapping many symbols and severely distorting the communications signals [Ref. 4, 5]

Fading and intersymbol interference are more difficult to overcome than ambient noise. The effects of fading can be compensated for by communications systems if frequency or spatial diversity techniques are employed. To mitigate intersymbol interference, complex signal processing algorithms and communications techniques are required. Much research is dedicated to equalizing the effects of intersymbol interference, since that can potentially lead to higher data rates.

C. CURRENT RESEARCH IN UNDERWATER COMMUNICATIONS

In support of the Navy's goal of improving underwater acoustic communications, the Office of Naval Research (ONR) is sponsoring Science & Technology initiatives in the area of underwater acoustic communications. The goal of many of these projects is the "development of new signaling schemes and signal processing algorithms." [Ref. 1] Aside from Navy sponsored research, private organizations and universities are conducting research into underwater acoustic communications as well, focusing on modulation schemes or equalization methods. [Ref. 5, 7, 8, 9, 10, 11, 12, 13, 14, 15]

As summarized by Kilfoyle and Baggeroer, the modulation schemes that are being employed use both coherent and non-coherent detection. In coherent detection, the typical modulation schemes currently investigated in research are Phase Shift Keying (PSK) and Quadrature Amplitude Modulation (QAM). More specifically, they are Binary PSK (BPSK), Quadrature PSK (QPSK) and 8PSK, as well as 8QAM and 16QAM. In the non-coherent modulation schemes, Differential Phase Shift Keying (DPSK) and M-ary Frequency Shift Keying (MFSK) are being tested. [Ref. 1, 2]

Researchers who are focusing on equalization methods are improving old methods as well as developing new techniques. The majority of current research centers on ways to equalize adaptively the ocean channel using Least Mean Squares (LMS) and Recursive Least Squares (RLS) algorithms. These algorithms range in application from single-channel adaptive equalization [Ref. 13] to multi-channel adaptive equalization [Ref. 12, 15], and from Decision Feedback Equalization (DFE) [Ref. 14] to Block Decision Feedback Equalization (Block-DFE) [Ref. 16]. Newer methods of equalization are also being researched. These methods include Spread Spectrum Communications [Ref. 4] and Spatial Filtering using an adaptive beamformer [Ref. 17].

Results of much of the research have been tabulated by Kilfoyle and Baggeroer [Ref. 2] and are reproduced in Table 1. Particulars of the research conducted by the principal investigators in Table 1 can be found in [Ref. 5, 9, 18, 19, 20, 21]. From this table it can be seen that bit error rates below 10^{-2}, and in some research below 10^{-4}, are achievable. These results are also reflected in the threshold and objective in-water exit

criteria of the Navy's Undersea Search and Survey and Communications/Navigation Aid Demonstration Broad Area Anouncement (BAA) Informational Paper. The threshold bit error rate criteria is 10^{-2}, and the objective bit error rate is 10^{-4} [Ref. 22].

Table 1.   Some Completely Coherent Telemetry Systems. After [Ref. 2]

Principal Investigator	Modulation Method	Data Rate (kbps)	Bandwidth / Carrier Frequency (kHz)	Range[a] (km)	Prob. of Error[b]
Stojanovic (1993, 1994)	4, 8PSK 8QAM	$0.6 - 3.0$	$0.3 - 1.0$ /10	$89 - 203$ $_{S,D}$	$<10^{-2}$
Goalic (1994)	QPSK	6	3 / 60	0.04 $_S$	N/A
Tarbit (1994)	BPSK	20	20 / 50	0.9 $_S$	$\sim10^{-3}$
Jarvis (1995)	B, QPSK	$1.1 - 2.2$	$0.6 - 2.2$ / N/A	$0.5 - 8.0$ $_{S,D}$	$<10^{-3}$
Jarvis (1997)	N/A	$0.9 - 1.8$	N/A / N/A	4.0 $_S$, 8.0 $_D$	$<10^{-4}$

[a] Ranges with an "S" subscript indicate a shallow-water result, while a "D" subscript indicates a deep-water or line-of-sight result.

[b] Error probabilities are typical values reported by the authors.

D.   THESIS OBJECTIVES

The goal of most of the research in underwater acoustic communications signal processing is to equalize, or 'undo', the spreading and multipath effects caused by the shallow water ocean channel. As discussed in the previous paragraphs, there are many techniques available to achieve the goal of equalizing the ocean channel. The purpose of this thesis is to study and compare the feasibility of using a passive time-reversed filter, inverse filter or an Infinite Impulse Response (IIR) filter to enhance the reliability of underwater acoustic communications, as an alternative to the more common Finite Impulse Response (FIR) filter. The advantage of these filters is simplicity of design. In addition, an IIR filter requires fewer parameters than a FIR filter to design [Ref. 23]. However, potential instability issues can arise due to the feedback paths that make up an IIR filter.

E.   THESIS OUTLINE

Following this introductory chapter, the remainder of this thesis is organized into three chapters. Chapter II presents some of the theory and methods that are used in recovering underwater acoustic signals and describes some of the basic filter methods available. Chapter III describes the actual methods implemented in this study and presents the results of the computer simulations tests of these methods. And finally, Chapter IV presents conclusions based on this research project and provides suggestions for future research.

II.   SIGNAL PROCESSING METHODS AND ALGORITHMS

A.   PROBLEM STATEMENT

In any communications system, there is a transfer of data or information from a sender to a receiver through a channel. The objective of communications is the transmission of specific data or information from a transmitter through a channel to a receiver in a way that reproduces the original data or information with fidelity. Though this is a simple concept, it can be a very difficult task to accomplish because of the inevitable interference (noise) and distortion of the signal caused by the channel through which the signal is transmitted. Depending on the type of channel, this distortion can have either a major or a minor effect on the signal. In underwater acoustic communications, the ocean is the transmission channel and it greatly distorts the transmitted signal. Therefore, for any underwater communications system to be effective, it must be able to overcome the significant distortional effects of the ocean channel.

There are many methods for countering the distortional effects of a transmission channel. Each method is highly dependent on the individual requirements or needs of the communications system. Broad methods include proper selection of data rate, modulation scheme, or signal processing techniques. This thesis focuses on equalization through signal processing techniques to eliminate the distortional effects of the ocean.

B.   EQUALIZATION

The crux of the signal processing techniques is to undo or reverse the distortional effects of the ocean environment. This approach, known as equalization, can be implemented through pre-processing of the signal at the transmitter, post-processing of the signal at the receiver, or a combination of both.

However the communications system is designed, the processing technique must be able to equalize adequately the distortional effects of the transmission channel. If designed properly, the output of the receiver will approximate the original transmitted signal. To successfully reproduce the transmitted signal, the combined effect of the

7

ocean impulse response and the receiver filter should approximate a delta function. The closer this approximation, the more effective is the communications system at equalizing the effects of the transmission channel and recovering the transmitted signal (see Figure 1).
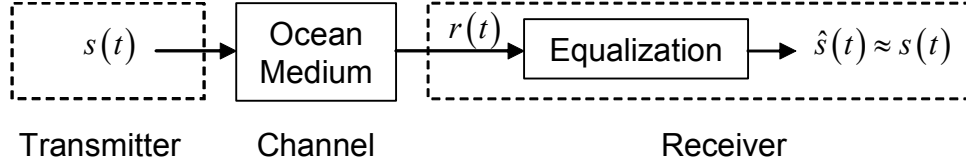

Figure 1.   Channel Equalization

If the equalization filter were ideal, then the result of filtering the ocean impulse response would be a delta function. This can be seen mathematically as follows. Let $h(t)$ denote the ocean impulse response. Then the signal arriving at the receiver is given by

$$r(t) = s(t) * h(t) \qquad \text{(II.1)}$$

where the $*$ denotes linear convolution, i.e.,

$$r(t) = \int_{-\infty}^{\infty} s(\tau) h(t-\tau) d\tau = \int_{-\infty}^{\infty} s(t-\tau) h(\tau) d\tau .$$

If the equalization filter has an impulse response $\hat{h}(t)$, then the output of the filter is given by

$$\hat{s}(t) = r(t) * \hat{h}(t) = s(t) * h(t) * \hat{h}(t) . \qquad \text{(II.2)}$$

Denote the convolution of $h(t)$ and $\hat{h}(t)$ by $g(t)$. In the ideal situation

$$g(t) = h(t) * \hat{h}(t) = \delta(t) \qquad \text{(II.3)}$$

so Equation (II.2) becomes

$$\hat{s}(t) = s(t) * \delta(t) = s(t) . \qquad \text{(II.4)}$$

8

Since it is not possible to design an ideal processor, signal processing algorithms and methods are continuously sought to improve the processor's ability to equalize the ocean's effects. Three filters that are used in this thesis are presented here. Since all three filters are intended for implementation using digital signal processing (DSP), discrete-time equations are used, rather than continuous-time equations.

1.   Passive Time-reversed Filter

As the name suggests, the passive time-reversed filter, $\hat{h}[n]$, is derived by simply reversing the ocean impulse response in time. In this case, the passive time-approach applies a matched filter repeatedly at a receiver, in contrast to the active approach that physically re-transmits a time-reversed signal from the receiver location [Ref. 24]. If $h[n]$ denotes the ocean impulse response, then

$$\hat{h}[n] = h[N-n], \quad 0 \le n \le N.$$
(II.5)

The result of processing the ocean impulse response with the passive time-reversed filter is thus

$$g[n] = h[n] * \hat{h}[n] = \sum_{k=0}^{2N-1} \hat{h}[k] h[n-k] = \sum_{k=0}^{2N-1} h[N-k] h[n-k]$$
(II.6)

where the convolution operation $(*)$ is now represented in discrete time. By performing a variable substitution, where $l = N - k$, Equation (II.6) can be re-written as

$$g[n] = \sum_{l=0}^{2N-1} h[l] h[n-(N-l)] = \sum_{l=0}^{2N-1} h[l] h[n-N+l].$$
(II.7)

This operation can be recognized as correlation and written as

$$g[n] = h[n] \diamond h[n-N]$$
(II.8)

where $(\diamond)$ denotes the correlation operator.

The motivation for choosing $\hat{h}[n]$ as the reversed ocean impulse response is that $g[n]$ will hopefully be a good approximation to an impulse. In fact, as the ocean

9

impulse response becomes more complicated due to environmental factors, $g[n]$ tends to become more impulse-like in character. Thus time-reversal is well-motivated and is quite simple to implement.

2. Frequency Inverse Filter

One method of equalization analyzed in this thesis is a frequency inverse filter. As the name implies, this filter is designed by taking the reciprocal values of each component of the frequency spectrum of the ocean impulse and calculating the time response. The filter's effect is to normalize all the ocean response frequency components to unity. By doing so, the filtered ocean time response should be ideally a delta function and the signal received would be identical to the signal transmitted.

If the frequency response of the ocean is denoted by

$$H(f) = |H(f)| e^{j\phi(f)}, \quad -\frac{f_s}{2} < f < \frac{f_s}{2}, \quad (II.9)$$

where $|H(f)|$ is the magnitude of $H(f)$, $\phi(f)$ is the phase of $H(f)$, and f_s is the sampling frequency, then the inverse filter is defined by

$$\hat{H}(f) = H^{-1}(f) = \frac{1}{|H(f)|} e^{-j\phi(f)}, \quad -\frac{f_s}{2} < f < \frac{f_s}{2}. \quad (II.10)$$

The result of processing by the ideal inverse filter is thus

$$G(f) = H(f)\hat{H}(f) = 1, \quad -\frac{f_s}{2} < f < \frac{f_s}{2}, \quad (II.11)$$

which corresponds to the result of Equation (II.3), in the time domain.

In a practical implementation of the inverse filter, the receiver would sample the ocean impulse response in the time domain. Therefore, in order to design the frequency inverse filter, the frequency spectrum of the ocean must first be determined by taking the Discrete Fourier Transform (DFT) of the sampled ocean impulse response sequence. The frequency response of the filter is defined to be the reciprocal of the spectrum of the

impulse response at each discrete frequency. The filter is brought back to the time domain using an inverse DFT.

3. Infinite Impulse Response (IIR) Filter

Infinite Impulse Response (IIR) and Finite Impulse Response (FIR) filters are derived from the general form of the difference equation

$$y[n] = a_1 y[n-1] + a_2 y[n-2] + \ldots + a_P y[n-P] + b_0 x[n] + \ldots + b_Q x[n-Q] \quad \text{(II.12)}$$

where $y[n]$ is the filter output and $x[n]$ is the filter input. If all the coefficients, a_i, are zero, the filter is a FIR filter; the impulse response is a finite-length sequence with values $\{b_0, \ldots, b_Q\}$. If any of the a_i are not equal to zero, the impulse response will be infinite in length and the filter is an IIR filter. Because the output $y[n]$ in Equation (II.12) is expressed in terms of previous values of the output, an IIR filter is sometimes referred to as a *recursive* filter.

As a simple example of an IIR filter, consider

$$y[n] = a y[n-1] + x[n] \quad \text{(II.13)}$$

By taking $x[n] = \delta[n]$ and evaluating this equation recursively, the impulse response can be shown to be

$$h[n] = a^n u[n] \quad \text{(II.14)}$$

where $u[n]$ is the unit step function. This filter possesses a single parameter, but has an infinite length impulse response.

The use of an IIR filter has several advantages over using an FIR filter, as well as some disadvantages. A key advantage is that, in general, fewer parameters are required to design the filter. In addition, with respect to computer implementation, an IIR filter may require considerably less computation and storage. Stability issues and phase distortion are two drawbacks to an IIR filter, however. Due to the lack of feedback terms in the FIR filter, the FIR filter possesses only zeros. This guarantees stability. Also, FIR

11

filters can be designed to have perfect linear phase. Since, the IIR filter uses feedback paths, it possesses both zeros and poles, and misplaced poles can lead to unstable IIR filter designs. In addition, the phase of an FIR filter is never perfectly linear and this leads to what is referred to as phase distortion. If some phase distortion is not important or tolerable however, then an IIR filter can be the preferable choice. [Ref. 25]

Since for most cases of interest the ocean behaves like a linear system, the received signal, $r[n]$, can be modeled as the weighted sum of past and present values of the transmitted signal, $s[n]$,

$$r[n] = \sum_{k=0}^{N} h[k] s[n-k] \tag{II.15}$$

where the weights $h[k]$ are the terms of the ocean impulse response. (This is simply the convolution of the impulse response $h[n]$ with the input $s[n]$.) The IIR filter can be determined by taking the z-transform of Equation (II.15) and writing the ocean system function in the z-domain as

$$H(z) = \frac{R(z)}{S(z)} = \sum_{k=0}^{N} h[k] z^{-k} . \tag{II.16}$$

The desired IIR filter response to equalize the effect of the ocean is the inverse of $H(z)$, given by

$$\hat{H}(z) = \frac{1}{H(z)} = \frac{1}{\sum_{k=0}^{N} h[k] z^{-k}} = \frac{\hat{S}(z)}{R(z)} . \tag{II.17}$$

With some manipulation Equation (II.17) can be rewritten as

$$\hat{S}(z) = \frac{R(z) - \sum_{k=1}^{N} h[k] z^{-k} \hat{S}(z)}{h[0]} . \tag{II.18}$$

This corresponds in the time domain to the equation

$$\hat{s}[n] = \frac{r[n] - \sum_{k=1}^{N} h[k]\hat{s}[n-k]}{h[0]} \tag{II.19}$$

which is the difference equation for an IIR filter.

An important aspect of our consideration of the IIR filter is that it may be able to be designed using just a few significant terms. This aspect leads to a faster and more simply implemented filter. This point is illustrated further in Chapter III section B subsection 3.

C. THEORETICAL MODEL FOR UNDERWATER ACOUSTIC COMMUNICATIONS

This section describes the basic procedures required to properly transmit and receive underwater acoustic communications. Figure 2 is a simplified block diagram of an underwater acoustic communications system.
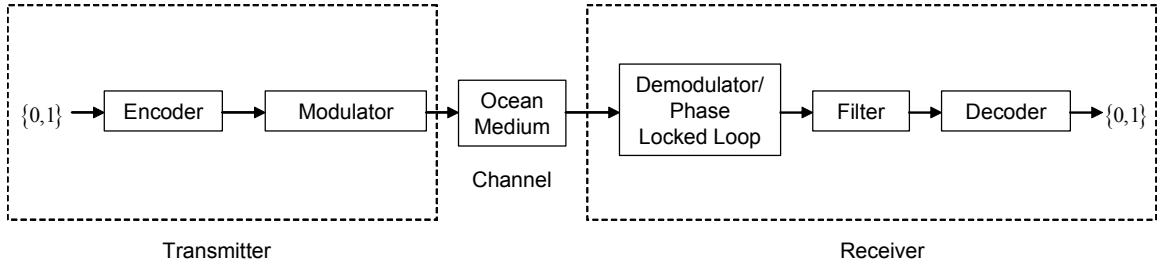
Figure 2. Underwater Acoustic Communications System

1. Signal Generation and Transmission

To transmit a binary sequence of data, the information must first be converted to a usable analog signal. This is done by converting the data to an analog signal via a Digital to Analog Converter (DAC), and then modulating the information signal onto a carrier signal. Many varieties of modulating techniques exist, but for this thesis a Binary Phase Shift Key (BPSK) modulation technique was chosen. The data signal is of the form

$$s(t) = \sqrt{2}d(t)\cos(2\pi f_c t) \tag{II.20}$$

13

where f_c is the carrier frequency and the variable $d(t)$ represents the data message to be transmitted. In BPSK, the signal has only two states and the two states are represented by the phase of the carrier (0 or π radians). This can be represented equivalently however as an amplitude modulation of ± 1. If the ith data bit, d_i, is a binary '1' then $d(t)$ is set equal to 1 for the bit period. Otherwise, if d_i is a binary '0', then $d(t)$ is equal to -1 for the bit period. In the physical sense, $d(t)$ represents a voltage amplitude that is used by the transmission system to generate the analog signal. The equation is scaled by a factor of $\sqrt{2}$ to simplify the mathematical calculations.

Once the signal is electrically generated, the signal must be transmitted through the communication channel to the receiver. In underwater acoustic communications, the signal is transmitted by imposing pressure variations on the ocean. These pressure variations (sound or ultrasound) then propagate through the ocean and are detected by the receiver. In order for the transmitter and receiver to send and detect the pressure changes, transducers must be used. Transducers convert electrical voltage signals to proportional pressure signals and vice versa, through the use of piezoelectric or ferroelectric materials [Ref. 26, 27]. Figure 3 shows a block diagram of a typical BPSK transmitter with the transducer (XDCR).
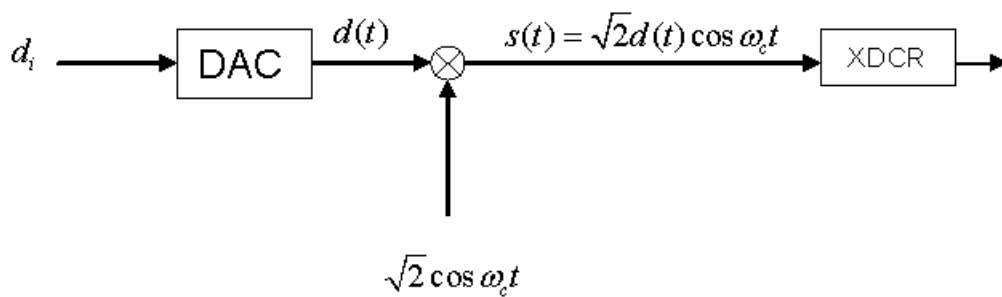
Figure 3.   BPSK Transmitter

2. Signal Reception and Demodulation

Since the ocean can be modeled as a linear system, the signal detected at the receiver, $r(t)$, is the result of convolving the input signal, $s(t)$, with the ocean impulse response, $h(t)$

$$r(t) = s(t) * h(t) = \int_{-\infty}^{\infty} h(\tau) s(t - \tau) d\tau .$$ (II.21)

This convolution is in reality an analog operation as shown here, although it has previously been represented as a discrete-time operation when discussing the equalization filtering.

After the acoustic signal is received and converted to an electrical signal by the transducer, the data must be extracted. Since the received signal consists of a baseband information signal, $r_{bb}(t)$, on a sinusoidal carrier signal

$$r(t) = r_{bb}(t) \cos(2\pi f_c t) ,$$ (II.22)

the baseband information is extracted by demodulation. The most common method of demodulating a signal is by heterodyning the signal with a local oscillator. The local oscillator generates a sinusoidal signal at the designed carrier frequency of the form, $2\cos(2\pi f_c t)$. This signal is then multiplied with the received signal producing the demodulated signal, $x(t)$, [Ref. 28]

$$x(t) = r(t) \cdot 2\cos(2\pi f_c t) = r_{bb}(t) \cdot 2\cos^2(2\pi f_c t) .$$ (II.23)

By using trigonometric properties of the cosine, Equation (II.23) can be rewritten as a function of two terms,

$$x(t) = r_{bb}(t) \cdot \left(1 + \cos(2\pi(2f_c)t)\right) = r_{bb}(t) + r_{bb}(t) \cos(2\pi(2f_c)t) .$$ (II.24)

The first of these terms is the baseband signal, or envelope, while the other term is the baseband signal modulated at twice the original modulation frequency. The signal at twice the original modulation frequency is removed by low-pass filtering the heterodyned

signal. The resultant signal is the demodulated baseband signal, $x_{bb}(t)$, which is the received envelope, [Ref. 28]

$$x_{bb}(t) = r_{bb}(t).$$ (II.25)

This envelope (which ideally in the absence of noise takes on values of ± 1) represents the received data.

For proper reception of a BPSK signal, the receiver local oscillator must be phase synchronized, or "coherent," with the transmitter. To synchronize the receiver local oscillator, some version of a Phase Locked Loop (PLL) circuit is generally employed in modern communications systems. This circuit detects the phase of the incoming signal, and synchronizes the receiver by minimizing the phase error between the signal and receiver. Any error between the two phases alters the frequency of the voltage controlled oscillator (VCO) until the phase error is zero. Many variations of a PLL exist, and are each useful depending on the specific application. Figure 4 shows an example of the Costas PLL. It should be noted that demodulation of the incoming circuit occurs within the PLL circuitry, so a separate demodulator is not necessary. [Ref. 28]
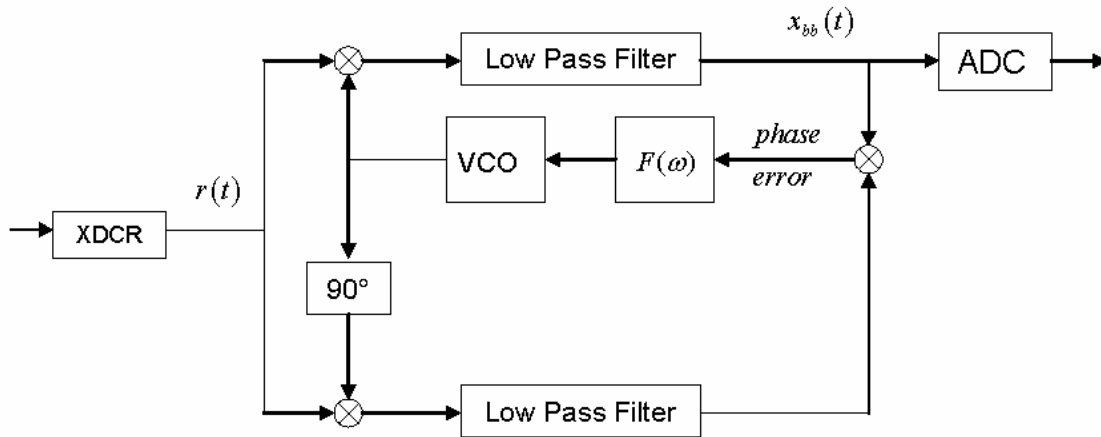
Figure 4.   Costas Phase Locked Loop Circuit

After the signal has been demodulated, it can be sampled and converted to a digital sequence for processing using an Analog to Digital Converter (ADC). Given a sampling frequency, f_s, in Hertz, the generated digital sequence is the analog signal sampled at every T_s seconds, where $T_s = \dfrac{1}{f_s}$:

$$x_{bb}[n] = x_{bb}(t)\big|_{t=nT_s} = x_{bb}(nT_s). \tag{II.26}$$

Since digital sampling of a signal causes the frequency spectrum to be repeated periodically at the sampling frequency, f_s, an undersampled signal can cause spectral overlap in the frequency band of interest. This effect, known as aliasing, produces distortion and more errors in the decoding. To ensure proper recovery of the signal, the sampling frequency must be sufficiently fast enough to generate a digital sequence that uniquely describes the analog signal in the frequency bandwidth of interest. If f_{max} is the maximum frequency of interest in the communications system, then the minimum sampling frequency to achieve uniqueness is twice the maximum frequency of interest, $f_s \geq 2f_{max}$.

Since the output signal of the ADC is a digital sequence, all follow-on filtering and manipulations of the data signal can be performed by a computer with a Digital Signal Processing (DSP) chip. Depending on the type of filter utilized, the demodulated signal can be filtered either recursively, or by convolution with the filter time response, or by using Fast Fourier Transform (FFT) techniques. Factors contributing to the filter method can include the length of the filter sequence, the length of the transmitted signal, and the computational power of the computer and complexity of the filter algorithm.

Once the signal has been filtered, the data can be decoded using a correlator and detector. For the BPSK signal, a basic correlator is the integrator. The integrator sums up the signal amplitude at each sampling point, over one bit period, and then samples the value at the end of the bit period. If the sampled value is greater than zero then the system assigns a value of 1 to the data point; otherwise the detector assigns a value of 0. An error occurs if the detector assigns a 1 when the original signal data point was a 0, and vice versa. The detector can be developed from a statistical point of view and is optimal

for a signal in Gaussian white noise [Ref. 29]. For the integrator and detector to function properly, they must be synchronized with the start of the bit period, otherwise the integrator and detector will sum up values belonging to two different bits and errors will increase. This can be accomplished by using a symbol timing recovery circuit.

D.   SIMULATION METHOD

In simulating the acoustic communications system, two programs were used. The first was the Monterey-Miami Parabolic Equation (MMPE) program, and the second was a simulation written in MATLAB. The MMPE program generates the frequency response data for ocean environments, while the MATLAB programs use the data generated by MMPE to simulate a communications system. An inherent shortcoming of any computer simulation is that everything is processed with discrete signals, or sequences. The transmitted signal and the ocean impulse response are in reality analog signals. Once the received signal is sampled, however, the simulation reflects how the computer would be able to handle and process all the data.

1.   Monterey Miami Parabolic Equation (MMPE) Program

The Monterey-Miami Parabolic Equation (MMPE) program is used to generate frequency responses of an ocean environment. This program is "a broadband, full-wave acoustic propagation model based on the parabolic approximation to the Helmholtz equation." [Ref. 30] Given appropriate input parameters, such as the bathymetry, source location, frequency band of interest, and desired depth and range bands, the program calculates the frequency response using a split-step Fourier parabolic equation algorithm. Details of the program modeling and validation studies can be found in [Ref. 31].

The output of the MMPE program is a binary file that contains the frequency response over the specified positive frequency range of the ocean at the depths and ranges defined by the input parameters.   Since these frequencies are only the positive frequencies in the bandwidth of interest, the calculated time response using the Fast Fourier Transform (FFT) of this data is the baseband complex envelope time signal of the ocean response (see Appendix A).

2. Communications System Simplification

A practical communications system is a complex system with many sub-systems that are needed to ensure proper transmission and reception of a transmitted signal. In order to analyze the capabilities of the different filters of interest, assumptions were made to simplify the programming and complexity of the communications system, and to remove sources of errors that could arise from sub-systems not directly associated with the filtering algorithms.

The first simplification to be made in this model is the removal of the carrier frequency used to modulate the BPSK signal. Since the information being transmitted is a baseband signal before modulation, all calculations can be performed using the baseband components, or complex envelopes, of the signal, ocean medium, and the filters. Appendix A contains a detailed derivation showing that it is sufficient to use only the baseband signals. The baseband signal of the BPSK communications signal is the analog data stream, $d(t)$, as mentioned previously in this chapter. For the ocean environment, the baseband envelope is to be derived from the complex baseband envelope.

As previously mentioned, phase synchronization of the receiver with the transmitter is necessary to properly receive a BPSK transmission. Not only does the receiver's local oscillator phase need to be synchronized, but the symbol timing must be synchronized to ensure the signal is being sampled at the proper time. For simplicity, and to remove potential errors due to tracking errors of the synchronizers, it is assumed that the receiver is both phase synchronized and symbol synchronized with the transmitter.

Assumptions are also used to simplify the complexity of the ocean medium. First it is assumed that the ocean is time-invariant. By applying this assumption, a non-adaptive approach to filtering the signal could be taken. With time-variability of the ocean, it is recognized that it would be necessary to incorporate an adaptive capability into the filtering process to ensure that the filter matches the current ocean condition.

Another assumption made to remove the necessity for an adaptive capability in the filter is that the transmitter and receiver are stationary. With this assumption, Doppler effects are removed, and it is ensured that the ocean medium maintains consistency for evaluation. If the two platforms are moving then the ocean would become variable with time, due to the spatial variability of the ocean, thus negating the assumption that the ocean is time-invariant.

The following list summarize the assumptions and simplifications that have been made in simulating the communications system:

- The ocean medium is time-invariant.
- The transmitter and receiver are stationary.
- The receiver is phase synchronized with the transmitter.
- The receiver's symbol timing is synchronized with the transmitter.
- The baseband equivalent signals are used for the signal, ocean and filter.

III. ALGORITHM TESTING AND RESULTS

A. OCEAN PROFILE

In order to adequately define the ocean environment two categories of parameters are needed. One category is the physical parameters of the ocean, and the other category is the frequency and time parameters for the bandwidth and time interval of interest.

1. Physical Parameters

In defining the physical parameters of the ocean, an appropriate set of spatial dimensions must be specified, as well as the sound speed characteristics of the ocean. Since a short range, shallow water ocean was desired, the depth of the ocean was set at 200 meters, and the range of interest was limited to approximately one kilometer. Also, the transmitter was set at a depth of 100 meters. In modeling the ocean's sound speed profile (SSP), an average SSP based on multiple true ocean sound speed profiles was used, as provided by Professor Kevin Smith of the Naval Postgraduate School. The ocean SSP is shown in Figure 5.
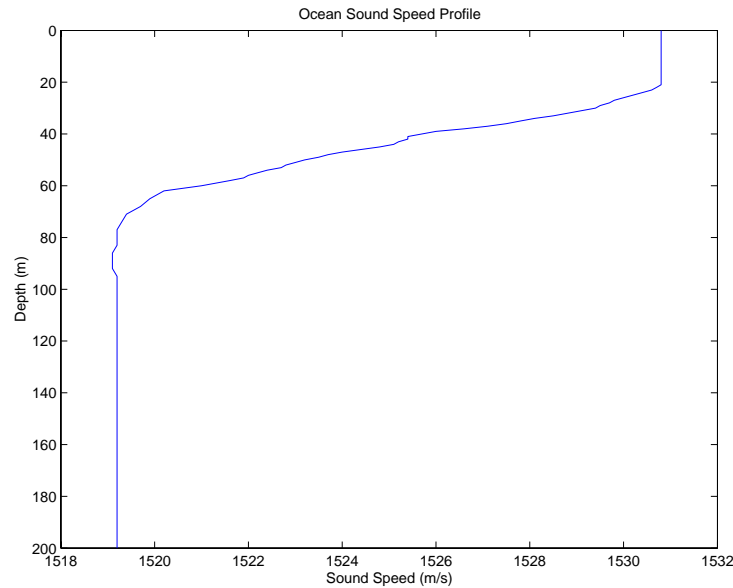
Figure 5.   Ocean Sound Speed Profile for the Experiments

2. Frequency and Time Parameters

For the simulations, a 20,000 Hz frequency bandwidth, B, with a center frequency, f_c, of 50,000 Hz was used. These parameters were based on values used in previous research for comparison, as discussed in Chapter I. In addition, the number of frequencies, n_f, specified to be generated by the MMPE model within the 20,000 Hz bandwidth was 512. By using 512 frequencies the frequency resolution, Δf, was calculated to be

$$\Delta f = \frac{B}{n_f - 1} = \frac{20,000 Hz}{511} = 39.14 Hz .\qquad\text{(III.1)}$$

The frequency resolution directly affects the overall time interval calculated in determining the ocean's impulse response. The overall time period, T_p, of the ocean's impulse response is given by

$$T_p = \frac{1}{\Delta f} = \frac{1}{39.14 Hz} = 0.02555 s .\qquad\text{(III.2)}$$

By zero-padding the frequency response vector produced by the MMPE model, the sampling frequency, f_s, was set to 60,078 Hz. This sampling frequency was needed to ensure a small enough sampling time, T_s, to prevent aliasing of the frequencies in the bandwidth of interest for the maximum bit rate simulated, 30,000 bits per second. A sampling frequency of 60,078 Hz ensured that a bit rate of 30,000 bits per second satisfied the Nyquist criterion. The sampling time was calculated to be

$$T_s = \frac{1}{f_s} = \frac{1}{60,078 Hz} = 16.6 \mu s .\qquad\text{(III.3)}$$

A summary of the physical and frequency and time parameters is listed in Table 2.

Table 2.   Ocean Parameters for the Experiments

Bottom Depth	200 meters
Transmitter Depth	100 meters
Range	0 to 1.05 kilometers
Center Frequency (f_c)	50,000 Hz
Bandwidth (B)	20,000 Hz
Number of Frequencies (n_f)	512
Frequency Resolution (Δf)	39.14 Hz
Sampling Frequency (f_s)	60078 Hz
Time Interval (T_p)	0.02555 seconds
Sampling Time (T_s)	16.6 microseconds

B.   FILTER RESPONSE SIMULATIONS

Prior to performing any bit error rate (BER) simulations, the ocean impulse responses for various locations in the ocean were filtered through the respective inverse filter, passive time-reversed filter, and IIR filter. These simulations were conducted to determine the abilities of the filters to remove any multipath signals for receivers positioned at these locations. The chosen range and depth locations are shown in Table 3. These ranges and depths are not necessarily round numbers because of the algorithms used by the MMPE model.

Table 3.   Ocean Range and Depth Locations

Ranges (kilometers)	0.39; 0.52; 0.65; 0.79; 0.92; 1.05
Depths (meters)	3.1; 50.0; 100.0; 150.0; 196.9

23

By combining the six ranges and the five depths, thirty scenarios were simulated. Each of these scenarios was separated into two categories based on the ocean impulse response. The first category consisted of ocean impulse responses with multipath structures with a short delay between the main return and the first multipath return; the second category had a long delay between the main return and the first multipath return. The first multipath return was considered to have a short delay, if it arrived within 0.005 seconds of the main return. These two categories of multipath were subjectively chosen to see if there was any correlation between the performance of the filter and the time of multipath arrival. Figures 6 and 7 show examples of each type of multipath arrival. The amplitude of the ocean impulse response is a relative amplitude referenced to a zero dB signal.
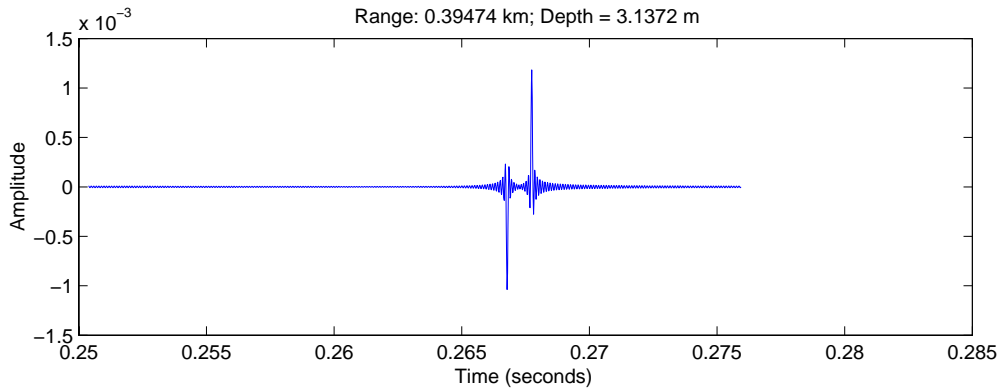
Figure 6.   Ocean Impulse Response for Short Delay Multipath
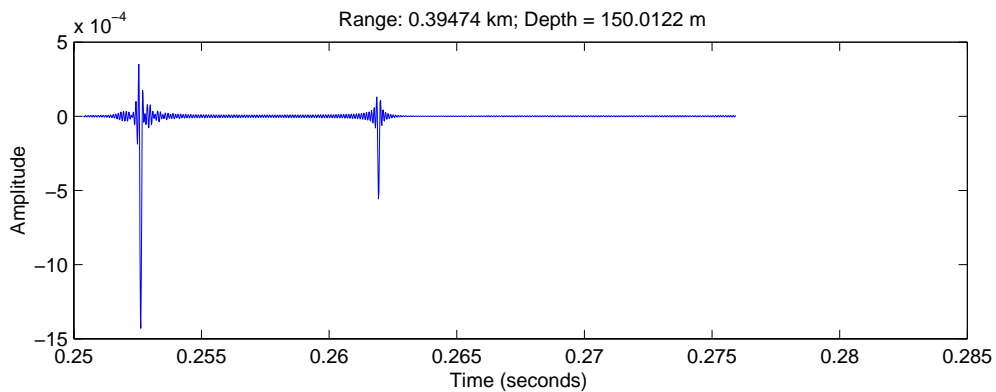
Figure 7.   Ocean Impulse Response for Long Delay Multipath

Of the thirty cases, 20 had multipath structures with a short delay, and 10 had structures with a long delay. Each section of Appendix B contains plots of the ocean impulse responses, along with each filter response.

1.   Passive Time-reversed Filter

Since the passive time-reversed filter is effectively performing an autocorrelation of the ocean impulse response, it was expected that the multipath signals would not be eliminated. However, since the maximum correlation of a signal with itself occurs when the correlation lag is zero, the magnitude of the multipath signals are expected to be reduced, thus emphasizing the main return signal. The ability of the receiver to properly decode the transmitted signal is dependent on how much attenuation the filter provides for multipath signals. Figure 8 shows an example of an ocean impulse response and the effect of the passive time-reversed filter.

Based on the thirty cases, it was determined that the passive time-reversed signal, on average, reduced the magnitude of multipath signals to 0.4 of the main path signal magnitude. The largest reduction in magnitude was 0.2, and occurred at a range of 0.39 kilometers and a depth of 100 meters. Section A of Appendix B contains figures of the passive time-reversed filter responses for all test cases.

2.   Inverse Filter

Theoretically, the inverse filter should have the effect of eliminating the multipath signals, since the output of the filter should ideally be a delta function. However, inverse filtering is known to be an ill-conditioned problem in many instances, since large errors may result from measurement uncertainties and quantization errors [Ref. 32]. By visual inspection of the graphical representations of the thirty scenarios, it was determined that the inverse filter did not consistently and effectively eliminate the multipath signals. Two effects were evident that could have contributed to the poor performance. The first effect was the erratic nature of the time response of the inverse filter. That is, the impulse response of the inverse filter fluctuated rapidly in time. The second effect was the large magnitudes of the filter's time responses with respect to the magnitudes of the actual
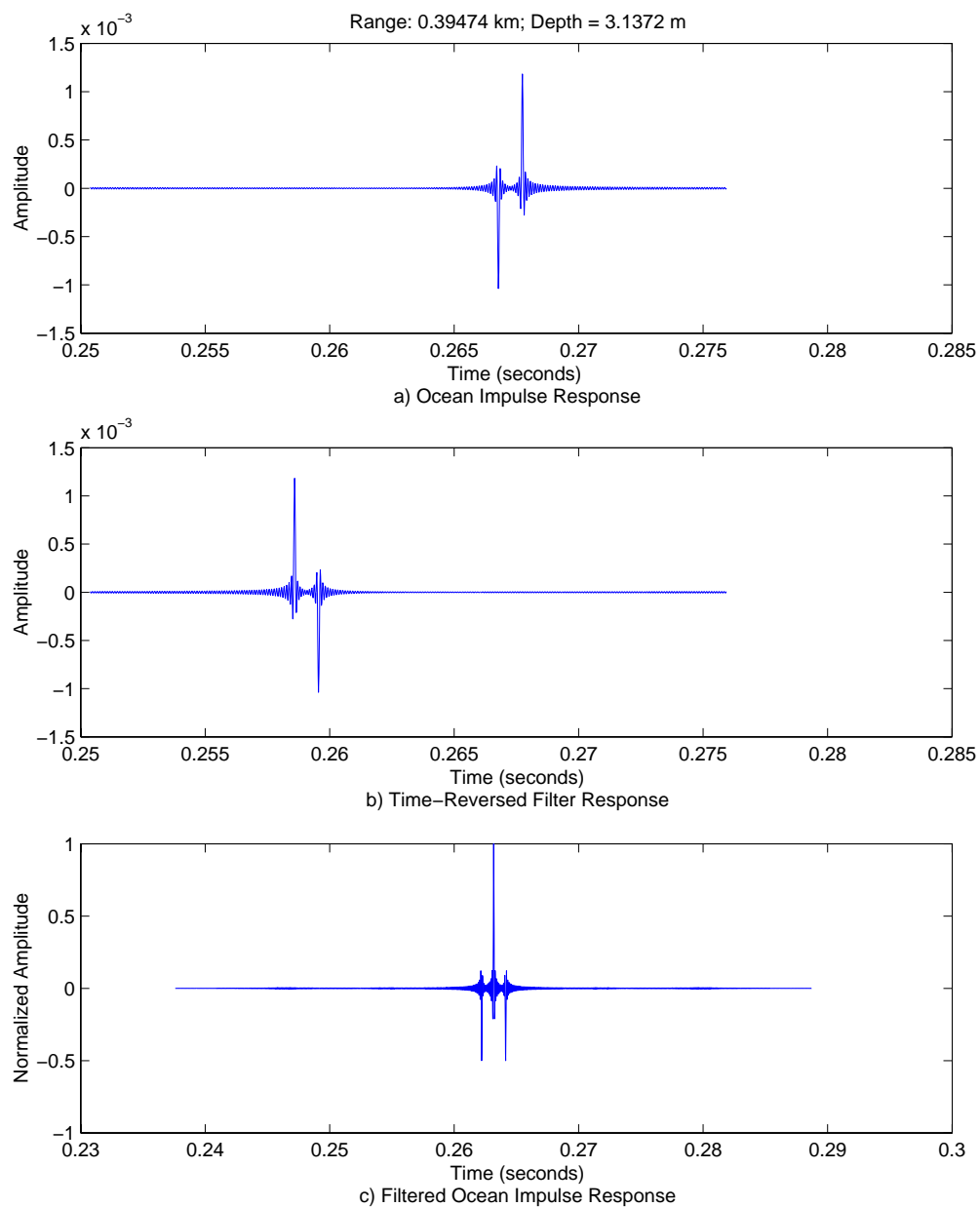
Figure 8.   Passive Time-reversed Filter

26

signals. Specifically, the inverse filter's time response was on the order of hundreds (10^2) as opposed to thousandths (10^{-3}) like the received signal. Any small errors in the signal or computational accuracy were greatly magnified. Figure 9 shows an example of an ocean impulse response and the effect of the inverse filter. Section B of Appendix B contains figures of the inverse filter responses for all the test cases.
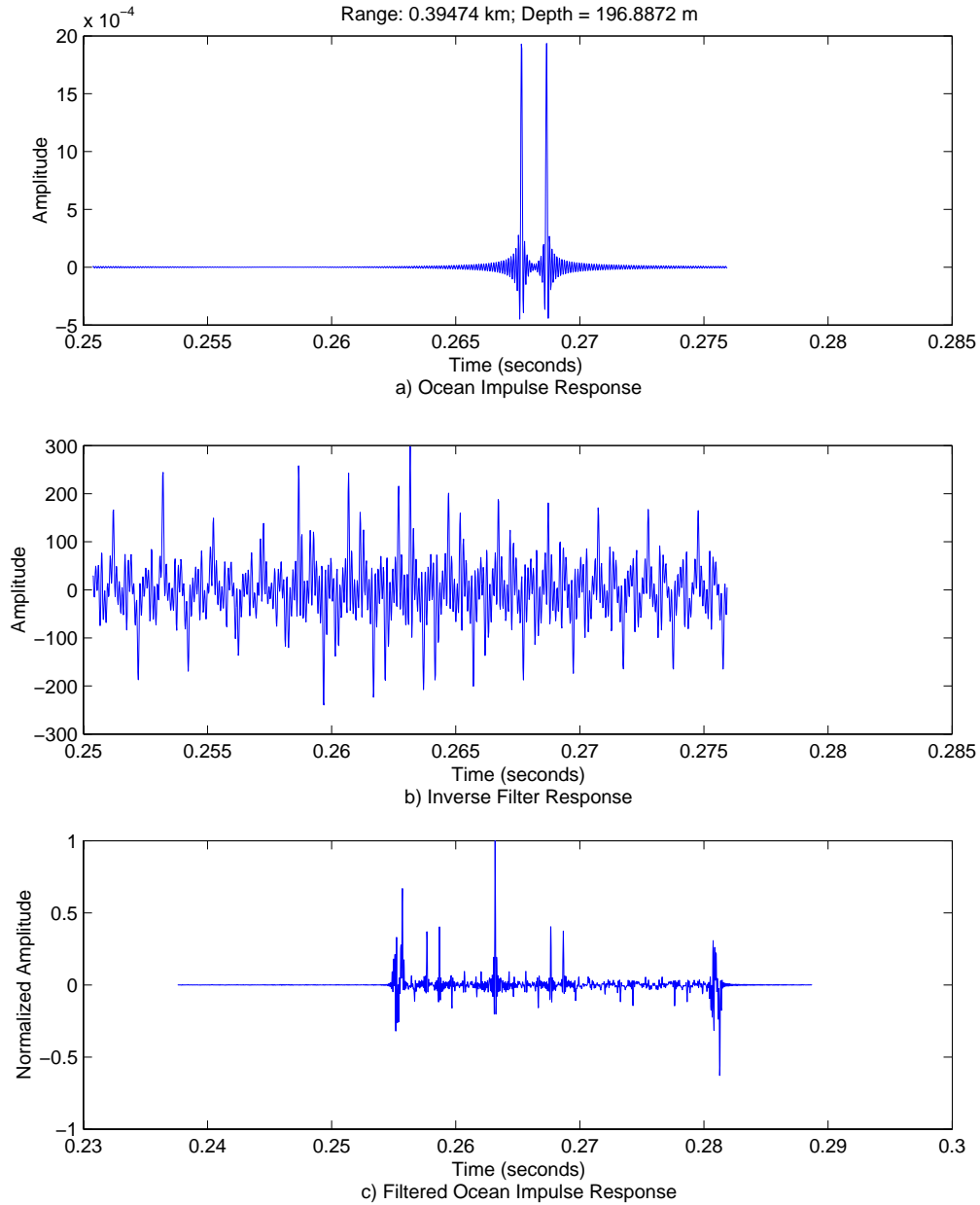
Figure 9.   Inverse Filter

3.   Infinite Impulse Response Filter

For the IIR filter, tap points were selected to determine portions of the ocean impulse response judged to be significant contributors to the distortion of the signal. These tap points were then used as the filter parameters. In Figure 10 it can be seen that the ocean impulse response has three significant returns, and the IIR filter tap points are the magnitudes of these returns with appropriate time delays referenced to the first main return. The number of tap points ranged from one to five, depending on the number of multipath signals received.   Once the tap points were determined, the ocean impulse response was then filtered through the IIR filter, to determine its effectiveness.   The responses of the filters were classified into three categories.
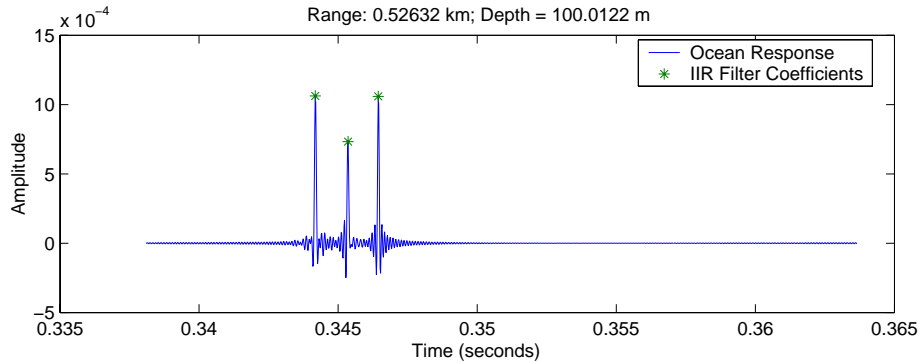
Figure 10.   Ocean Impulse Response and IIR Tap Points

The first and worst case category was the unstable response in which the filter output oscillated with an ever increasing magnitude. With these responses, a number of different combinations of tap points were used to attempt to stabilize the filter. Despite the different combinations, suitable tap points were not found to stabilize the filter. An example of an unstable IIR filter response is shown in Figure 11. Because of the filter instabilities, it was anticipated that the unstable IIR filters would perform poorly.
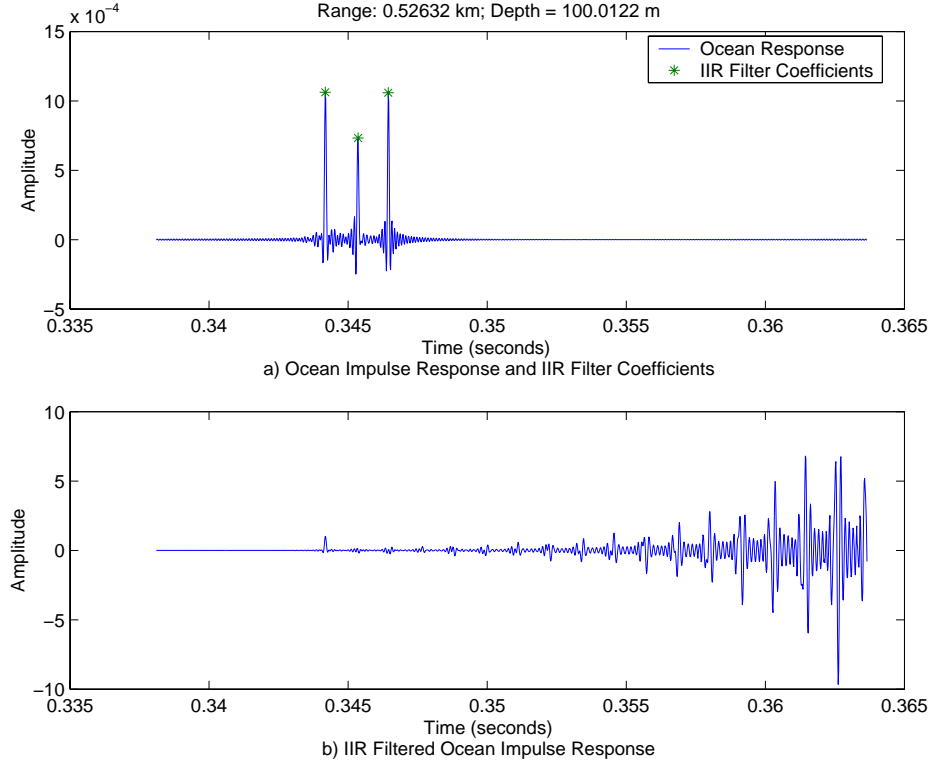
Figure 11.   Unstable IIR Filter

The second category of IIR filters was the IIR filter with a stable response, but having residual multipath components. These cases were able to reduce significantly the magnitude of the multipath signal, but were unable to eliminate completely the multipath signal and repetitive residual structures were present in the filter's output. An example of a stable IIR filter response with residual multipath signals is shown in Figure 12.

The last category, and best performing, was the stable IIR filter with no residual multipath component. The stable IIR filter was able to eliminate the multipath signals at the filter output. An example of such a filter is shown in Figure 13. Section C of Appendix B contains figures of the IIR filter responses for all test cases.
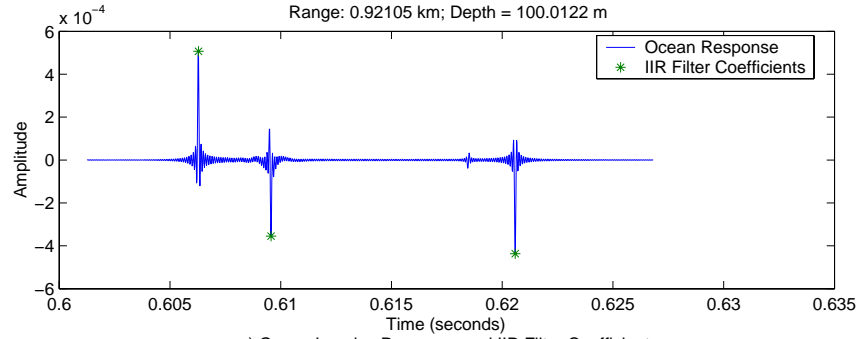
29
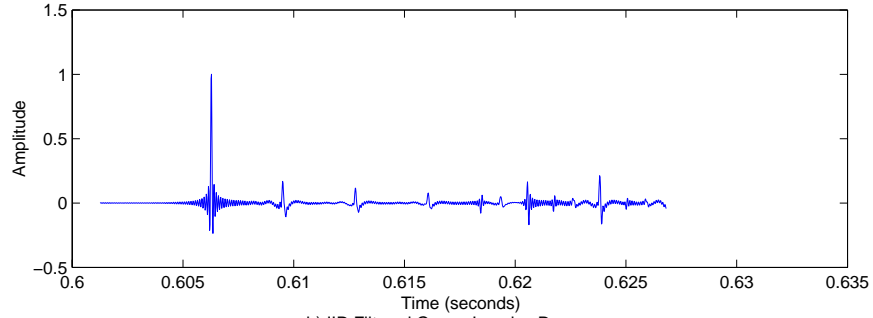
Figure 12.   Stable IIR Filter with Residual Multipaths
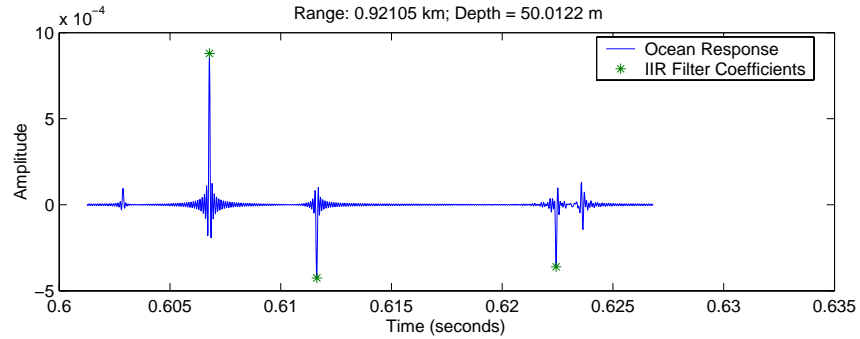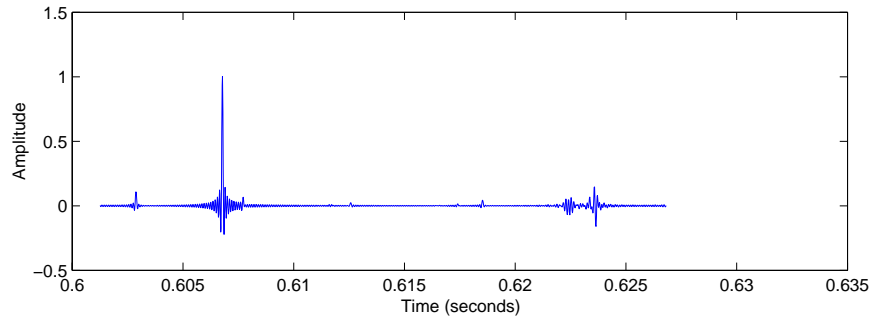
Figure 13.   Stable IIR Filter

With these three categories defined, the thirty cases corresponding to receivers at different ranges and depths were categorized as shown in Table 4.

Table 4.　　IIR Filter Stability Categories

Stability Type	Number of Cases
Unstable	14
Stable with Residual Multipaths	10
Stable	6

C.　BIT ERROR RATE SIMULATIONS

Simulated data transmissions were conducted for the ranges and depths listed in Table 3 and repeated in Table 5. For each location, or case, simulations were conducted over a range of bit rates as shown in Table 5. The bit rates are not necessarily round numbers because they were calculated by dividing the sampling frequency by the desired number of samples per bit period (e.g., 3 samples per bit period equals a bit rate of 60078 Hz/3 samples per bit, or 20,026 bits per second). The numbers are representative of typical practical communication rates of 10 to 30 kilobits per second.

Table 5.　　Data Transmission Parameters

Ranges (kilometers)	0.39; 0.52; 0.65; 0.79; 0.92; 1.05
Depths (meters)	3.1; 50.0; 100.0; 150.0; 196.9
Bit Rates (bits per second)	10,013; 12,015.6; 15,019.5; 20,026; 30,039

The number of bits, n_{bits}, in the data transmission was set at 2^{17}. This value was chosen to provide bit error rate accuracy smaller than 10^{-5}.

$$BER\ accuracy = \frac{1\ bit\ error}{2^{17}\ bits} = 7.63 \times 10^{-6}\ . \tag{III.4}$$

The total transmission time, T_{total}, of the data signal is dependent on the bit rate and the total number of bits sent, and is given by

$$T_{total} = \frac{n_{bits}}{R_b}\ . \tag{III.5}$$

The total transmission times for each bit rate are listed in Table 6.

Table 6.   Data Transmission Times

Bit Rate, R_b (bits per second)	Bit Period, $\frac{1}{R_b}$ (seconds per bit)	Total Transmission Time, T_{total} (seconds)
10,013	99.9x10^{-6}	13.09
12,015.6	83.2x10^{-6}	10.9
15,019.5	66.5x10^{-6}	8.73
20,026	49.9x10^{-6}	6.55
30,039	33.3x10^{-6}	4.36

1.   Passive Time-reversed Filter

The ability of the passive time-reversed filter to achieve bit error rates below 10^{-2} was very limited. In only three cases was the passive time-reversed filter able to achieve BERs equal to or better than 10^{-2}.   In those three cases, these low bit error rates corresponded to transmission rates below 20,000 bits per second and the magnitude of the residual multipath structures were less than thirty percent of the magnitude of the main path signal. The data indicated that the passive time-reversed filter is not an effective

means of recovering a signal since there are inherent residual multipath components in the filter output.

2.   Inverse Filter

The inverse filter was the overall worst performing of all three filters. The best performance of the inverse filter was to achieve a bit error rate of 10^{-1}. As previously stated, the poor performance of the inverse filter appeared to be caused by the erratic nature of the time response of the filter and the associated large magnitudes resulting from direct inversion in the frequency domain. Further research and simulation designs would be needed to understand the specific causes of the poor performance of the filter, and perhaps to try to improve the design of the inverse filter.

3.   Infinite Impulse Response Filter

The infinite impulse response filter was successful in a limited number of cases. This was an improvement over the performance of the other filters however. In five of the 30 cases the IIR filter was able to achieve a BER below 10^{-2}. All five of these cases were stable IIR filters with no residual multipaths. The remaining stable IIR filter with no residual multipaths produced a BER of 0.5, though it is not apparent why this case did not perform well.

All ten of the unstable IIR filters produced a BER of 0.5. In addition, the stable IIR filters with residual multipath signals performed poorly. Of the fourteen stable IIR filters with residual multipath signals, only five were able to produce a BER better than 0.5. Two produced a BER greater than 10^{-1} and less than 0.5, and three were able to achieve a BER between 10^{-1} and 10^{-2}. A summary of the performance of the IIR filter and the passive time-reversed filter is given in Tables 7 and 8.

Comparisons of the BER with the stability of the IIR filters revealed some correlations between the effectiveness of the IIR filter and its stability. First, it was clear

Table 7.   IIR Filter and Passive Time-reversed Filter Performance (Cases 1 to 15)

Case	Range (km)	Depth (m)	Number of Multipath Components (incl. main path)	Stability	IIR Filter BER	Time-reversed Filter BER
1	0.39	3.14	2	Unstable	0.5	~0.1 to ~0.2
2	0.39	50.0	2	Stable (w/ residuals)	0.5	~0.1 to ~0.2
3	0.39	100.0	2	Stable	$<10^{-3}$	$\sim10^{-1}$ to $<10^{-4}$
4	0.39	150.0	2	Stable	$\sim10^{-3}$	$\sim10^{-1}$ to $<10^{-4}$
5	0.39	196.9	2	Unstable	0.5	~0.1 to ~0.2
6	0.52	3.14	2	Stable	$<10^{-4}$	~0.1 to ~0.2
7	0.52	50.0	2	Stable	$<10^{-1}$ to $<10^{-4}$	<0.2 but $>10^{-3}$
8	0.52	100.0	3	Unstable	0.5	~0.1 to ~0.2
9	0.52	150.0	3	Stable	0.5	~0.1 to ~0.2
10	0.52	196.9	2	Unstable	0.5	~0.1 to ~0.2
11	0.65	3.14	4	Stable (w/ residuals)	$<10^{-1}$ but $>10^{-2}$	~0.1 to ~0.2
12	0.65	50.0	3	Stable (w/ residuals)	<0.5 but $>10^{-1}$	~0.1 to ~0.2
13	0.65	100.0	3	Stable (w/ residuals	$<10^{-1}$ but $>10^{-2}$	~0.1 to ~0.2
14	0.65	150.0	3	Stable (w/ residuals)	<0.5 but $>10^{-1}$	~0.1 to ~0.2
15	0.65	196.9	3	Stable (w/ residuals)	$<10^{-1}$ but $>10^{-2}$	<0.2 but $>10^{-2}$

Table 8.　　IIR Filter and Passive Time-reversed Filter Performance (Cases 16 to 30)

Case	Range (km)	Depth (m)	Number of Multipath Components (incl. main path)	Stability	IIR Filter BER	Time-reversed Filter BER
16	0.79	3.14	3	Stable (w/ residuals)	0.5	~0.1 to ~0.2
17	0.79	50.0	3	Unstable	0.5	~0.1 to ~0.2
18	0.79	100.0	3	Stable (w/ residuals)	0.5	<0.2 but >10^{-2}
19	0.79	150.0	4	Stable (w/ residuals)	0.5	~0.1 to ~0.2
20	0.79	196.9	3	Stable (w/ residuals)	0.5	~0.1 to ~0.2
21	0.92	3.14	3	Unstable	0.5	~0.1 to ~0.2
22	0.92	50.0	3	Stable	$<10^{-2}$ to $<10^{-4}$	~0.1 to ~0.2
23	0.92	100.0	3	Stable (w/ residuals)	0.5	~0.1 to ~0.2
24	0.92	150.0	5	Stable (w/ residuals)	0.5	~0.1 to ~0.2
25	0.92	196.9	4	Unstable	0.5	~0.1 to ~0.2
26	1.05	3.14	4	Unstable	0.5	~0.1 to ~0.2
27	1.05	50.0	5	Stable (w/ residuals)	0.5	~0.1 to ~0.2
28	1.05	100.0	3	Unstable	0.5	~0.1 to ~0.2
29	1.05	150.0	3	Stable (w/ residuals)	0.5	~0.1 to ~0.2
30	1.05	196.9	5	Unstable	0.5	~0.1 to ~0.2

that if the IIR filter is unstable no decoding of a signal was possible. This is not a surprise. In addition, the data suggested that a stable IIR filter is also unable to effectively decode a signal, if there are any significant residual multipath components. The combined effects of all the residual multipath components in an IIR filter, though small at times, seem to dominate the main return, much like the residual components of the passive time-reversed filter. In stable filters that have no residual multipath components, the receiver was able to effectively decode the transmitted signal with bit error rates less than 10^{-2} for transmitted bit rates around 20,000 bits per second. At lower bit rates, the bit error rates decreased to less than 10^{-3}, and in three cases to below 10^{-4}.

The data indicated that the effective IIR filters were the stable filters with no residual multipath components. Comparisons of the stability of the IIR filters with the number of multipath signals including the main path revealed that the stability of the IIR filter had some dependency on the number of multipath components. Four of the five stable IIR filters that performed well possessed only two multipath components, including the main path signal, while the fifth had three multipath components, including the main path signal. Neither of the two non-main path components for the fifth case was significantly dominant. Both magnitudes were about fifty percent of the magnitude of the main path signal. The results of this study suggest that any correlation between the stability of the IIR filter and its range or depth from the transmitter can be more appropriately attributed to the multipath structure and not to the range or depth. The farther the receiver is from the transmitter, the more likely there will be multipath components, since there is more opoortunity for the transmitted signal to reflect off the surface and bottom multiple times.

Plots of the bit error rates versus bit rate for all three filters were generated and are contained in section A of Appendix C. An example of the BER versus bit rate plots is shown in Figure 14. This plot shows the BER for a range of 0.92 kilometers and a depth of 50.0 meters.

BER vs Bit Rate (Range: 0.92105 km, Depth: 50.0122 m)
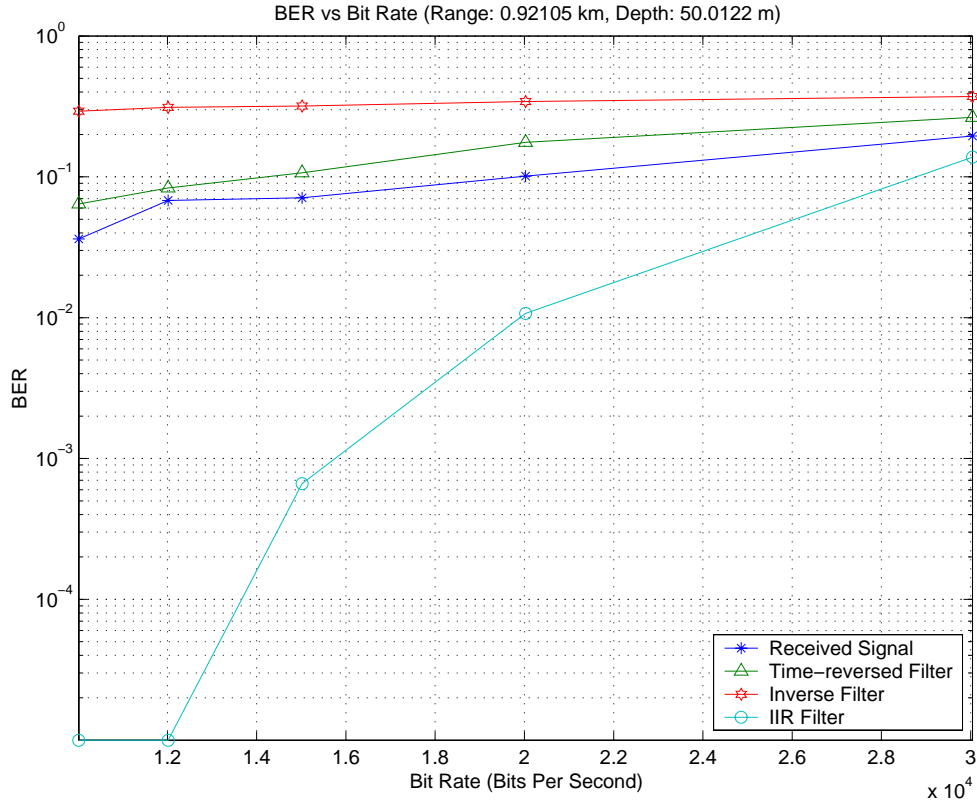
Figure 14.   BER versus Bit Rate

In addition, spatial plots of the BER were generated and are contained in section B of Appendix C. An example of a spatial plot is shown in Figure 15. This plot shows the BER for a signal transmitted at 20,026 bits per second. In these plots, red hues represent bit error rates around 10^{-1} and greater, blue hues represent bit error rates around 10^{-3} and lower, and yellow and green hues signify bit error rates between 10^{-3} and 10^{-1}. From this example, it can be seen that the IIR filter performs adequately at close ranges in a limited number of instances.
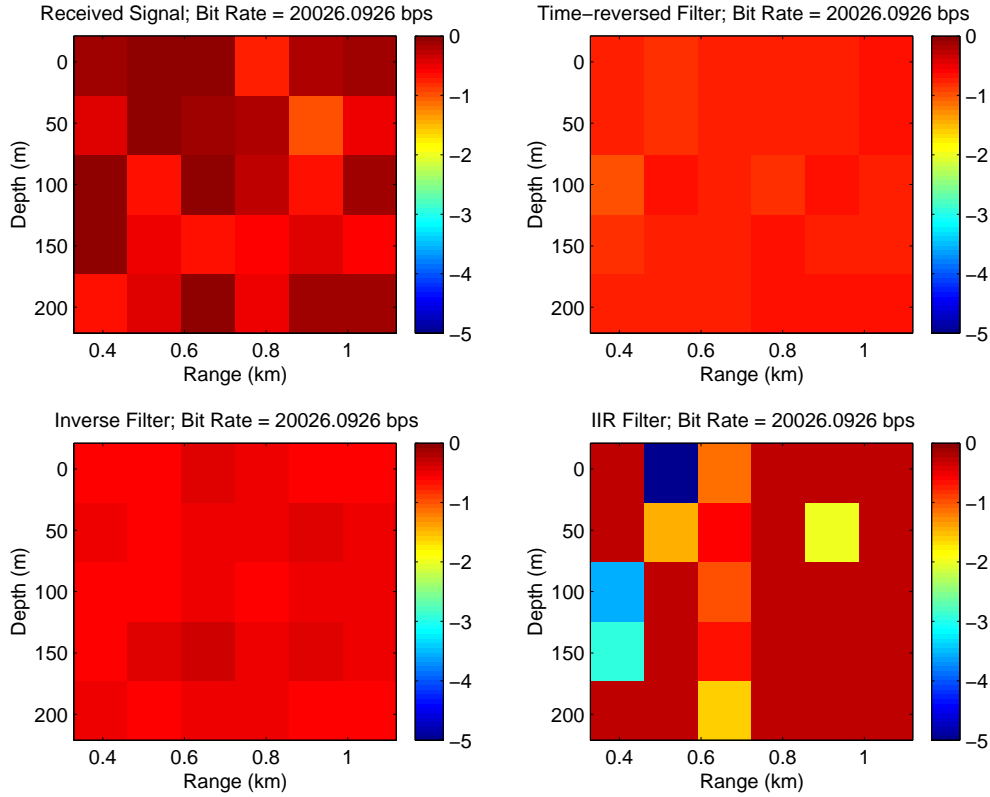
Figure 15.   Log BER for Bit Rate of 20,026 bps

D.   LESSONS LEARNED ON MODELING AND SIMULATIONS

In the process of developing and implementing the simulations, obstacles and learning points occurred that provided a greater appreciation and understanding of engineering and the complexity of designing simulations. To begin with, simulation run times are a very important factor when conducting simulations and analyses. For the ocean model developed by the MMPE program, the execution time lasted upwards of a week to develop one ocean. Once the ocean frequency response was obtained, the MATLAB simulations required about three hours for each case. The long simulation run times were due to the long data vectors required to achieve specific desired accuracies for the bit error rates and to achieve small enough sampling intervals to simulate the desired bit rates.

With regard to the run times needed to perform simulations, one major lesson learned was the importance of choosing appropriate parameters. In learning the details of

the MMPE model, four different ocean environments were modeled, although ultimately only one was used. The need to build multiple ocean environments occurred because what originally appeared as benign values for some of the parameters actually caused significant inaccuracies in the ocean model. For example, the number of frequencies calculated within the bandwidth greatly affected the time response of the ocean. Originally a small number of frequencies were calculated, which led to a large frequency resolution. The application of the Fourier Transform, a property of which stipulates that the frequency resolution is the inverse of the total time interval, led to a small total time interval. The ultimate consequence of choosing a small number of frequencies was that the time response exceeded the time window of the Discrete Fourier Transform; therefore the time signal was circularly wrapped around in the time window (an effect known as aliasing). This is a most undesirable result.

THIS PAGE INTENTIONALLY LEFT BLANK

IV.   CONCLUSIONS AND RECOMMENDATIONS

A.   CONCLUSIONS

In this thesis, three types of filters were examined to determine their potential viability for equalization in underwater acoustic communications systems. The objective was to analyze the abilities of the filters to mitigate the distortional effects of a shallow water channel associated with littoral regions of the ocean. Such distortional effects cause intersymbol interference (ISI) and prevent effective communication with modern digital communications systems. Underwater acoustic communications is important to the Department of Defense's Network Centric Warfare and the U.S. Navy's "Forward, From the Sea" doctrines which emphasize information dominance in the battlespace. The shallow water channel is of particular interest because of the vast number of littoral regions throughout the world in which the U.S. Navy operates.

Two performance aspects of each filter were analyzed to determine the ability of each filter to equalize the ocean channel. The first aspect was the ability of the filter to remove multipath components from the ocean time response. The second performance aspect was the ability to receive transmitted signals with minimal bit error rates. This performance aspect was analyzed by simulating the transmission of a communications signal and decoding the signal after filtering and calculating the bit error rate. The three filters analyzed were the passive time-reversed filter, the inverse filter, and the IIR filter. Of the three filters, the inverse filter performed poorly while the passive time-reversed filter and the IIR filter performed with limited success.

The passive time-reversed filter performed best over the range of cases. This filter consistently achieved bit error rates on the order of 10%. Earlier results from previous research have shown time-reversal to be a feasible filtering technique with better bit error rates than those produced in this thesis. However, these results were based on time-reversal arrays, rather than a single receiver [Ref. 8, 9, 12, 14, 15, 18, 20]. The passive time-reversed filter was unable to consistently achieve bit error rates below 10%, because of the presence of residual multipath structures inherent in the output of the passive time-reversed filter.

The inverse filter was incapable of recovering any communications signal without bit error rates greater than 10^{-1}. It was determined that the inability of the inverse filter to perform adequately was due to the erratic time response of the filter and the associated large magnitudes. These results were not completely unexpected since the design of inverse filters is known to be ill-conditioned at times. In addition, small errors in the calculation of the frequency response are greatly magnified for magnitudes of the frequency response that are less than one.

The IIR filter achieved adequate results, although on a limited basis. The IIR filter was able to produce the best bit error rates (below 10^{-2}) when stable, however this occurred in only five of the thirty cases. Performance was degraded quite significantly when residual multipath structures exist at the filter output or when the filter is unstable. However, further investigation and development of this approach may prove fruitful in the development of an IIR filter as a useful equalization method, especially if applied to data collected from multiple sensors and combined with suitable array processing for spatial focusing.

B.   RECOMMENDATIONS FOR FUTURE WORK

The results of this thesis show that the passive time-reversed filter and the IIR filter might be viable methods for equalizing the ocean channel and removing multipath structures. In order to improve the ability of the passive time-reversed filter, it is recommended that development and optimization of an array receiver should be investigated. Before an IIR filter can be considered a reliable means of recovering underwater acoustic communications, two major obstacles still exist that need to be researched and eliminated. First, methods need to be researched and developed that can efficiently and consistently produce stable IIR filters. Because of time limitations, methods for stabilizing unstable filters were not investigated in this thesis. Secondly, algorithms should be researched and developed that can take a stable IIR filter and produce filter outputs that remove all multipath structures from the ocean time response. Finally, if these studies continue to show feasibility, it would be useful to develop an adaptive IIR filter that can account for the time-varying nature of the ocean medium.

APPENDIX A. BASEBAND DISCUSSION

This appendix briefly discusses a property of a communications system, which allows for the simplification of the simulations in this study. Specifically, all the pertinent information and transmission distortions are carried out with the (real) envelope of the signal.* This useful property allows the use of baseband signals, instead of the bandpass signal, for all calculations and manipulations.

A. TRANSMITTED DATA SIGNAL

The transmitted signal is a baseband data signal $d(t)$ modulated onto a sinusoidal carrier with frequency f_c and phase γ,

$$s(t) = d(t)\cos(2\pi f_c t + \gamma). \tag{A.1}$$

This transmitted signal is a bandlimited or bandpass signal since the spectrum is non-zero only in some limited region centered about the carrier $(\pm f_c)$.

B. OCEAN IMPULSE RESPONSE

The ocean impulse response over the band of interest can also be modeled as a baseband signal, or envelope, $\hat{h}(t)$ modulated onto a carrier with frequency f_c and phase $\phi(t)$

$$h(t) = \hat{h}(t)\cos(2\pi f_c t + \phi(t)). \tag{A.2}$$

---

* An equivalent analysis can be carried out in terms of the complex envelope, but the present approach avoids the discussion of complex valued signals.

C.   RECEIVED DATA SIGNAL

The received signal, $r(t)$, is the convolution of the transmitted data signal and the ocean impulse response,

$$r(t) = s(t) * h(t) = \int_{-\infty}^{\infty} h(\tau) s(t - \tau) d\tau. \qquad (A.3)$$

By substituting Equations (A.1) and (A.2) into Equation (A.3), $r(t)$ can be expressed in terms of the real envelopes and the carrier frequencies,

$$r(t) = \int_{-\infty}^{\infty} \left[\hat{h}(\tau) \cos\left(2\pi f_c \tau + \phi(\tau)\right) \right] \left[d(t - \tau) \cos\left(2\pi f_c (t - \tau) + \gamma\right) \right] d\tau$$

$$= \int_{-\infty}^{\infty} \hat{h}(\tau) d(t - \tau) \cos\left(2\pi f_c \tau + \phi(\tau)\right) \cos\left(2\pi f_c (t - \tau) + \gamma\right) d\tau. \qquad (A.4)$$

This can be further simplified using trigonometric identities to obtain

$$r(t) = \frac{1}{2} \int_{-\infty}^{\infty} \hat{h}(\tau) d(t - \tau) \left[\cos\left(2\pi f_c t + \phi(\tau) + \gamma\right) + \cos\left(2\pi f_c (2\tau - t) + \phi(\tau) - \gamma\right) \right] d\tau. \quad (A.5)$$

D.   DEMODULATED DATA SIGNAL

The demodulated data signal, $x(t)$, is the received data signal heterodyned with a local oscillator with the carrier waveform, $\cos\left(2\pi f_c t + \theta(t)\right)$; thus

$$x(t) = r(t) \cos\left(2\pi f_c t + \theta(t)\right). \qquad (A.6)$$

The time varying phase $\theta(t)$ is for the purpose of tracking the phase of the received signal (see discussion in Chapter II, Section C).

Substitution of Equation (A.5) into Equation (A.6) leads to

$$x(t) = \frac{1}{2} \int_{-\infty}^{\infty} \hat{h}(\tau) d(t-\tau) \cdot \left[\cos\left(2\pi f_c t + \phi(\tau) + \gamma\right)\right.$$
$$\left. + \cos\left(2\pi f_c (2\tau - t) + \phi(\tau) - \gamma\right)\right] \cos\left(2\pi f_c t + \theta(t)\right) d\tau .$$

(A.7)

Through the use of trigonometric identities, $x(t)$ can be expressed in the form of the baseband signal multiplied by a constant and several components at twice the carrier frequency. The explicit expression is

$$x(t) = \frac{1}{4} \int_{-\infty}^{\infty} \hat{h}(\tau) d(t-\tau) \cdot \left[\cos\left(\phi(\tau) + \gamma - \theta(t)\right)\right.$$
$$+ \cos\left(2\pi f_c (2t) + \phi(\tau) + \gamma + \theta(t)\right)$$
$$+ \cos\left(2\pi f_c (2\tau) + \phi(\tau) - \gamma + \theta(t)\right)$$
$$\left. + \cos\left(2\pi f_c (2\tau - 2t) + \phi(\tau) - \gamma - \theta(t)\right)\right] d\tau .$$

(A.8)

E.   LOW PASS FILTERED DATA SIGNAL

The receiver in the communications system uses a low pass (LP) filter to recover the baseband signal prior to decoding the data signal. The LP filter is designed to remove the components at twice the carrier frequency, leaving the real envelope signals. Thus $x(t)$ in Equation (A.8) becomes

$$x_{LP}(t) = \frac{1}{4} \int_{-\infty}^{\infty} \hat{h}(\tau) d(t-\tau) \cos\left(\phi(\tau) + \gamma - \theta(t)\right) d\tau .$$

(A.9)

Without loss of generality, the phase of the transmitted signal, γ, can be set to zero. Further, since the phase of the received signal is acquired and tracked by a phase-locked loop, it can be assumed that $\theta(t) = \phi(t)$. In addition, if it is assumed that the phase due to the ocean is slowly varying (i.e., the signal duration is less than the channel coherence time), then over the integration time when $\hat{h}(t)$ is not zero, we have $\phi(\tau) \approx \phi(t)$ so that

$$\cos\left(\phi(\tau) + \gamma - \theta(t)\right) \approx 1$$

and Equation (A.9) can be written as

$$x_{LP}(t) = \frac{1}{4}\int_{-\infty}^{\infty} \hat{h}(\tau)d(t-\tau)d\tau = \frac{1}{4}\hat{h}(t)*d(t) = x_{bb}(t). \qquad (A.10)$$

Equation (A.10) demonstrates that, except for a constant scale factor (¼), the demodulated and LP filtered signal is the convolution of the real envelopes of the transmitted data signal and ocean impulse response. In other words, Equation (A.10) is the baseband equivalent of Equation (A.3). The terms $\hat{h}(t)$, $d(t)$, and $x_{bb}(t)$ are the real envelopes corresponding to the bandpass signals $h(t)$, $s(t)$ and $x(t)$.

APPENDIX B.   OCEAN AND FILTER PLOTS

This appendix contains plots of the ocean responses and the filter responses. They are separated into three sections, one for each of the filter types.   The ocean response is contained in each section for comparison. . The amplitudes of these plots are relative amplitudes referenced to a zero dB signal.

A.   PASSIVE TIME-REVERSED FILTER RESULTS

Figures 16 through 45 contain plots of the ocean impulse response, the passive time-reversed filter response, and the filtered ocean response for all thirty test cases. From these plots it can be seen that the passive time-reversed filter is able to reduce the magnitudes of multipath returns, however, it is unable to completely eliminate the multipath returns.
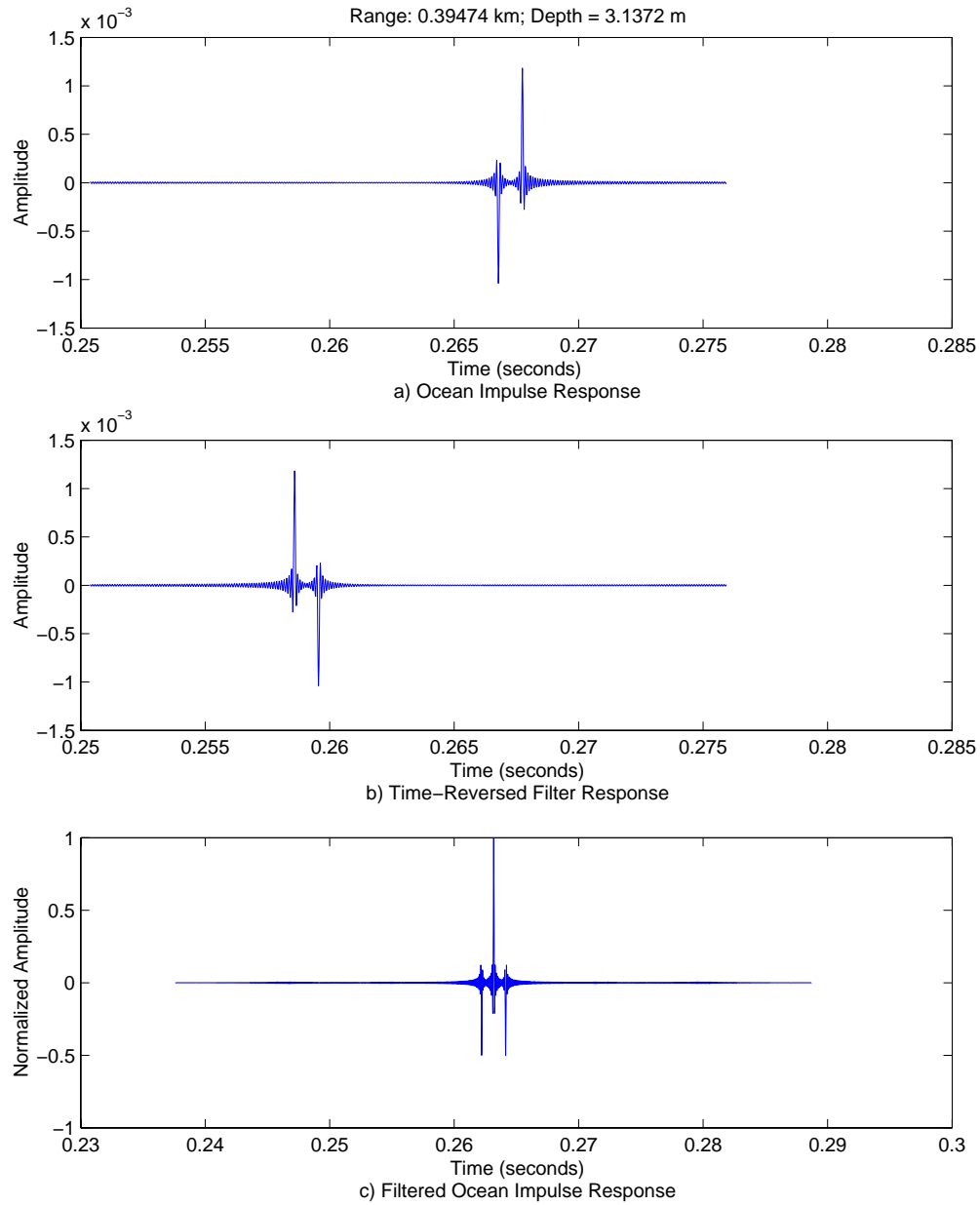
Figure 16.   Passive Time-reversed Filter, Case 1
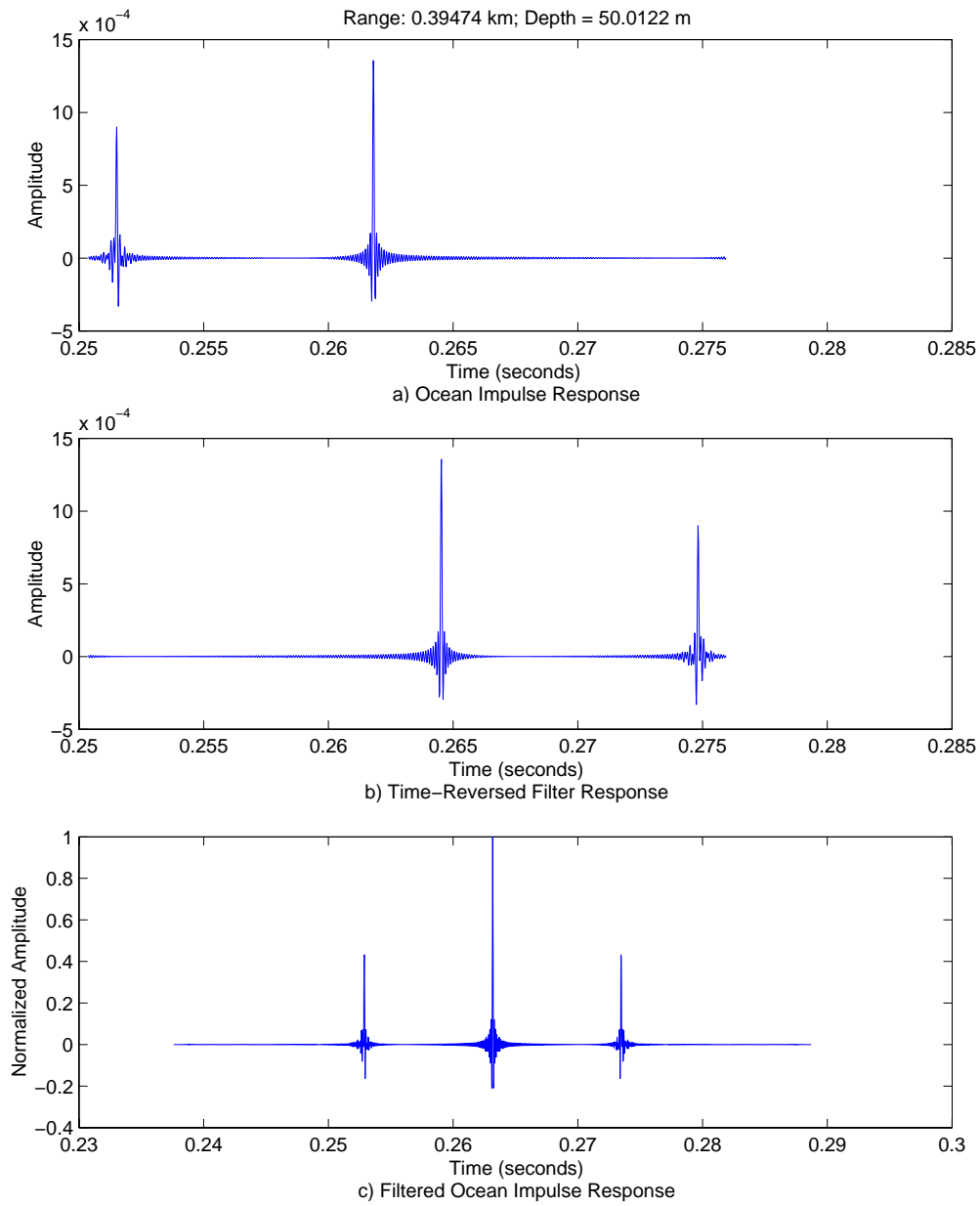
Figure 17.   Passive Time-reversed Filter, Case 2
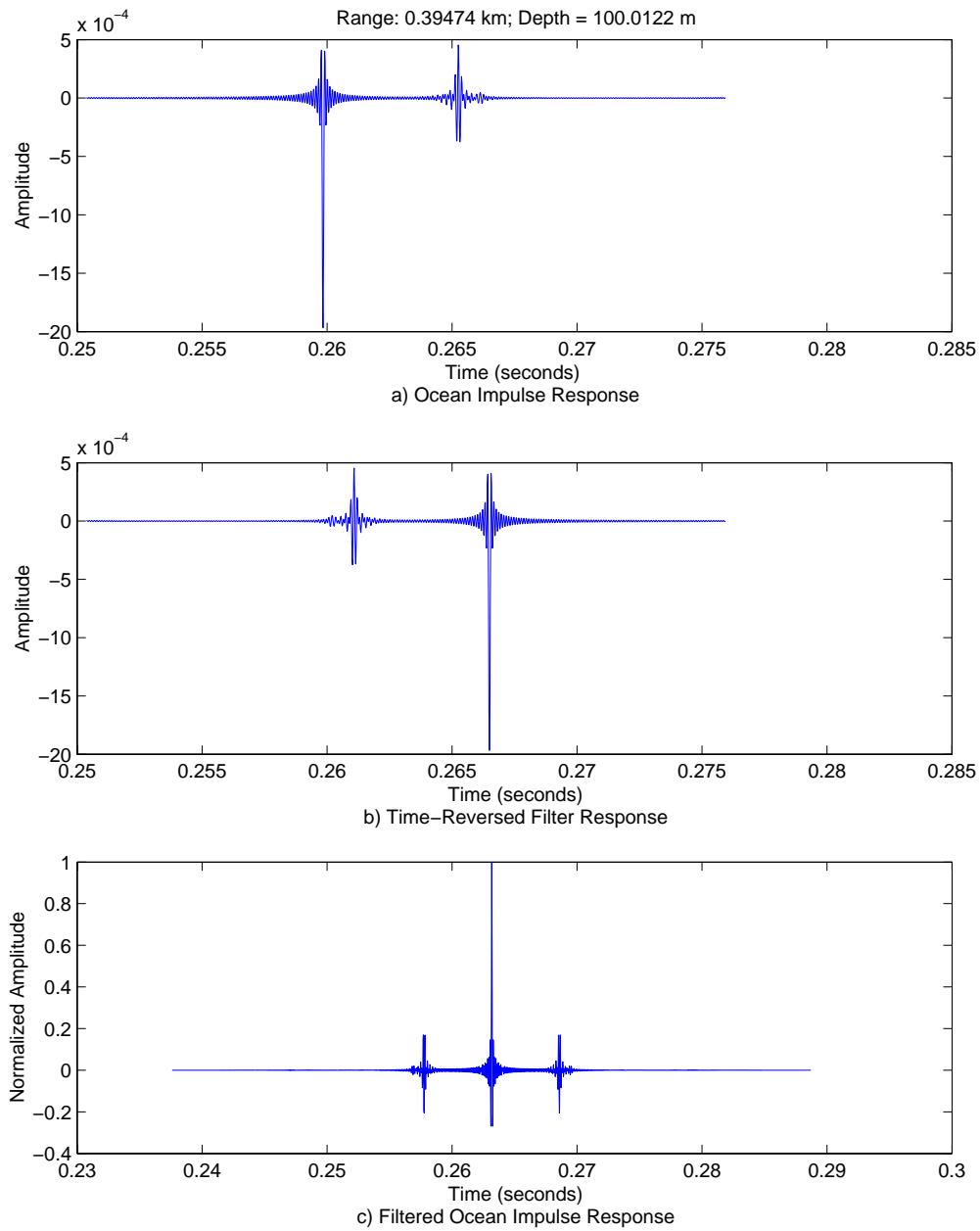
Figure 18.   Passive Time-reversed Filter, Case 3
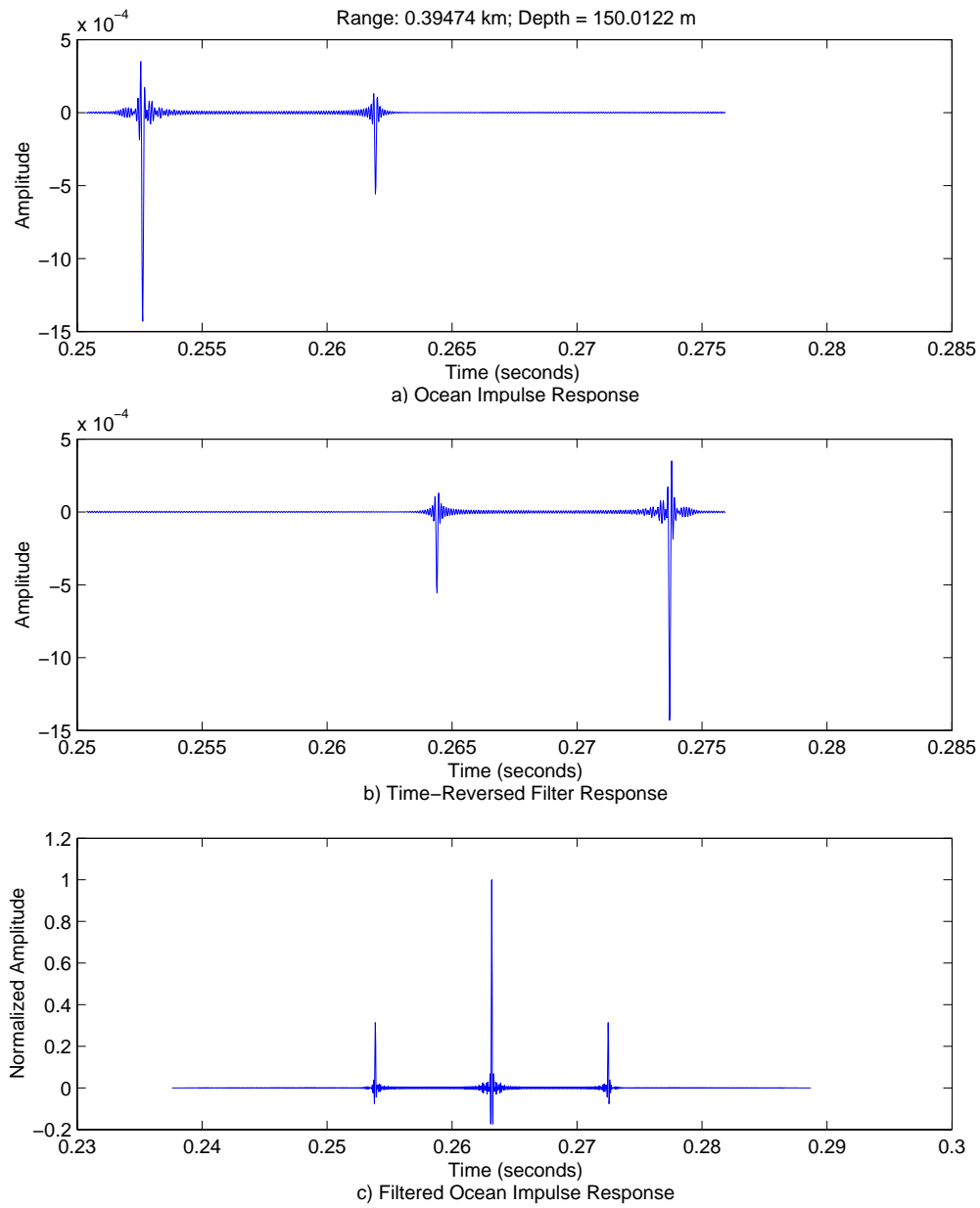
Figure 19.   Passive Time-reversed Filter, Case 4
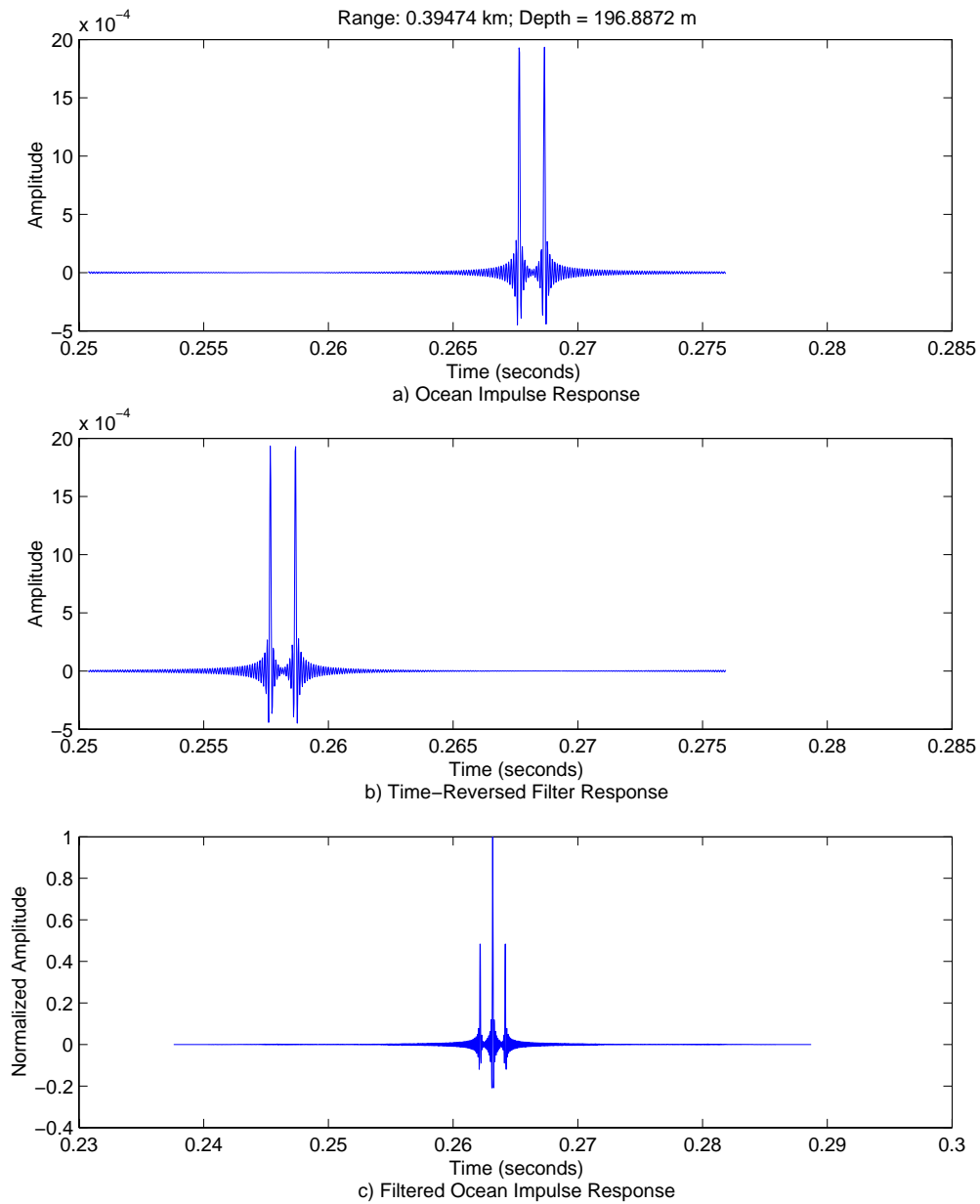
Figure 20.   Passive Time-reversed Filter, Case 5
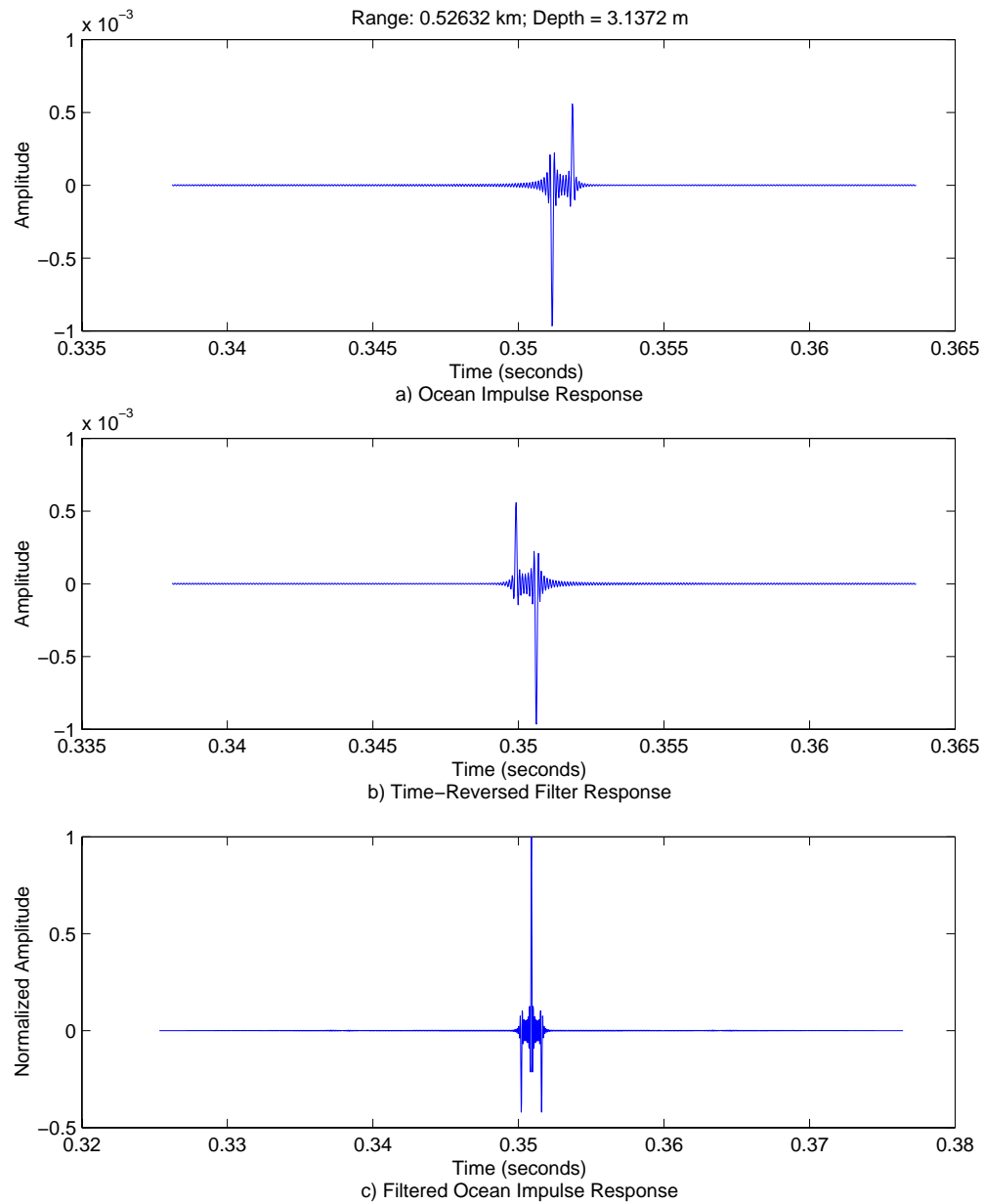
Figure 21.   Passive Time-reversed Filter, Case 6
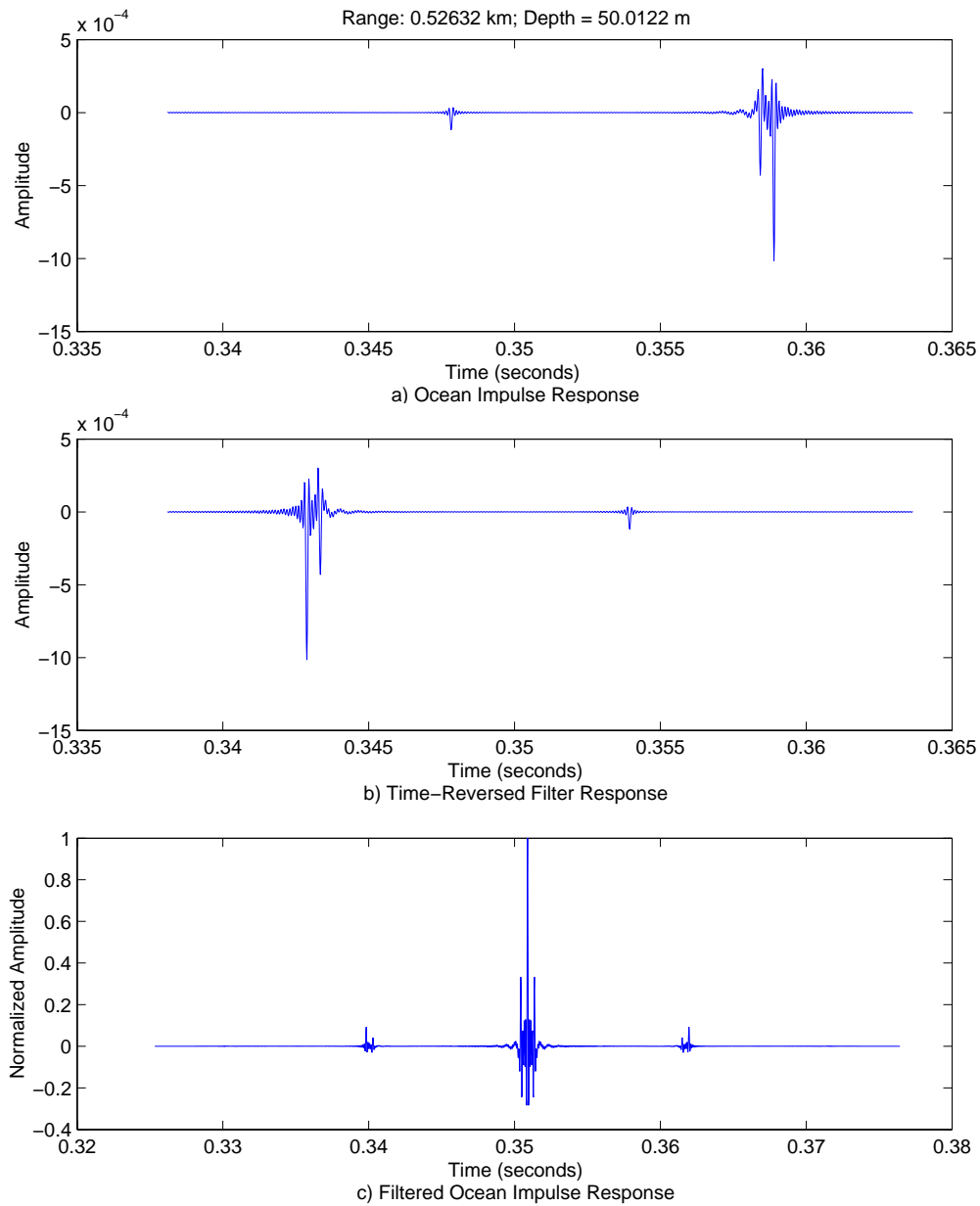
Figure 22.   Passive Time-reversed Filter, Case 7
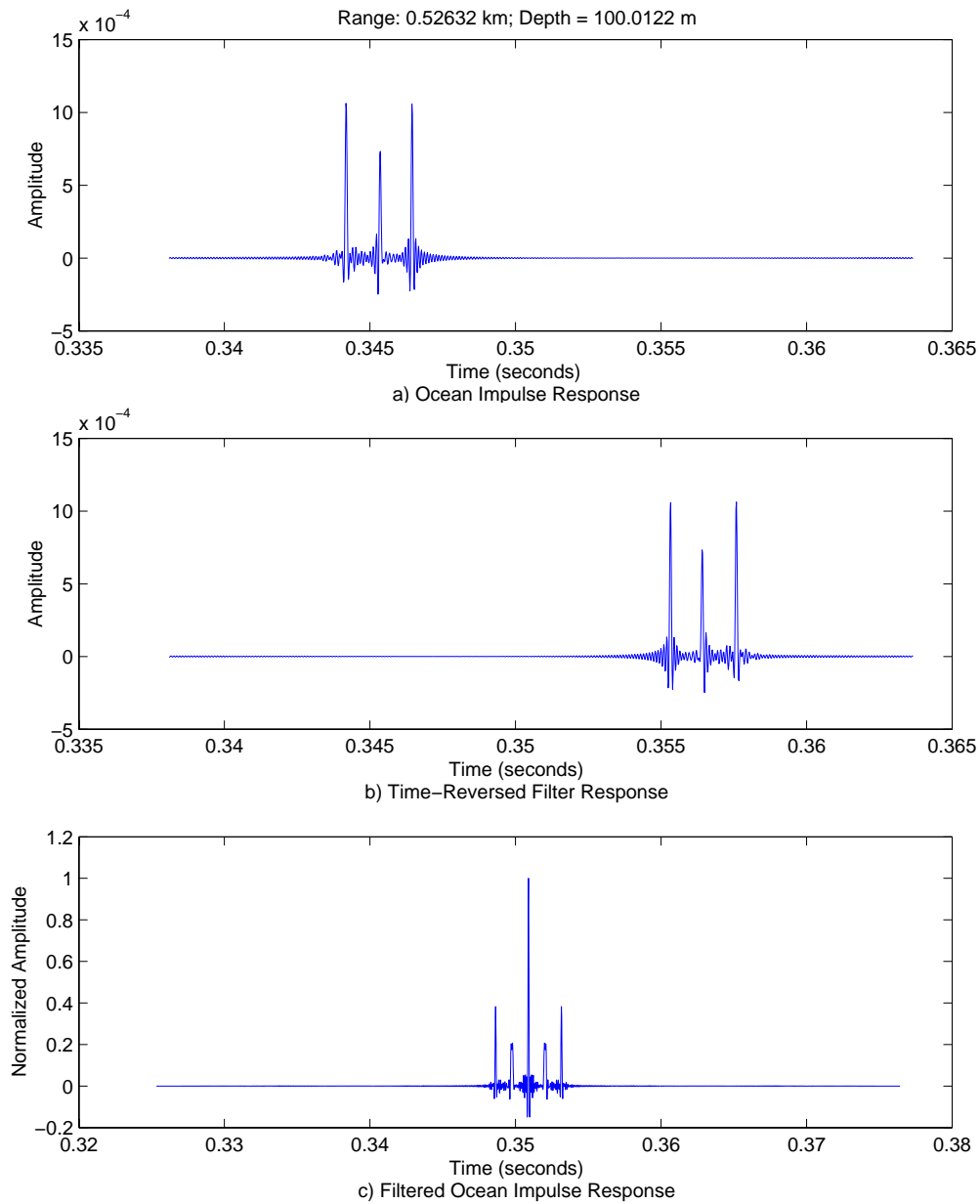
Figure 23.   Passive Time-reversed Filter, Case 8
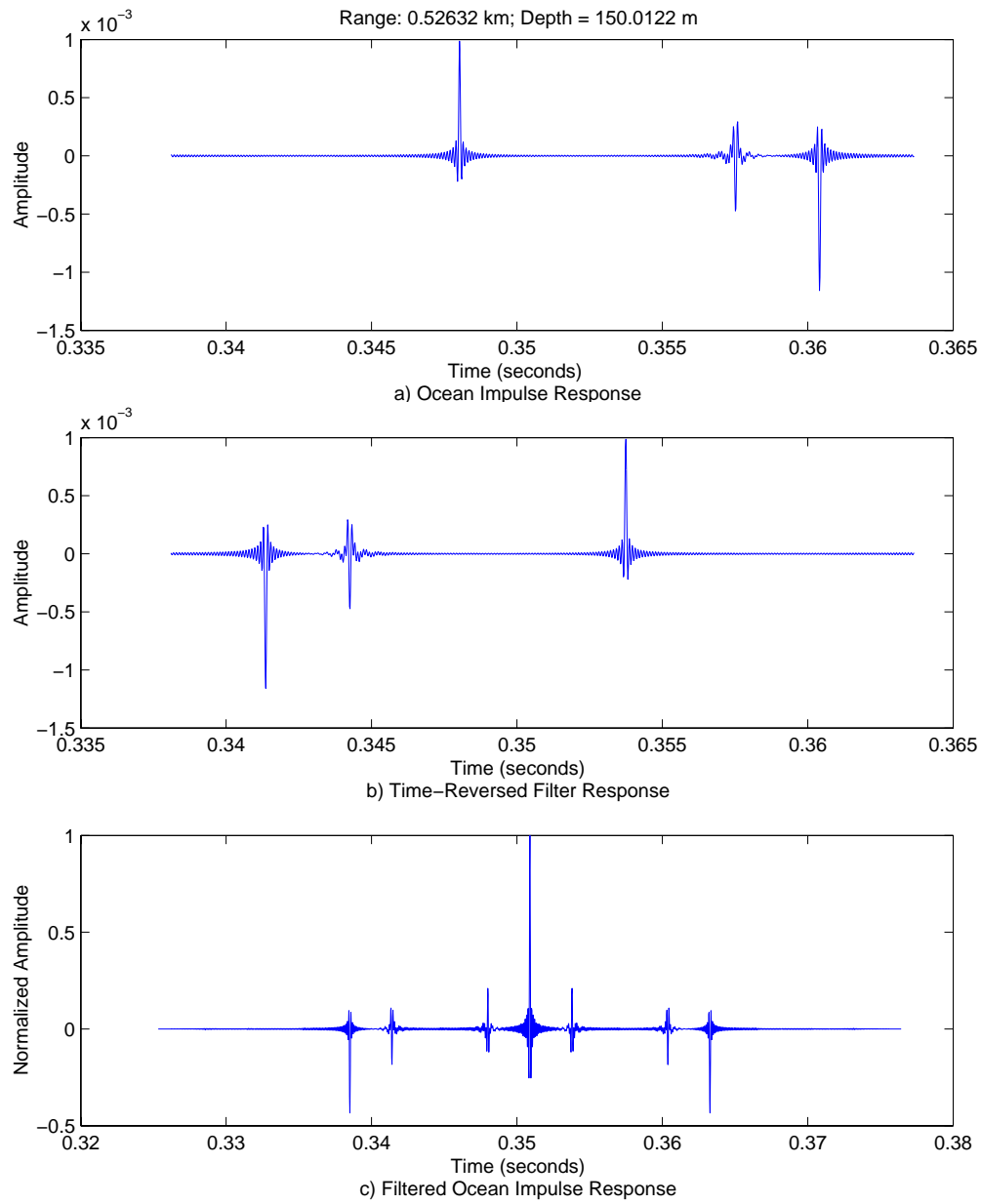
Figure 24.   Passive Time-reversed Filter, Case 9
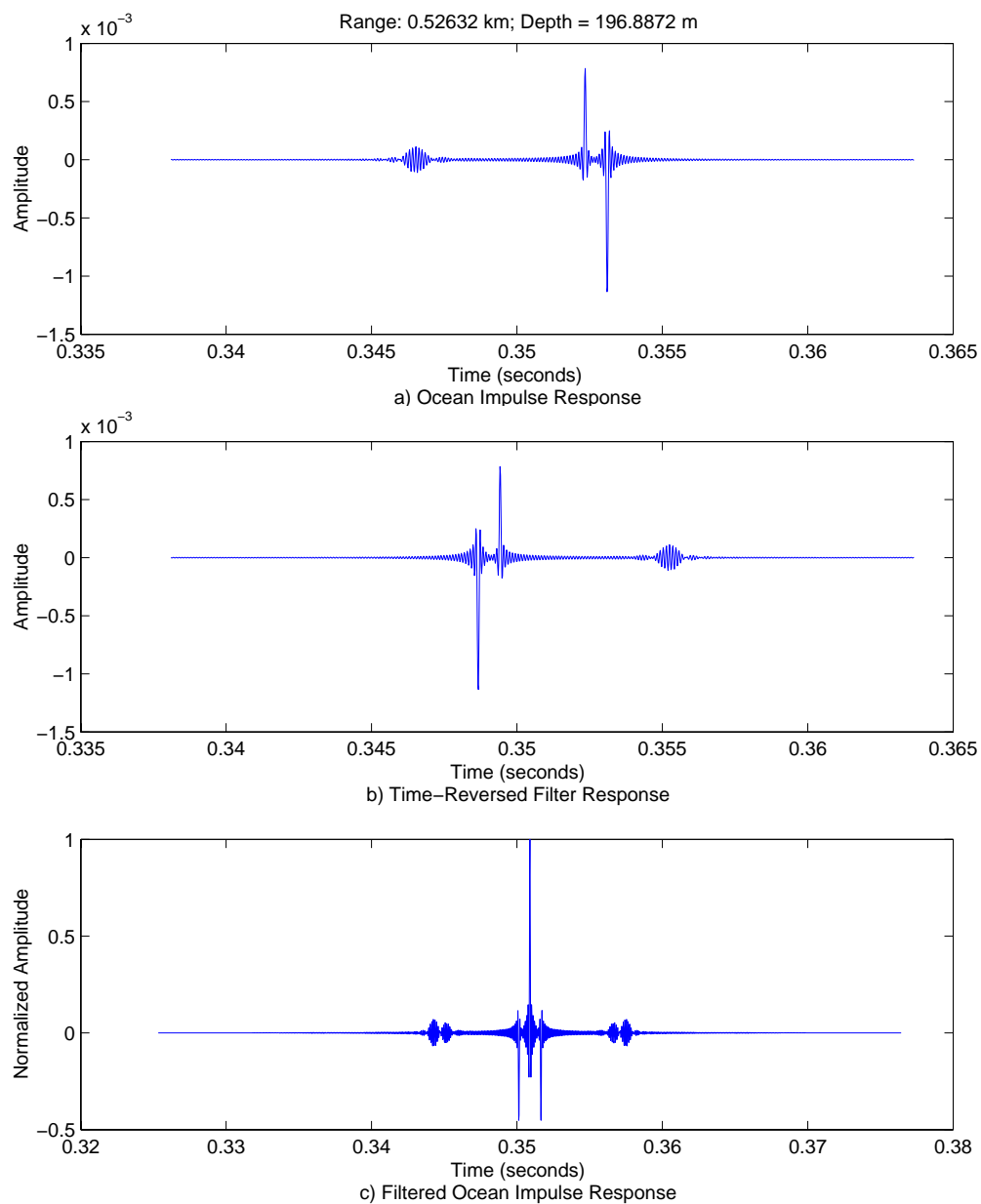
Figure 25.   Passive Time-reversed Filter, Case 10

57
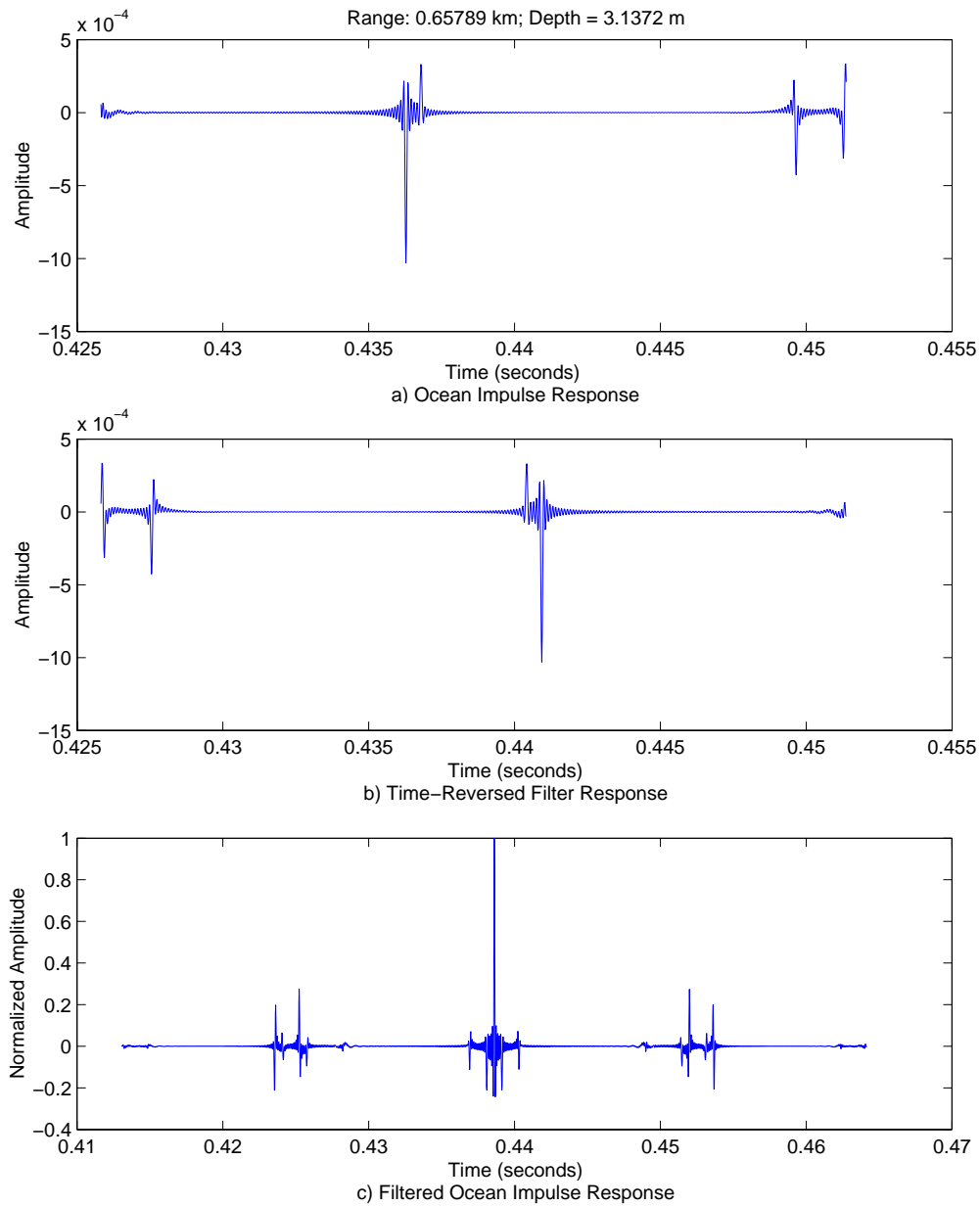
Figure 26. Passive Time-reversed Filter, Case 11
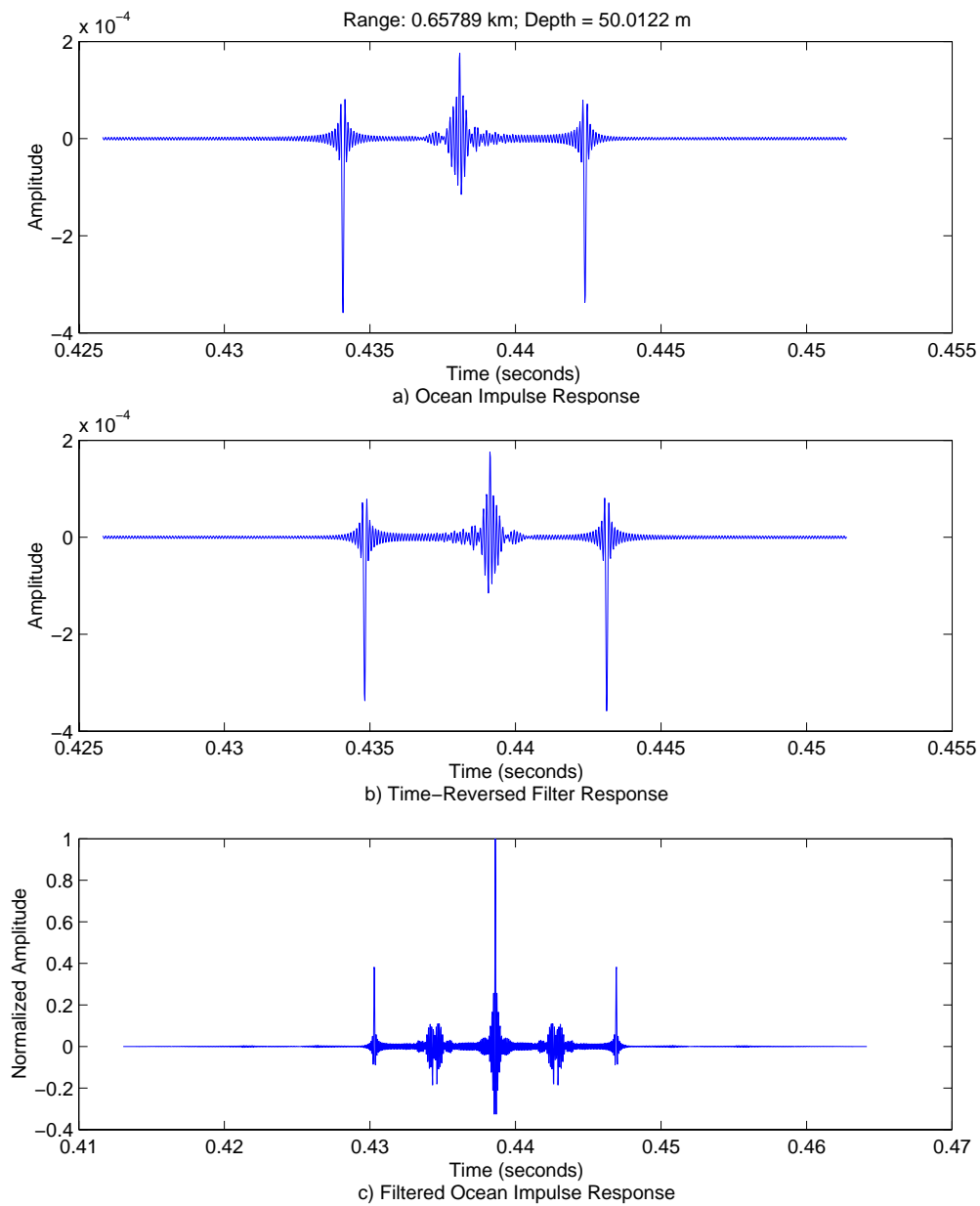
Figure 27.   Passive Time-reversed Filter, Case 12
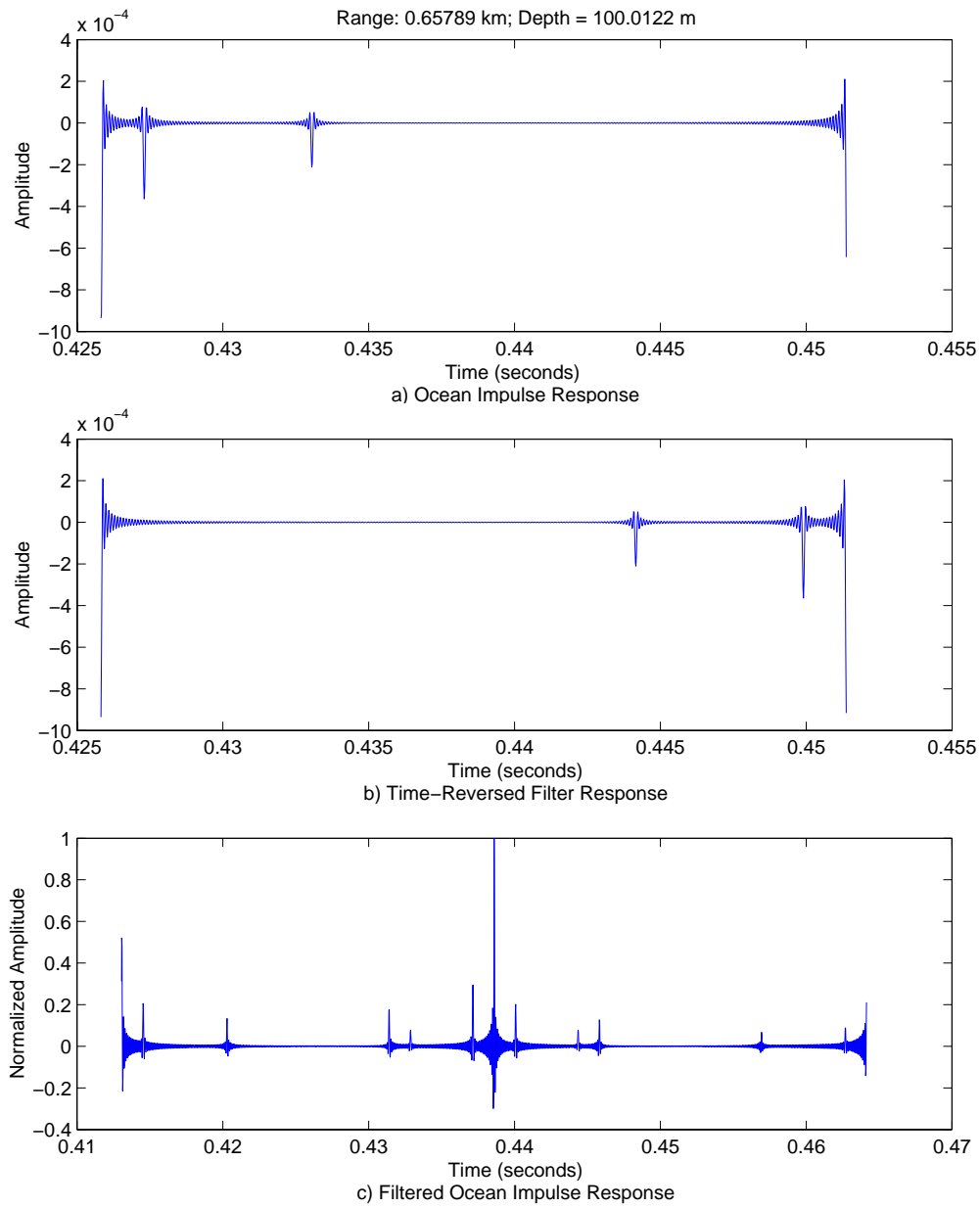
Figure 28.   Passive Time-reversed Filter, Case 13
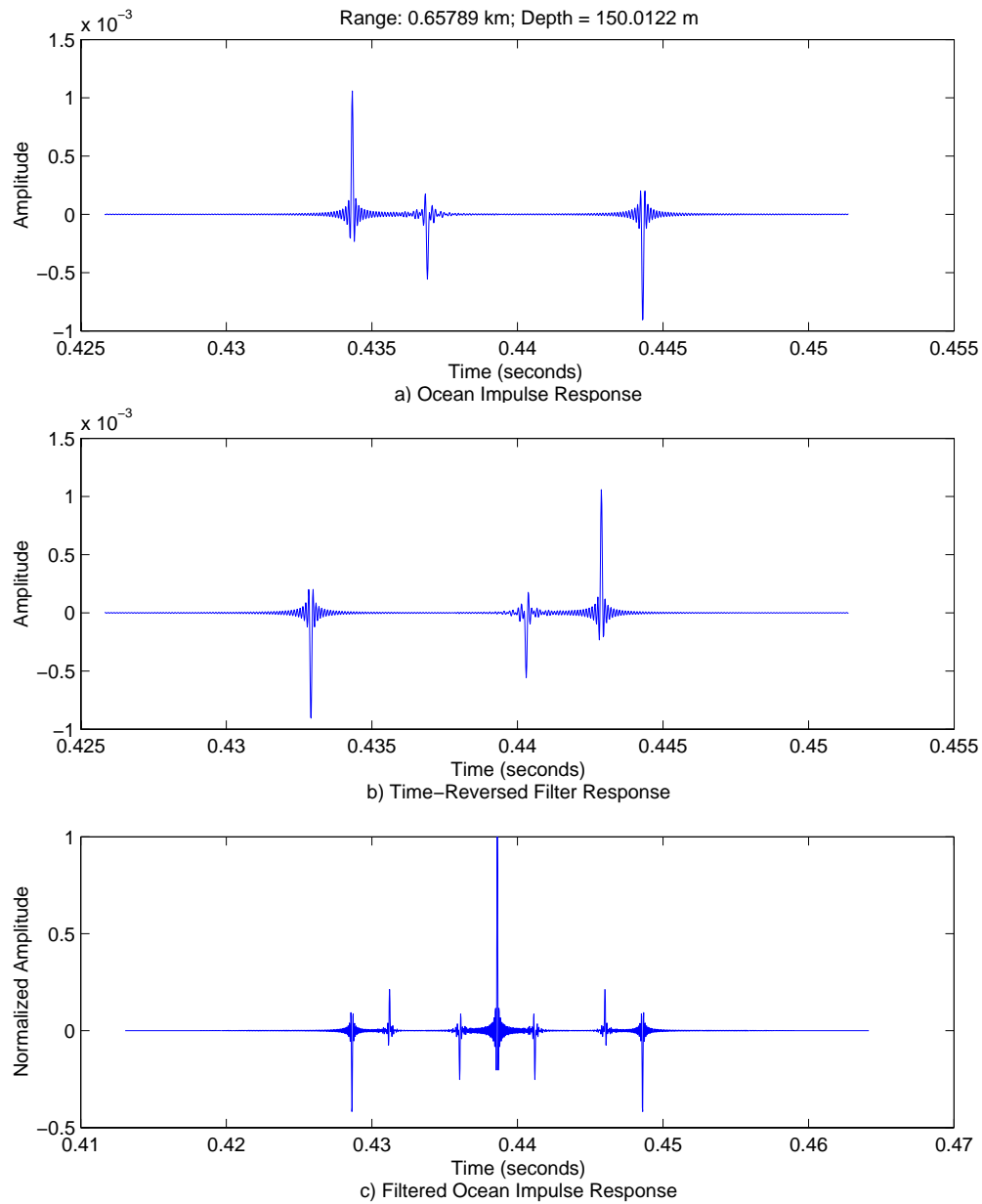
Figure 29.   Passive Time-reversed Filter, Case 14
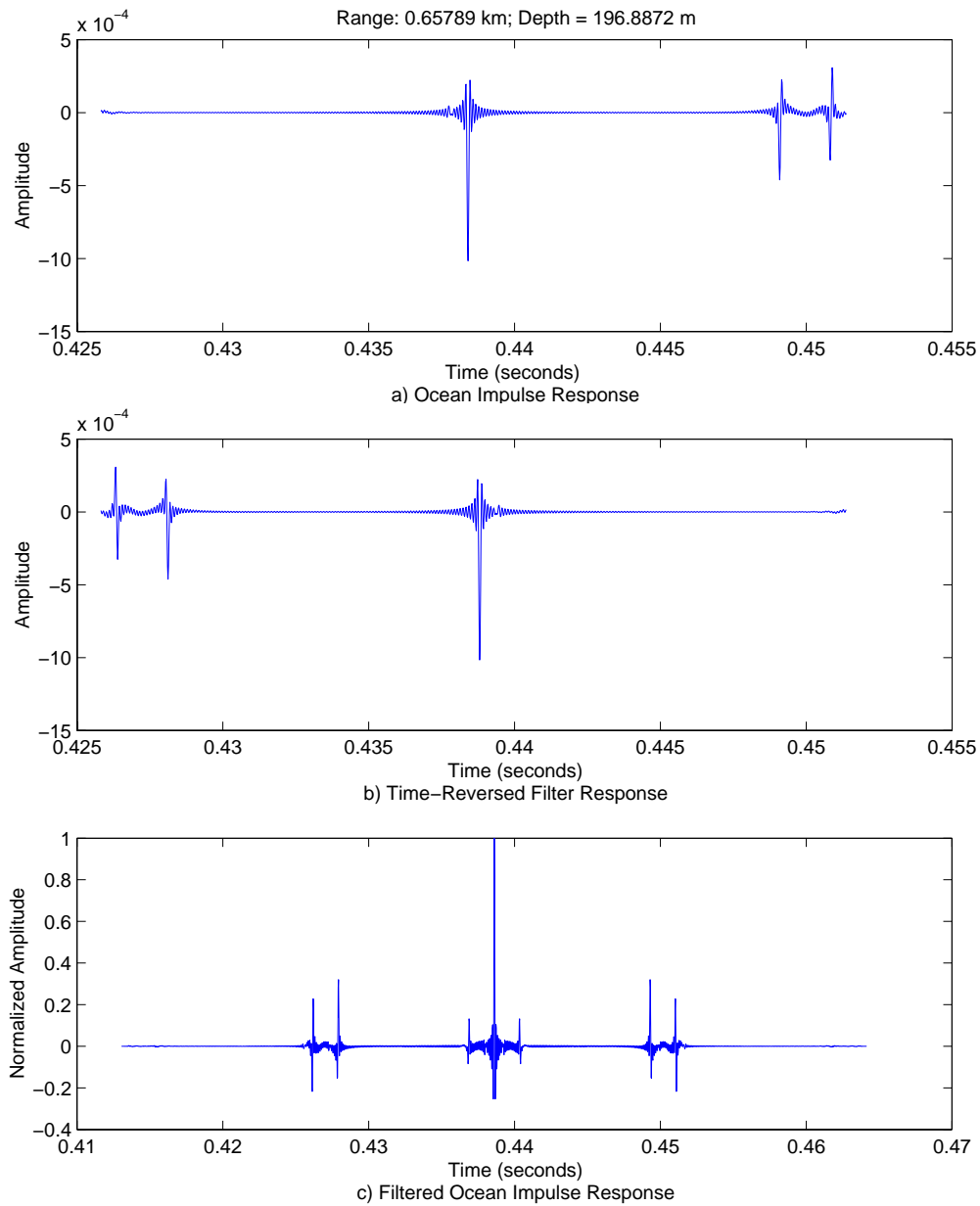
Figure 30.   Passive Time-reversed Filter. Case 15
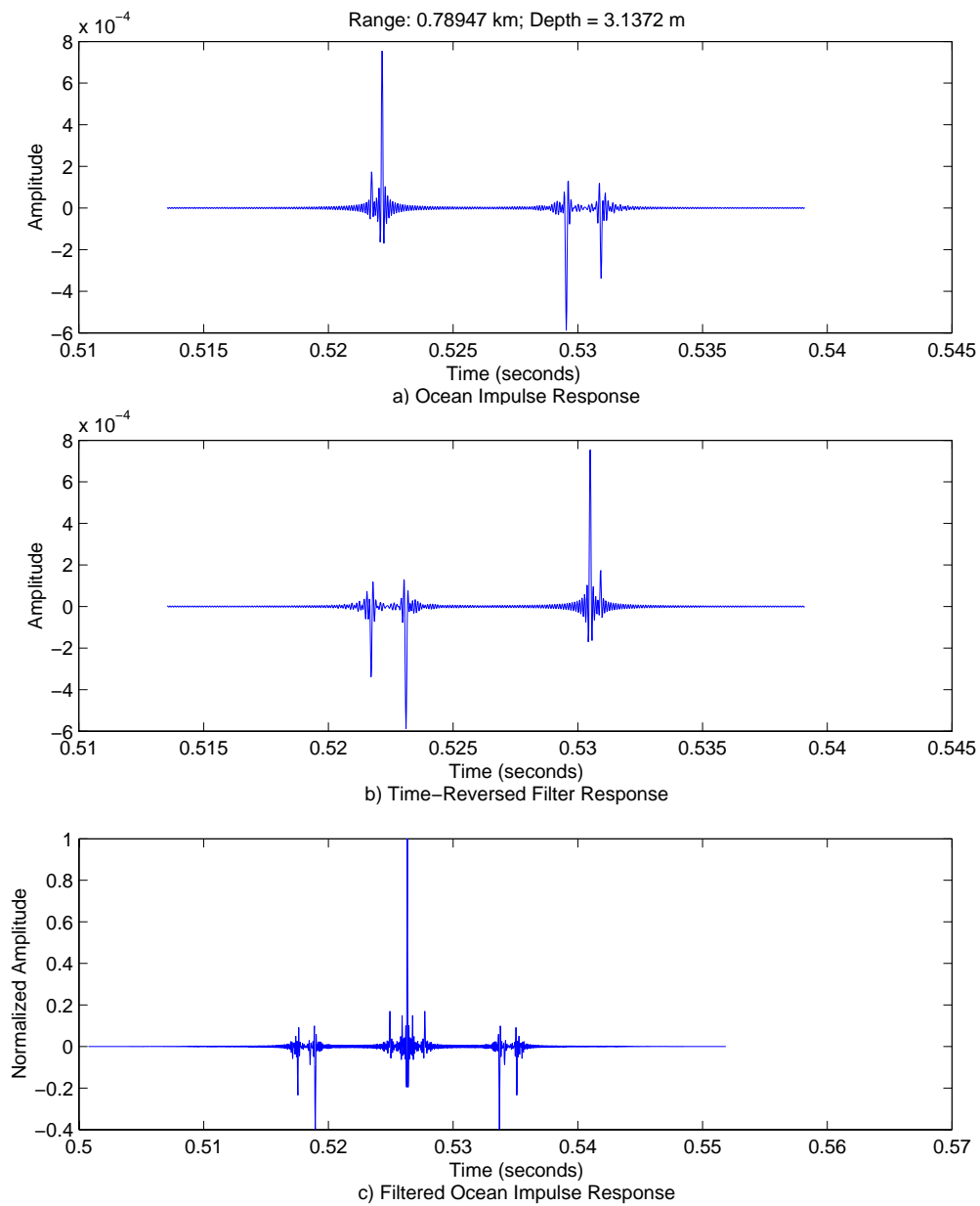
Figure 31.   Passive Time-reversed Filter, Case 16
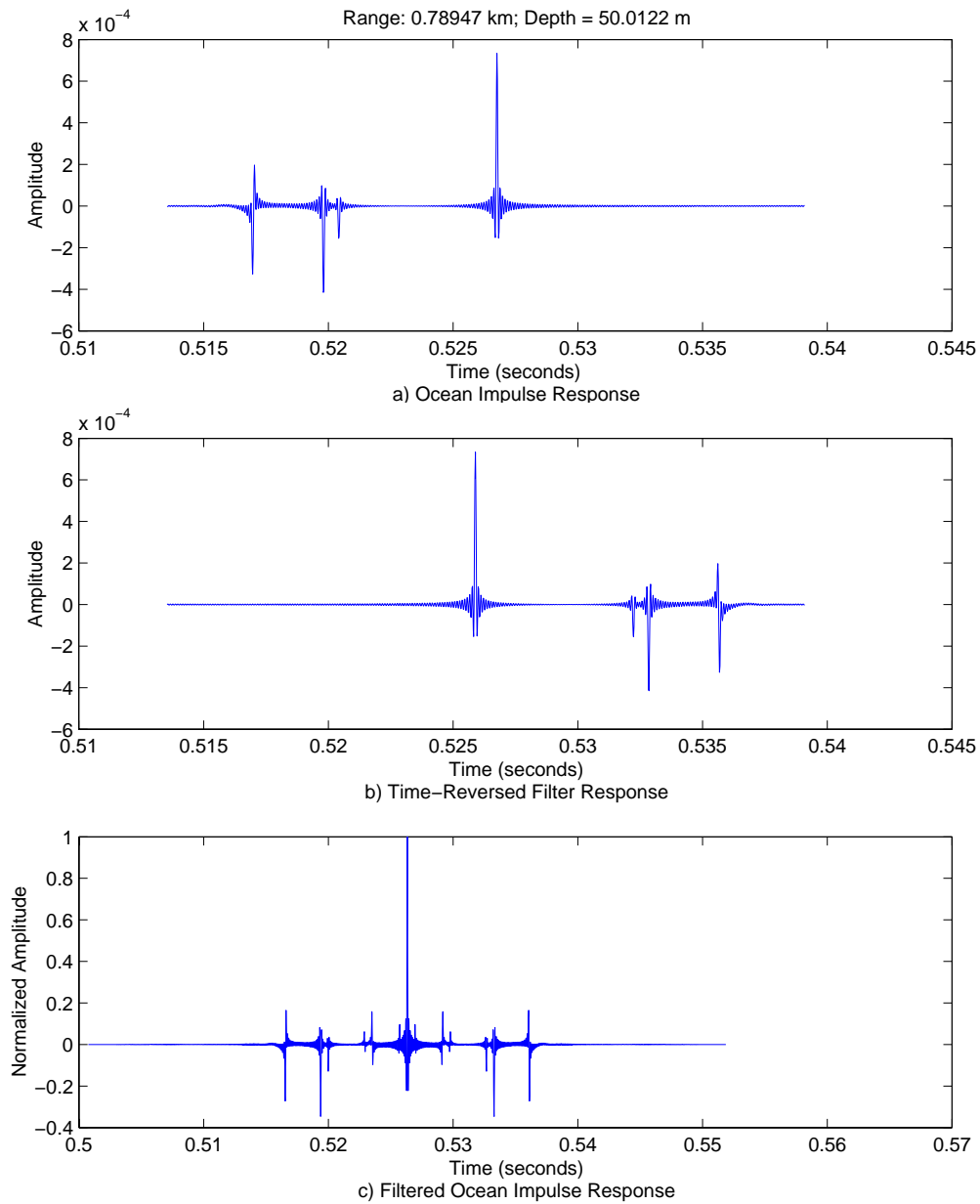
Figure 32.   Passive Time-reversed Filter, Case 17
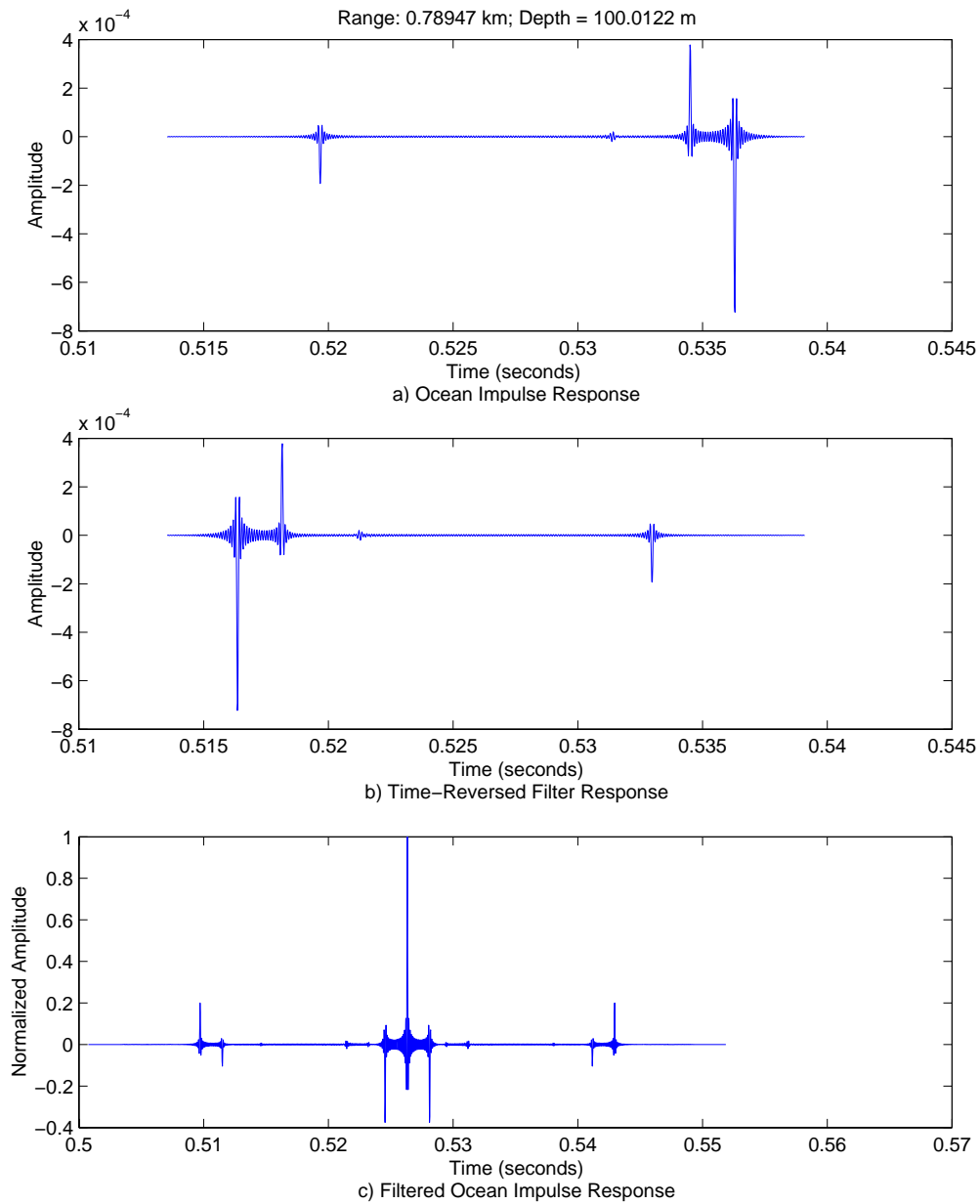
Figure 33.   Passive Time-reversed Filter, Case 18
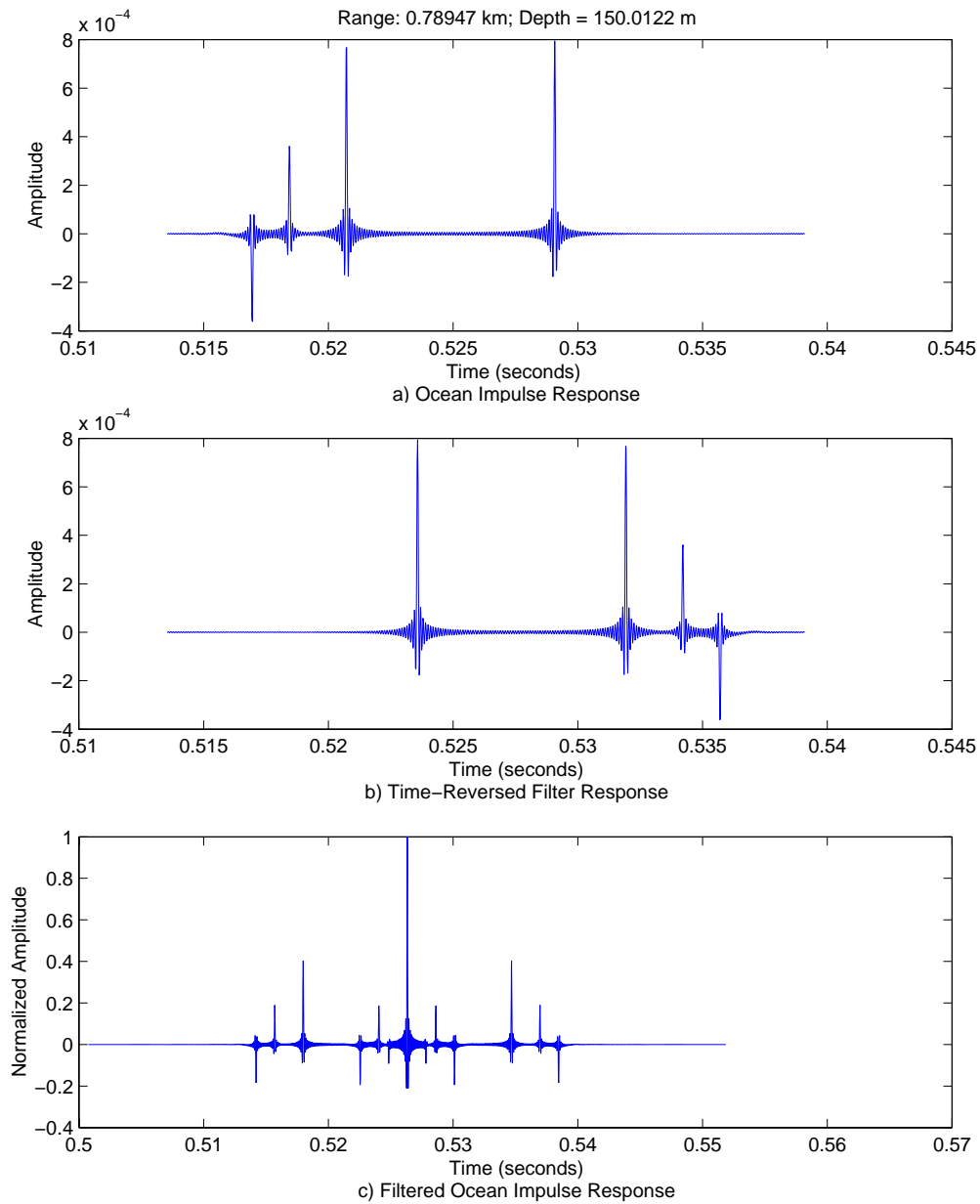
Figure 34.　Passive Time-reversed Filter, Case 19
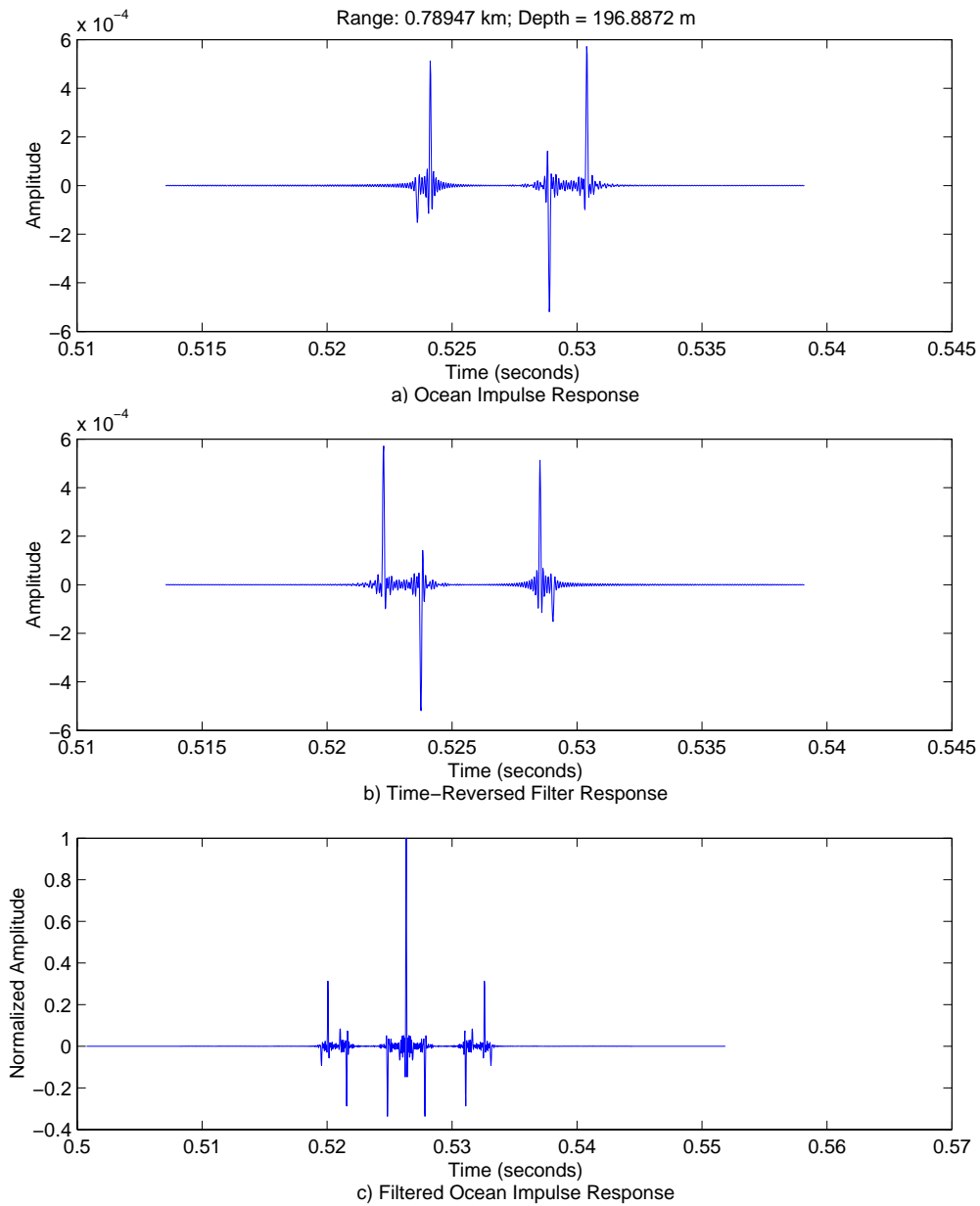
Figure 35.   Passive Time-reversed Filter, Case 20
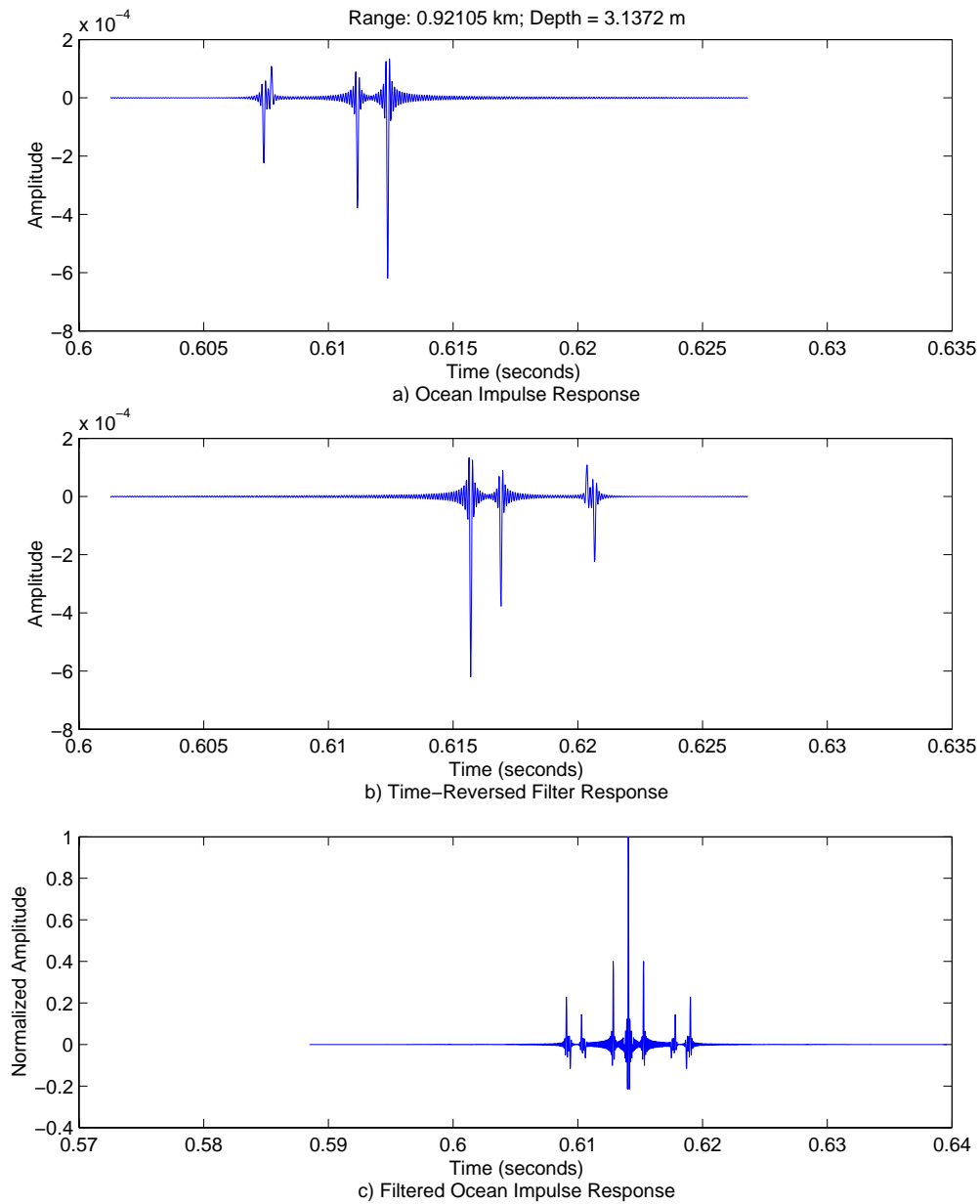
Figure 36.   Passive Time-reversed Filter, Case 21
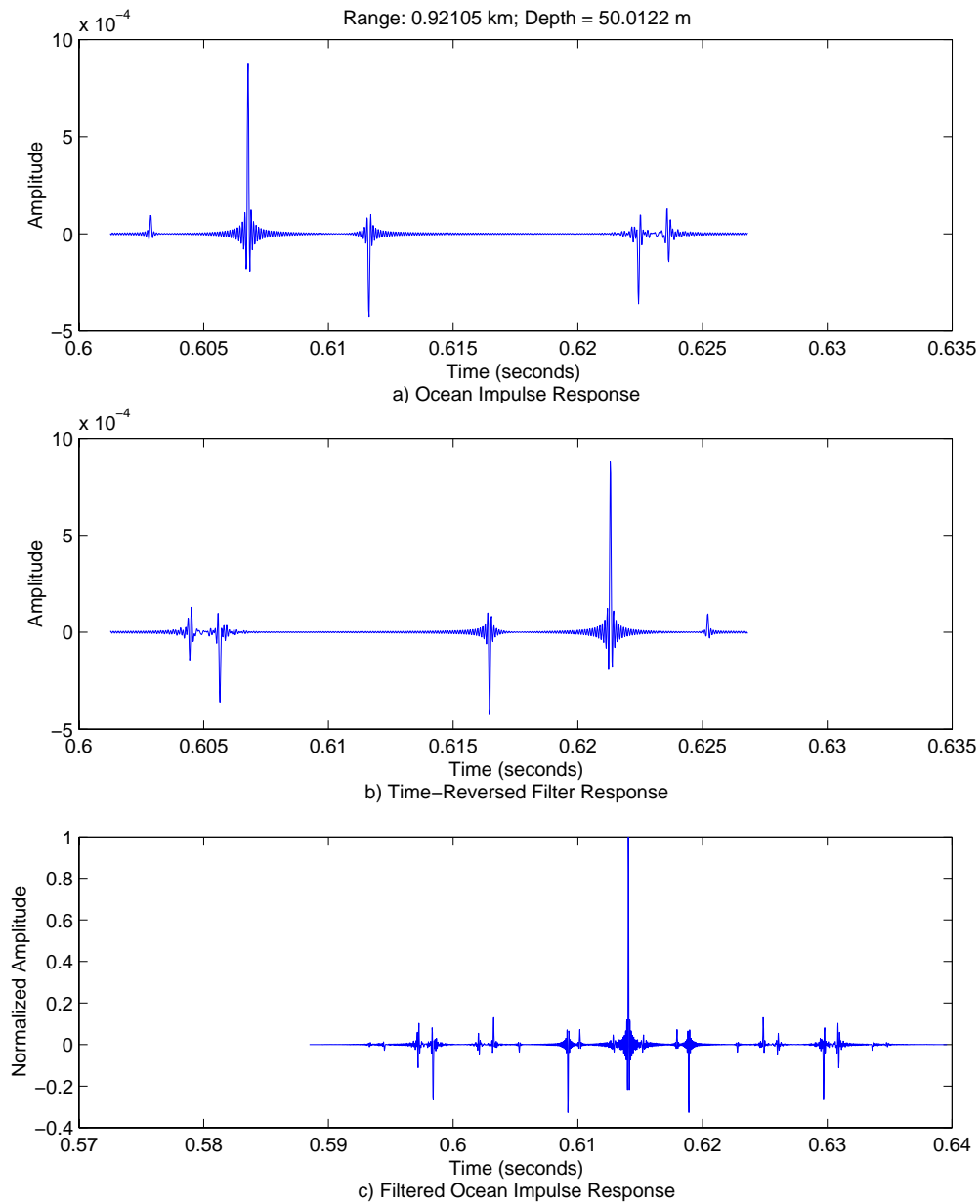
Figure 37.   Passive Time-reversed Filter, Case 22
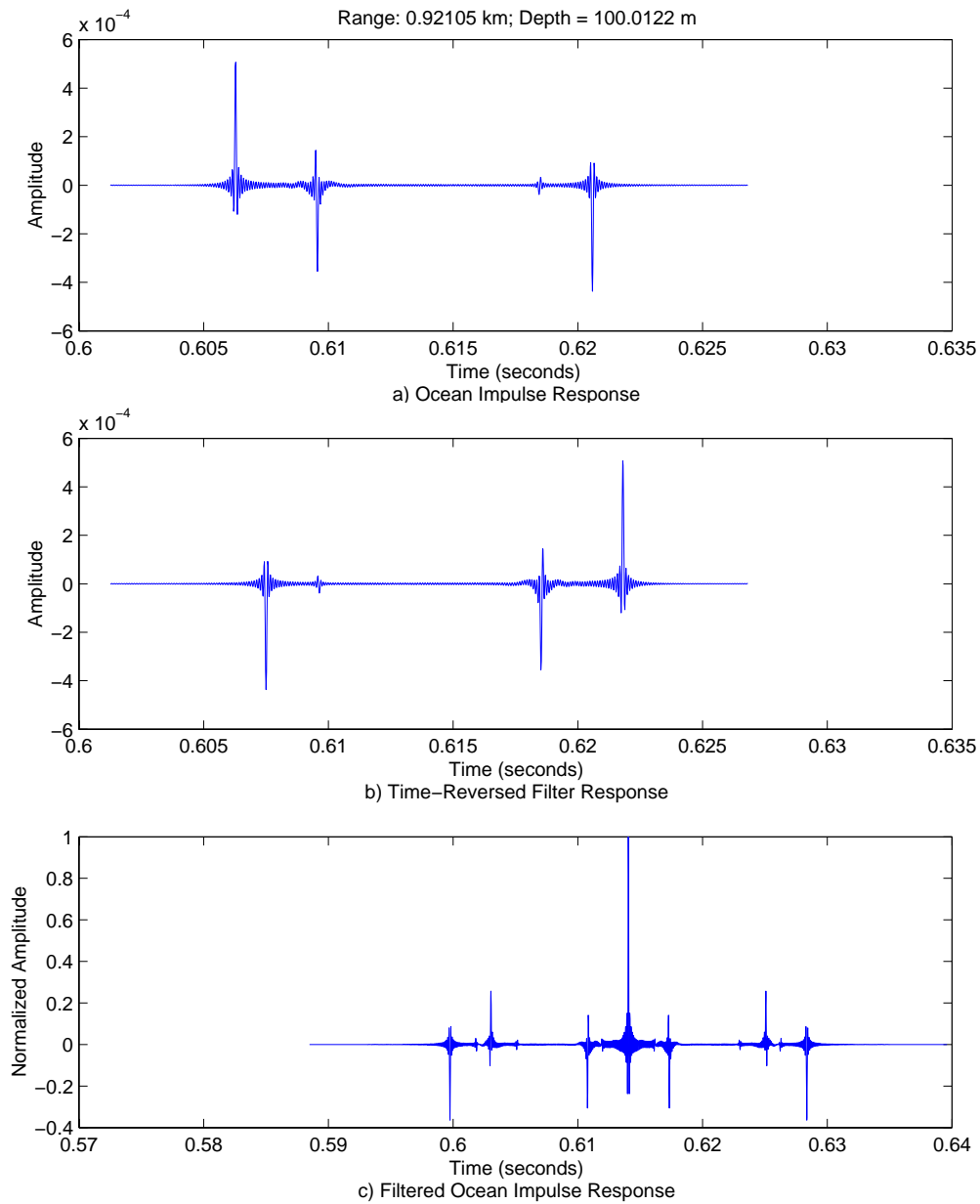
Figure 38.   Passive Time-reversed Filter, Case 23
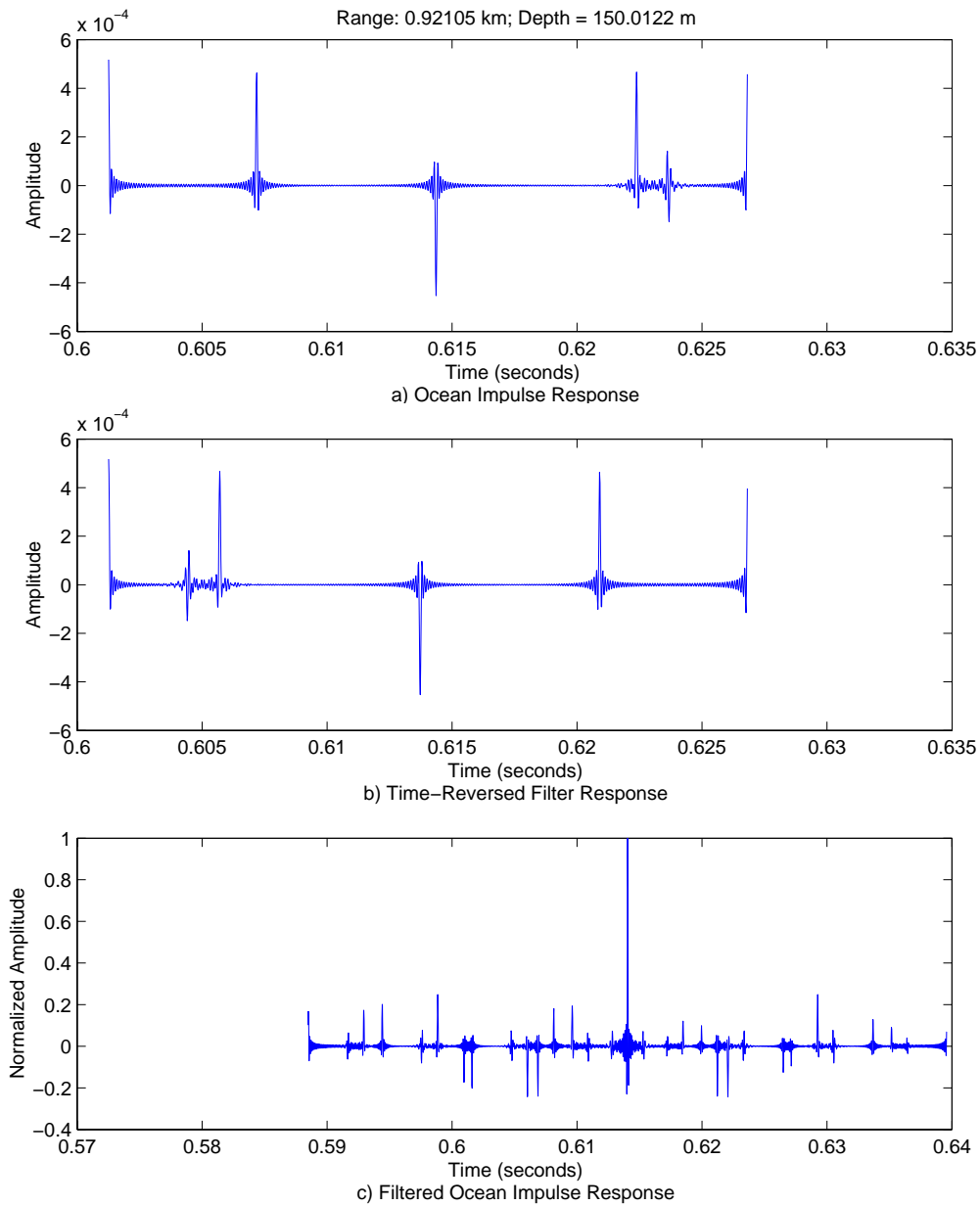
Figure 39.   Passive Time-reversed Filter, Case 24
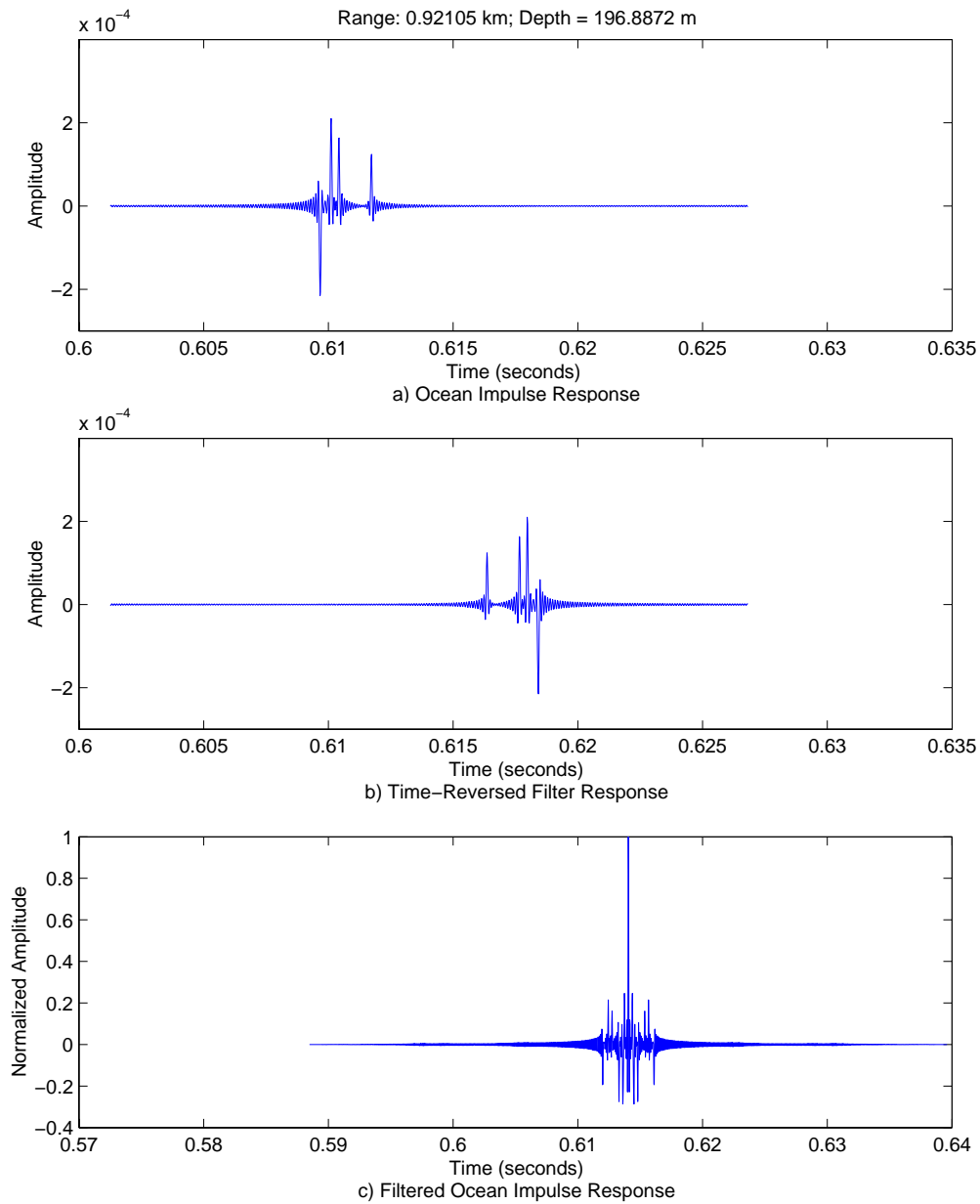
Figure 40.   Passive Time-reversed Filter, Case 25
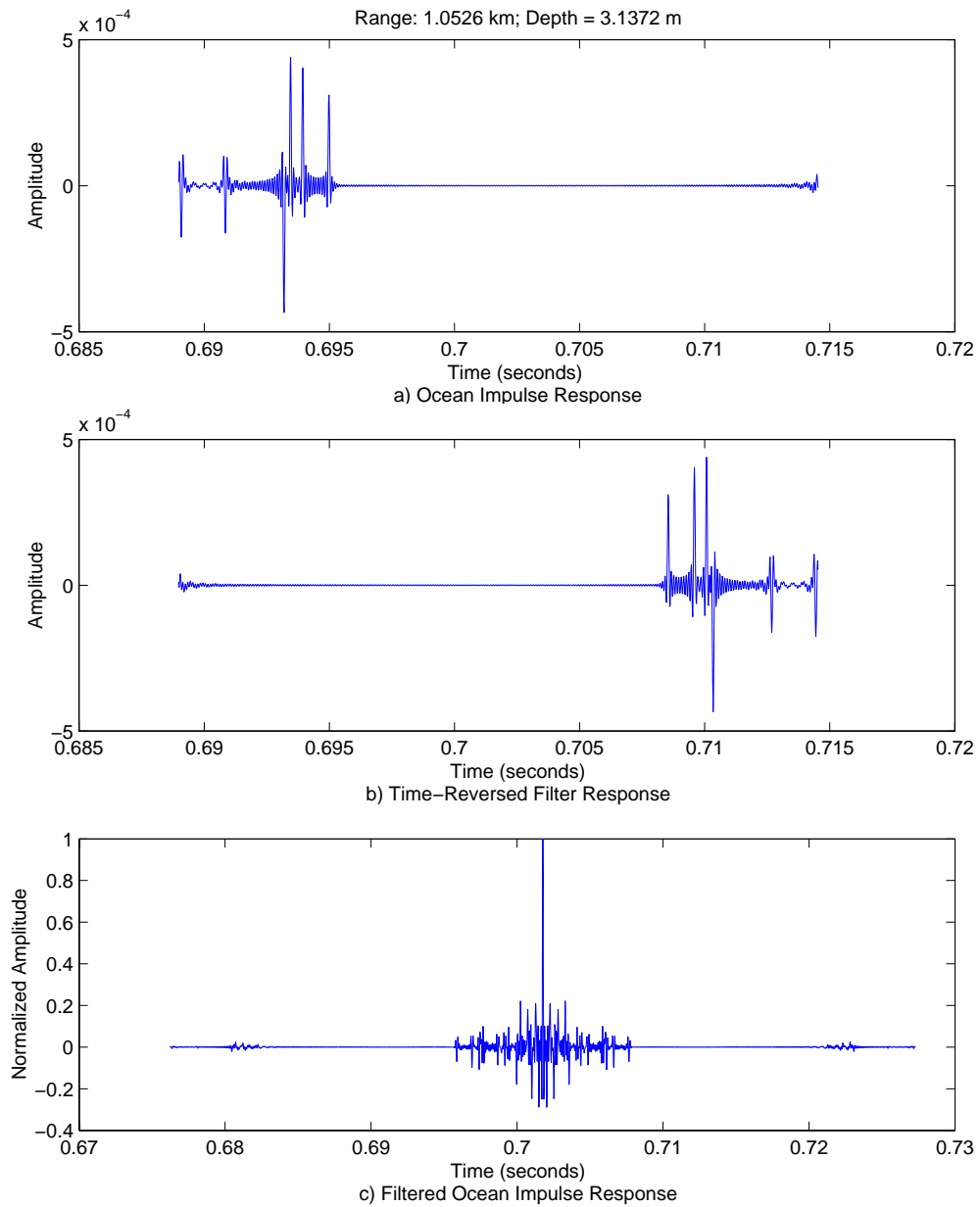
Figure 41.   Passive Time-reversed Filter, Case 26
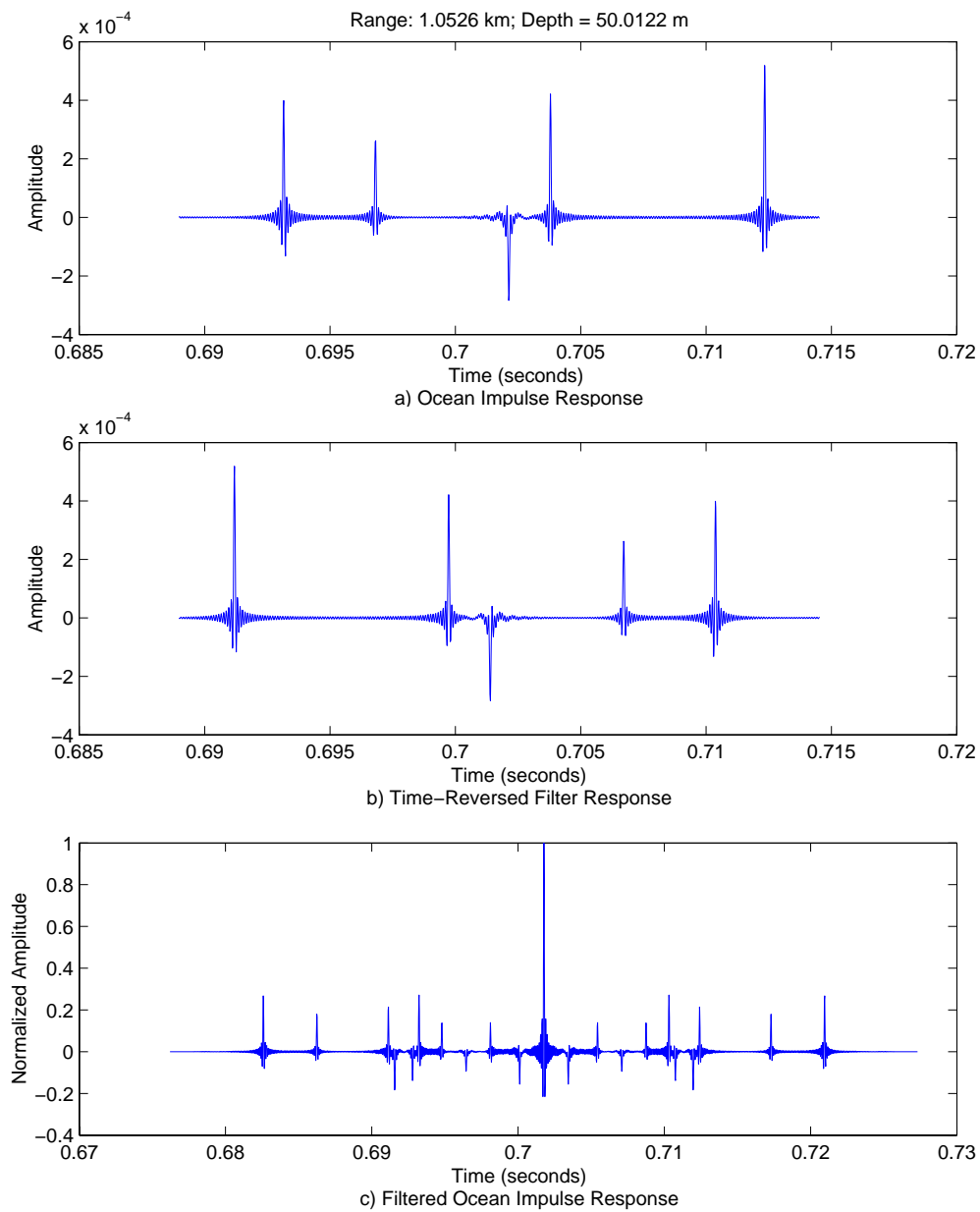
Figure 42.   Passive Time-reversed Filter, Case 27
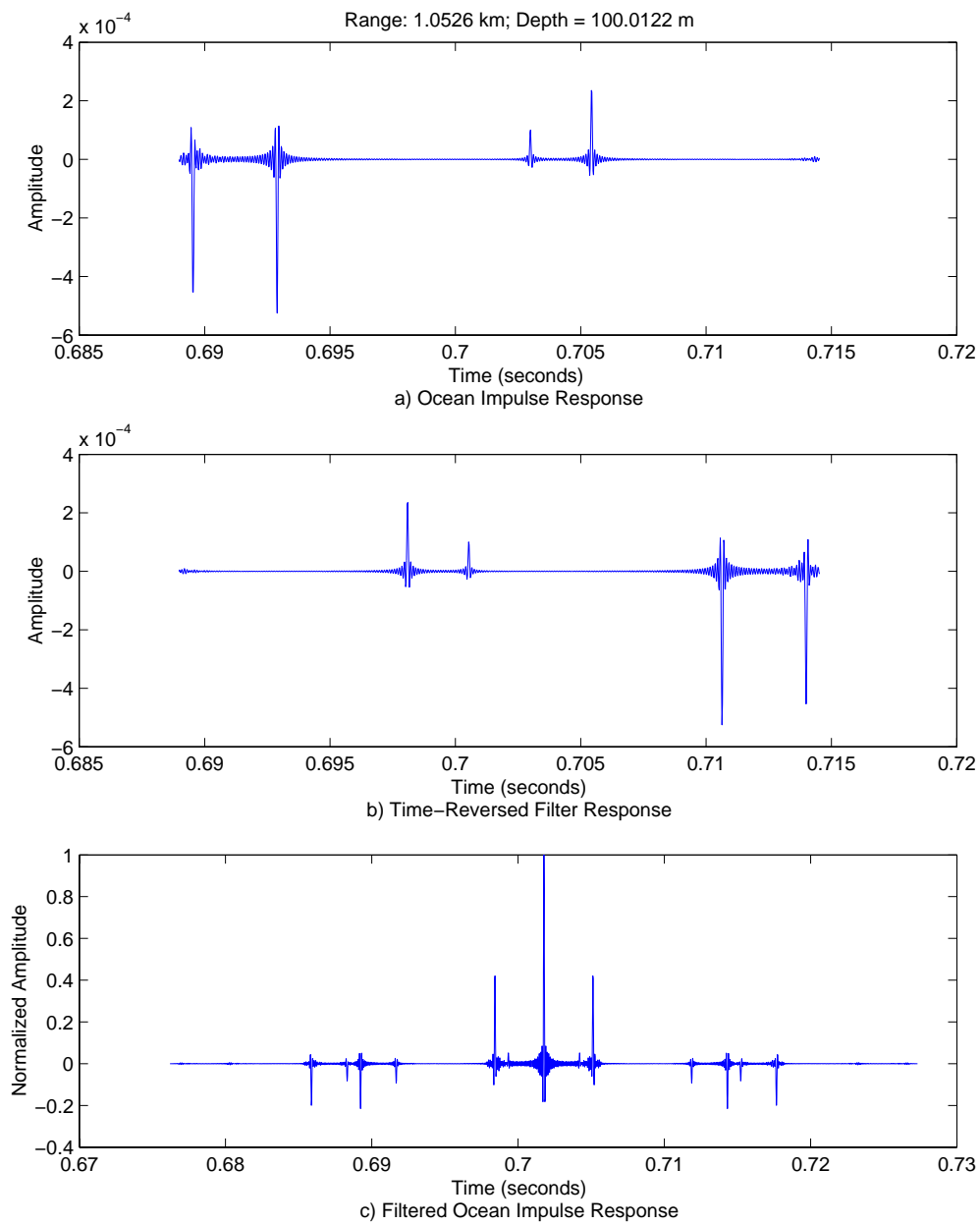
Figure 43.   Passive Time-reversed Filter, Case 28
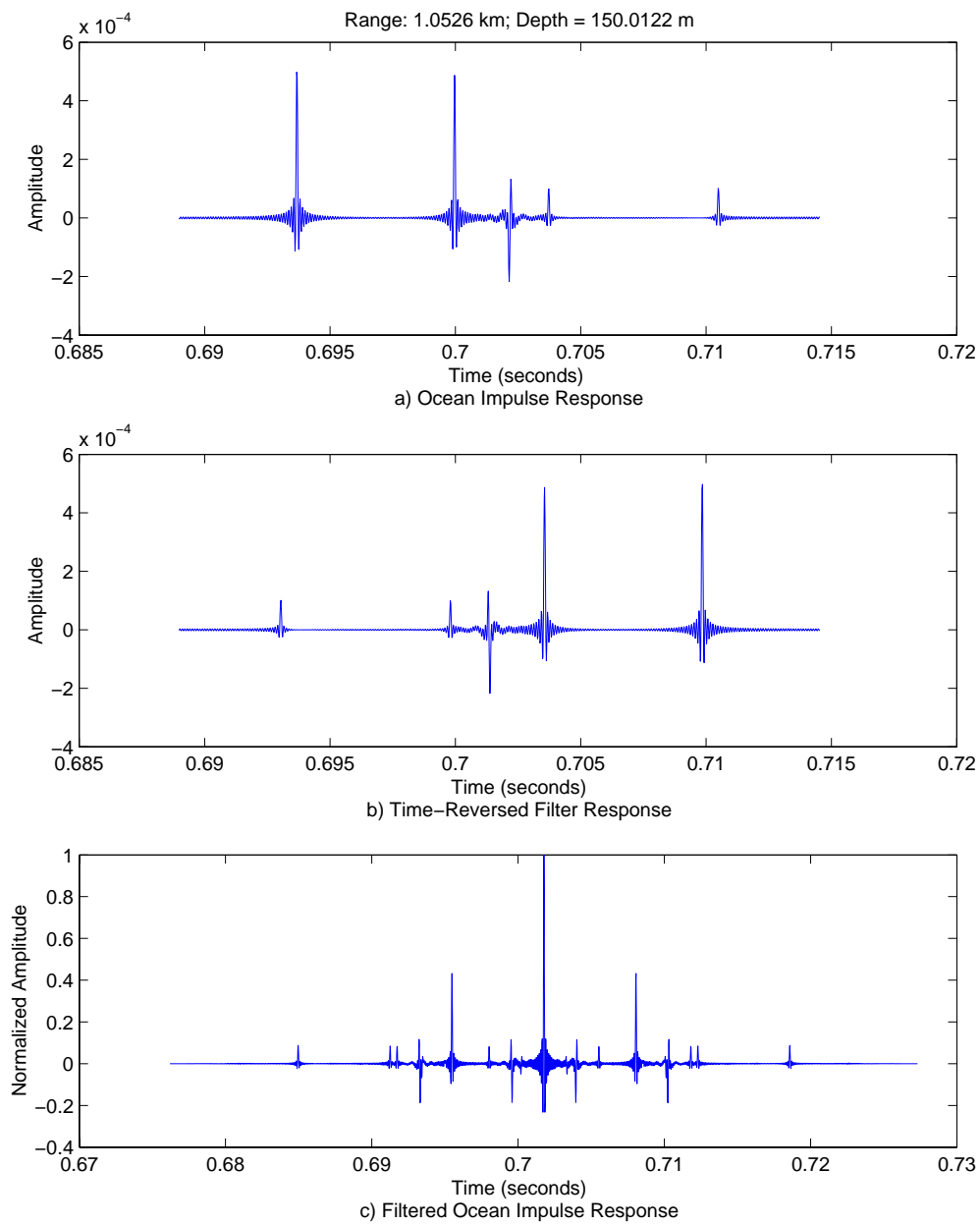
Figure 44.   Passive Time-reversed Filter, Case 29
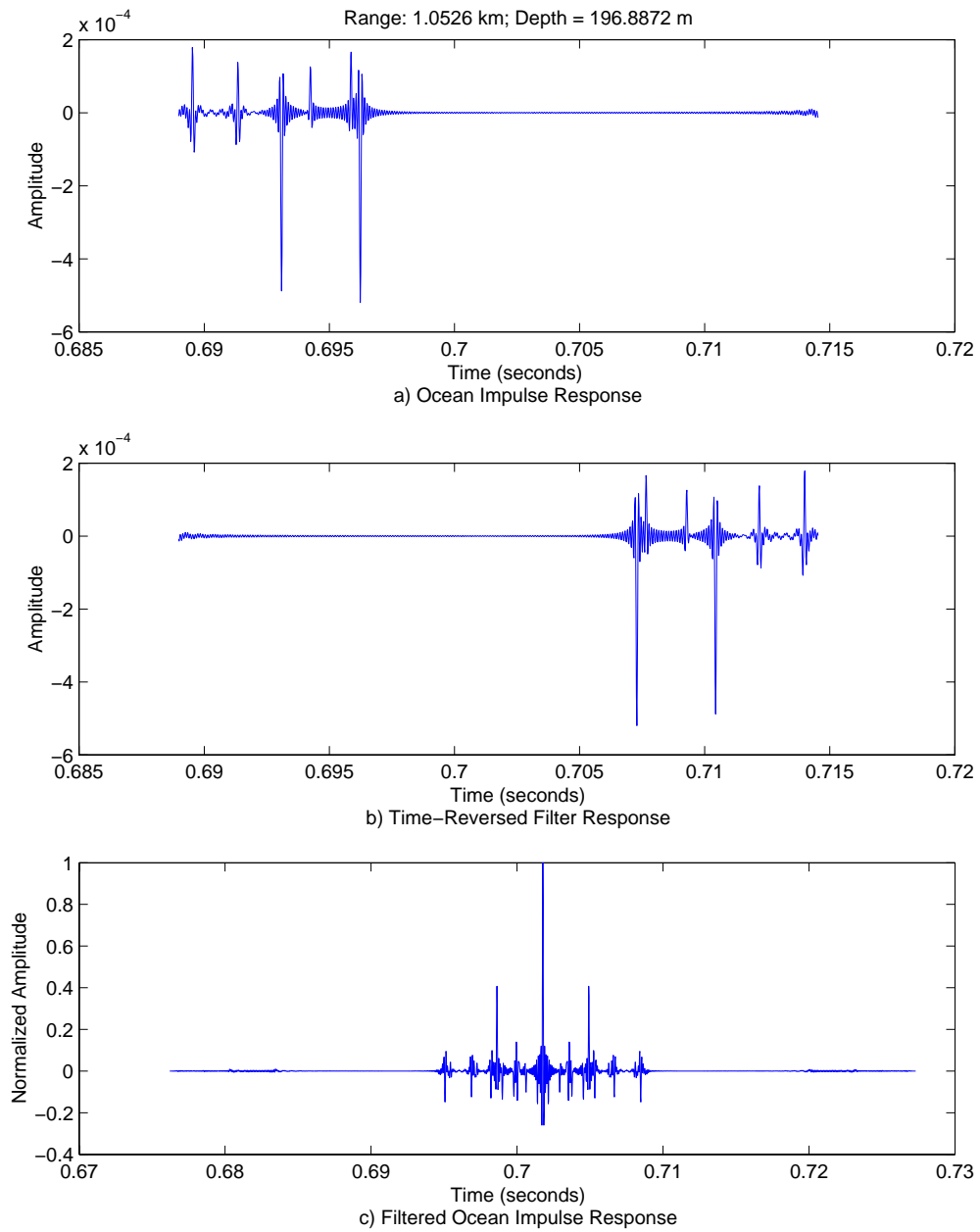
Figure 45.   Passive Time-reversed Filter, Case 30

B.   INVERSE FILTER RESULTS

Figures 46 through 75 contain plots of the ocean impulse response, the inverse filter response, and the filtered ocean response for all thirty test cases. From these plots, it can be seen that the time response of the inverse filter, subfigure b), is highly erratic and that the magnitudes are on the order of hundreds, as opposed to thousandths like the ocean response, subfigure a). These characteristics lead to filter outputs with excessive residual returns.
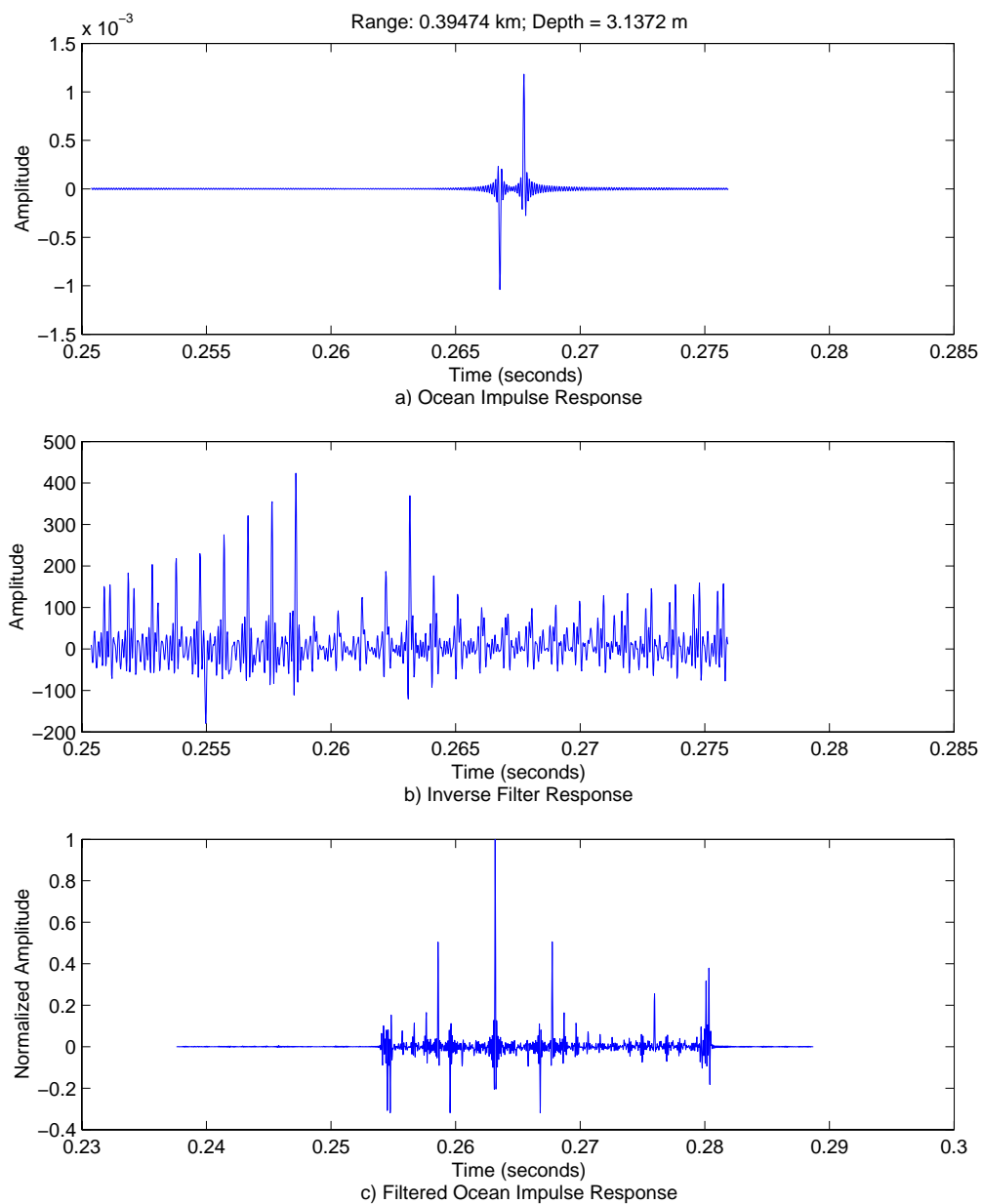
Figure 46.   Inverse Filter, Case 1
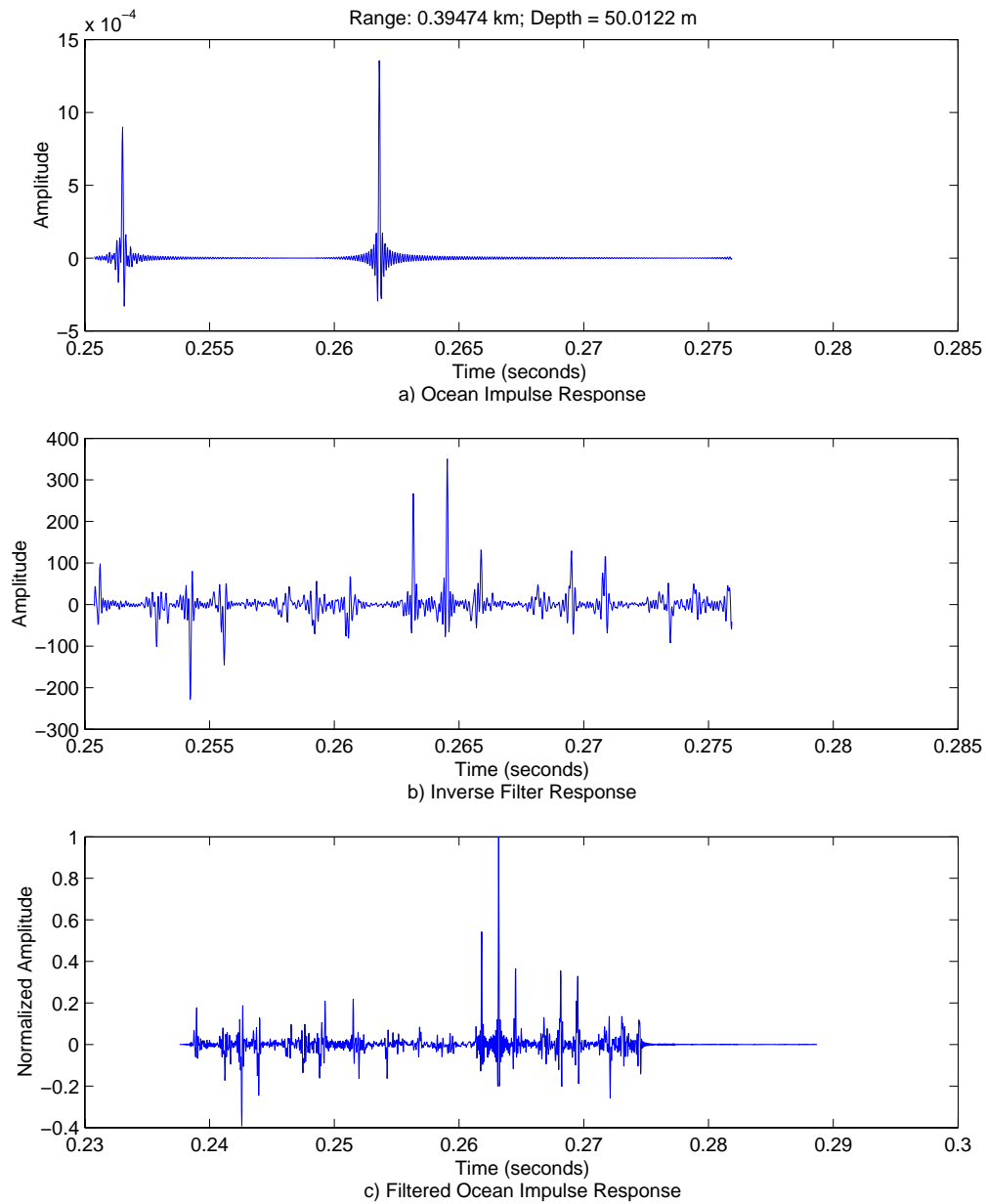
Figure 47. Inverse Filter, Case 2
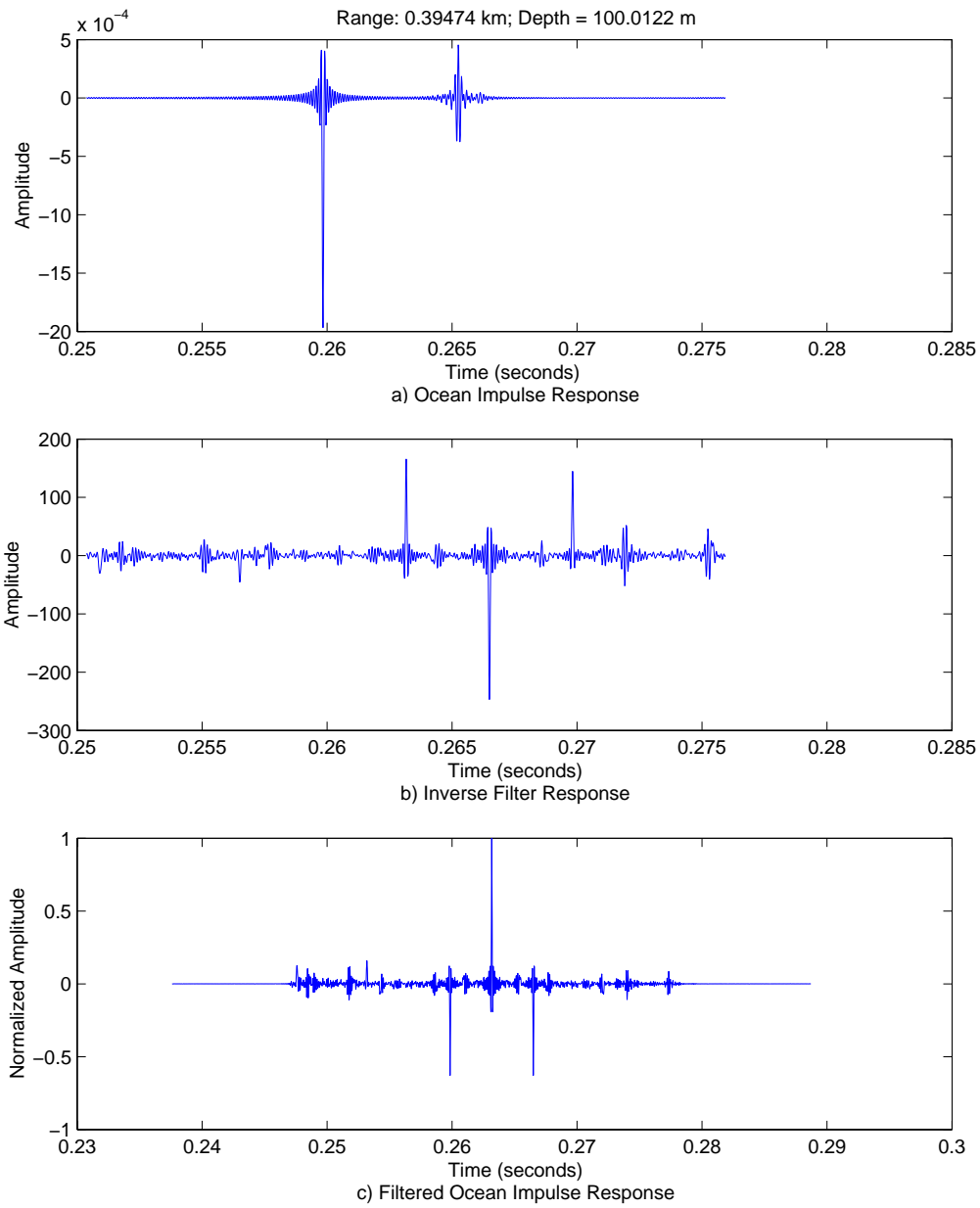
Figure 48.   Inverse Filter, Case 3
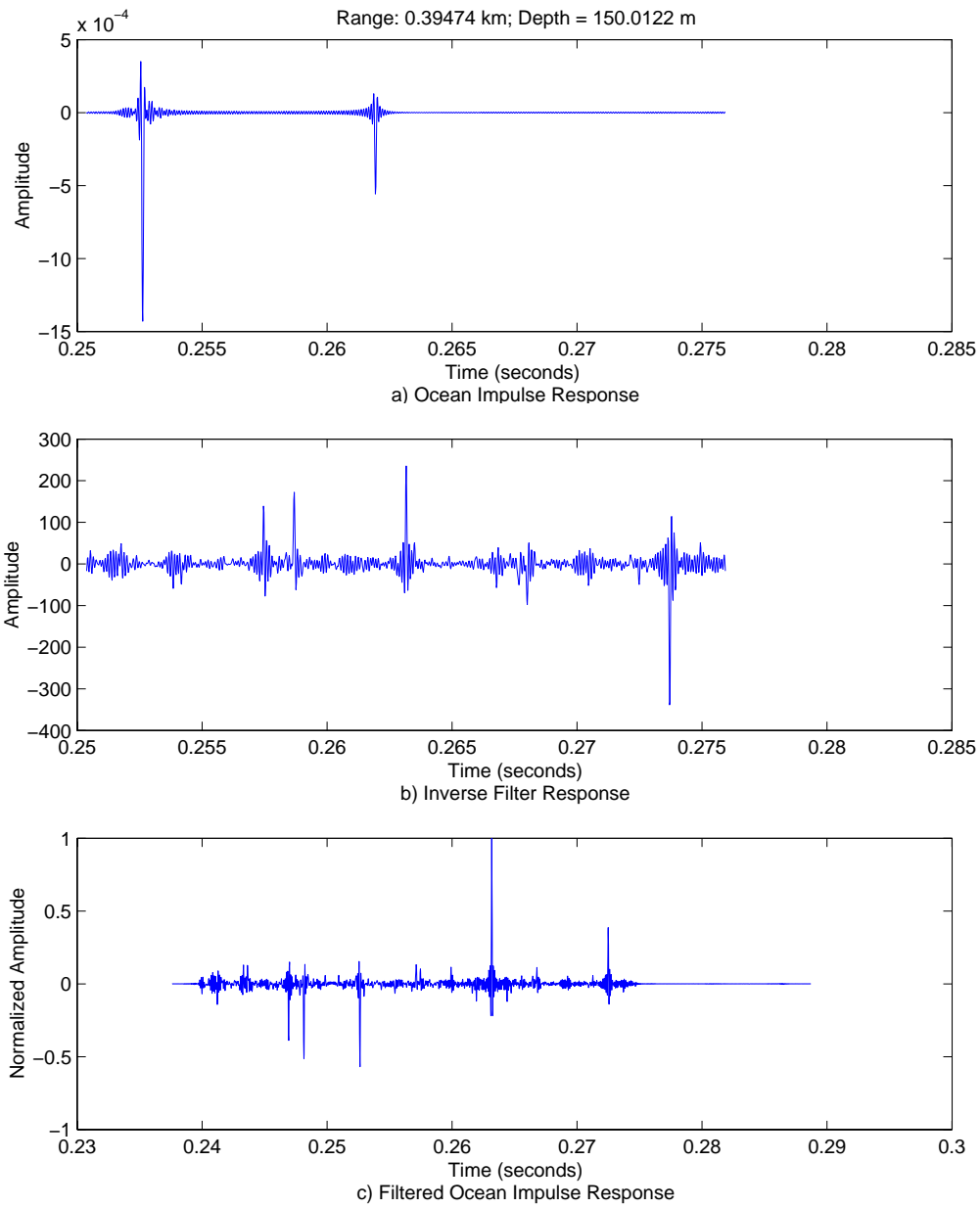
Figure 49.   Inverse Filter, Case 4
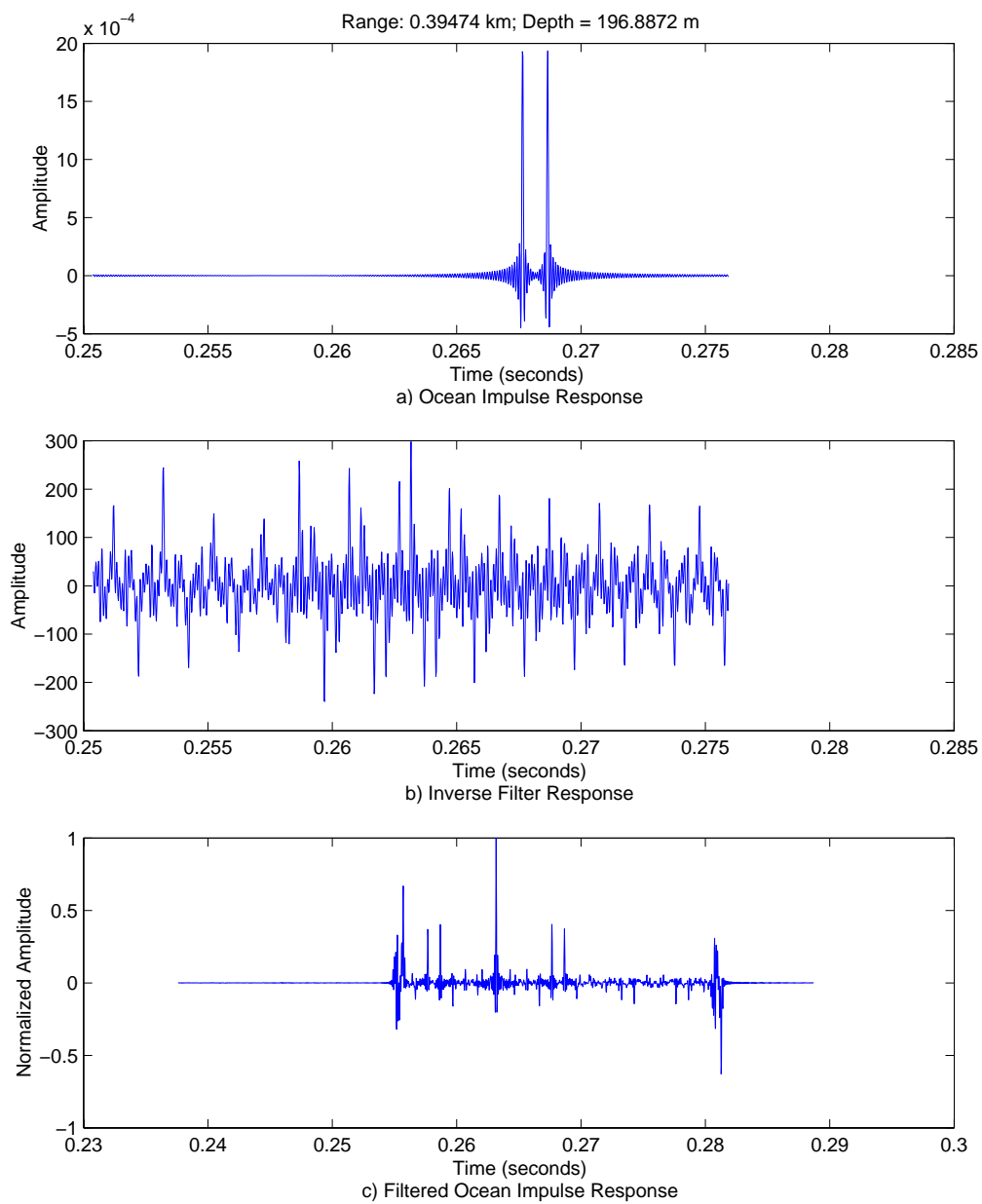
Figure 50.   Inverse Filter, Case 5
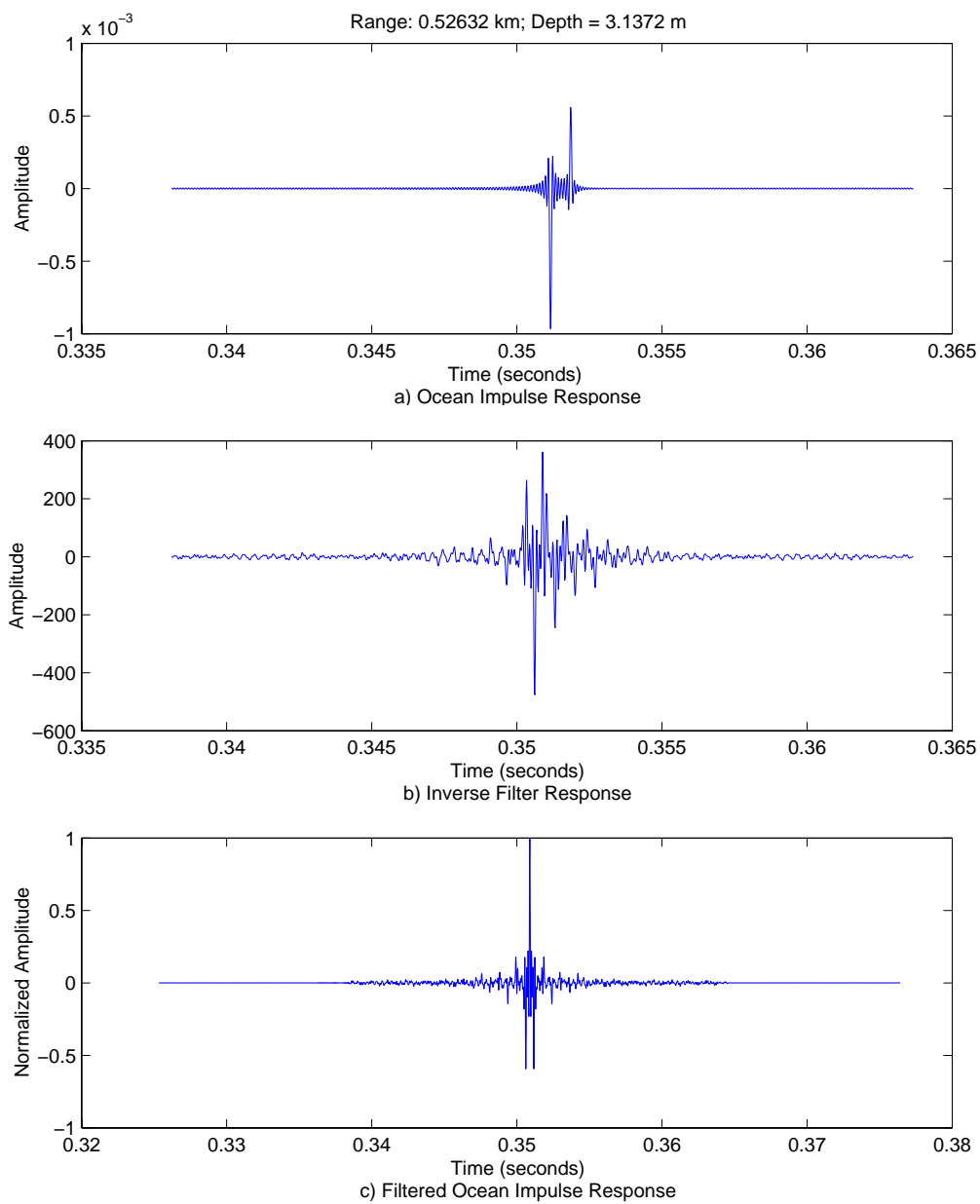
Figure 51.   Inverse Filter, Case 6
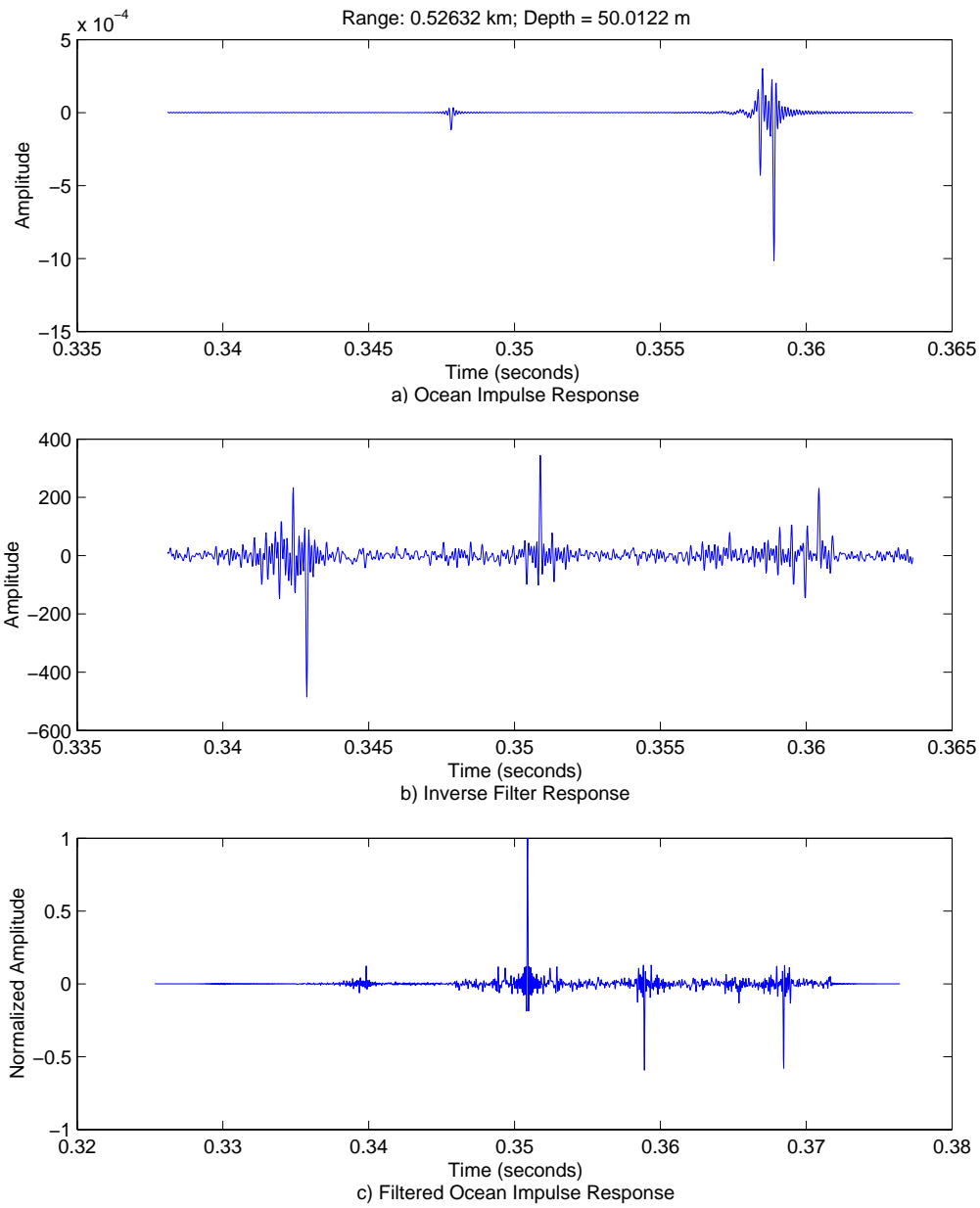
Figure 52.   Inverse Filter, Case 7
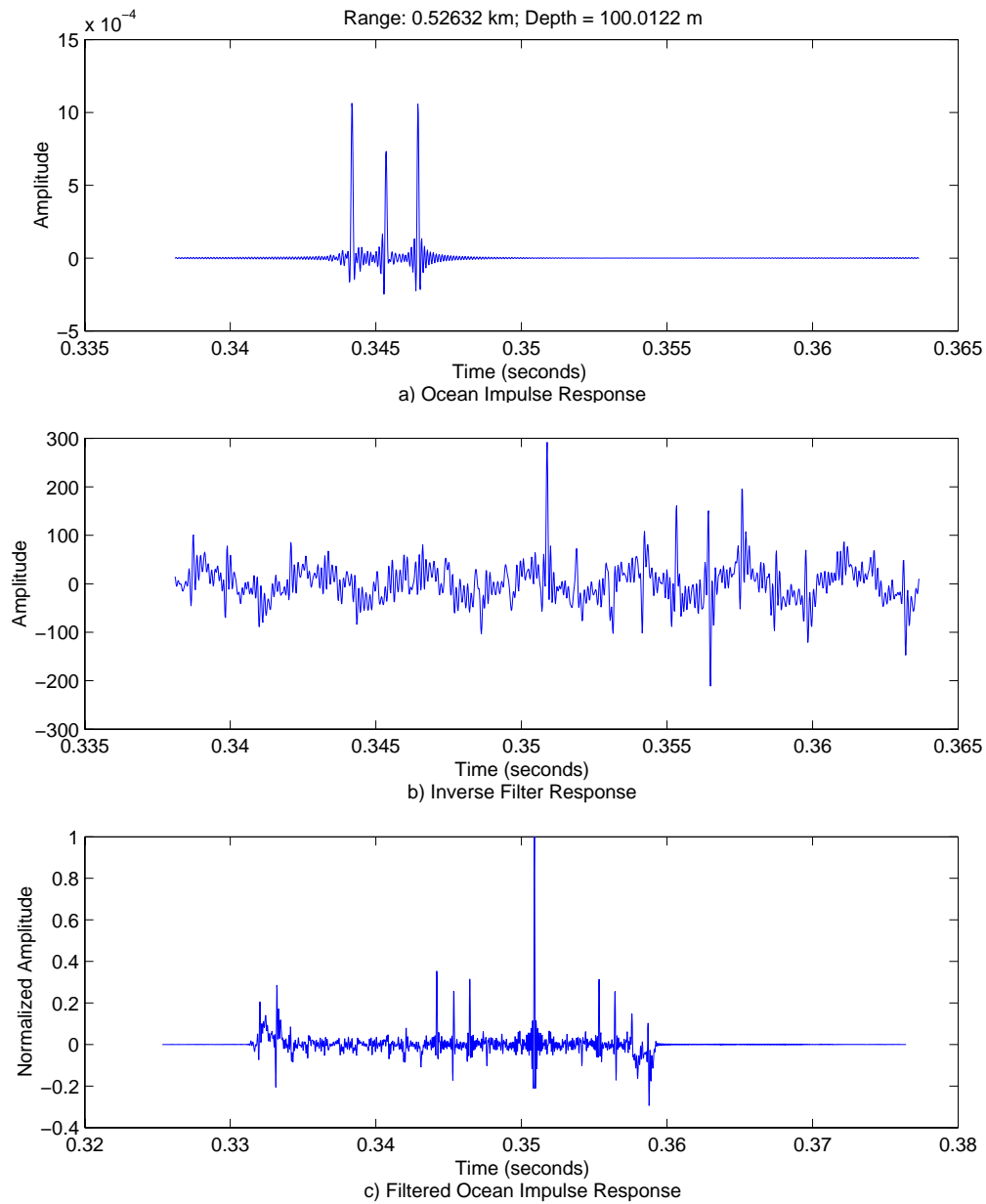
Figure 53.   Inverse Filter, Case 8
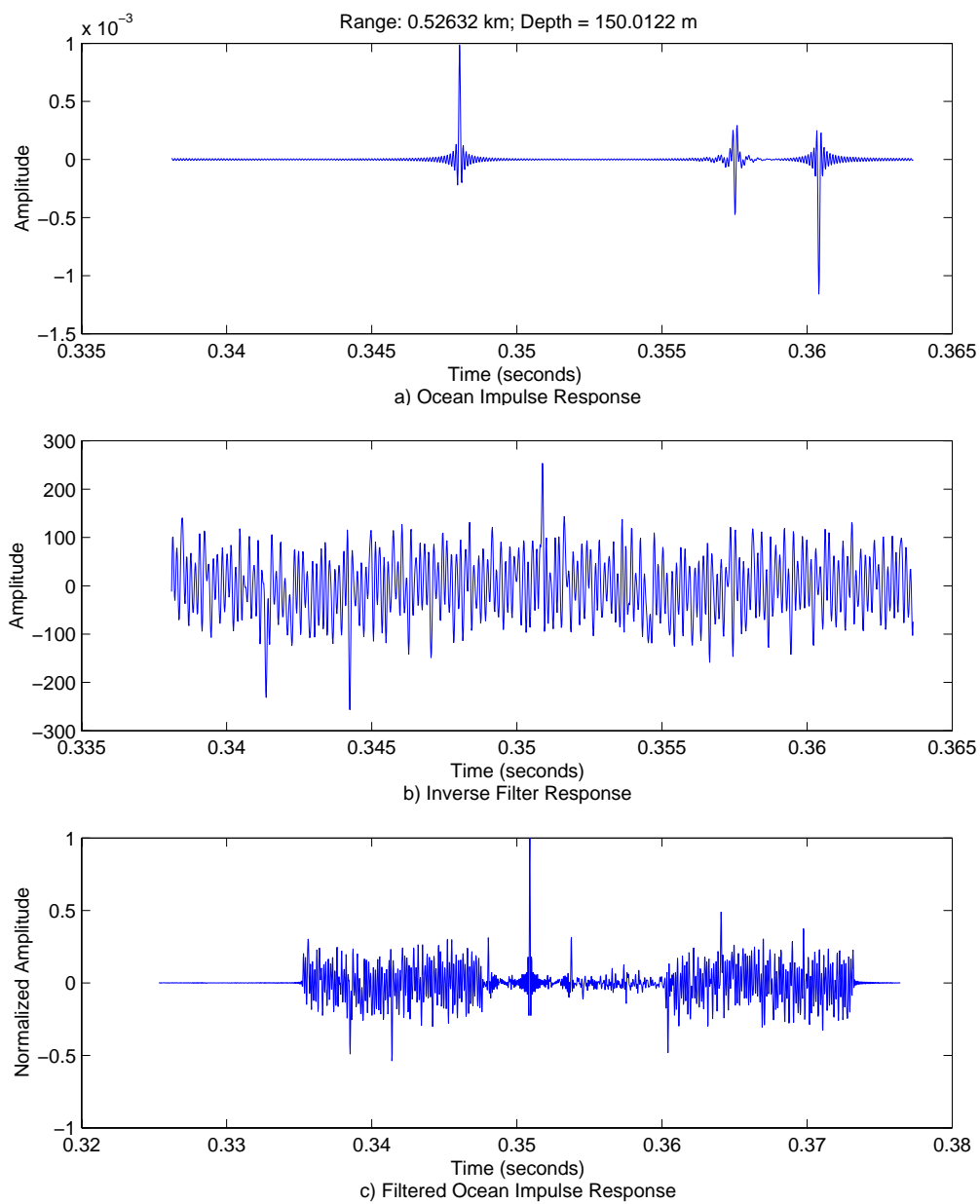
Figure 54.   Inverse Filter, Case 9
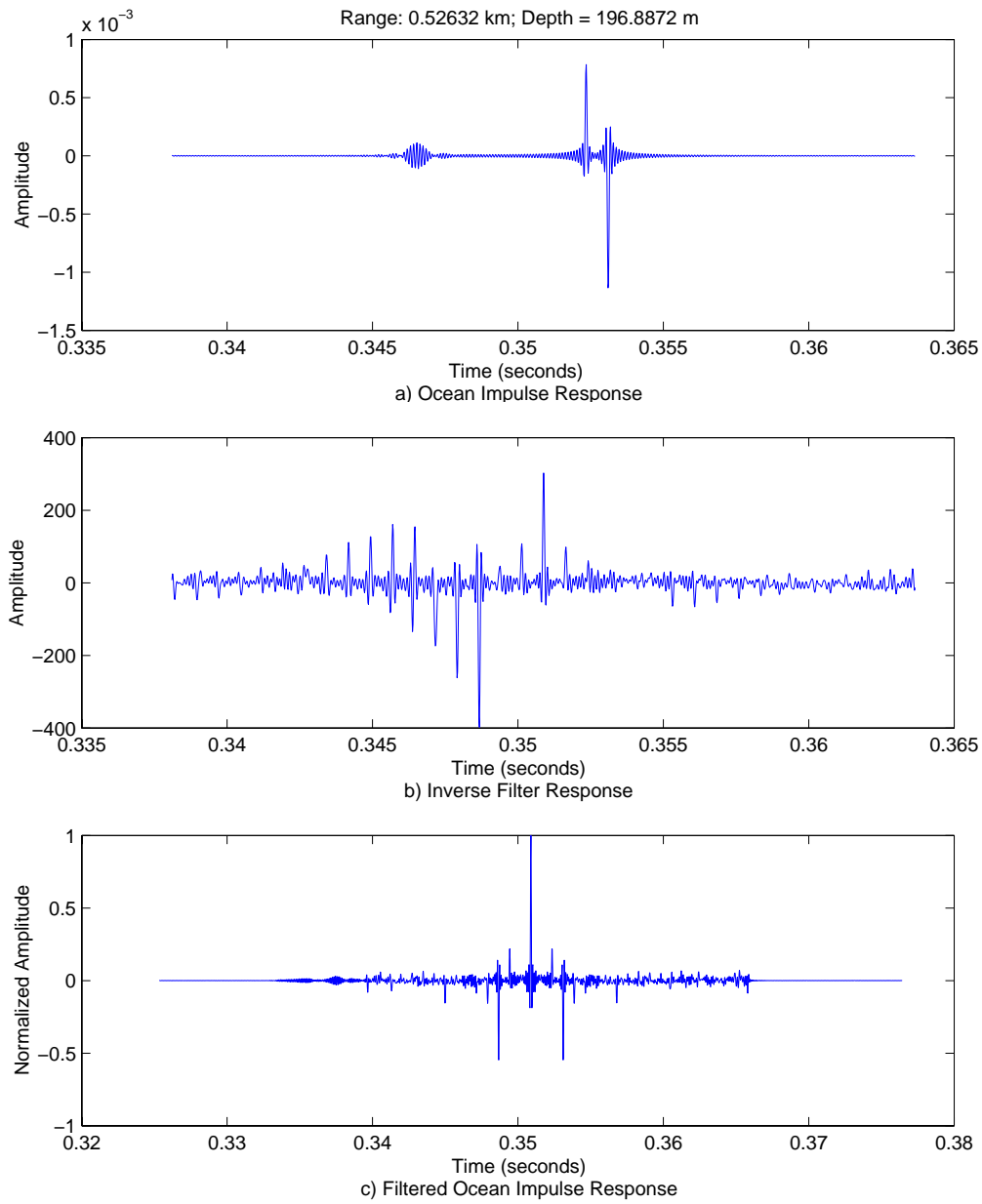
Figure 55.   Inverse Filter, Case 10
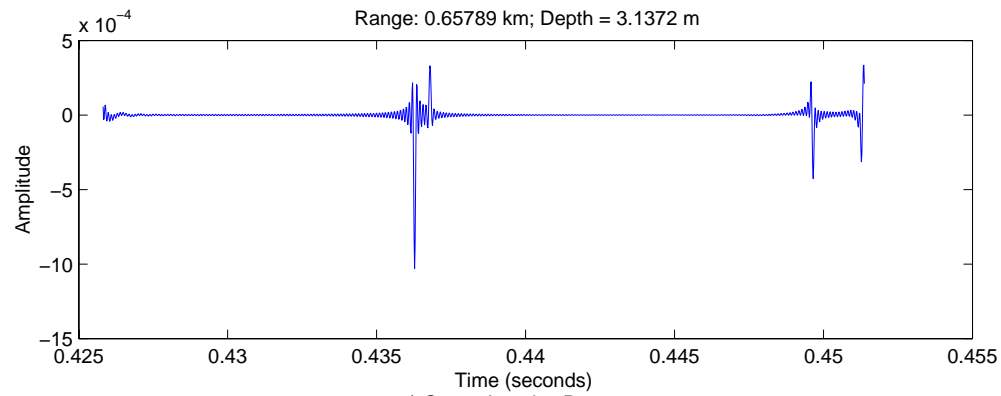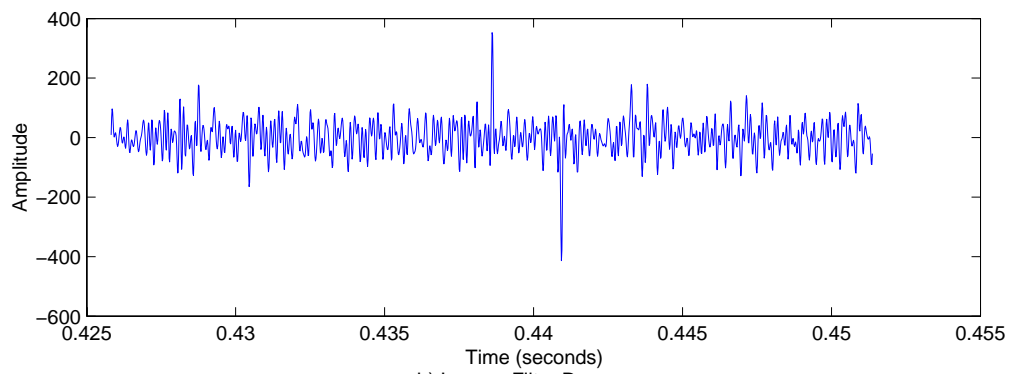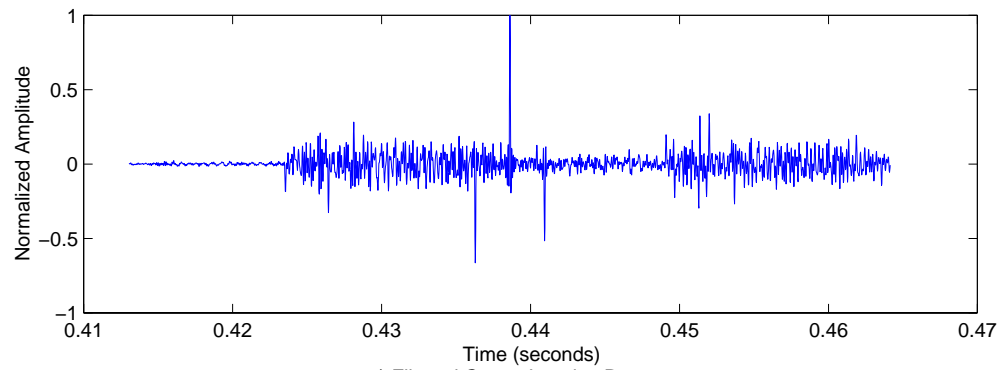
Figure 56.   Inverse Filter, Case 11
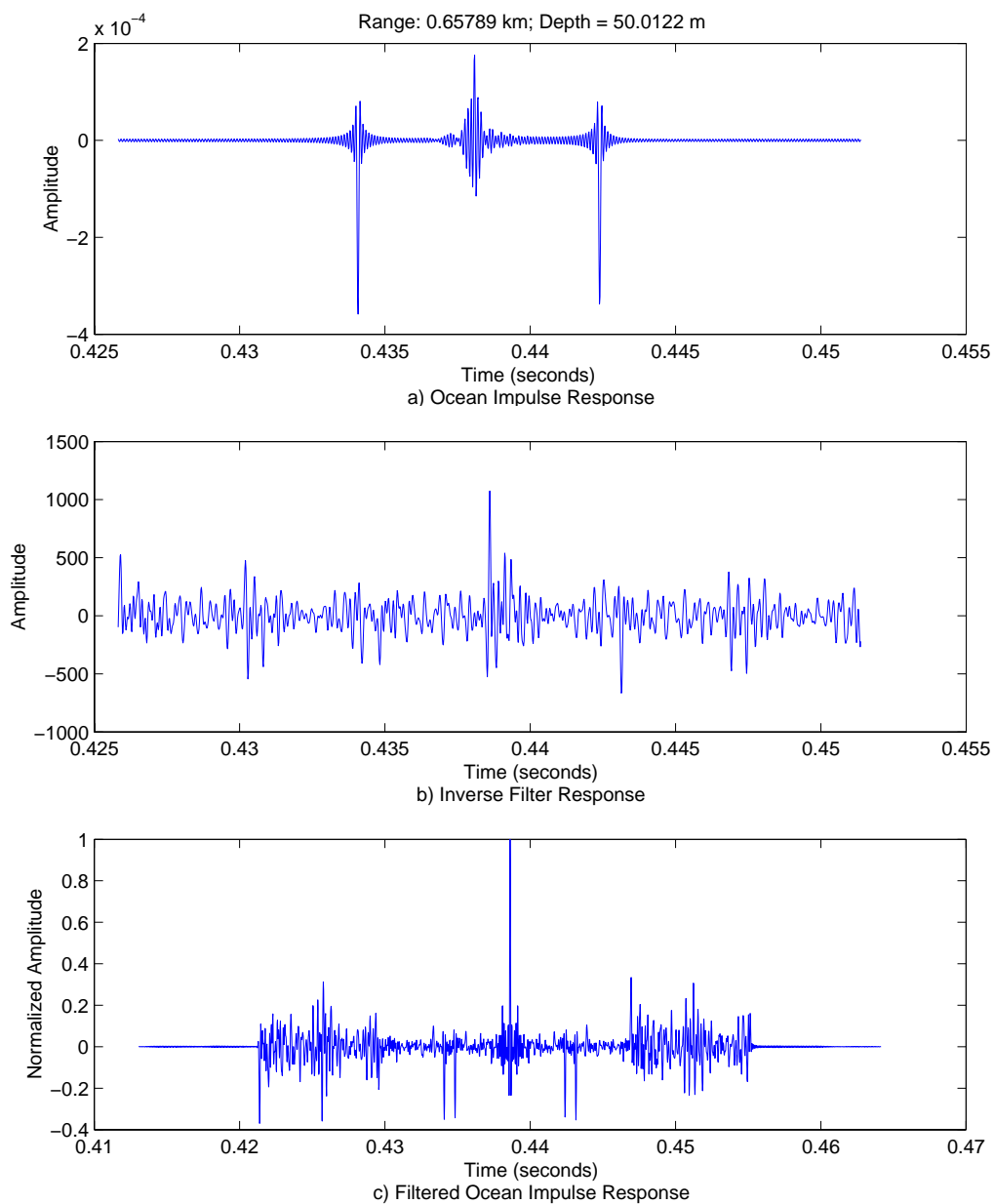
Figure 57.   Inverse Filter, Case 12

90
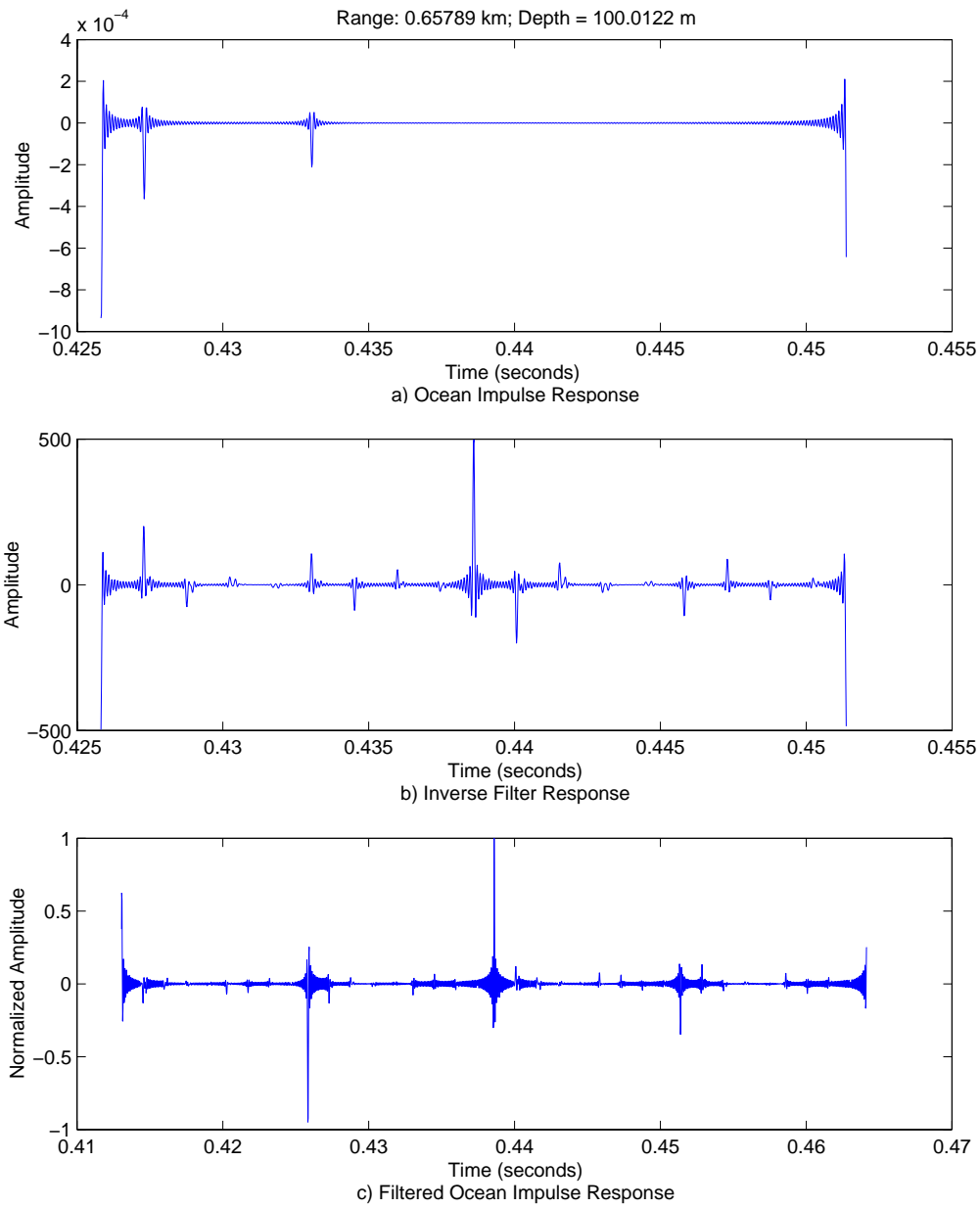
Figure 58.   Inverse Filter, Case 13

91
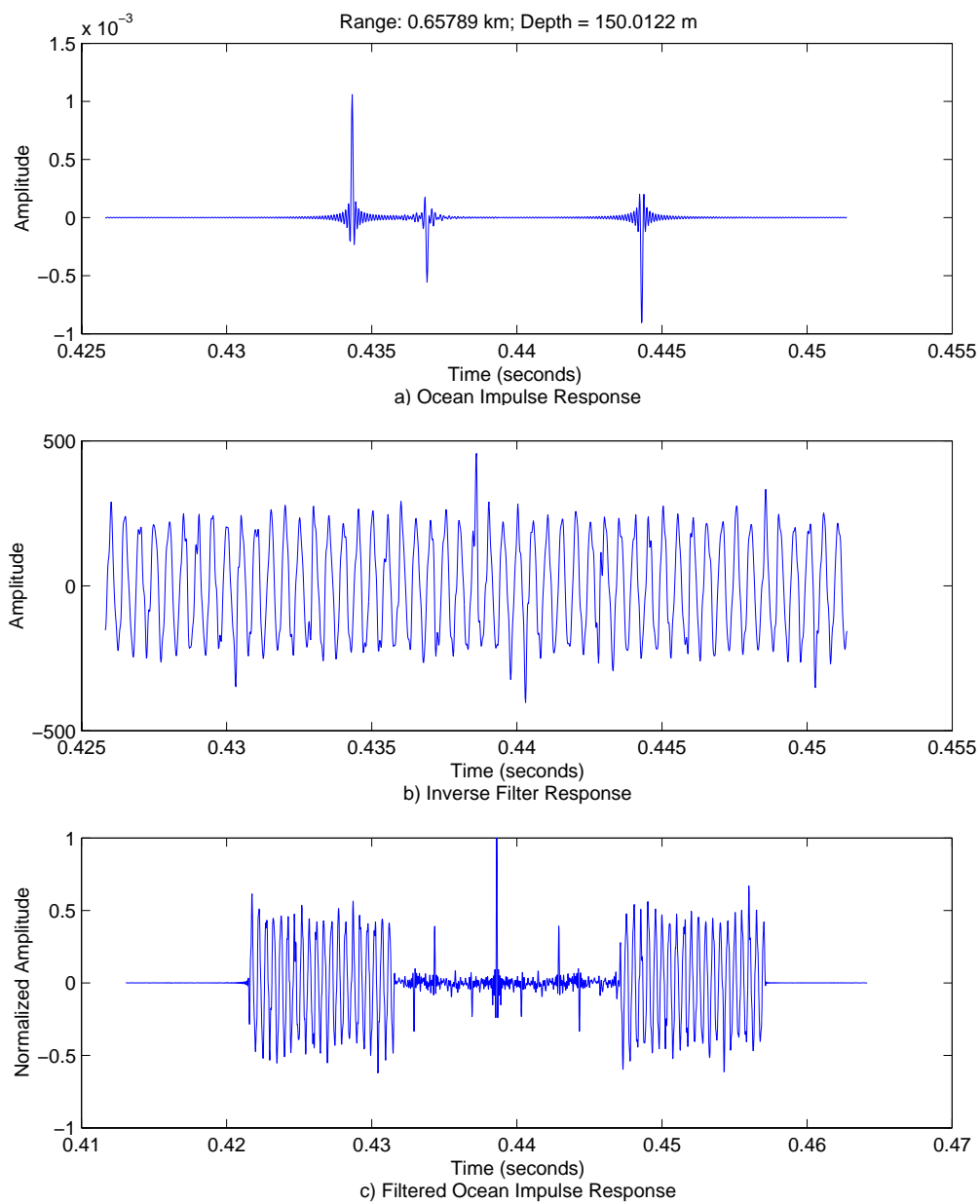
Figure 59.   Inverse Filter, Case 14

92
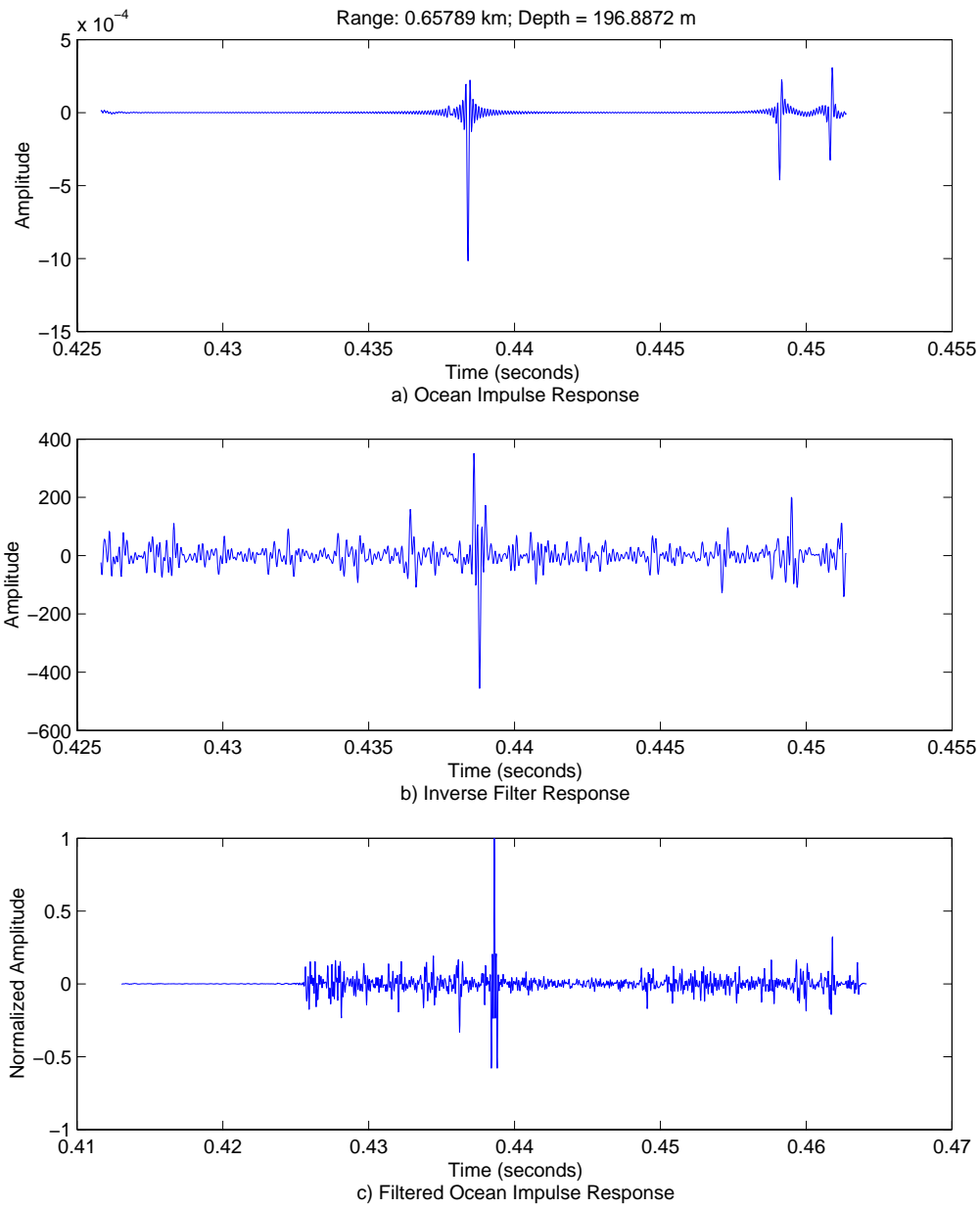
Figure 60.   Inverse Filter, Case 15
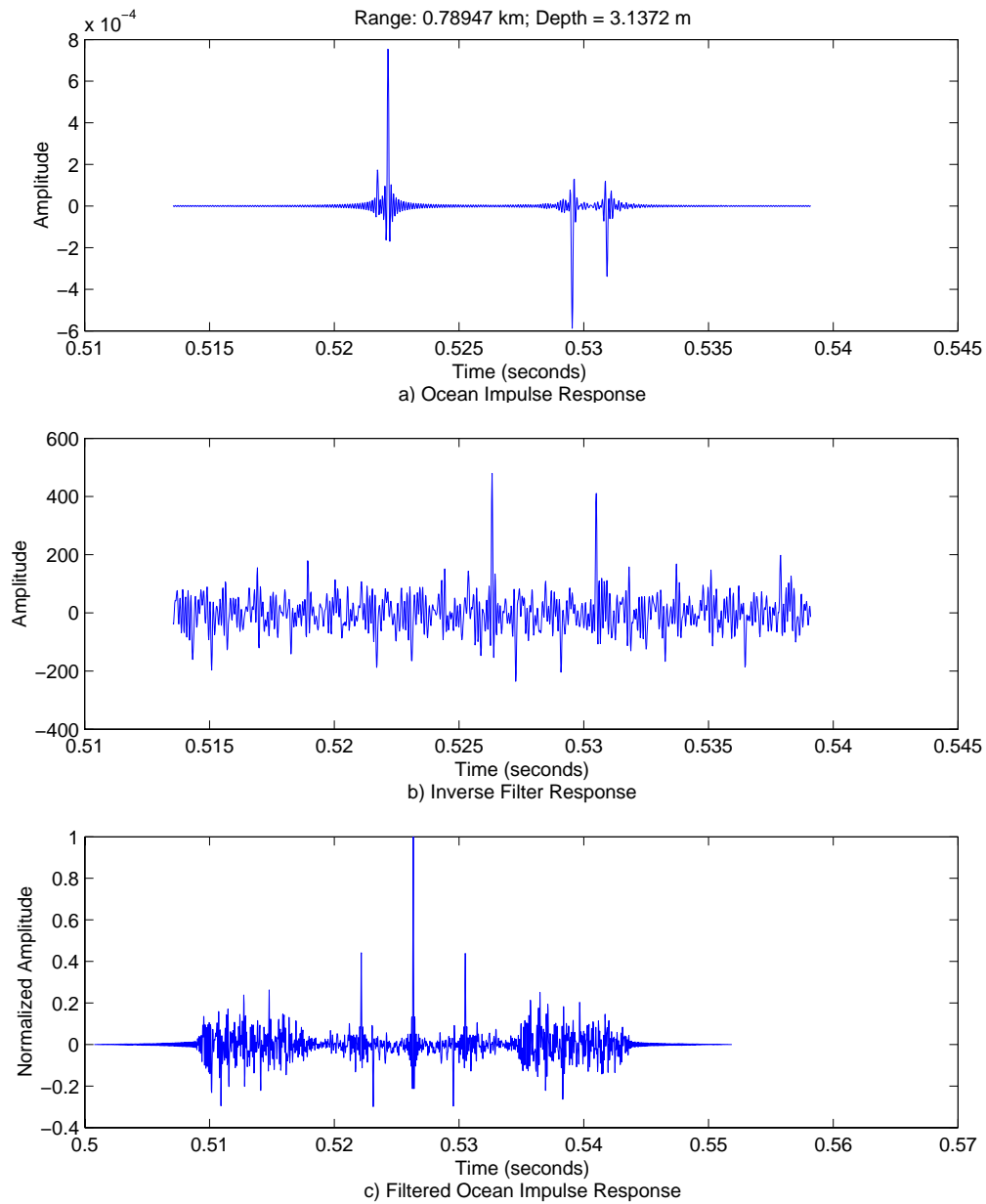
Figure 61.   Inverse Filter, Case 16

a) Ocean Impulse Response

b) Inverse Filter Response

c) Filtered Ocean Impulse Response
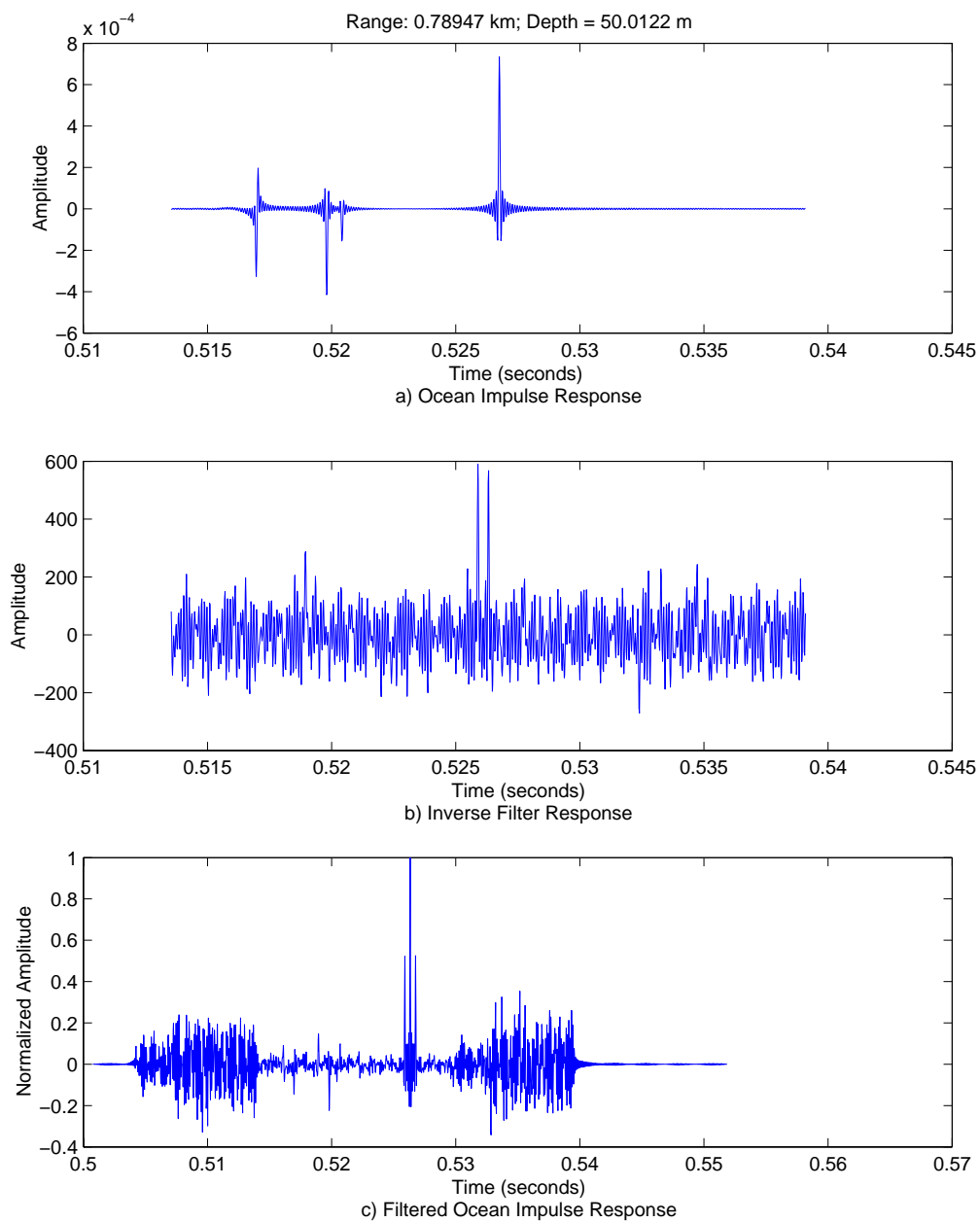
Figure 62.   Inverse Filter, Case 17

95
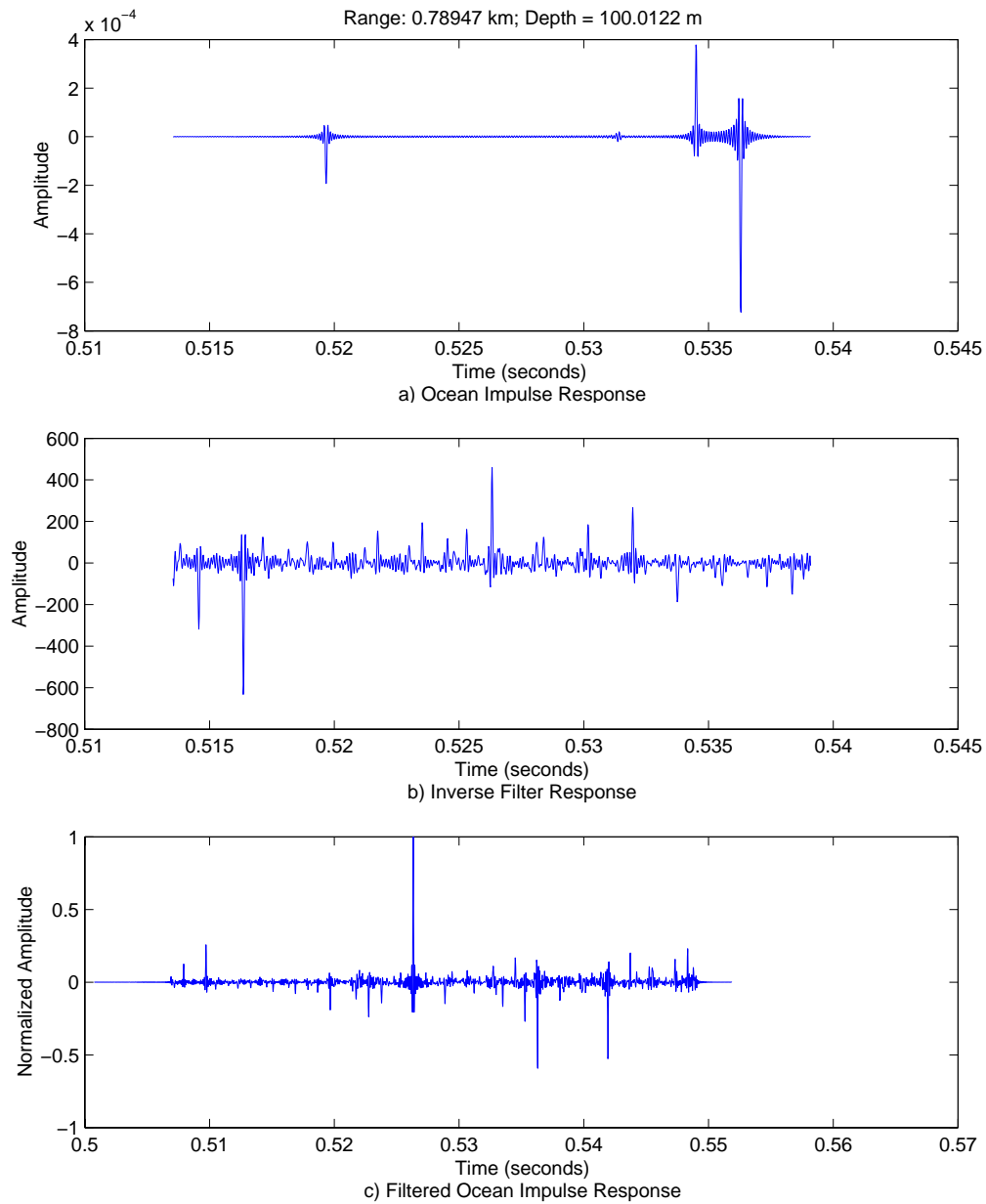
Figure 63. Inverse Filter, Case 18
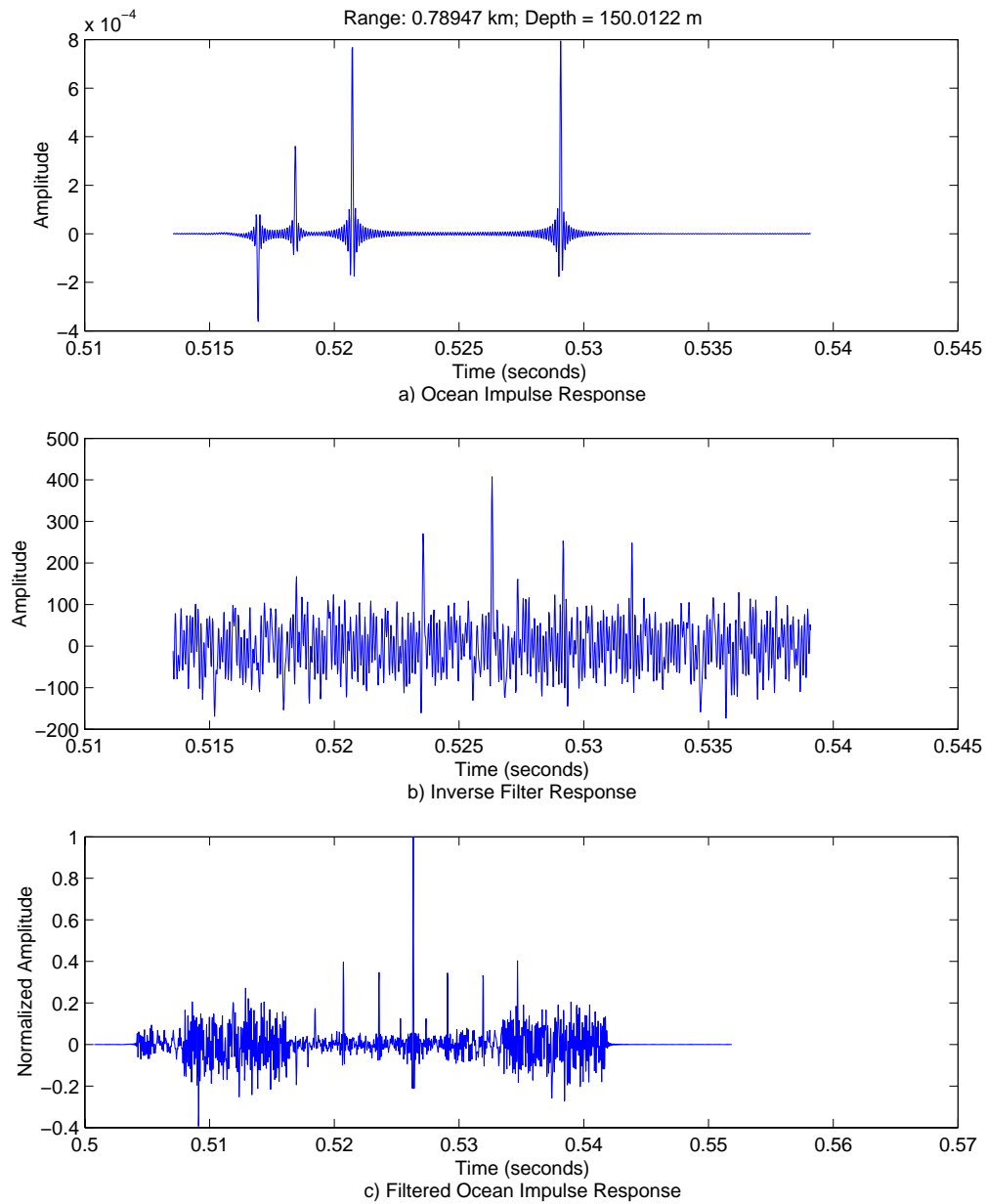
Figure 64.   Inverse Filter, Case 19
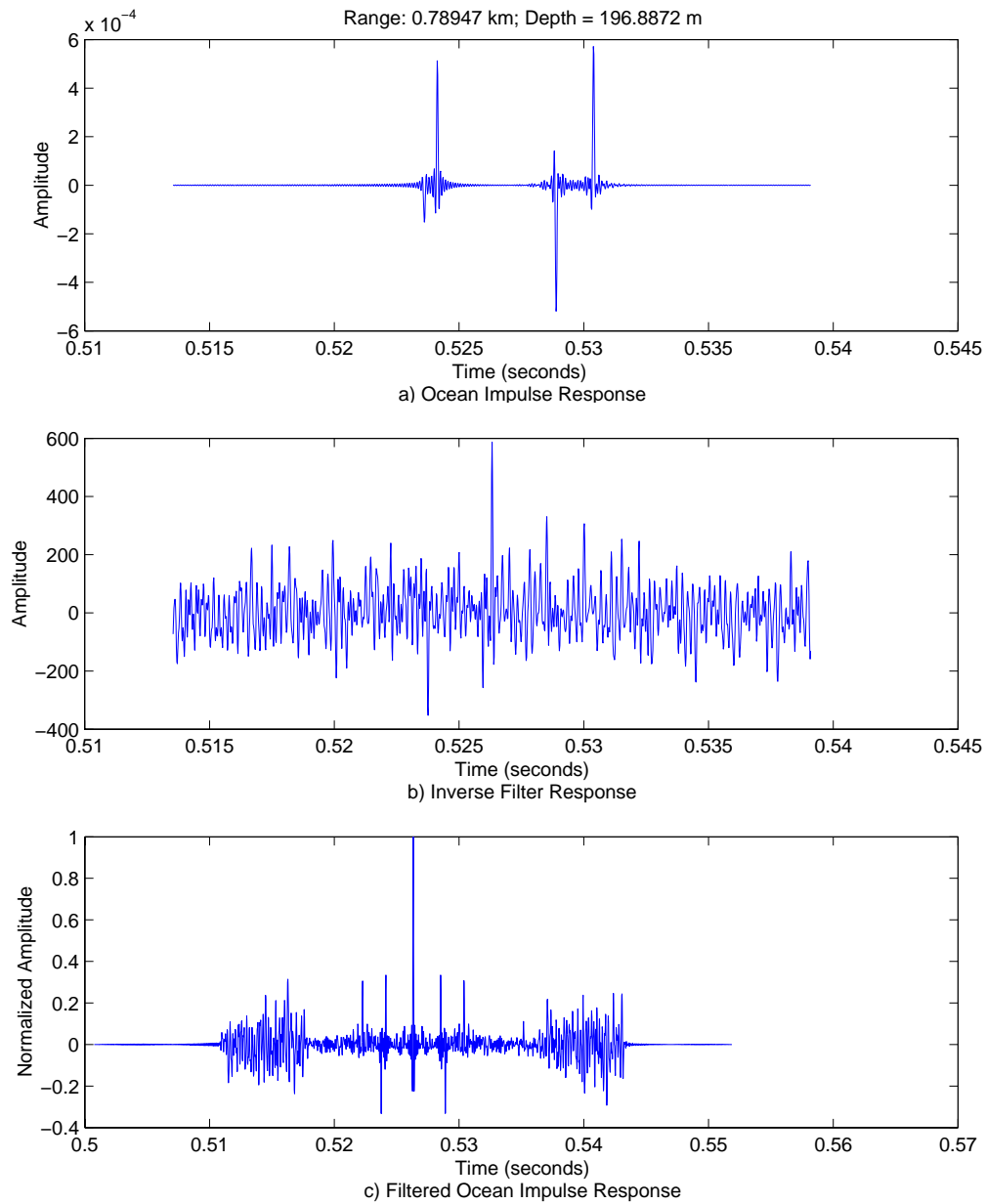
Figure 65.   Inverse Filter, Case 20

Range: 0.92105 km; Depth = 3.1372 m

a) Ocean Impulse Response

b) Inverse Filter Response

c) Filtered Ocean Impulse Response
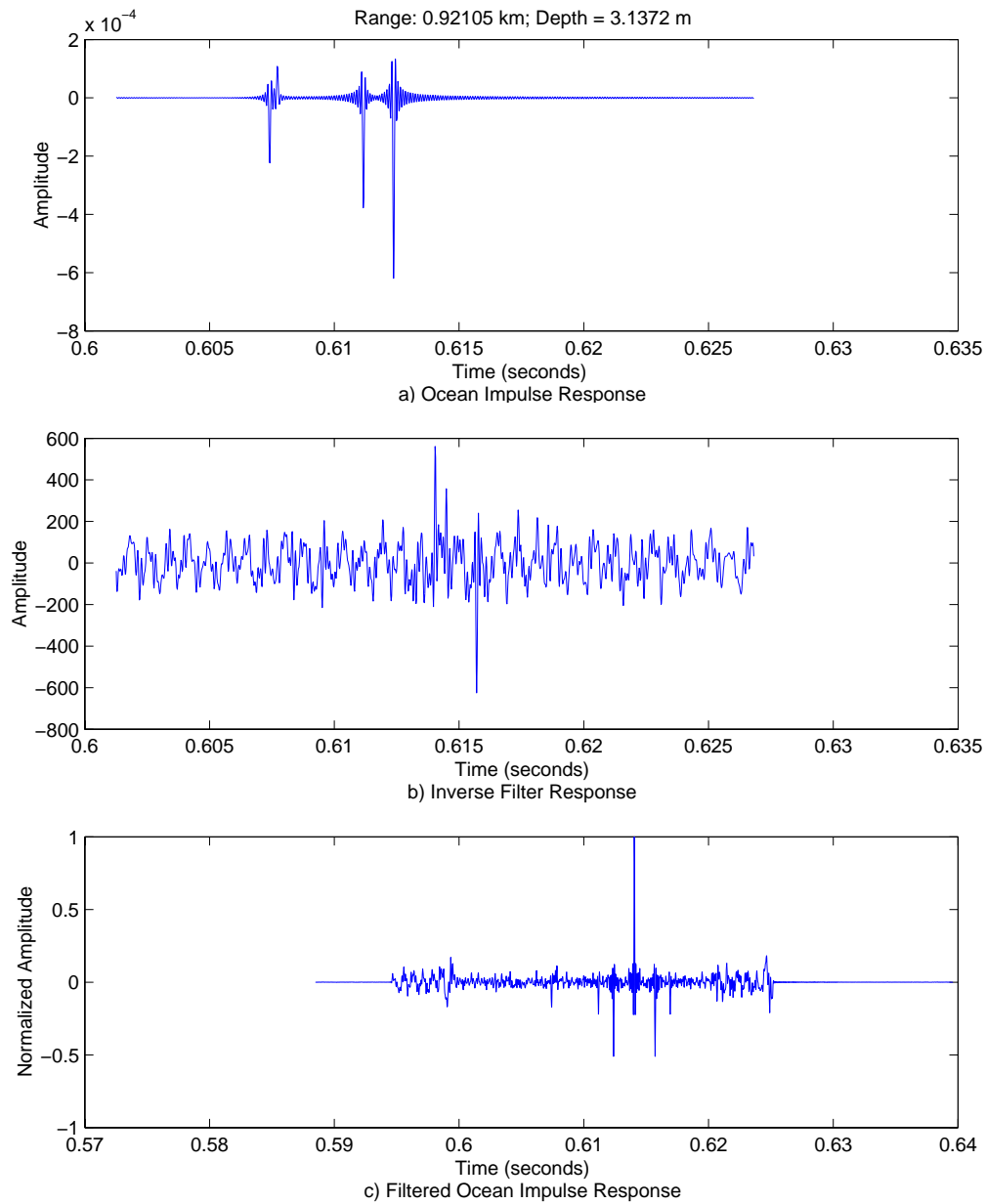
Figure 66.   Inverse Filter, Case 21
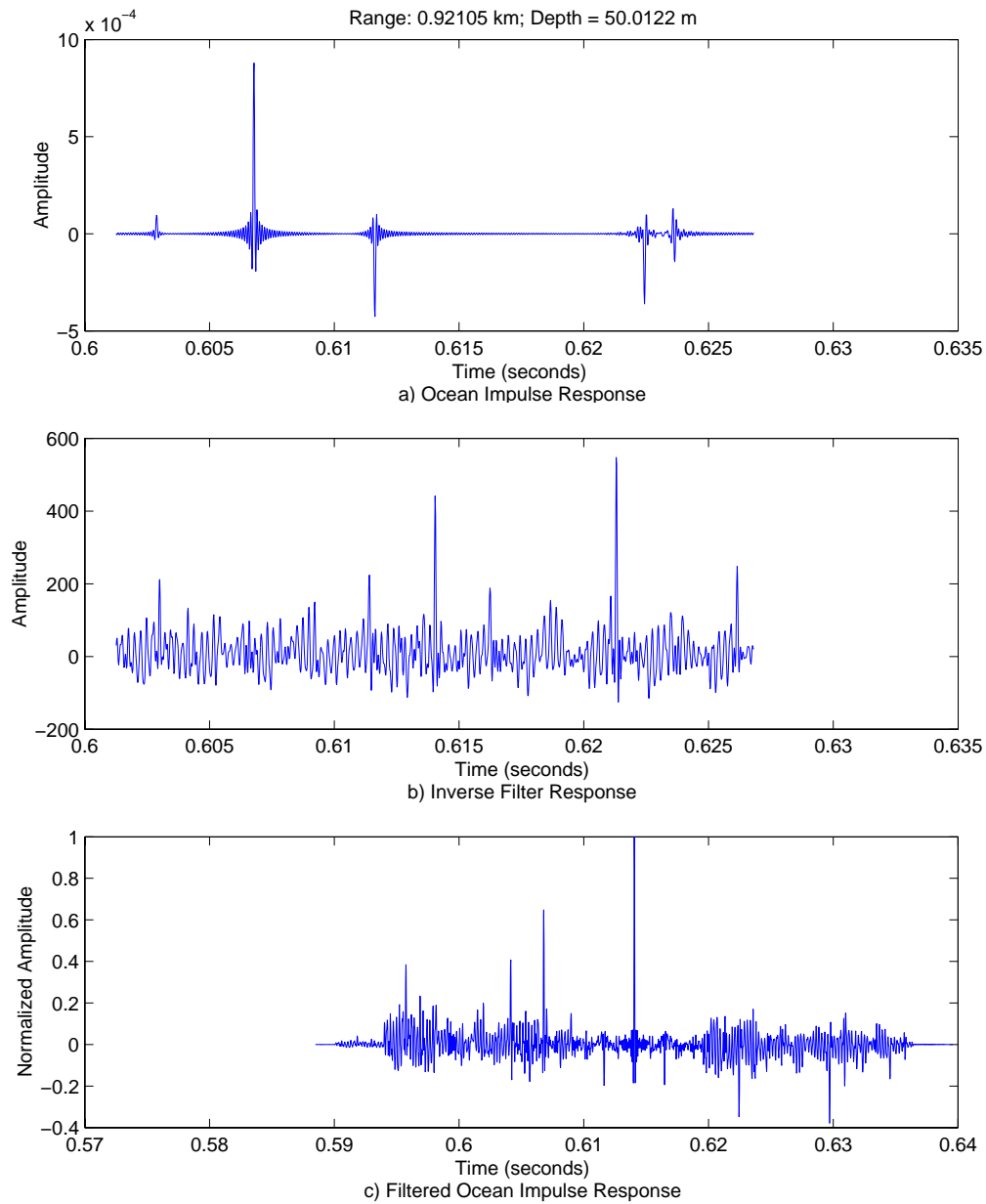
Figure 67.   Inverse Filter, Case 22

100
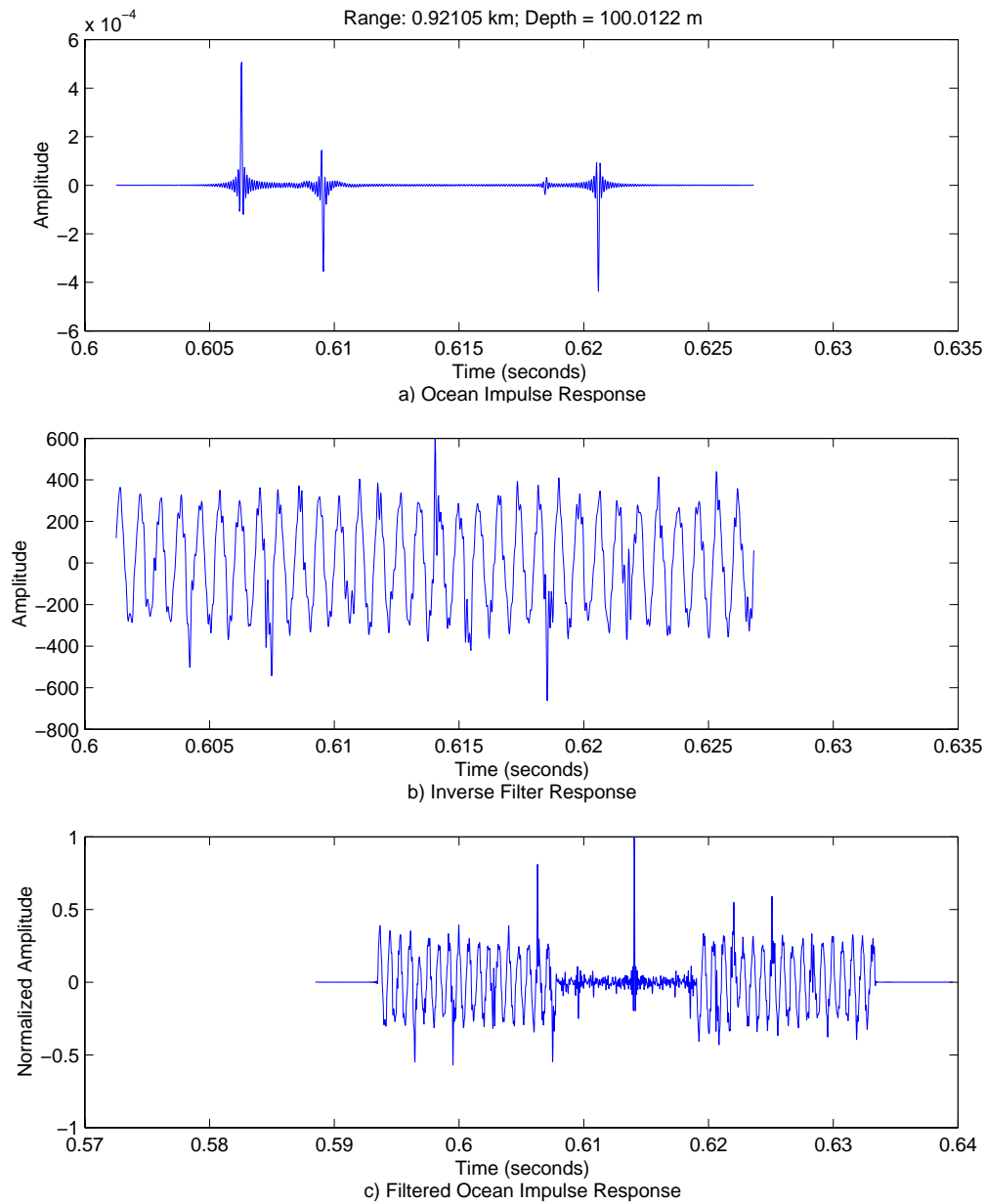
Figure 68.   Inverse Filter, Case 23
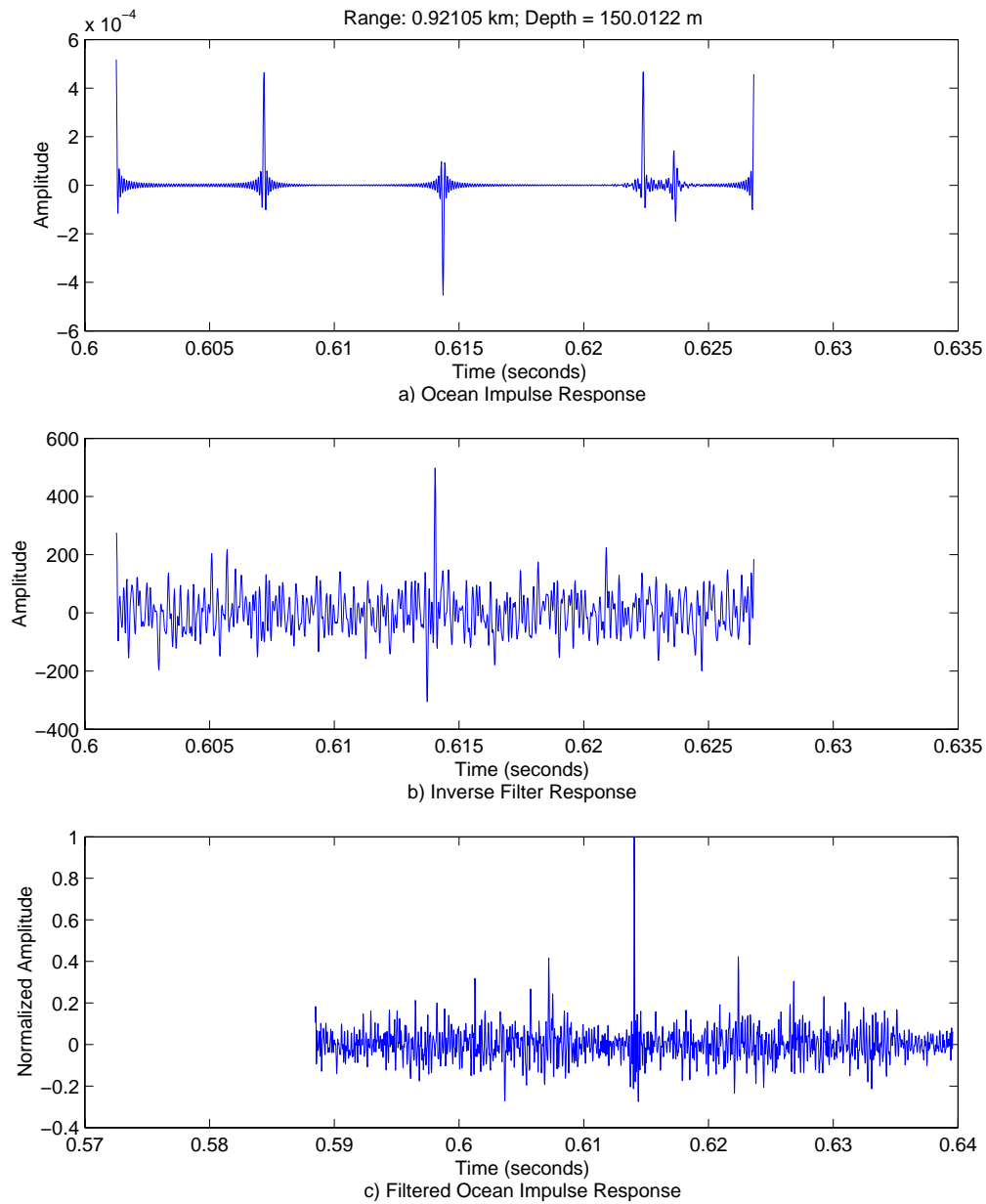
Figure 69.   Inverse Filter, Case 24

102
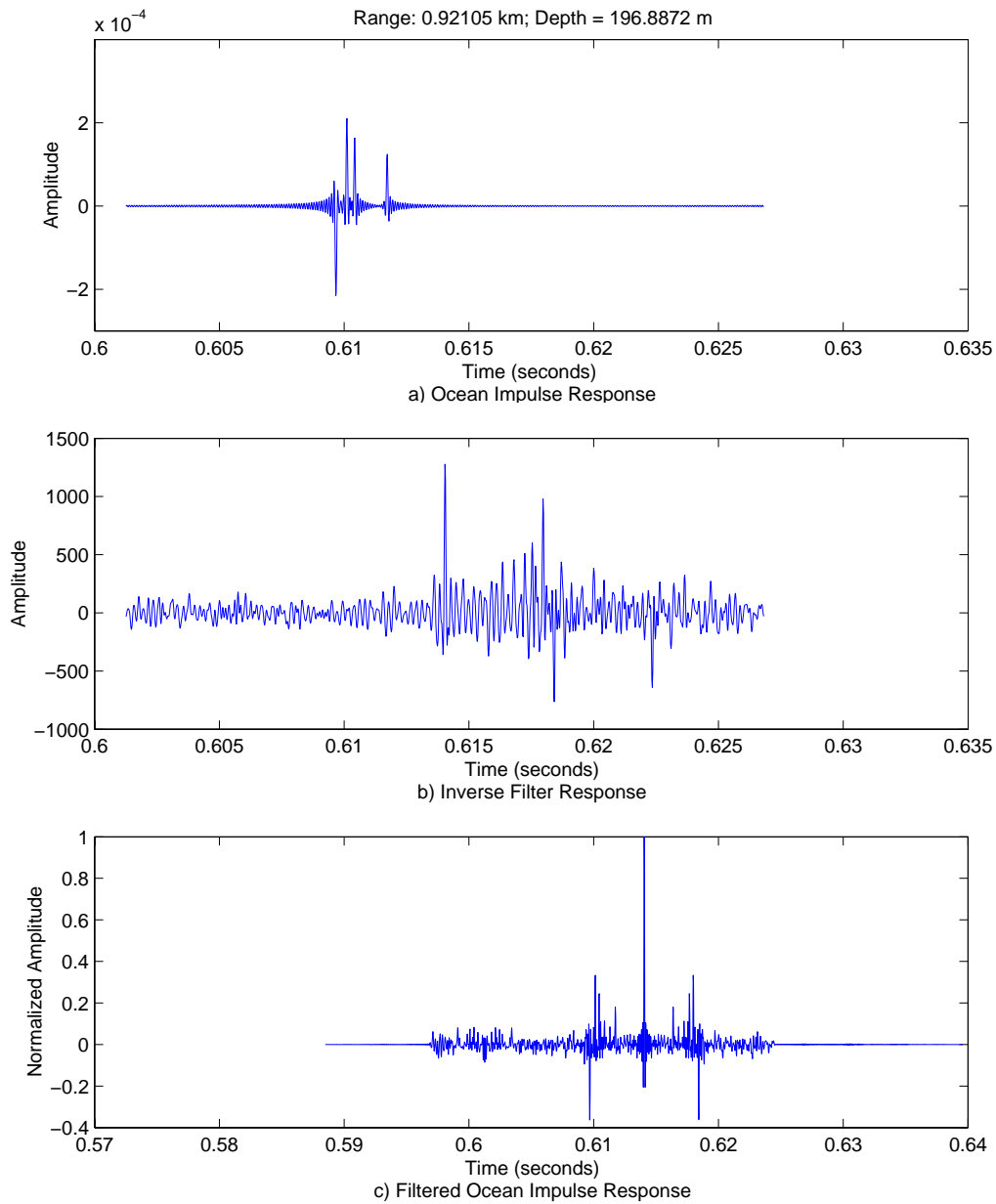
Figure 70.   Inverse Filter, Case 25
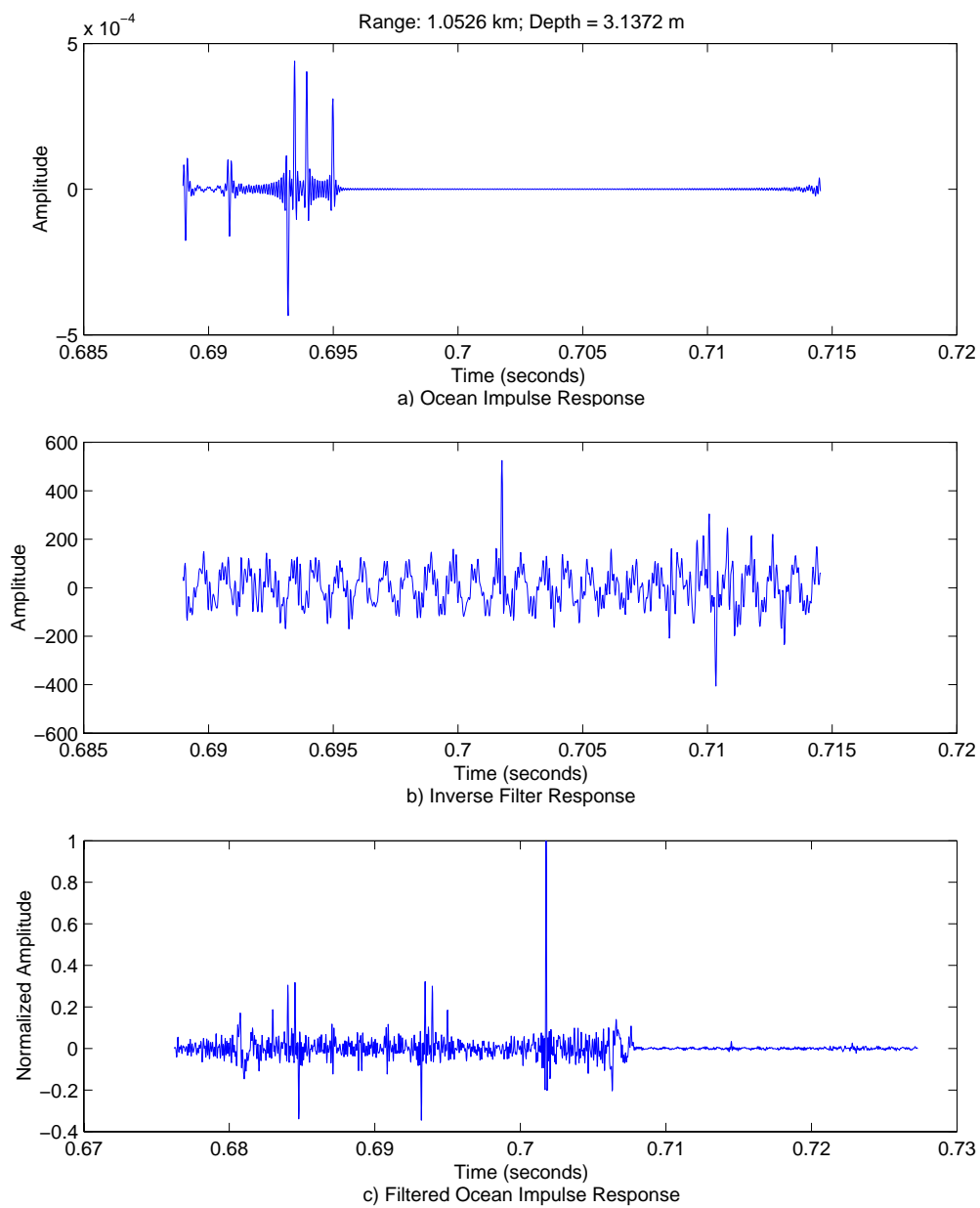
Figure 71.   Inverse Filter, Case 26

104
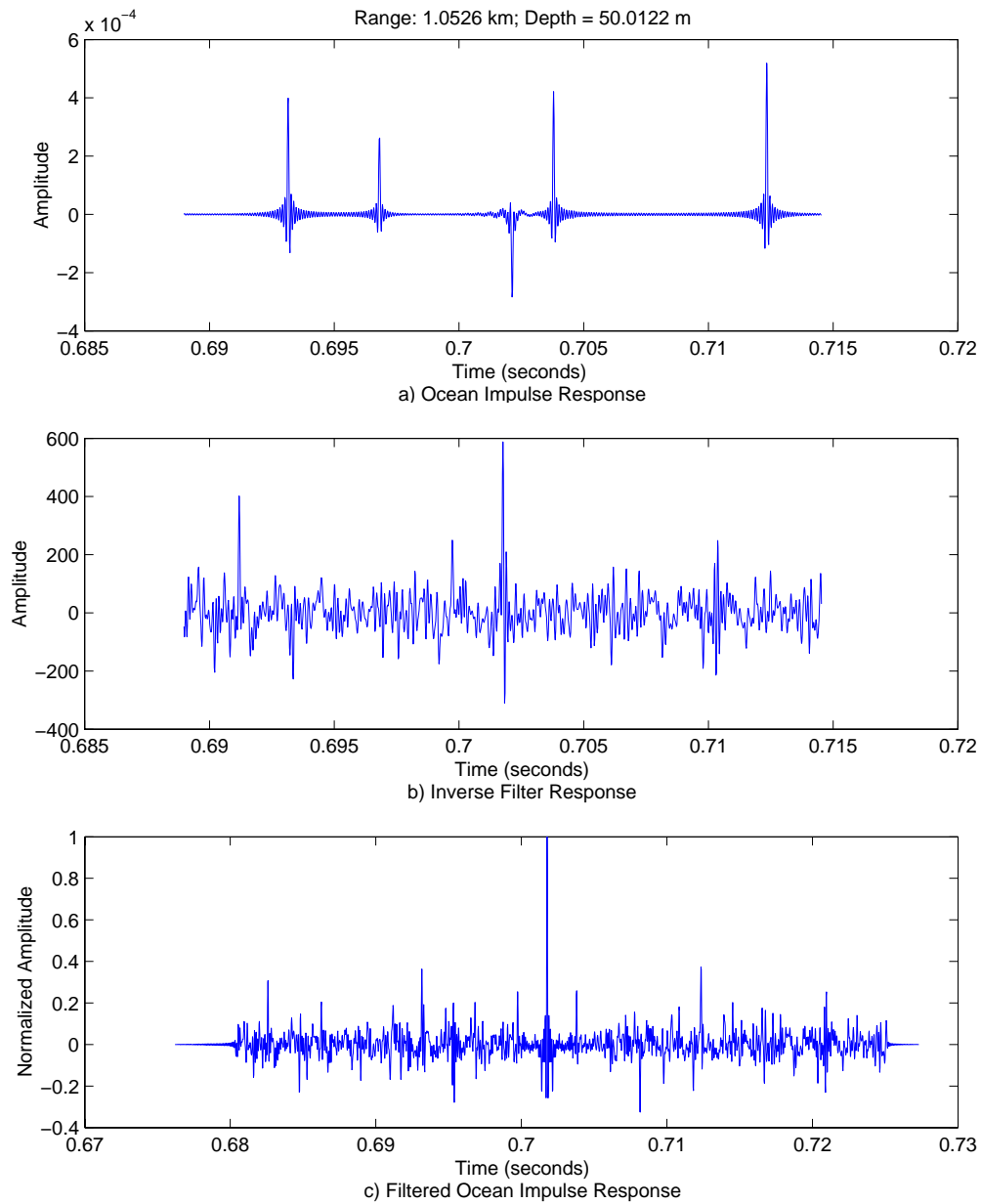
Figure 72.   Inverse Filter, Case 27
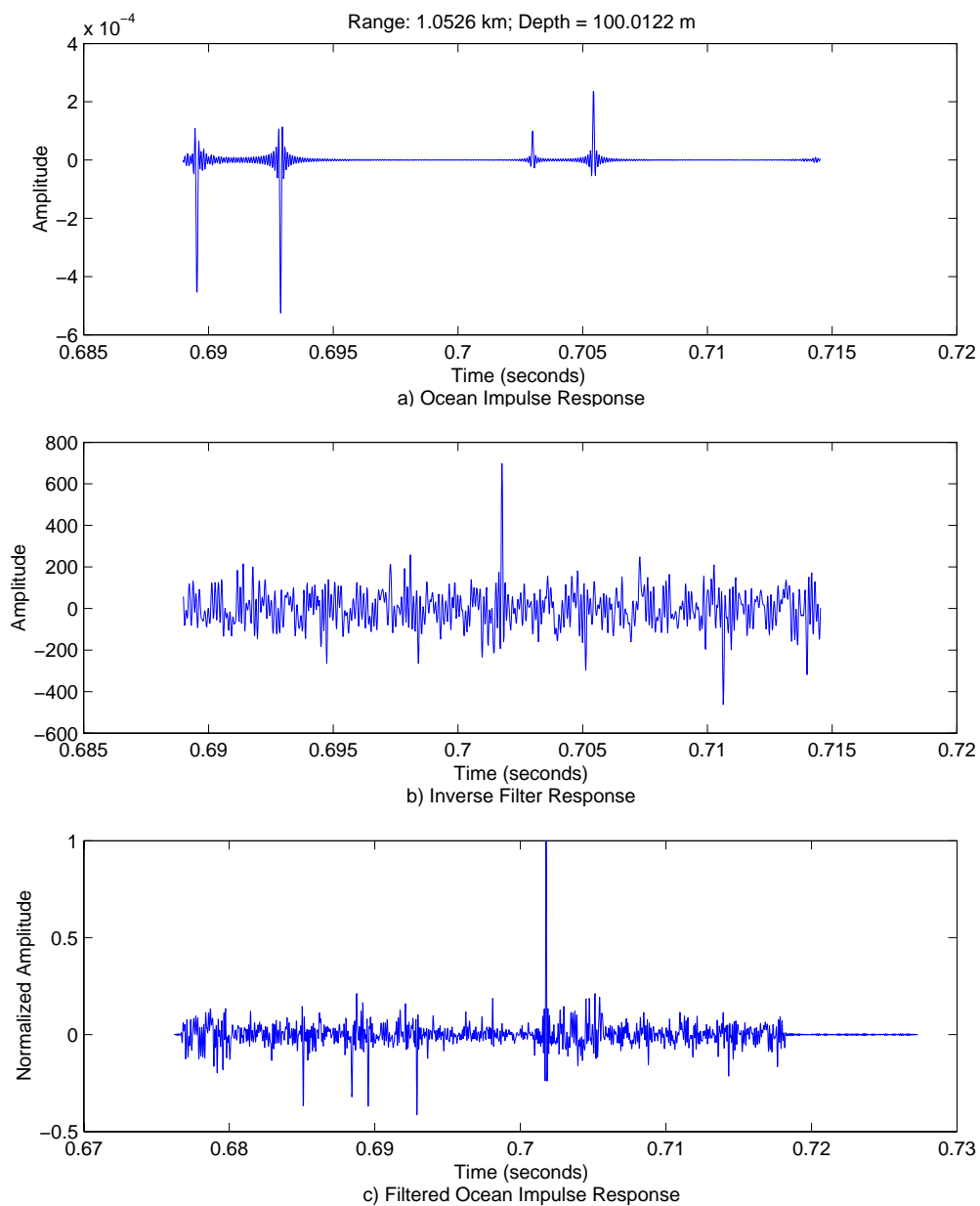
Figure 73.   Inverse Filter, Case 28

106
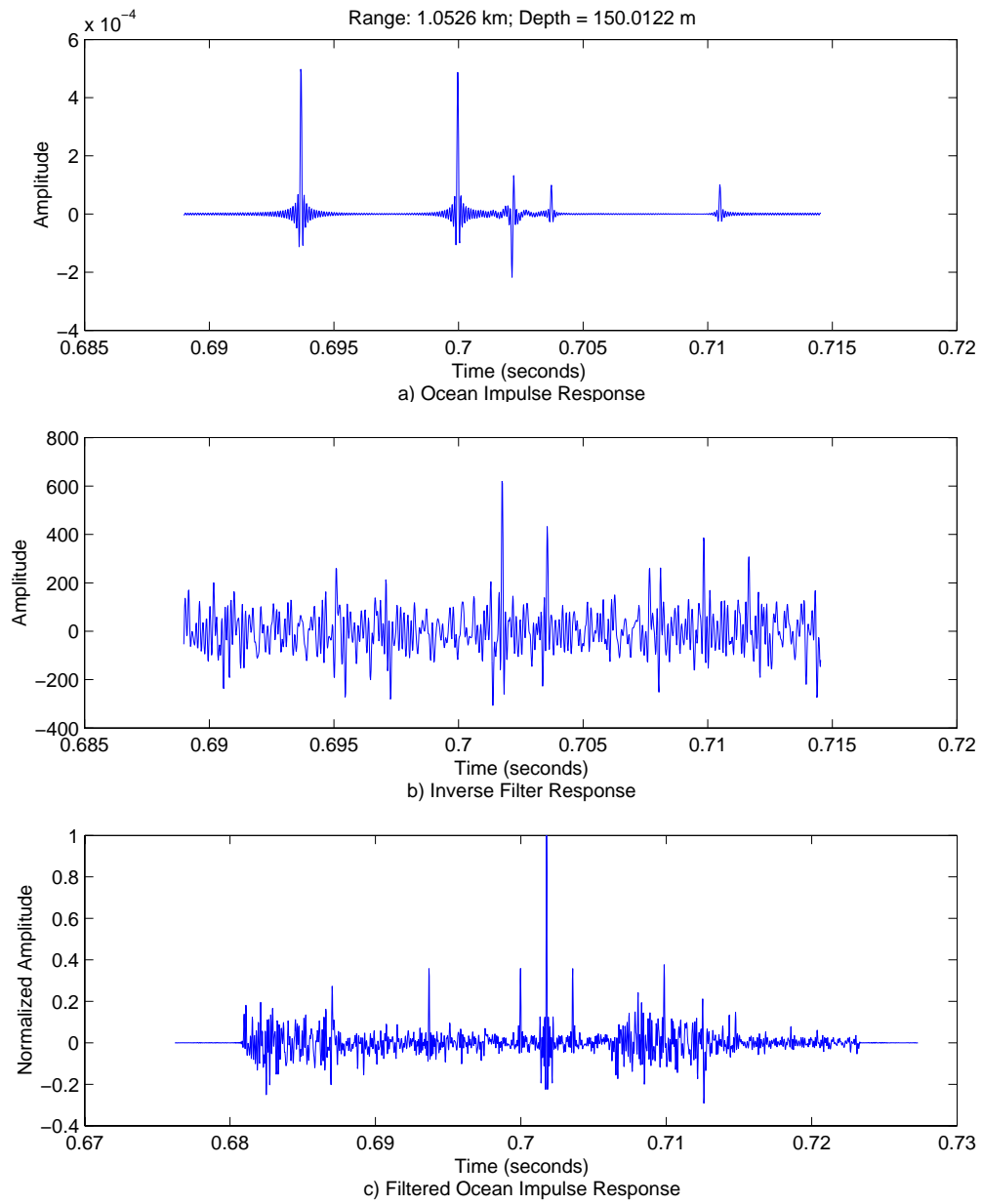
Figure 74.   Inverse Filter, Case 29
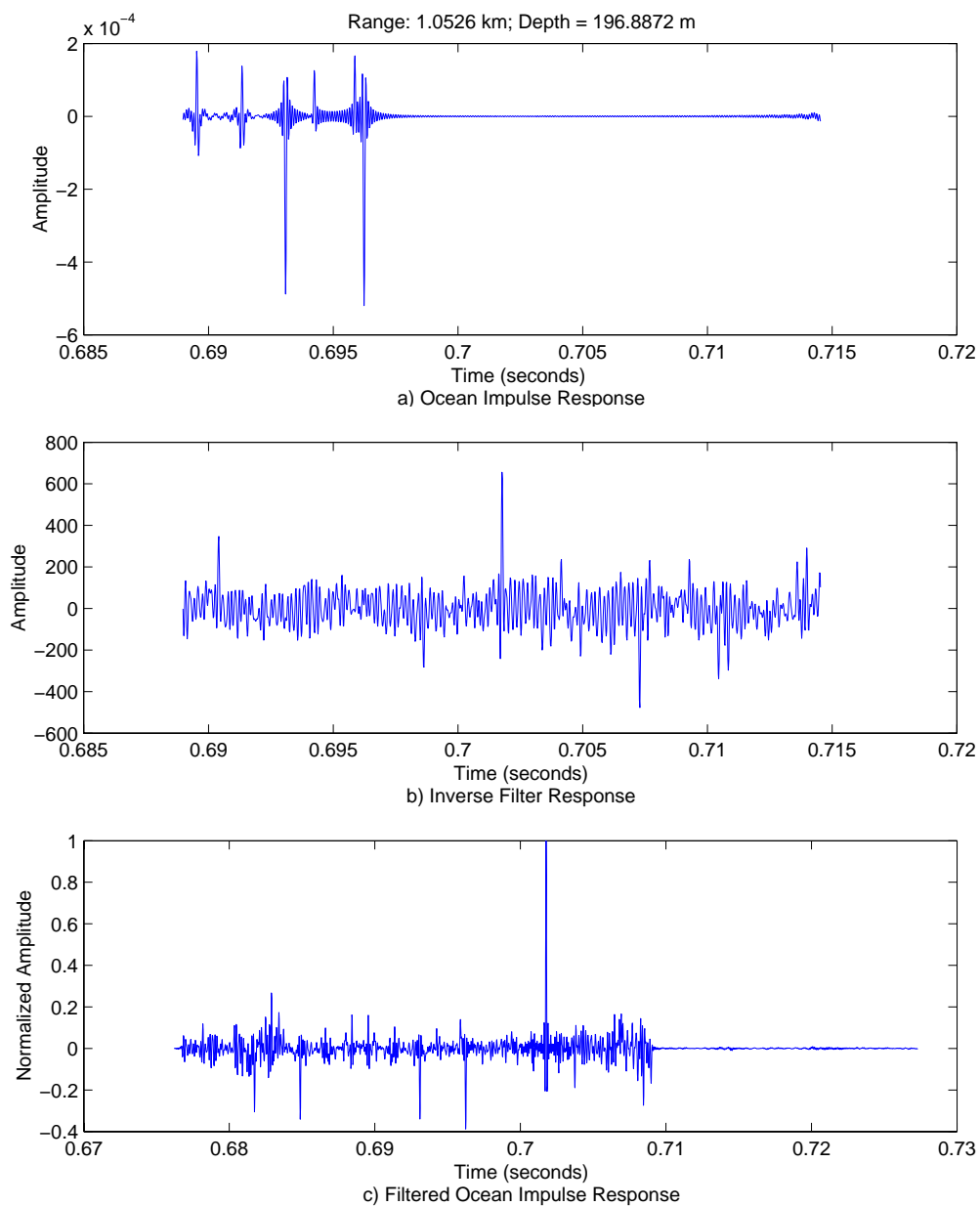
Figure 75.   Inverse Filter, Case 30

C. INFINITE IMPULSE RESPONSE FILTER RESULTS

Figures 76 through 105 contain plots of the ocean impulse response, IIR filter response, and the filtered ocean response for all thirty test cases. The IIR filter tap points were selected based on the magnitudes of the main signal and multipath returns. Three types of responses of the IIR filter can be seen in these plots. The worst response is the unstable filter with the output oscillating with increasingly larger magnitudes. A second response is the stable filter with residual multipath returns, and the final response is the stable filter with no residual multipath returns. A summary of the cases and their responses are contained in Tables 7 and 8 of Chapter III.
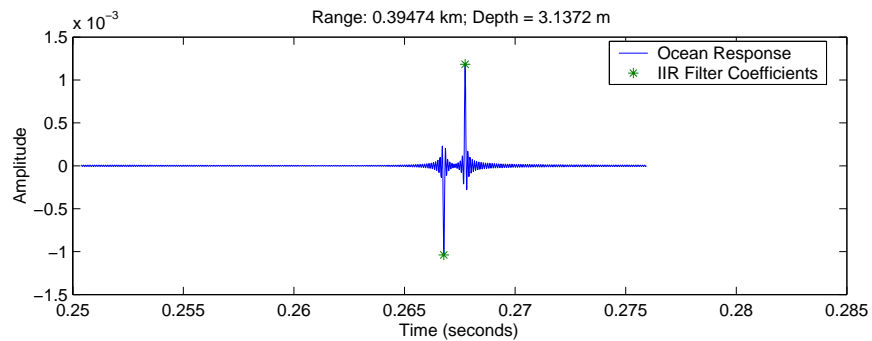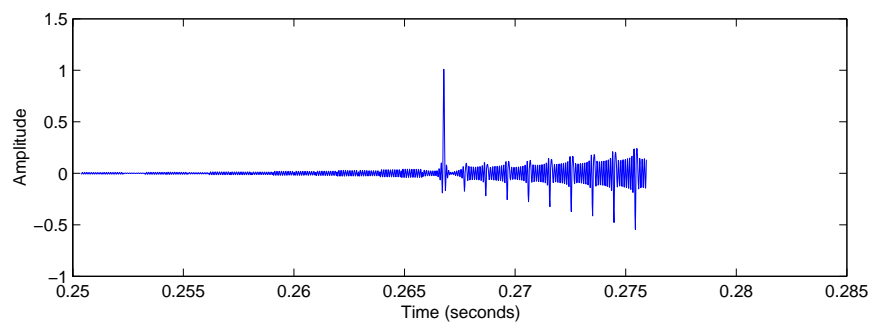
Figure 76.   IIR Filter, Case 1
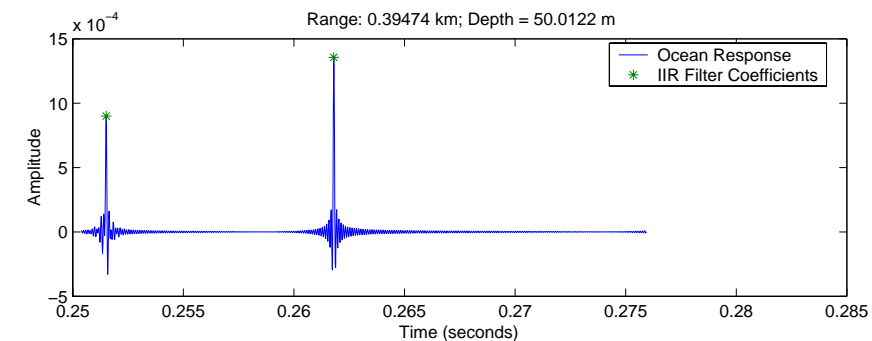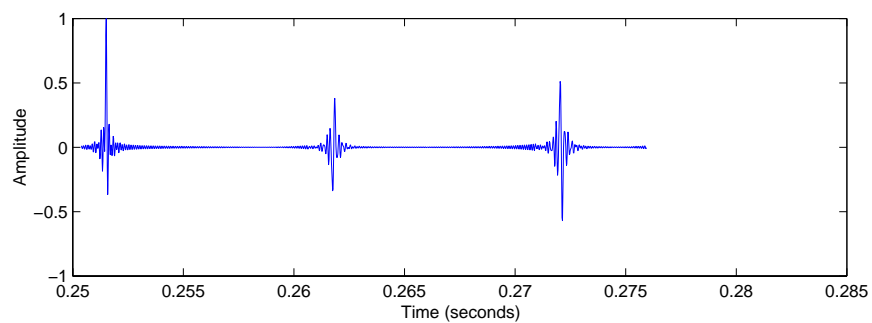
Figure 77.   IIR Filter, Case 2
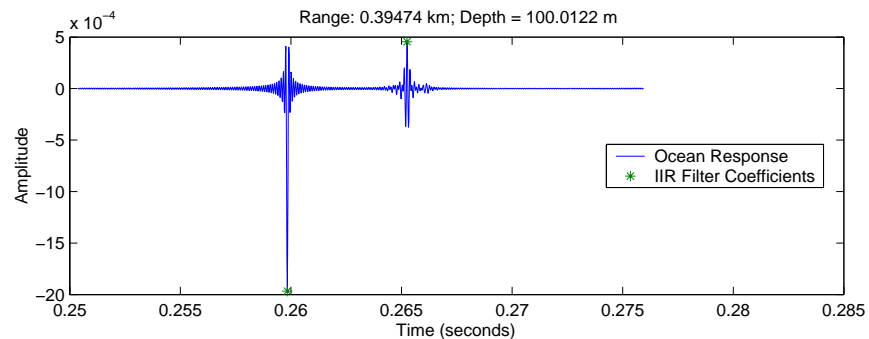
110
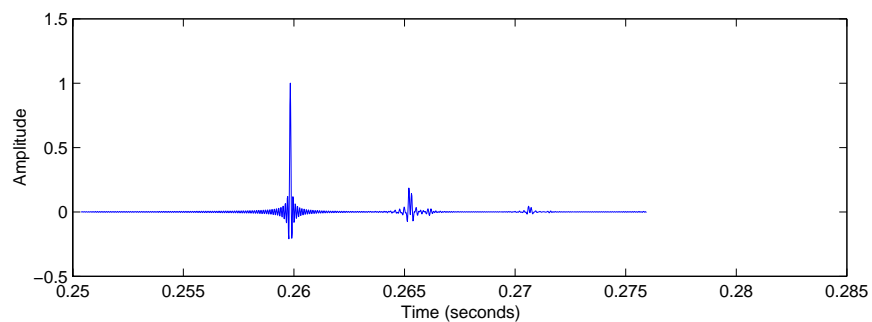
Figure 78.   IIR Filter, Case 3
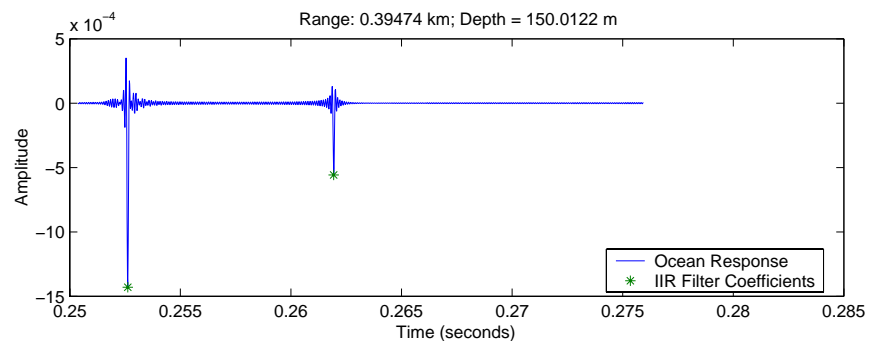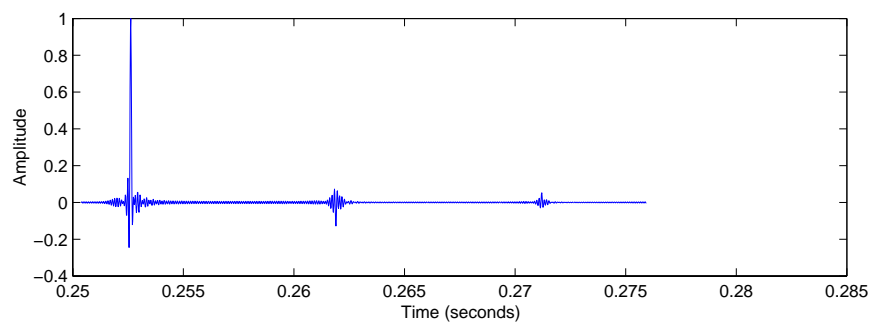
Figure 79.   IIR Filter, Case 4
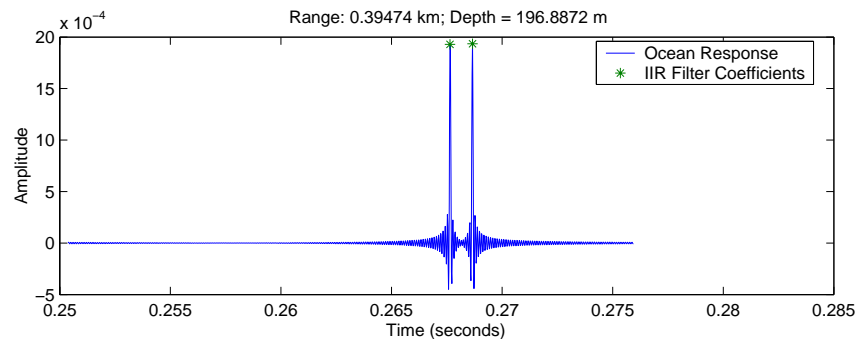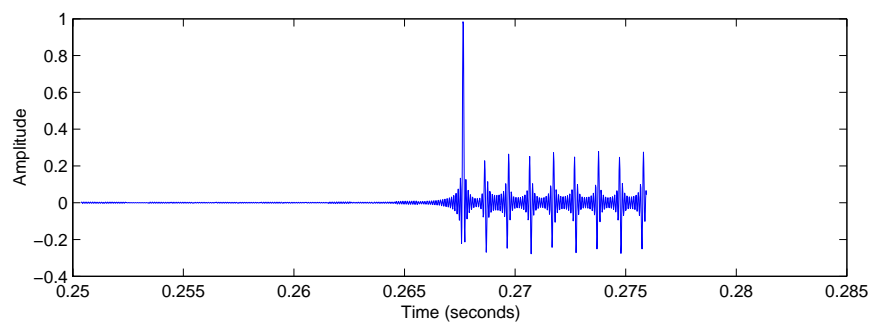
Figure 80.　IIR Filter, Case 5
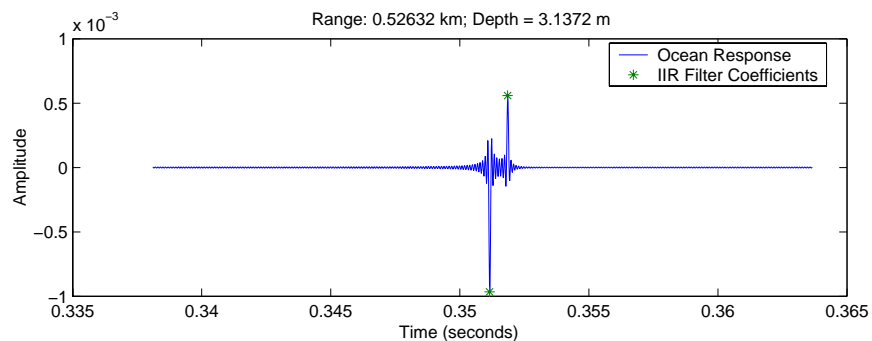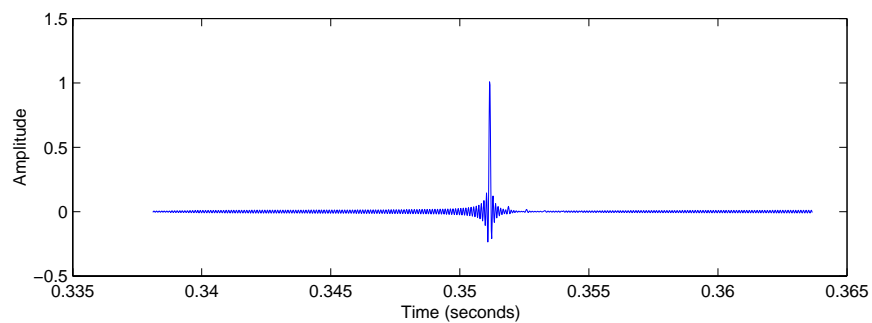
Figure 81.　IIR Filter, Case 6
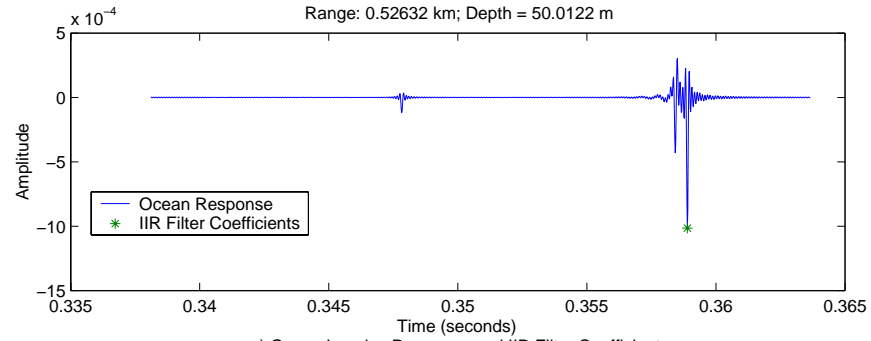
112
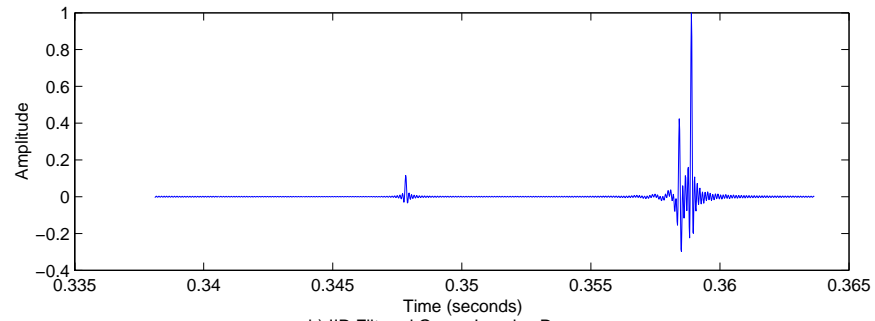
Figure 82.   IIR Filter, Case 7
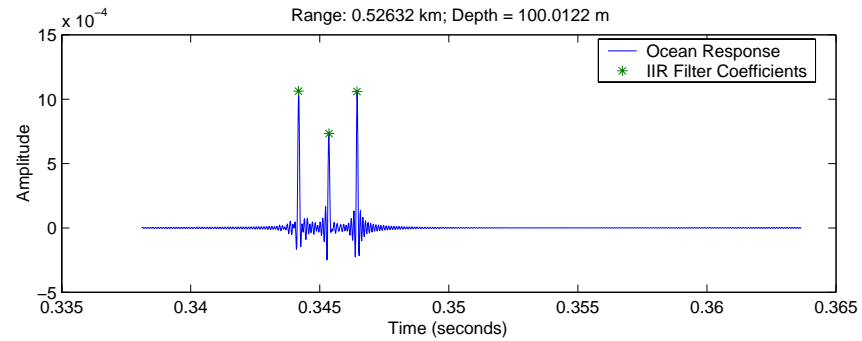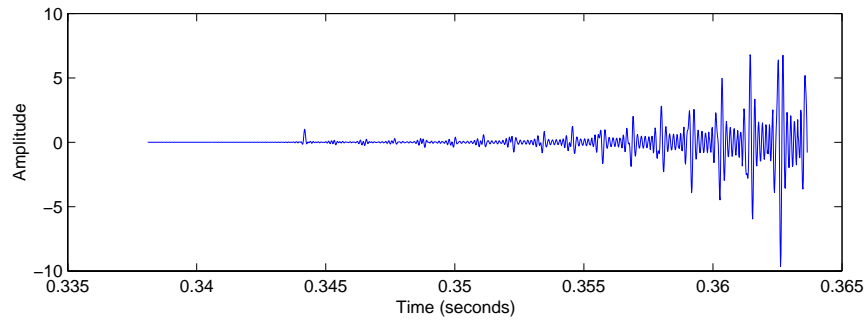
Figure 83.   IIR Filter, Case 8
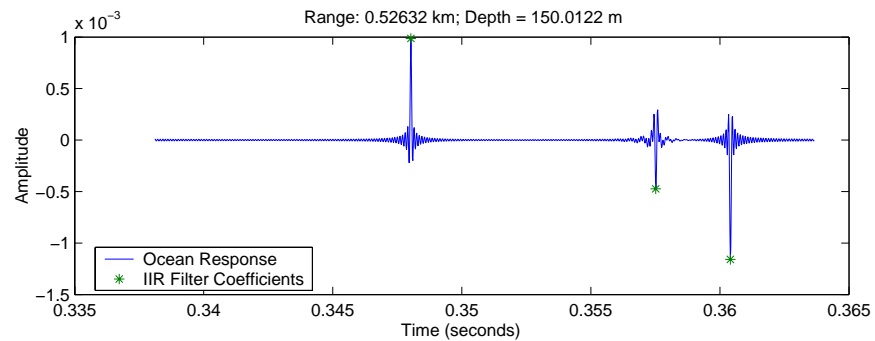
113
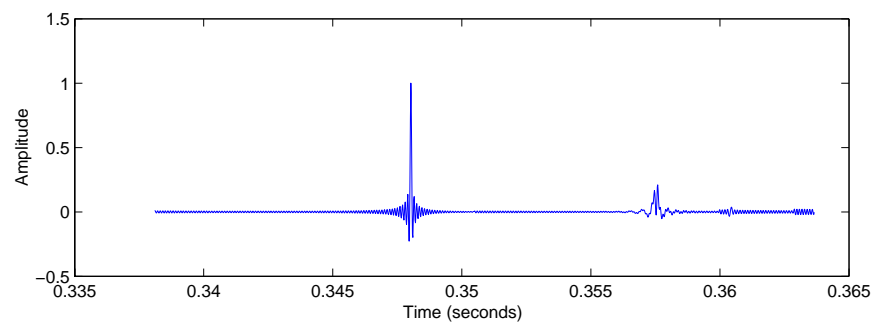
Figure 84.   IIR Filter, Case 9
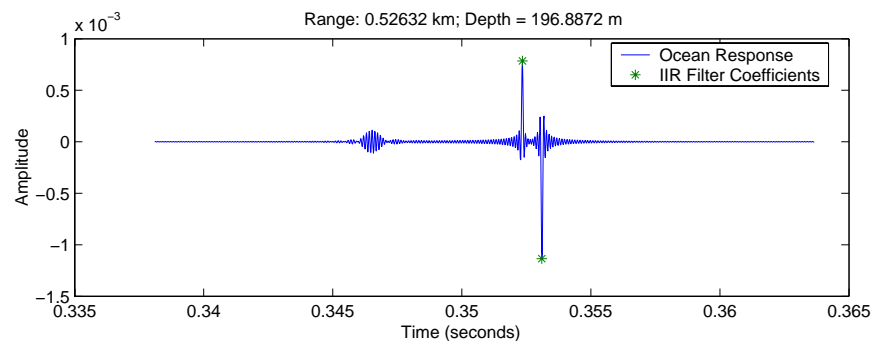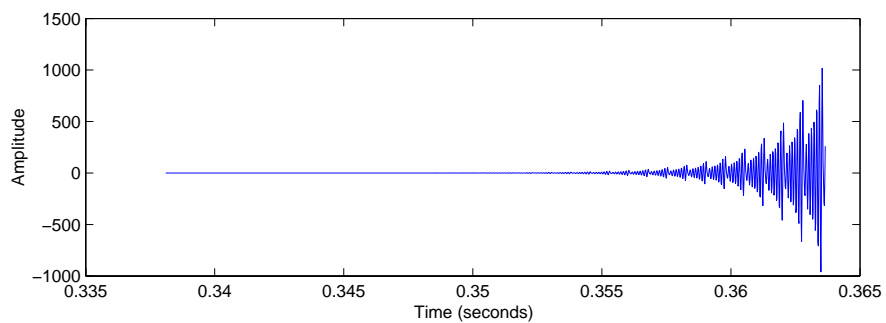
Figure 85.   IIR Filter, Case 10
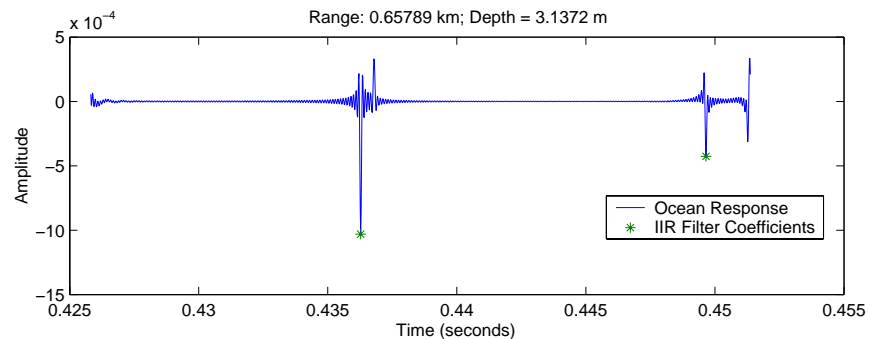
114
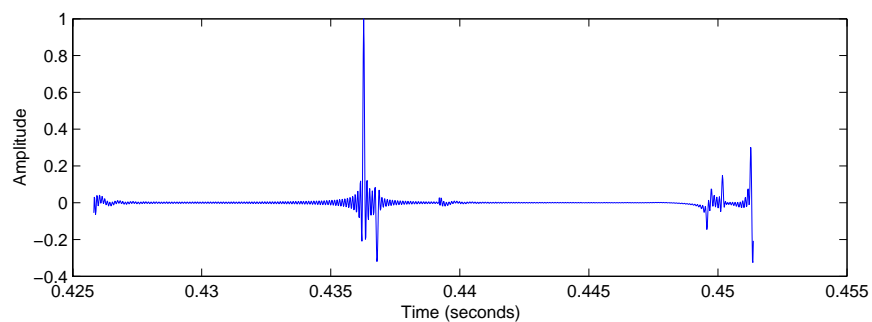
Figure 86.   IIR Filter, Case 11

Figure 87.   IIR Filter, Case 12

115

Figure 88.   IIR Filter, Case 13

Figure 89.   IIR Filter, Case 14

Figure 90.   IIR Filter, Case 15

Figure 91.   IIR Filter, Case 16
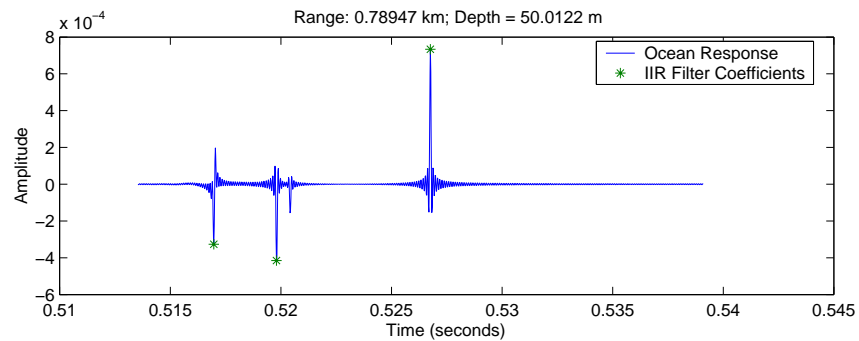
Figure 92.   IIR Filter, Case 17

Figure 93.   IIR Filter, Case 18
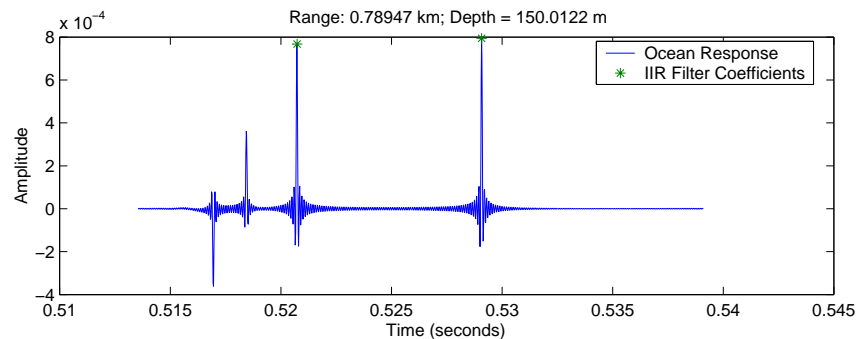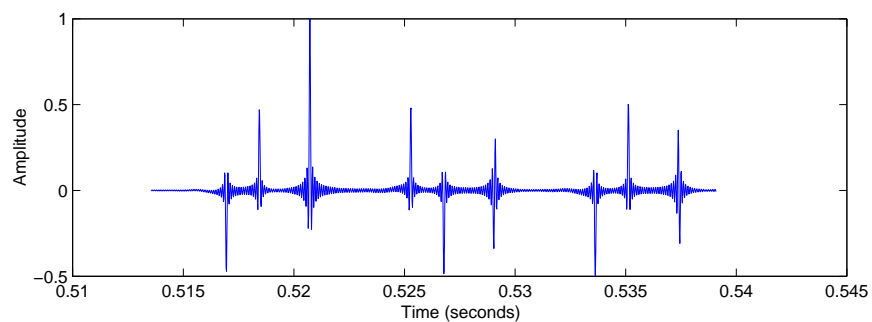
Figure 94.   IIR Filter, Case 19
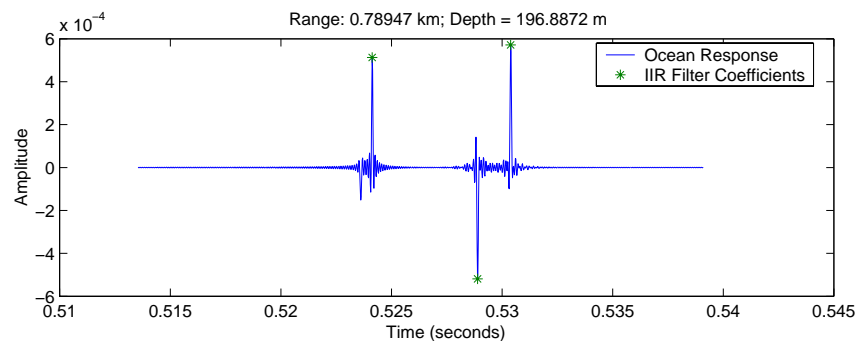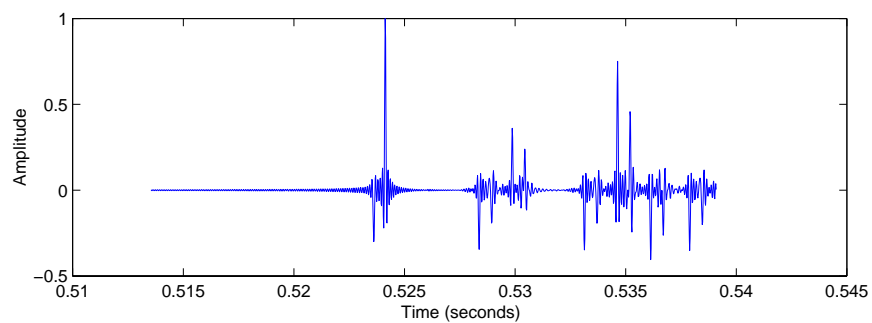
Figure 95.   IIR Filter, Case 20
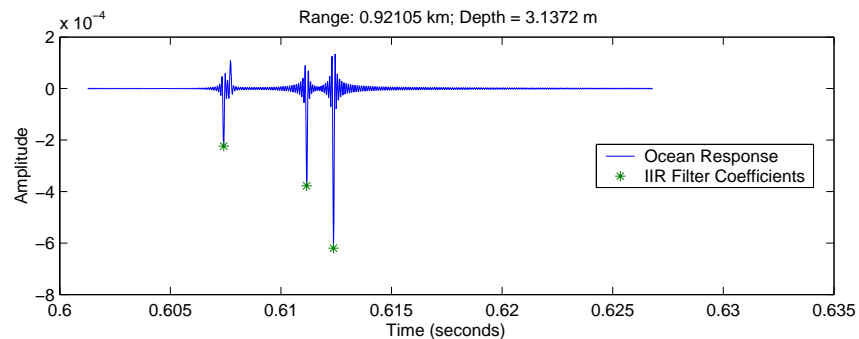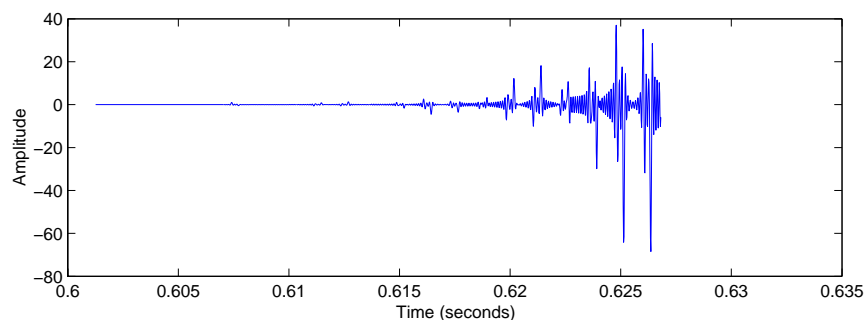
Figure 96.   IIR Filter, Case 21
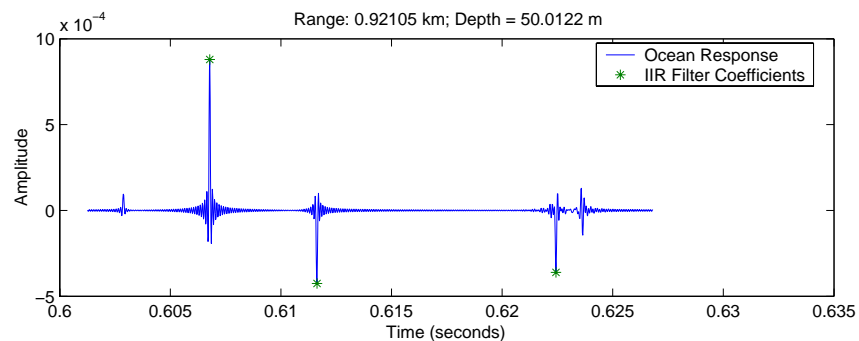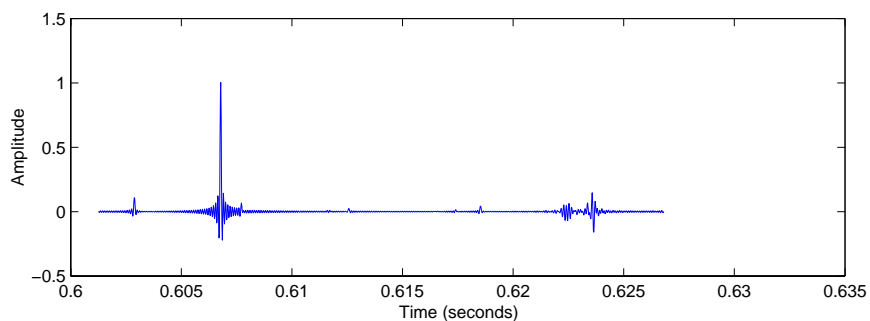
Figure 97.   IIR Filter, Case 22
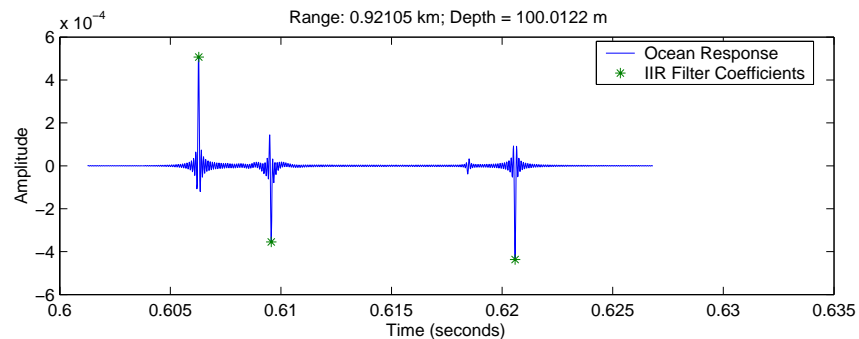
120
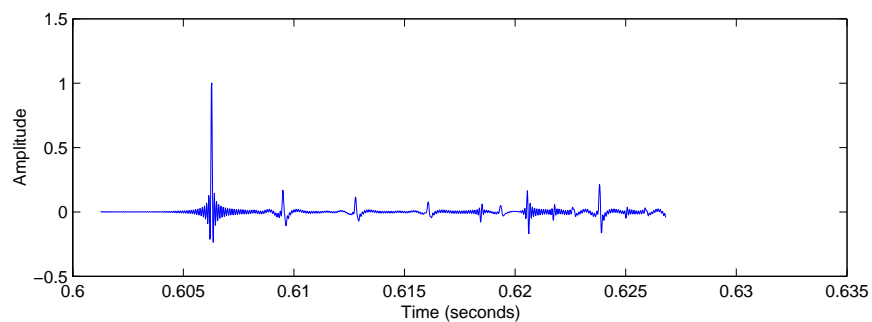
Figure 98.　IIR Filter, Case 23
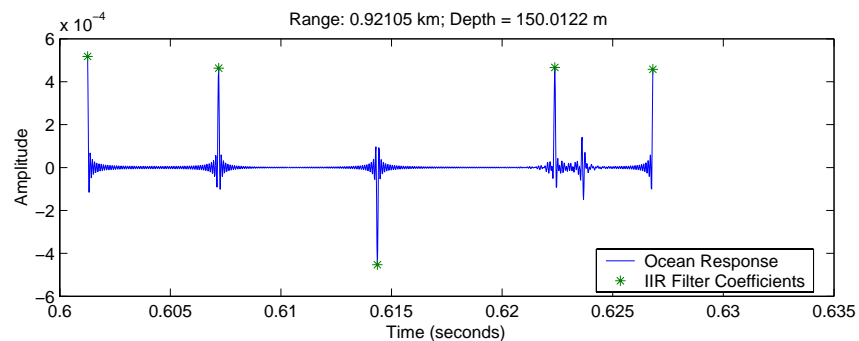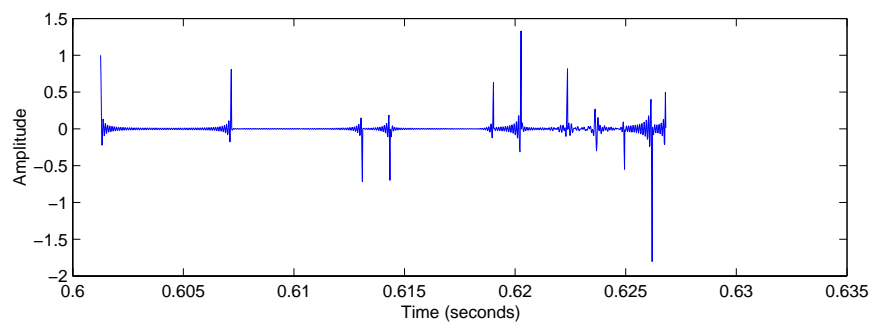
Figure 99.　IIR Filter, Case 24
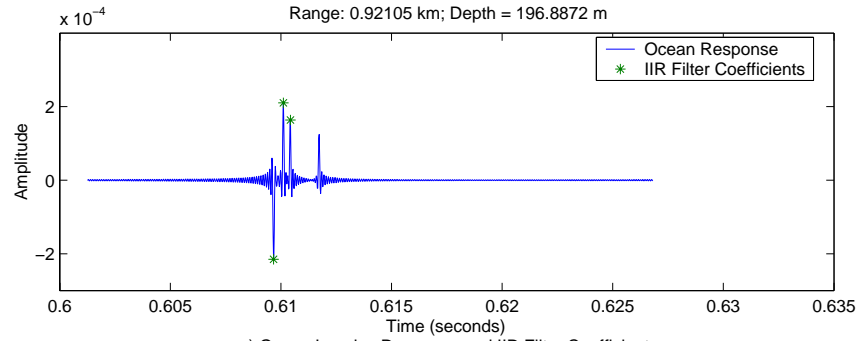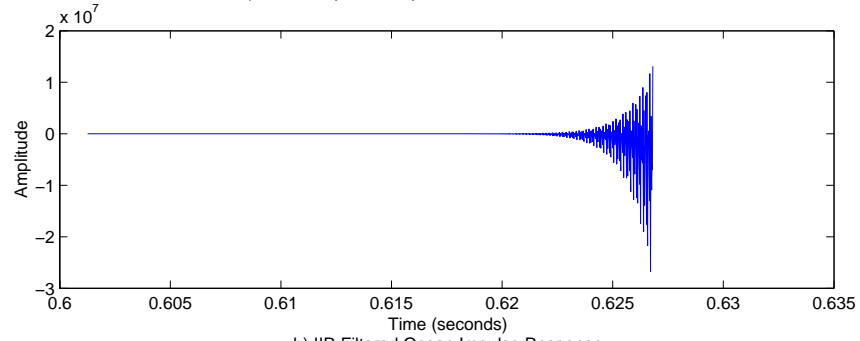
Figure 100.　IIR Filter, Case 25
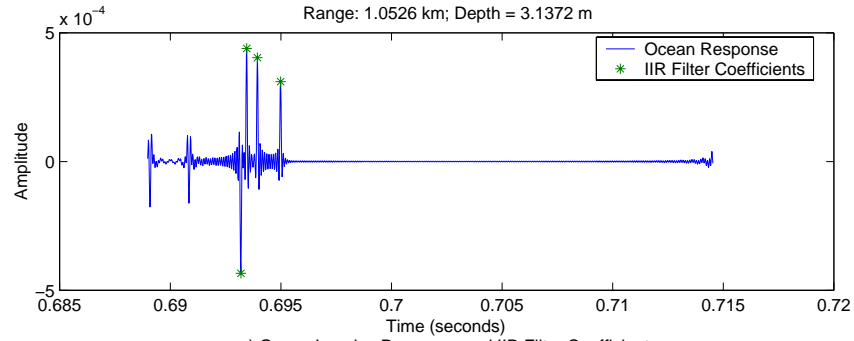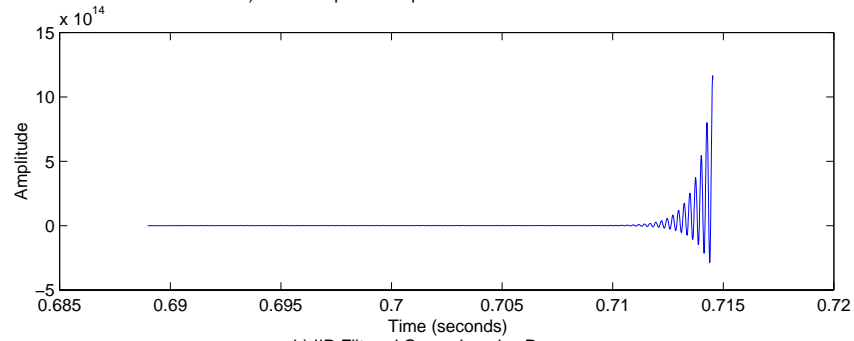
Figure 101.　IIR Filter, Case 26
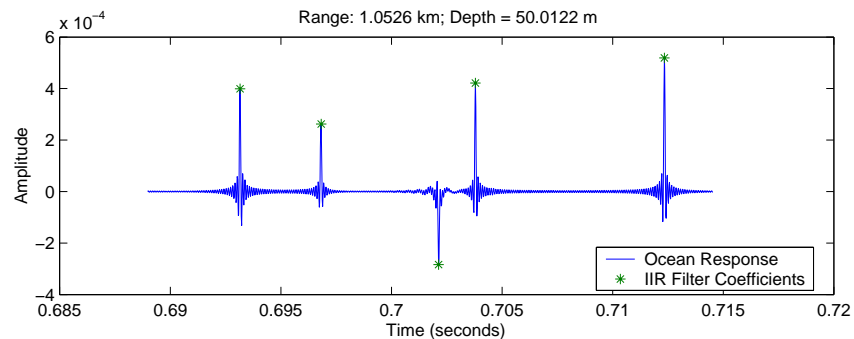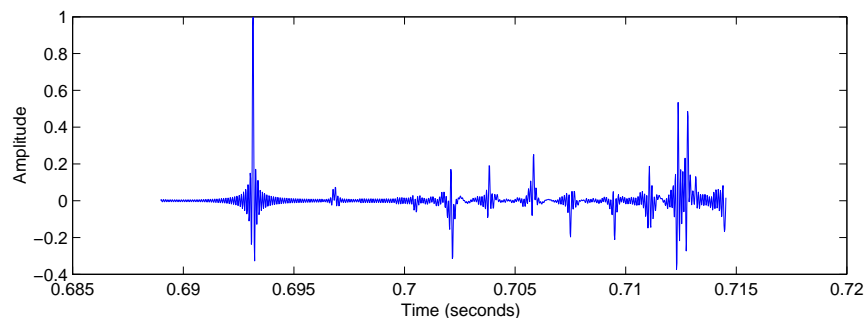
Figure 102.   IIR Filter, Case 27
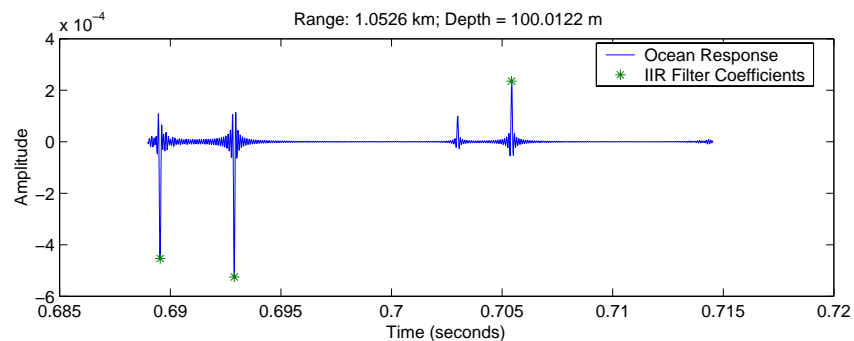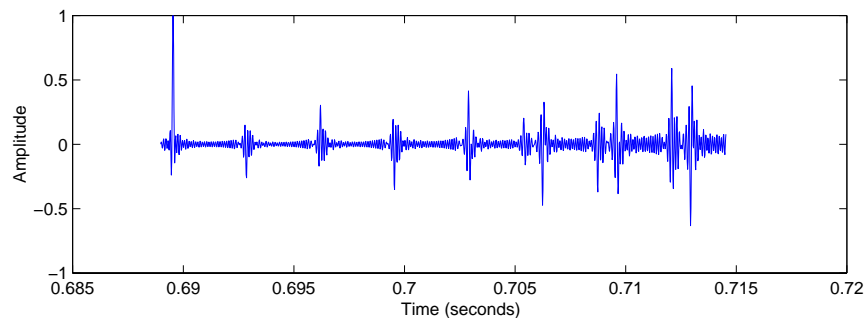
Figure 103.   IIR Filter, Case 28
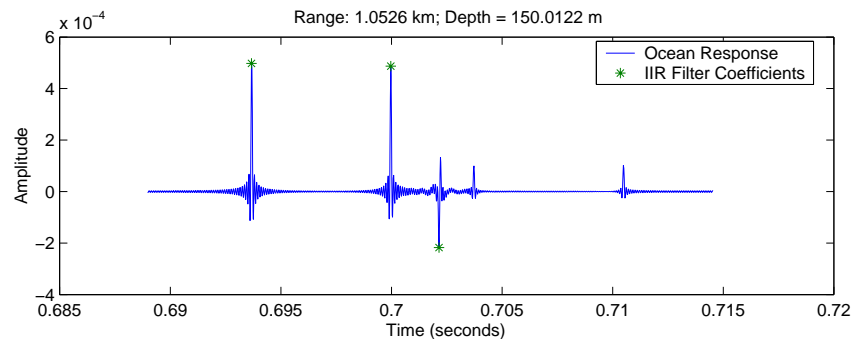
123
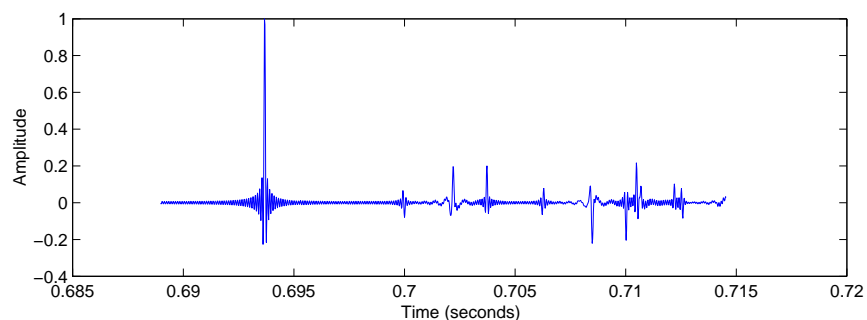
Figure 104.   IIR Filter, Case 29
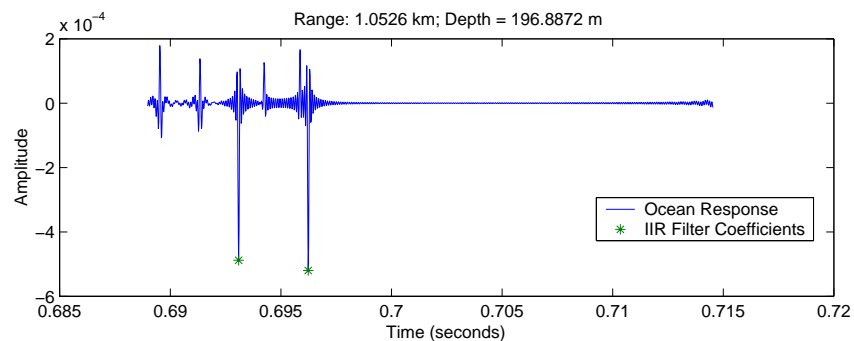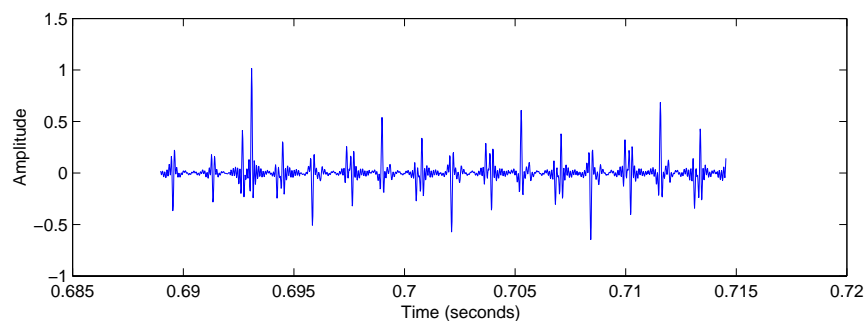
Figure 105.   IIR Filter, Case 30

124

APPENDIX C.   BIT ERROR RATE PLOTS

This appendix contains plots of the bit error rate simulations. It is separated into two sections. The first section contains plots of the bit error rate versus bit rate for all three of the filters and the received signal. The second section contains spatial plots of the bit error rate versus range and depth for all three of the filters and the received signal.

A.   BIT ERROR RATE VERSUS BIT RATE

Figures 106 through 135 contain plots of the bit error rates versus bit rate. Bit error rates for all three filters and the received signal for a single location in the ocean are contained on one plot. Because the simulation accuracy for bit error rates was 7.63×10^{-6}, any errors rates below 10^{-5} were rounded to 10^{-5}.
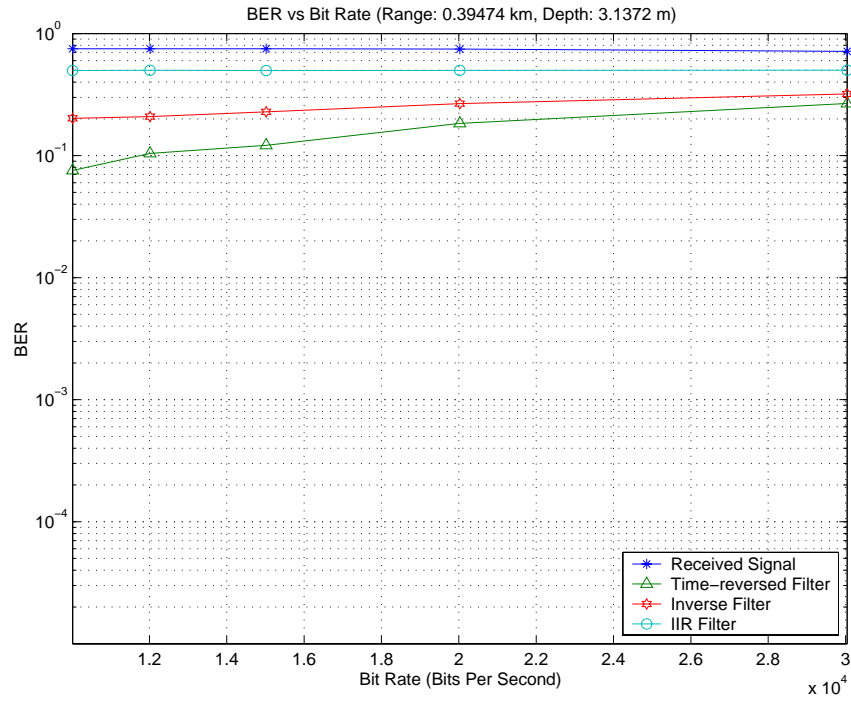
Figure 106.   BER vs Bit Rate, Case 1
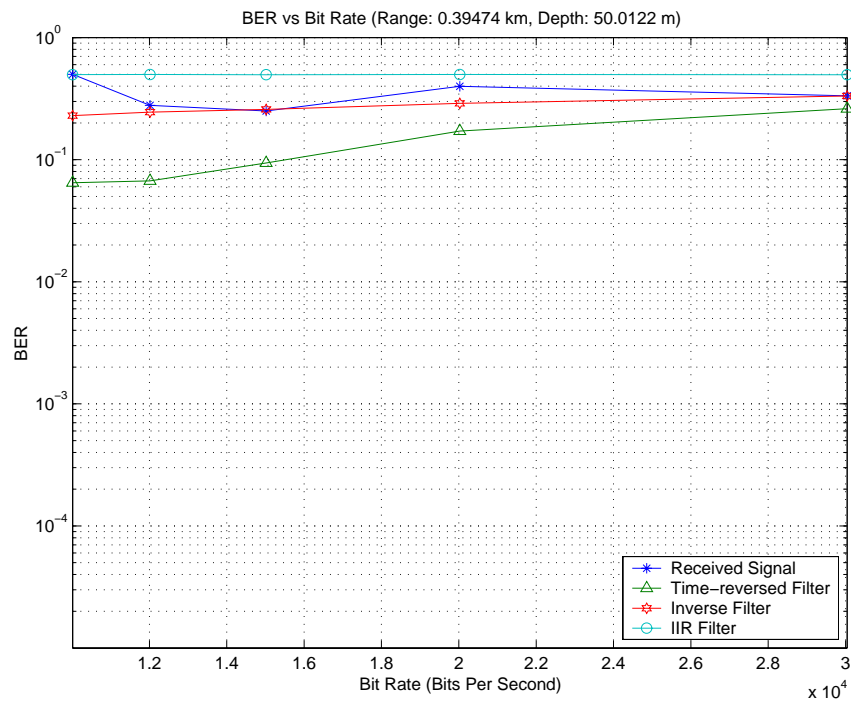
Figure 107.   BER vs Bit Rate, Case 2
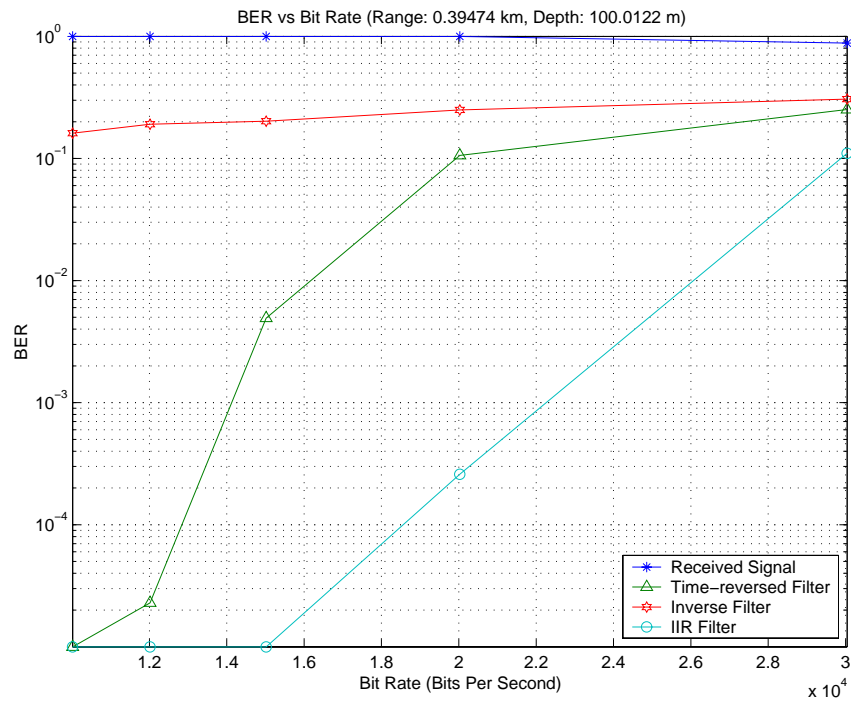
Figure 108.   BER vs Bit Rate, Case 3
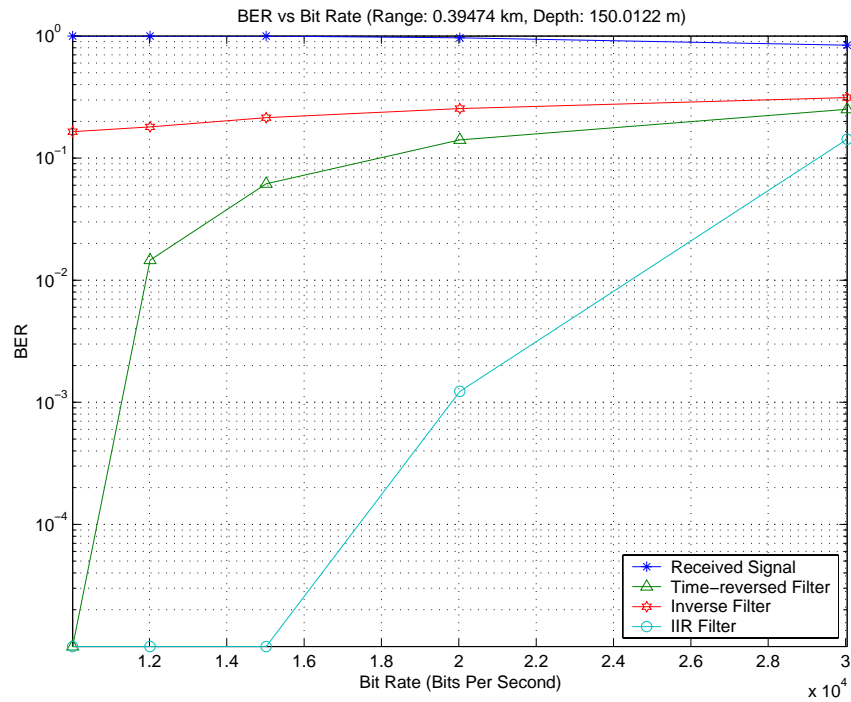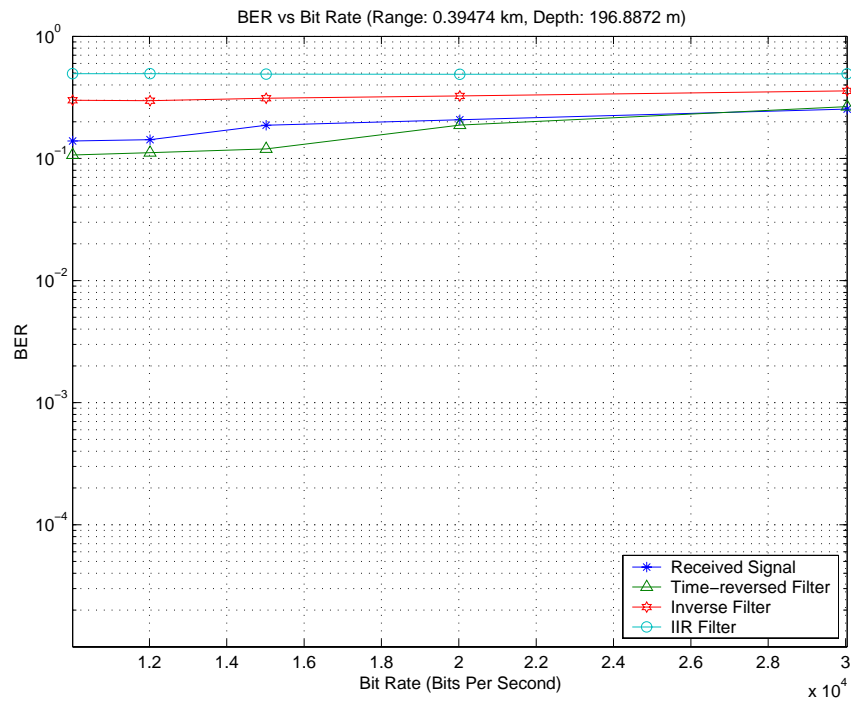

Figure 109.   BER vs Bit Rate, Case 4

127

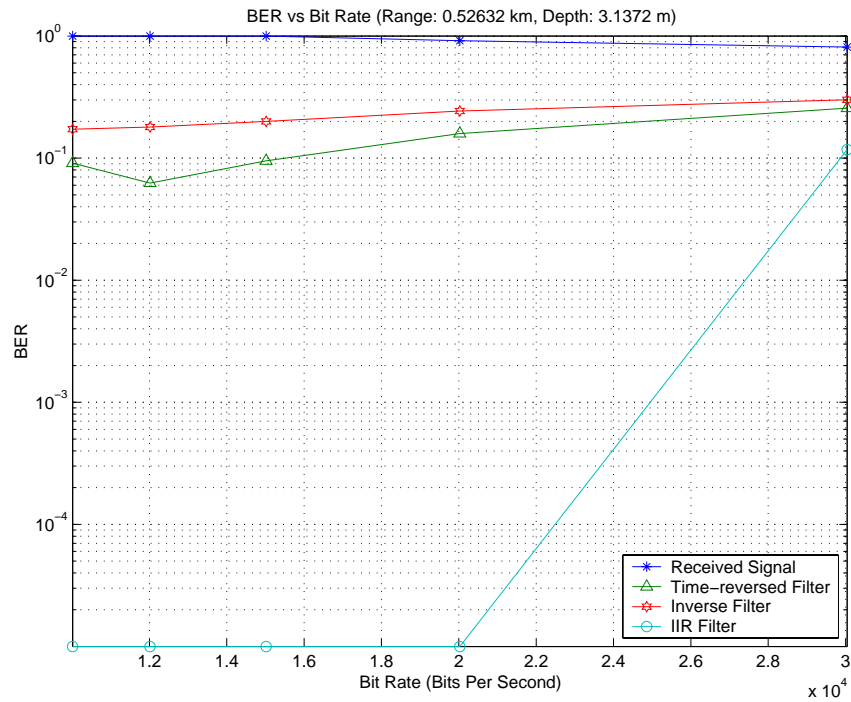Figure 110.   BER vs Bit Rate, case 5

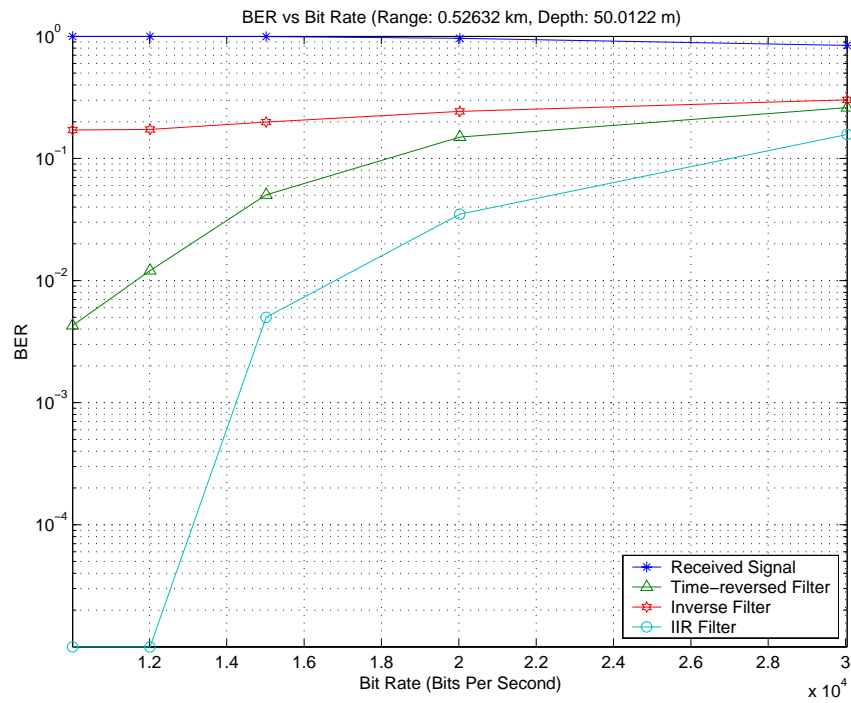

Figure 111.   BER vs Bit Rate, Case 6
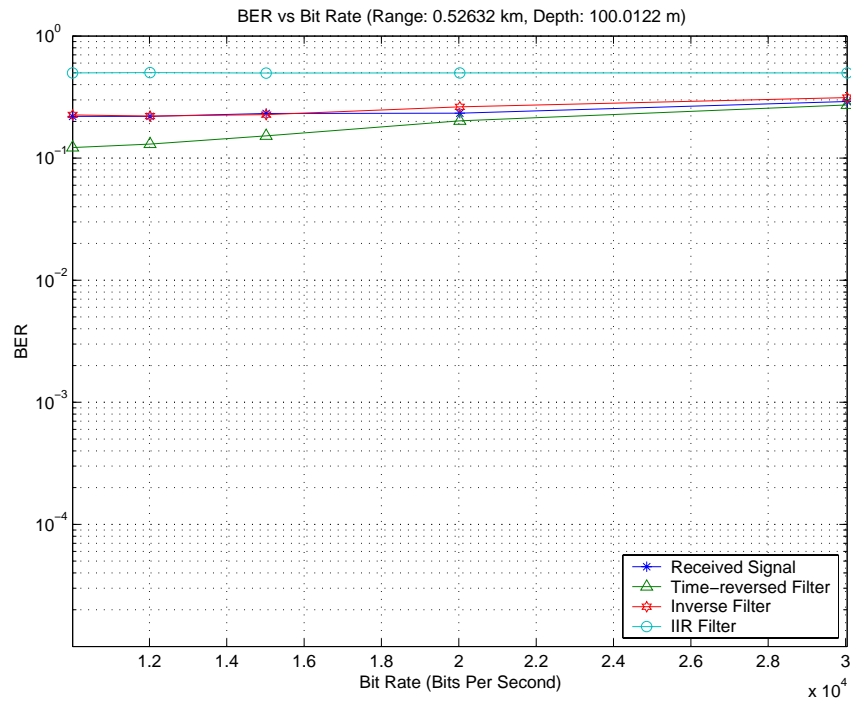
128

Figure 112.   BER vs Bit Rate, Case 7
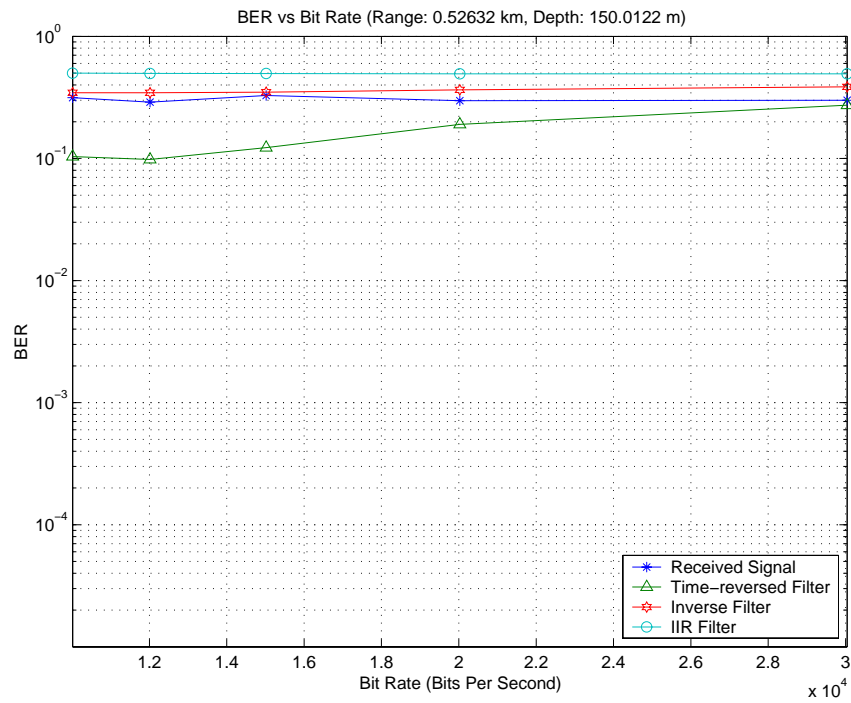

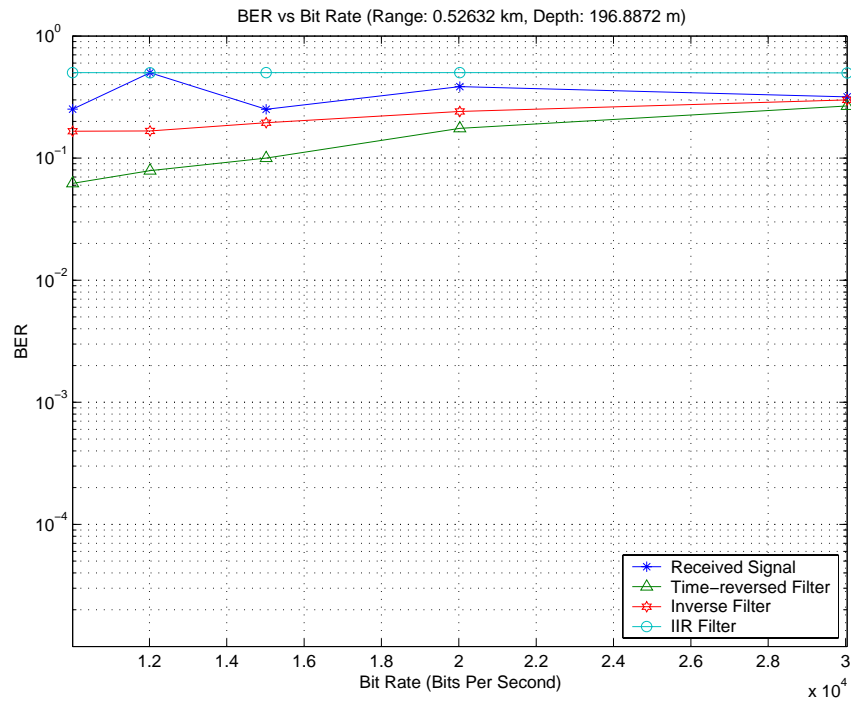Figure 113.   BER vs Bit Rate, Case 8

Figure 114.　BER vs Bit Rate, Case 9
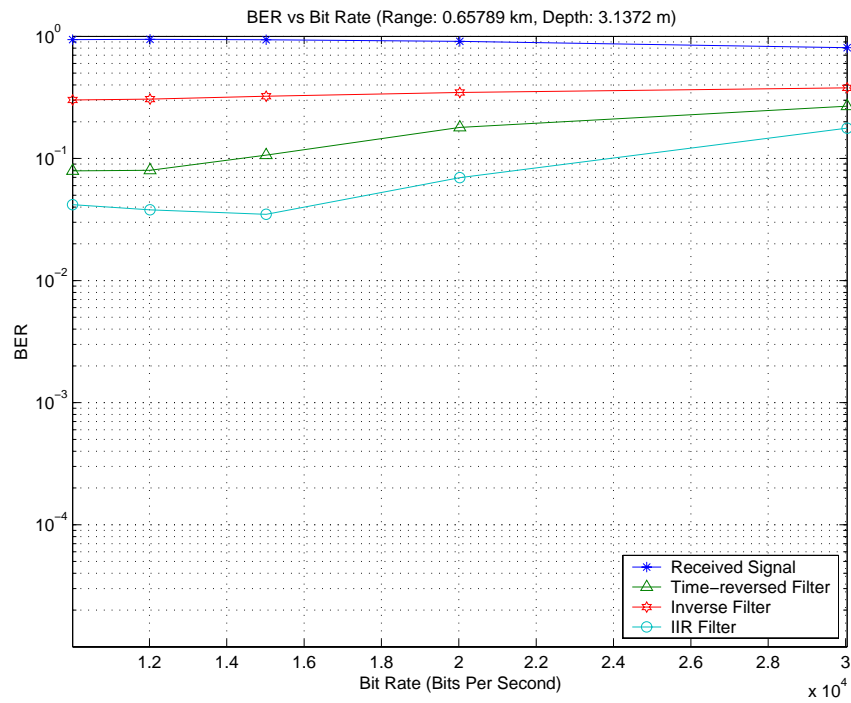

Figure 115.　BER vs Bit Rate, Case 10

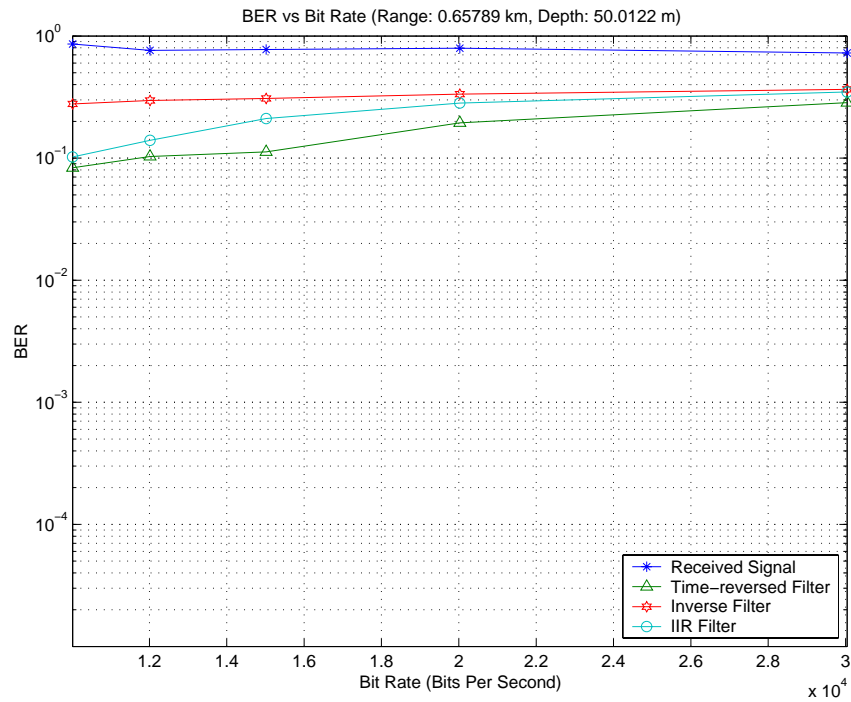Figure 116.   BER vs Bit Rate, Case 11

Figure 117.   BER vs Bit Rate, Case 12
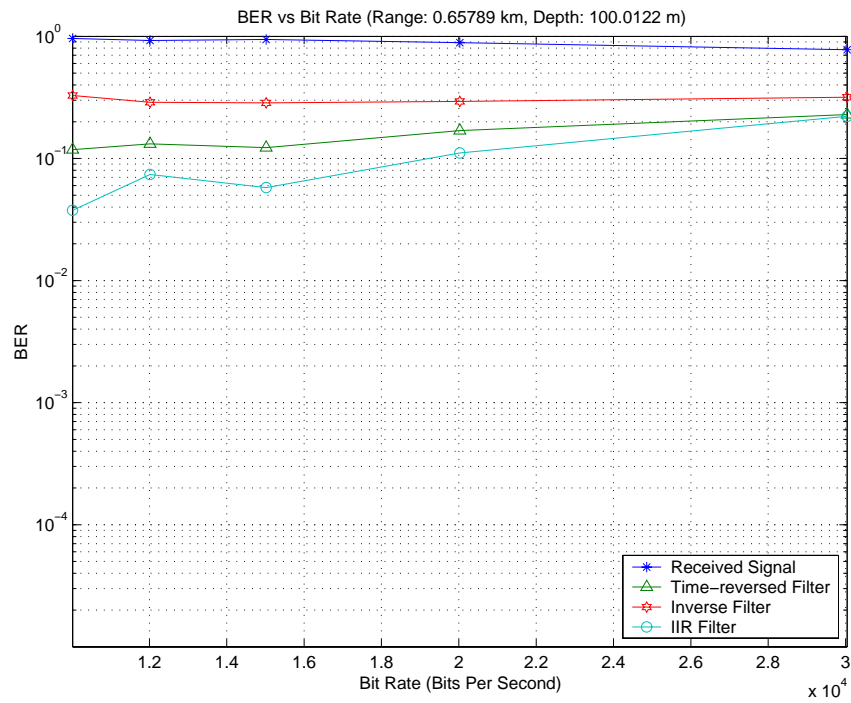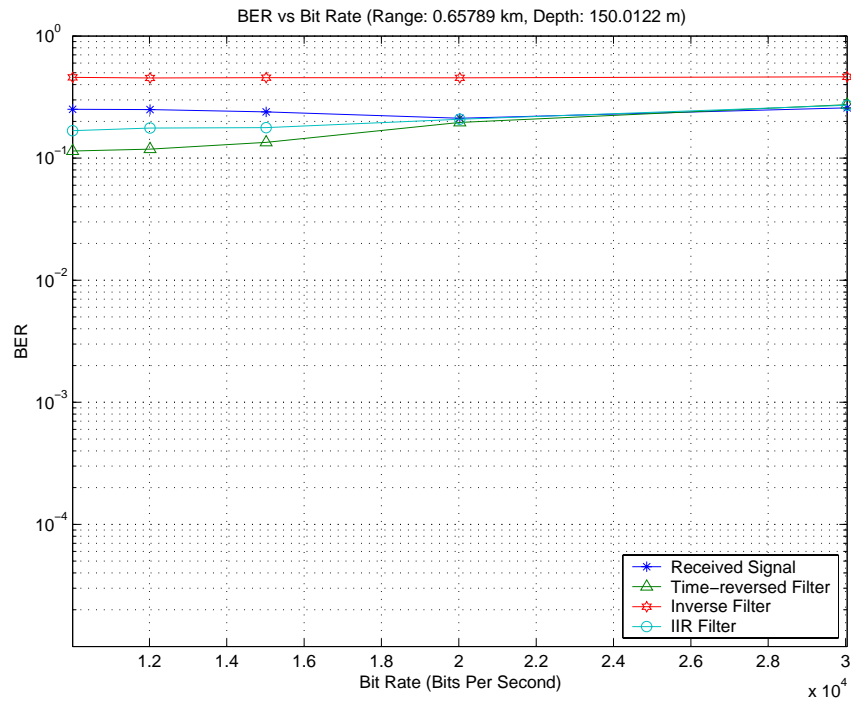
Figure 118.   BER vs Bit Rate, Case 13

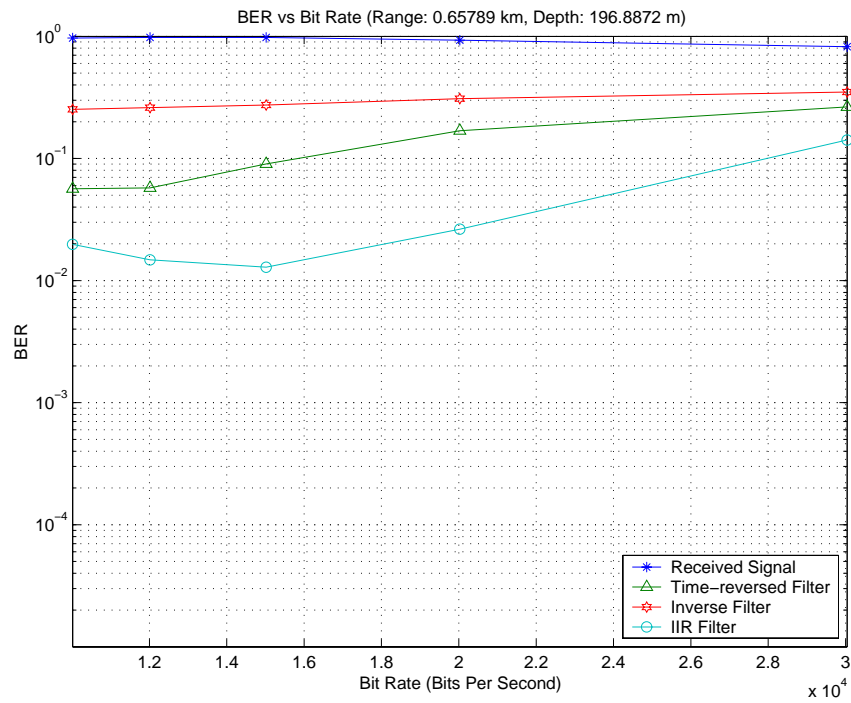Figure 119.   BER vs Bit Rate, Case 14

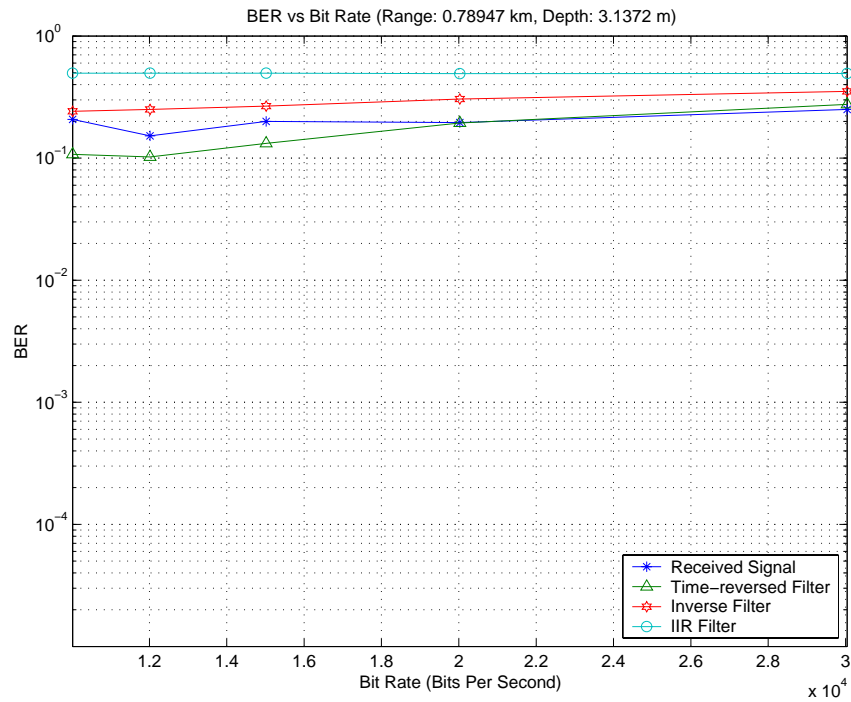Figure 120.　BER vs Bit Rate, Case 15

Figure 121.　BER vs Bit rate, Case 16
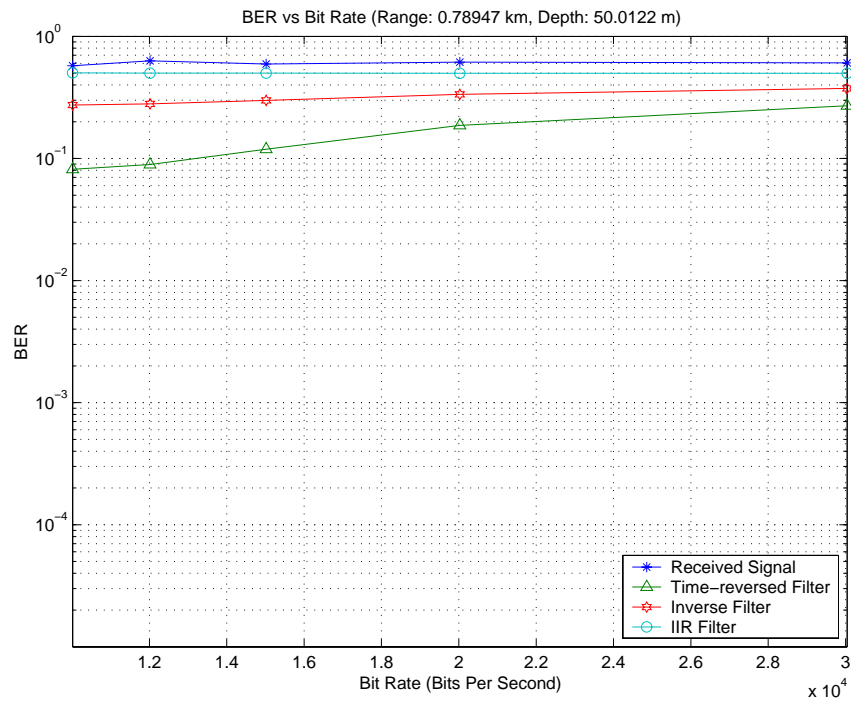
133

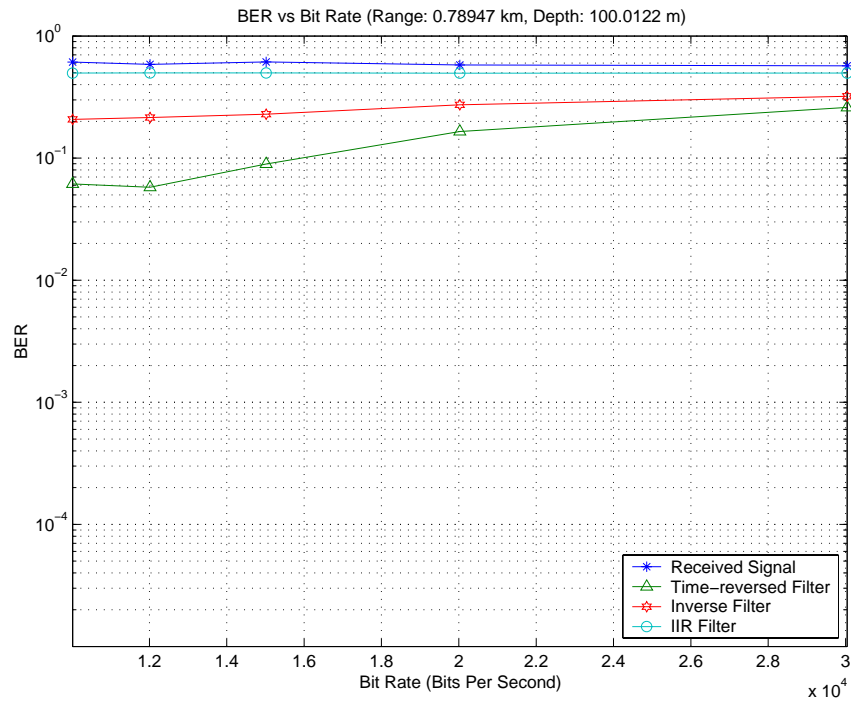Figure 122.   BER vs Bit Rate, Case 17

Figure 123.   BER vs Bit Rate, Case 18

Figure 124.   BER vs Bit Rate, Case 19

Figure 125.   BER vs Bit rate, Case 20

Figure 126.   BER vs Bit Rate, Case 21

Figure 127.   BER vs Bit Rate, Case 22

136

Figure 128.   BER vs Bit Rate, Case 23
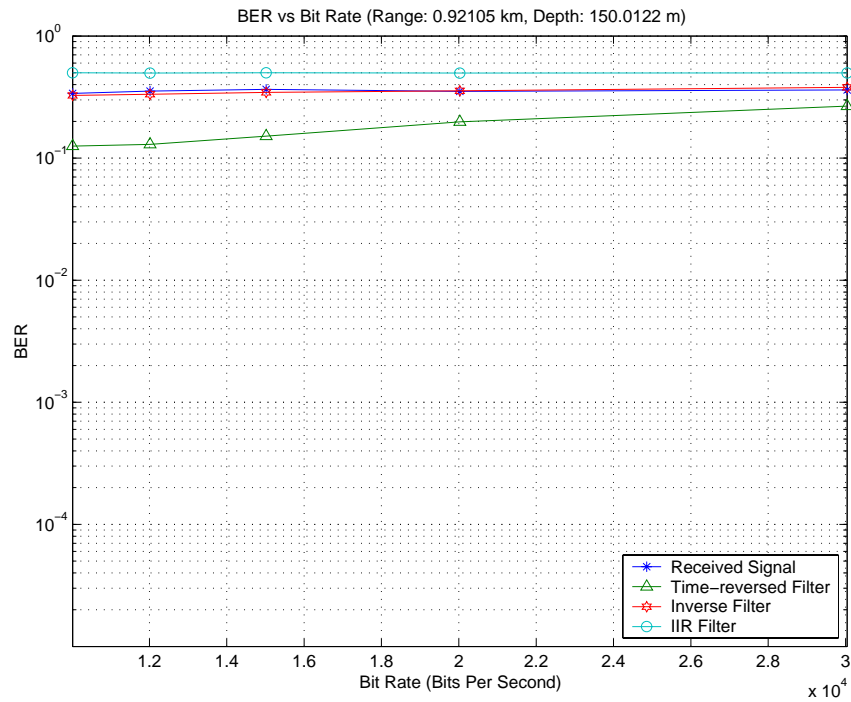
Figure 129.   BER vs Bit Rate, Case 24
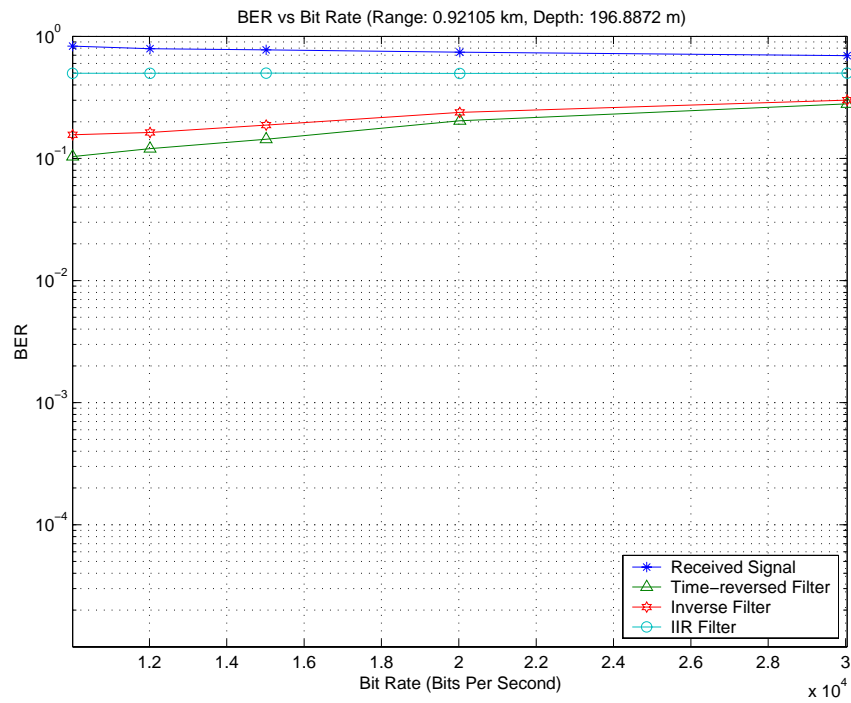
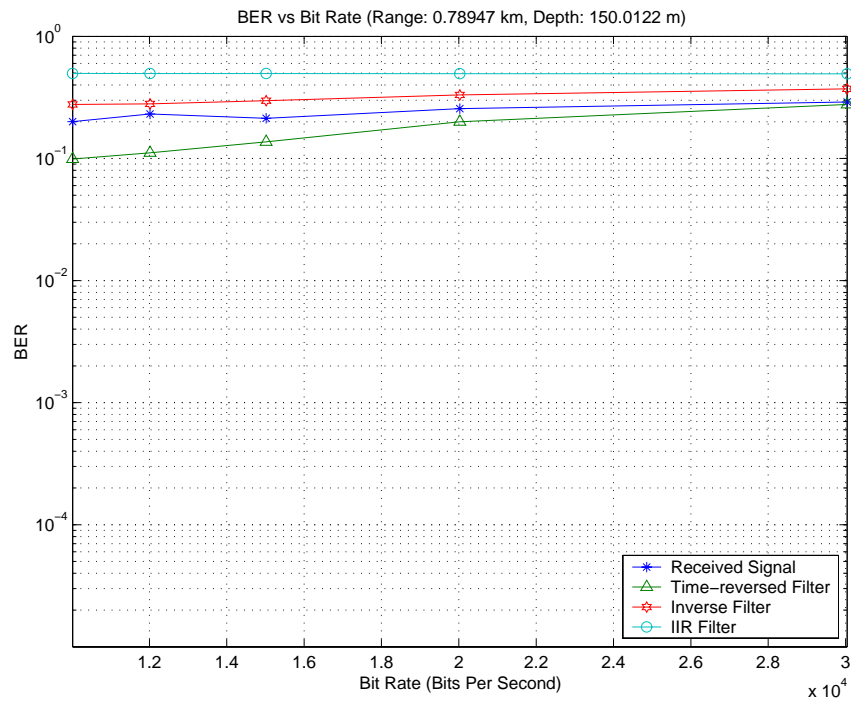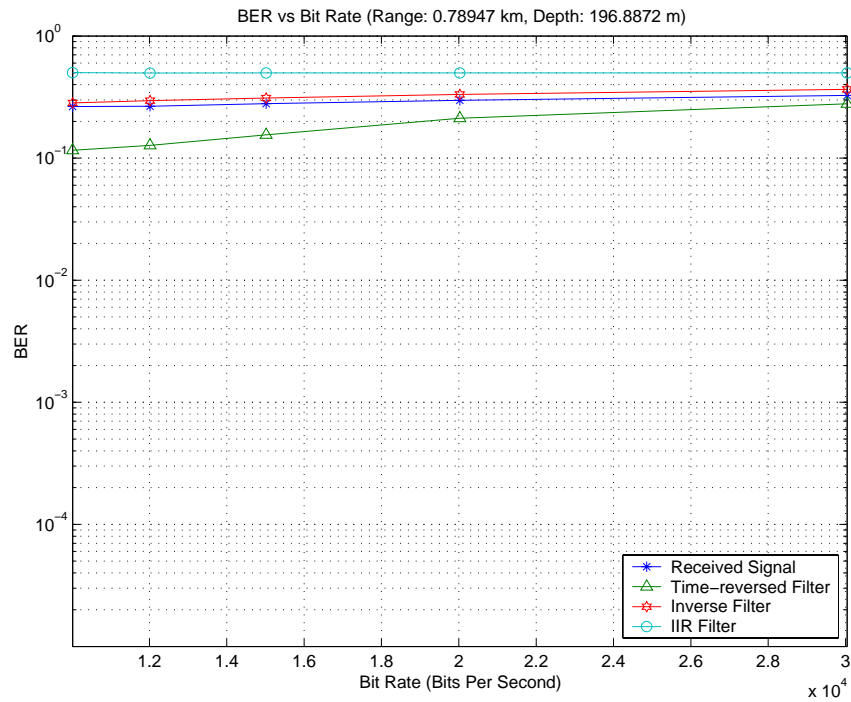Figure 130.   BER vs Bit Rate, Case 25
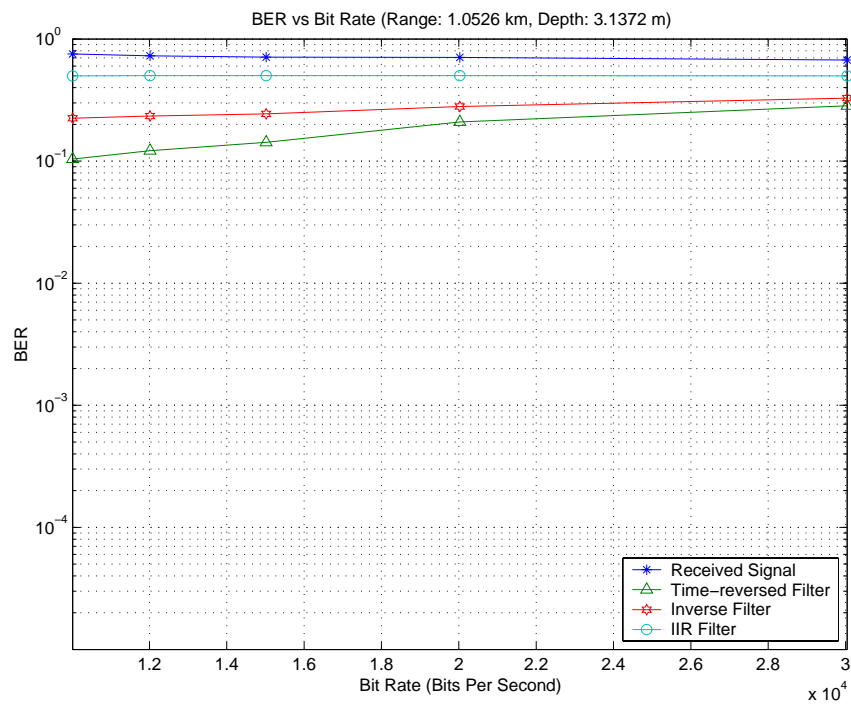
Figure 131.   BER vs Bit Rate, Case 26

138

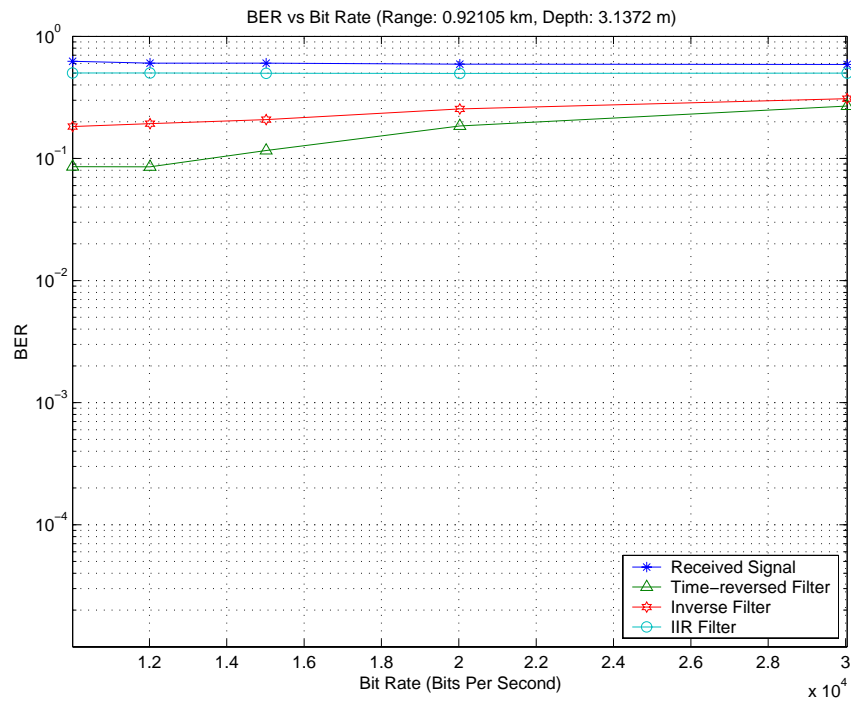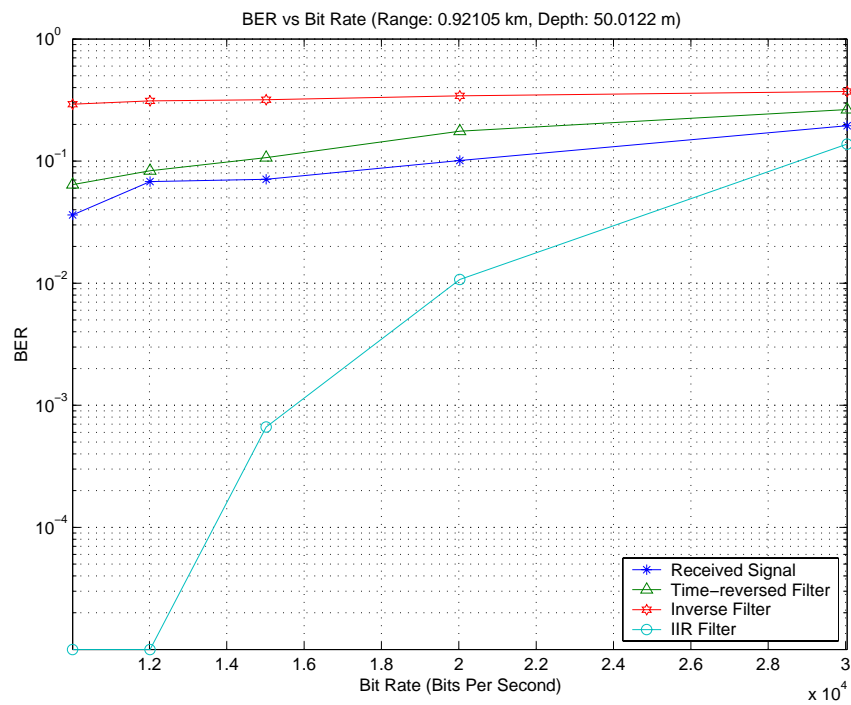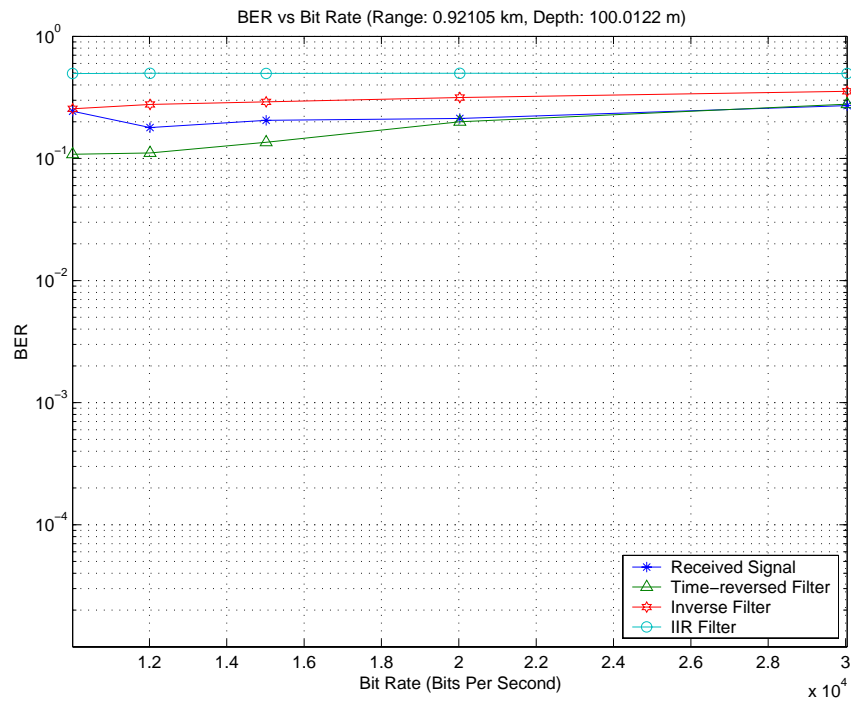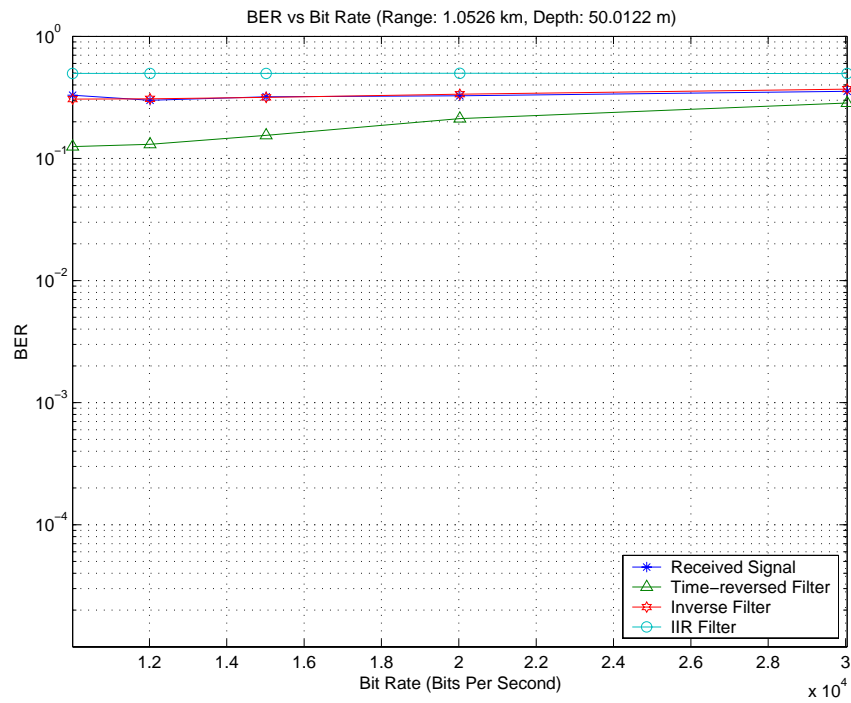Figure 132.   BER vs Bit Rate, Case 27
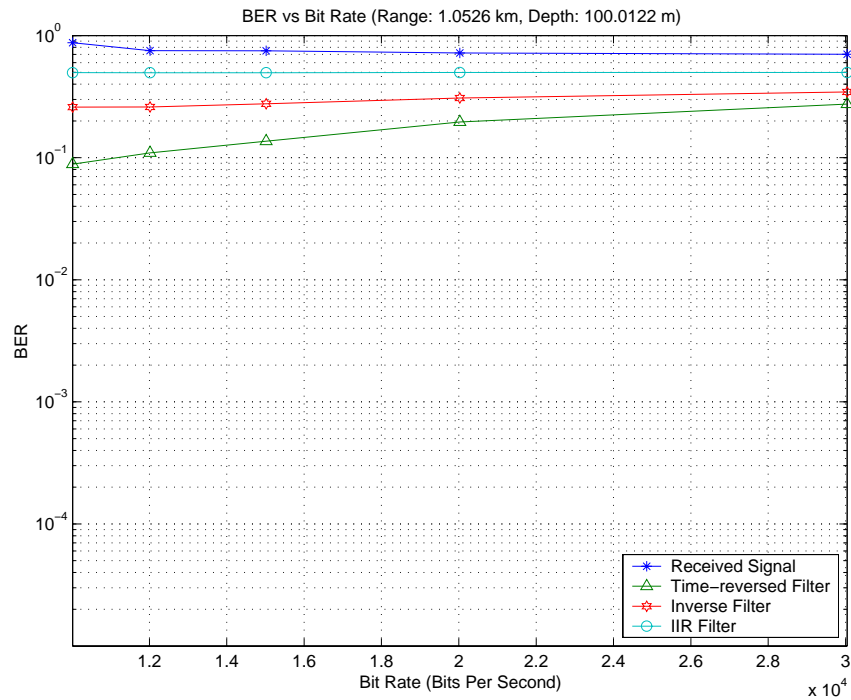
Figure 133.   BER vs Bit Rate, Case 28

139
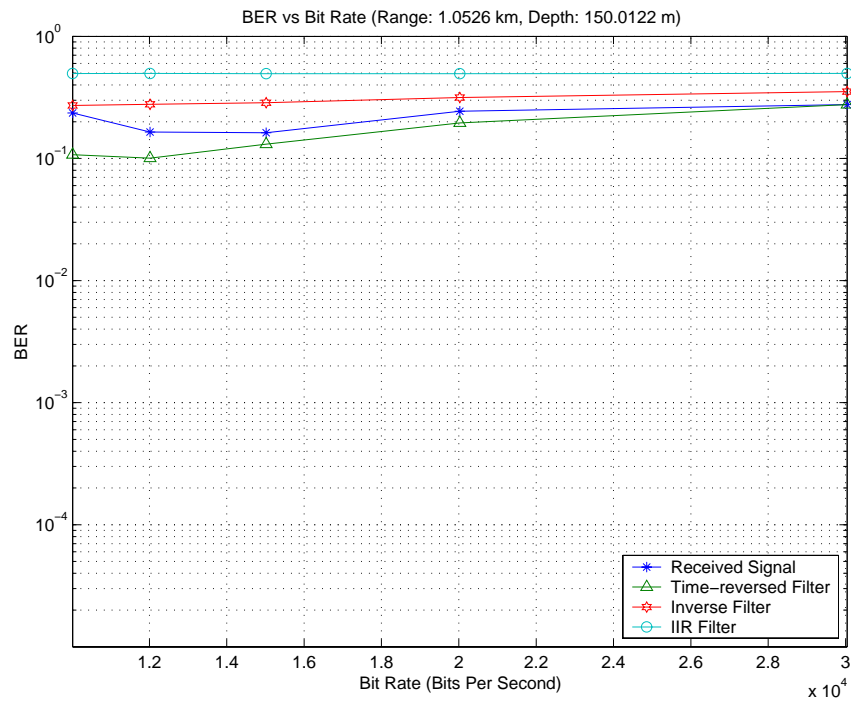
Figure 134.   BER vs Bit Rate, Case 29
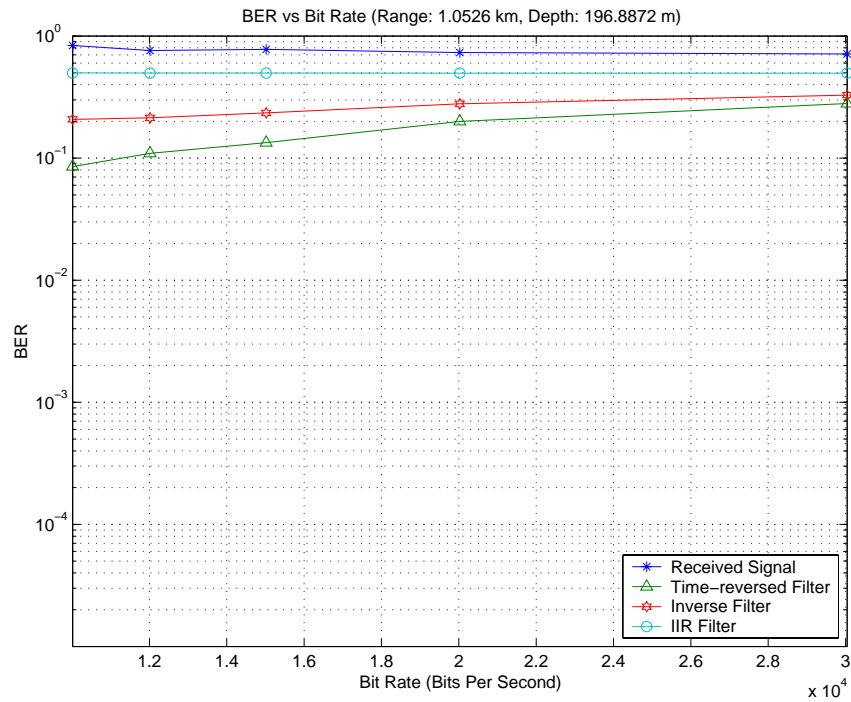
Figure 135.   BER vs Bit Rate, Case 30

B. BIT ERROR RATE VERSUS RANGE AND DEPTH

Figures 136 through 140 contain plots of the bit error rates versus range and depth for the specific bit rates. Each figure depicts one bit rate, but contains four plots; one for the received signal and one for each of the filters (passive time-reversed, inverse, and IIR). The axes are depth and range with the color representing the bit error rate. In these plots, red hues represent bit error rates around 10^{-1} and greater, the blue hues represent bit error rates around 10^{-3} and lower, and the yellow and green hues signify bit error rates between 10^{-3} and 10^{-1}.
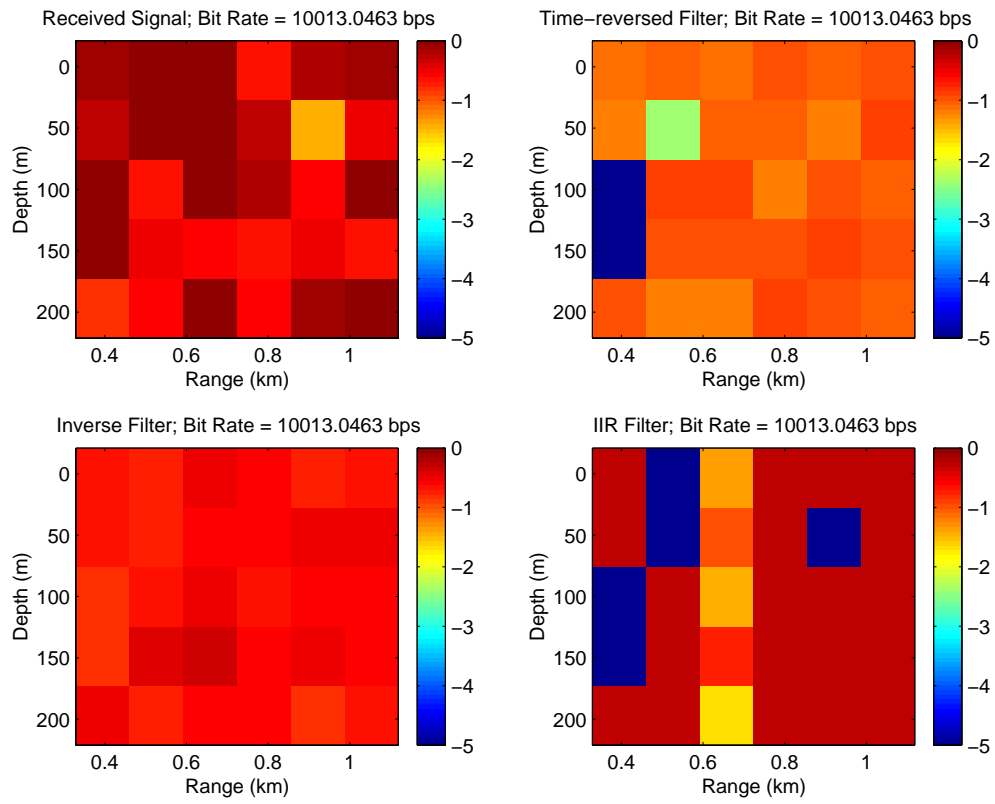
Figure 136.   Log BER for Bit Rate of 10013 bps
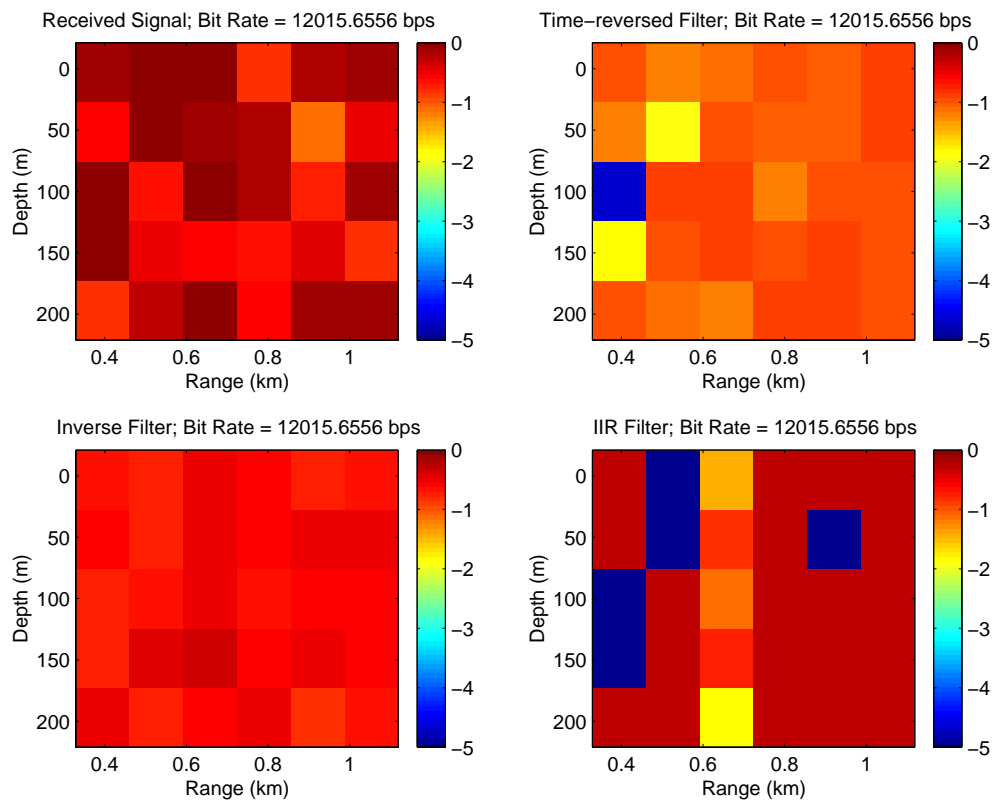
Figure 137.   Log BER for Bit Rate of 12015 bps
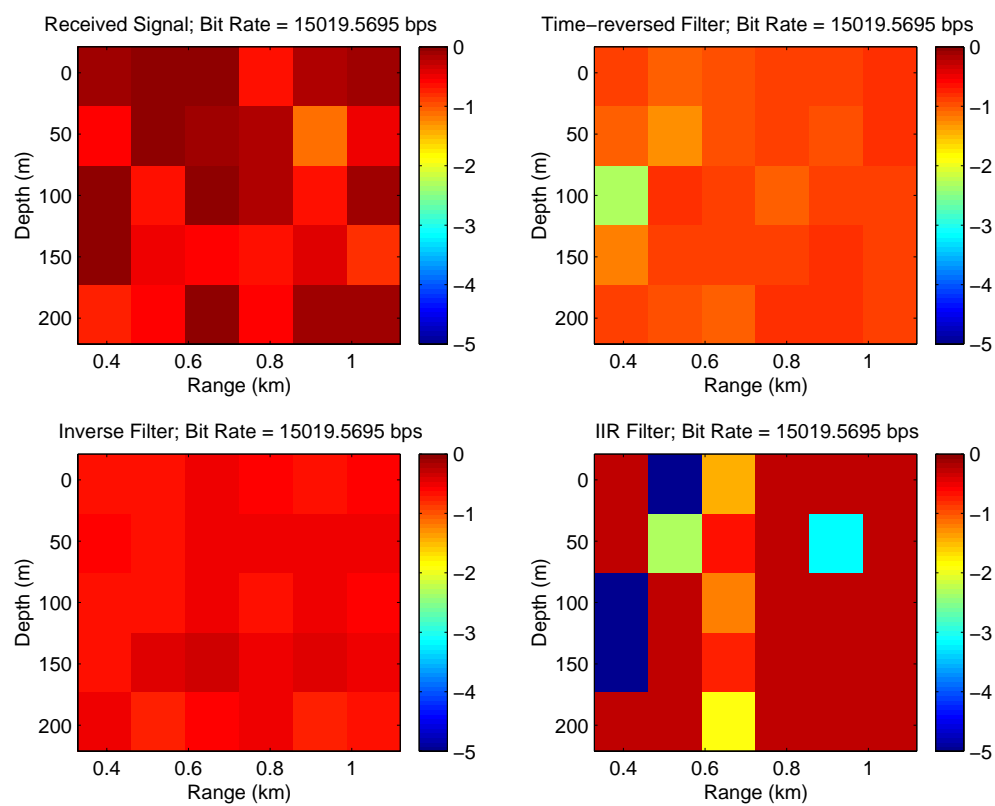
Figure 138.   Log BER for Bit Rate for 15019 bps

144
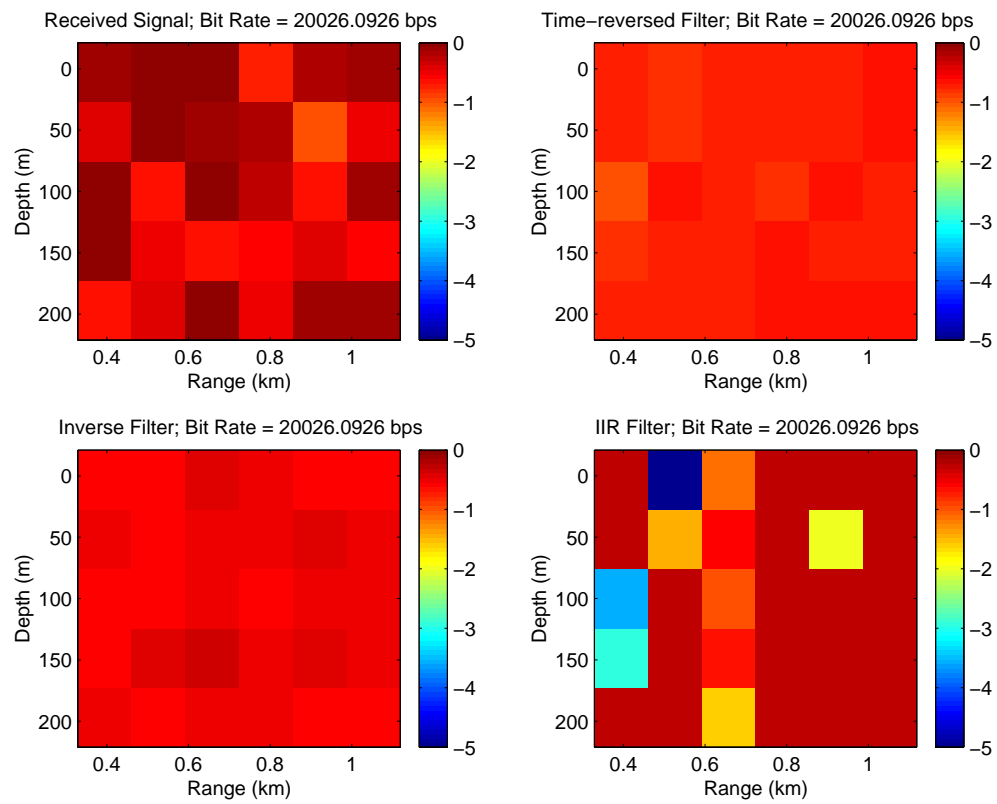
Figure 139.   Log BER for Bit Rate of 20026 bps

Figure 140.   Log BER for Bit Rate of 30039 bps

LIST OF REFERENCES

[1]   R. A. Benson, Jr. and T. Curtin, B., "Office of Naval Research Program in Underwater Acoustic Communications," Office of Naval Research, Arlington, VA.

[2]   D. B. Kilfoyle and A. B. Baggeroer, "The State of the Art in Underwater Acoustic Telemetry," *IEEE Journal of Oceanic Engineering*, vol. 25, pp. 4-27, January 2000.

[3]   B. Fletcher, "UUV Master Plan: A Vision for Navy UUV Development," Space and Naval Warfare Systems Center, San Diego.

[4]   G. Loubet, V. Capellano, and R. Filipiak, "Underwater Spread-Spectrum Communications," presented at OCEANS '97, 1997.

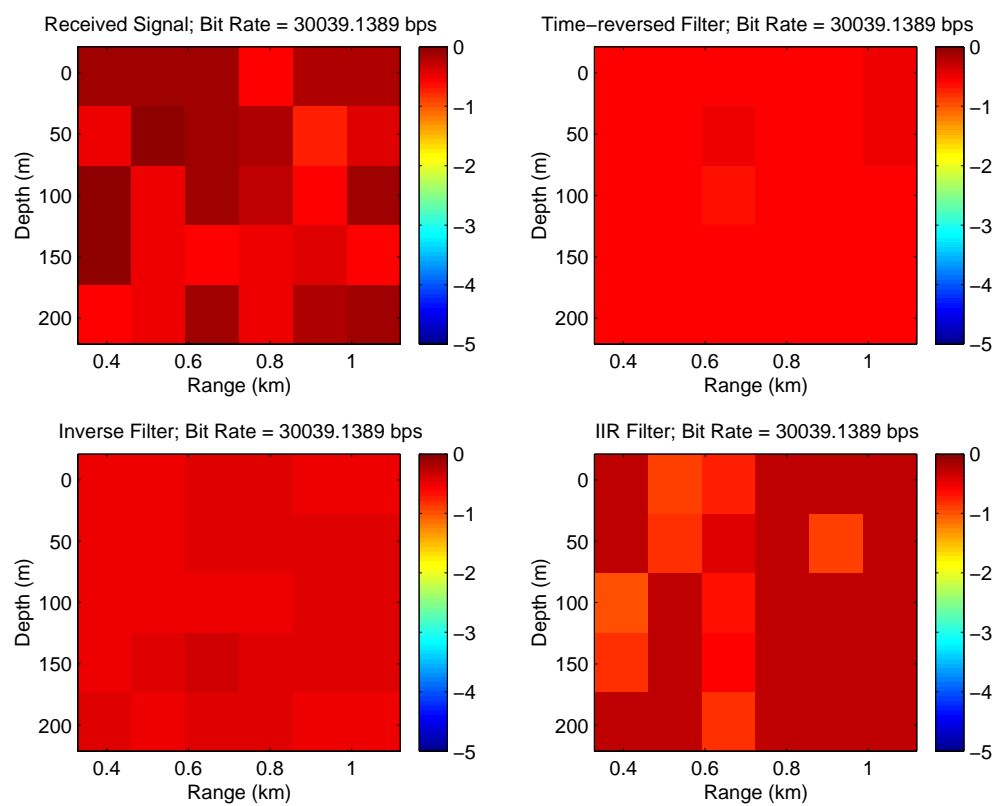[5]   M. Stojanovic, J. A. Catipovic, and J. G. Proakis, "Phase-Coherent Digital Communications for Underwater Acoustic Channels," *IEEE Journal of Oceanic Engineering*, vol. 19, pp. 100-111, 1994.

[6]   F. B. Jensen, W. A. Kuperman, M. B. Porter, and H. Schmidt, *Computational Ocean Acoustics*. New York: American Institute of Physics Press, 1994.

[7]   L. Freitag, M. Johnson, and M. Stojanovic, "Efficient Equalizer Update Algorithms for Acoustic Communication Channels of Varying Complexity," presented at OCEANS '97, 1997.

[8]   M. Stojanovic, L. Freitag, and M. Johnson, "Channel-Estimation-Based Adaptive Equalization of Underwater Acoustic Signals," presented at OCEANS '99, 1999.

[9]   P. S. D. Tarbit, G. S. Howe, O. R. Hinton, A. E. Adams, and B. S. Sharif, "Development of a Real-time Adaptive Equalizer for a High-rate Underwater Acoustic Data Communications Link," presented at OCEANS '94, 1994.

[10]   B. Geller, V. Capellano, and G. Jourdain, "Equalizer for Real Time High Rate Transmission in Underwater Communications," presented at ICASSP-95, 1995.

[11]   B. Geller, J. M. Brossier, and V. Capellano, "Equalizer for High Data Rate Transmission in Underwater Communications," presented at OCEANS '94, 1994.

[12]   V. Capellano, G. Loubet, and G. Jourdain, "Adaptive Multichannel Equalizer for Underwater Communications," presented at OCEANS '96, 1996.

[13]   B. Geller, V. Capellano, J.-M. Brossier, A. Essebbar, and G. Jourdain, "Equalizer for Video Rate Transmission in Multipath Underwater Communications," *IEEE Journal of Oceanic Engineering*, vol. 21, pp. 150-155, 1996.

[14]   V. Capellano, "Performance Improvements of a 50 km Acoustic Transmission Through Adaptive Equalization and Spatial Diversity," presented at OCEANS '97, 1997.

[15]   V. Capellano and G. Jourdain, "Comparison of Adaptive Algorithms for Multichannel Adaptive Equalizers. Application to Underwater Acoustic Communications.," presented at OCEANS '98, 1998.

[16]   D. E. Lambert, N. A. Pendergrass, and S. M. Jarvis, "An Adaptive Block Decision Feedback Receiver for Improved Performance in Channels with Severe Intersymbol Interference," presented at OCEANS '96, 1996.

[17]   G. S. Howe, P. S. D. Tarbit, O. R. Hinton, B. S. Sharif, and A. E. Adams, "Sub-sea Acoustic Remote Communications Utilising an Adaptive Receiving Beamformer for Multipath Suppression," presented at OCEANS '94, 1994.

[18]   M. Stojanovic, J. A. Catipovic, and J. G. Proakis, "Adaptive Multi-channel Combining and Equalization for Underwater Acoustic Communications," *Journal of the Acoustical Society of America*, vol. 94, pp. 1621-1631, 1993.

[19]   A. Goalic, J. Labat, J. Trubuil, S. Saoudi, and D. Rioualen, "Toward a Digital Acoustic Underwater Phone," presented at Oceans '94, Brest, France, 1994.

[20]   S. M. Jarvis and N. A. Pendergrass, "Implementation of a Multichannel Decision Feedback Equalizer for Shallow Water Acoustic Telemetry Using a Stabilized Fast Transversal Filters Algorithm," presented at OCEANS '95, 1995.

[21]   S. Jarvis, R. Janiesch, K. Fitzpatrick, and R. Morrissey, "Results from Recent Sea Trials of the Underwater Digital Acoustic Telemetry System," 1997.

[22]   "Undersea Search and Survey and Communications/Navigation Aid Demonstration BAA Informational Paper."

[23]   C. W. Therrien, *Discrete Random Signals and Statistical Signal Processing*. Englewood Cliffs, NJ: Prentice Hall, Inc., 1992.

[24]   C. Athanasiou, "Comparison of Alternative Methods of Environmentally Adaptive Underwater Acoustic Communication Systems," *M.S. Engineering Acoustics*. Monterey, California: Naval Postgraduate School, 2001.

[25]   J. G. Proakis and D. G. Manolakis, *Digital Signal Processing: Principles, Algorithms, and Applications*, Second ed. New York: Macmillan Publishing Company, 1992.

[26]   J. W. Caruthers, *Fundamentals of Marine Acoustics*, vol. 18. New York: Elsevier Scientific Publishing Company, 1977.

[27]   R. F. W. Coates, *Underwater Acoustic Systems*. New York: Halsted Press, 1989.

[28]   B. Sklar, *Digital Communications*, 2nd ed. Upper Saddle River, New Jersey: Prentice Hall PTR, 2001.

[29]   H. L. Van Trees, *Detection, Estimation, and Modulation Theory Part 1*. New York: John Wiley & Sons, 1968.

[30]   S. D. Kouteas, "Time Delay Estimation for Underwater Signals and Application to Localization," in *Department of Electrical and Computer Engineering*. Monterey, California: Naval Postgraduate School, 2001, pp. 232.

[31]   K. B. Smith, "Convergence, Stability, and Variability of Shallow Water Acoustic predictions Using a Split-Step Fourier Parabolic Equation Model," *Journal of Computational Acoustics*, vol. 9, pp. 243-285, 2000.

[32]   D. E. Dudgeon and R. M. Mersereau, *Multidimensional Digital Signal Processing*. Englewood Cliffs, New Jersey: Prentice-Hall, Inc., 1984.

THIS PAGE INTENTIONALLY LEFT BLANK

INITIAL DISTRIBUTION LIST

1. Defense Technical Information Center
   Ft. Belvoir, Virginia

2. Dudley Knox Library
   Naval Postgraduate School
   Monterey, California

3. Engineering and Technology Curricular Office, Code 34
   Naval Postgraduate School
   Monterey, California

4. Professor Jeffrey B. Knorr, Code EC/Ko
   Chairman, Department of Electrical and Computer Engineering
   Monterey, California

5. Professor Charles W. Therrien, Code EC/Ti
   Department of Electrical and Computer Engineering City, State
   Monterey, California

6. Professor Kevin B. Smith, Code PH/Sk
   Chairman, Engineering Acoustics Academic Committee
   Monterey, California

7. Ryan J. Kuchler, LT U.S. Navy
   Pacific Grove, California